Department of Electrical Engineering

Enhancing the Performance of Flexible AC Transmission Systems (FACTS) by Computational Intelligence

Ahmed Mohamed Othman

Aalto University

DOCTORAL DISSERTATIONS

Aalto University publication series
DOCTORAL DISSERTATIONS 55/2011

Enhancing the Performance of Flexible AC Transmission Systems (FACTS) by Computational Intelligence

Ahmed Mohamed Othman

Doctoral dissertation for the degree of Doctor of Science in Technology to be presented with due permission of the Aalto University School of Electrical Engineering for public examination and debate in Auditorium S5 at the School of the Electrical Engineering (Espoo, Finland) on the 6th of Sept. 2011 at 12 noon.

Aalto University
School of Electrical Engineering
Department of Electrical Engineering
Faculty of Engineering - Zagazig University

Supervisors
AALTO UNIVERSITY, Prof. Matti Lehtonen
ZAGAZIG UNIVERSITY, Prof. Mahdi El-Arini

Preliminary examiners
Prof. Abdel.maksoud Taalab, El.Menofia University, Egypt.
Prof. Mohan Kothari, Indian Institute of Technology, India.

Opponent
Prof. Mansour H. Abdel.Rahman, El.Mansoura University, Egypt.

Aalto University publication series
DOCTORAL DISSERTATIONS 55/2011

ISBN 978-952-60-4176-6 (pdf)
ISBN 978-952-60-4175-9 (printed)
ISSN-L 1799-4934
ISSN 1799-4942 (pdf)
ISSN 1799-4934 (printed)

Aalto Print
Helsinki 2011

Finland

The dissertation can be read at http://lib.tkk.fi/Diss/

Author
Ahmed Mohamed Othman Abd El.Maksoud

Name of the doctoral dissertation
Enhancing the Performance of Flexible AC Transmission Systems (FACTS) by Computational Intelligence

Publisher School of Electrical Engineering

Unit Electrical Engineering Department

Series Aalto University publication series DOCTORAL DISSERTATIONS 55/2011

Field of research Power Systems and High Voltage Engineering

Manuscript submitted 10 February 2011 **Manuscript revised** 16 May 2011

Date of the defence 6 September 2011 **Language** English

☒ **Monograph** ☐ **Article dissertation (summary + original articles)**

Abstract

The thesis studies and analyzes UPFC technology concerns the management of active and reactive power in the power networks to improve the performance aiming to reach the best operation criteria. The contributions of the thesis start with formatting, deriving, coding and programming the network equations required to link UPFC steady-state and dynamic models to the power systems. The thesis derives GA applications on UPFC to achieve real criteria on a real world sub-transmission network.

An enhanced GA technique is proposed by enhancing and updating the working phases of the GA including the objective function formulation and computing the fitness using the diversity in the population and selection probability. The simulations and results show the advantages of using the proposed technique. Integrating the results by linking the case studies of the steady-state and the dynamic analysis is achieved. In the dynamic analysis section, a new idea for integrating the GA with ANFIS to be applied on the control action procedure is presented.

The main subject of the thesis deals with enhancing the steady-state and dynamics performance of the power grids by Flexible AC Transmission System (FACTS) based on computational intelligence. Control of the electric power system can be achieved by designing the FACTS controller, where the new trends as Artificial Intelligence can be applied to this subject to enhance the characteristics of controller performance. The proposed technique will be applied to solve real problems in a Finnish power grid. The thesis seeks to deal, solve, and enhance performances until the year 2020, where the data used is until the conditions of year 2020. The FACTS device, which will be used in the thesis, is the most promising one, which known as the Unified Power Flow Controller (UPFC).

The thesis achieves the optimization of the type, the location and the size of the power and control elements for UPFC to optimize the system performance. The thesis derives the criteria to install the UPFC in an optimal location with optimal parameters and then designs an AI based damping controller for enhancing power system dynamic performance. In this thesis, for every operating point GA is used to search for controllers' parameters, parameters found at certain operating point are different from those found at others. ANFISs are required in this case to recognize the appropriate parameters for each operating point.

Keywords Unified Power Flow controller (UPFC), Genetic Algorithm (GA), Optimal location, Optimal settings

ISBN (printed) 978-952-60-4175-9 **ISBN (pdf)** 978-952-60-4176-6

ISSN-L 1799-4934 **ISSN (printed)** 1799-4934 **ISSN (pdf)** 1799-4942

Location of publisher Espoo **Location of printing** Helsinki **Year** 2011

Pages 174 **The dissertation can be read at** http://lib.tkk.fi/Diss/

Preface

This work has been carried out under joint supervision between both of ZAGAZIG UNIVERSITY, EGYPT and AALTO UNIVERSITY, School of Electrical Engineering, FINLAND. Professor Mahdi El-Arini participated from Zagazig University and Professor Matti Lehtonen participated from Aalto University. The author of this dissertation has had the main responsibility of all research work and publications.

It might be worthwhile to begin with a brief as a summary of the work that has introduced in this thesis. The first task, which formed a primary of the thesis survey, was to cover and investigate FACTS technology and concerns the management of active and reactive power in the power networks to improve the performance aiming to reach the best operation criteria.

The concept of FACTS technology has the ability to deal with many fields of both system and customer problems, where the power control can solve many of these problems with enhancing the quality of the performance. We can categorize the types of FACTS depends on the technique which applied in their implementation and the connection method to the power system.

The subject of the thesis is to study applications of FACTS to control an electric power system. There are some problems like the inability to achieve full utilising of the capacity of the transmission lines, undesirable voltage levels, higher losses, high or low voltages, blocking and outages that must be solved. FACTS devices can be used for adapting the phase angle and the voltage magnitude at certain buses and/or line impedances, which gives the ability to control the power flow in the networks.

The thesis derives the criteria to install the UPFC in an optimal location with optimal parameters and then designs an AI based damping controller for enhancing power system dynamic performance.

Dissertation's and Author’s Contribution

The contributions of the thesis start with formatting, deriving, coding and programming the network equations required to link UPFC steady-state and dynamic models to the power systems. One of the other contributions of the thesis is deriving GA applications on UPFC to achieve real criteria on a real world sub-transmission network.

An enhanced GA technique is proposed by enhancing and updating the working phases of the GA including the objective function formulation and computing the fitness using the diversity in the population and selection probability. The simulations and results show the advantages of using the proposed technique. Integrating the results by linking the case studies of the steady-state and the dynamic analysis is achieved. In the dynamic analysis section, a new idea for integrating the GA with ANFIS to be applied on the control action procedure is presented.

In addition to, packages of Software for genetic algorithm and adaptive neuro-fuzzy system are developed. In other related work, GA only was used to enhance the system dynamic performance considering all working range of power system at a time that gave a difficulty and inability in some cases to reach the solution criteria. In this thesis, for every operating point GA is used to search for controllers’ parameters, parameters found at certain operating point are different from those found at others. ANFISs are required in this case to recognize the appropriate parameters for each operating point.

This work has been carried out under joint supervision between both of ZAGAZIG UNIVERSITY, EGYPT and AALTO UNIVERSITY, FINLAND. Professor Mahdi El-Arini participated from Zagazig University and Professor Matti Lehtonen participated from Aalto University. The author of this dissertation has had the main responsibility of all research work and publications.

Acknowledgements

First of all I would like to acknowledge my greats debt in this work to my Merciful GOD who supported me with patience and strength to complete this thesis.

Cordial thanks and deep gratitude are offered to Prof. Dr. Matti Lehtonen, Electrical Engineering Department, Power Systems group, AALTO UNIVERSITY, Finland and to Prof. Mahdi El-Arini, Electrical Power and Machines Department, Faculty of Engineering, ZAGAZIG UNIVERSITY, Egypt for valuable guidance and supervision.

The support is provided by the Egyptian Educational Missions, Zagazig University, and Aalto University are thankfully acknowledged.

Special thanks are also offered to staff members and instructors of the Electrical Engineering Department in Aalto University School of Electrical Engineering, and in Zagazig University, for great help, guidance and for exerted efforts to overcome the difficulties that arose during the work. In addition, special thanks for William Martin, from Aalto University for reviewing and double-checking of the language issues of the thesis.

In fact, I would like to dedicate this thesis to all of our professors and ask GOD to help me to express clearly the aim of this thesis.

At the last, but not least, my deepest thanks also go to my family: my mother, my father, my brother, my sister, my father-in-law and my wife brother and sisters. Finally, my (HANA) and beloved wife, for their patience and endless support.

ESPOO, Aalto,

Ahmed Mohamed Othman Abd El-Maksoud.

Contents

List of Abbreviations

ANFIS	Artificial Neuro-Fuzzy Interference System
ANN	Artificial Neural Network
AVR	Automatic Voltage Regulator
DNS	Demand Not Supplied
DVR	Dynamic Voltage Restorer
ENS	Energy Not Supplied
FACTS	Flexible AC Transmission System
FL	Fuzzy Logic
GA	Genetic Algorithm
GTO	Gate Turn-Off (Thyristor)
HVDC	High Voltage Direct Current
IGBT	Insulated Gate Bipolar Transistor
IGCT	Integrated Gate Commutated Thyristor
LPF	Low Pass Filter
LP	Low Pressure (turbine)
PSS	Power System Stabilizer
PWM	Pulse Width Modulation
PQ	Power Quality
SSR	Subsynchronous Resonance
SSSC	Static Synchronous Series Compensator
STATCOM	Static (Synchronous) Compensator
SVC	Static Var Compensator
TCBR	Thyristor Controlled Braking Resistor
TCR	Thyristor Controlled Reactor
TCSC	Thyristor Controlled Series Capacitor
UPFC	Unified Power Flow Controller
UPQC	Unified Power Quality Conditioner
VSC	Voltage Source Converter
VSI	Voltage Source Inverter

1 Introduction on Power Flow Control

1.1 Introduction

FACTS Technology is concerned with the management of active and reactive power to improve the performance of electrical networks. The concept of FACTS technology embraces a wide variety of tasks related to both networks and consumers problems, especially related to power quality issues, where a lot of power quality issues can be improved or enhanced with an adequate control of the power flow.

In general, the concept of power flow control is concerned with two jobs: load support and voltage compensation. Through the demand operation, the tasks are to raise the amount of the network power factor, to increase the true power from the source, to compensate voltage regulation and to decrease harmonic components resulted from large and fluctuating nonlinear loads especially in industry applications. Voltage Support is mainly important to decrease voltage changes at the terminals of a transmission path. Reactive power support in transmission networks also enhances the stability of the networks by maximizing the active power that can be transferred. It also assists to keep a substantially regulated voltage profile at all sections of power transfer, it enhances HVDC (High Voltage Direct Current) feature performance, raises transmission efficiency, sets steady-state bus normal voltage and over voltages, and can avoid serious blackouts.

Series and shunt VAR compensators are able to alter the performance characteristics of electrical networks. Series compensators change the parameters of the transmission grids or distribution levels, where shunt compensators modify the impedance at the connected terminals. In both of them, the reactive power through the system can significantly improve the performance of the power system.

Classically, rotating and fixed capacitors or which uses mechanical in switching or inductors are applied to VAR power compensators. Even in recent decades, static VAR compensators based on thyristor switched capacitors and thyristor controlled reactors to give or take the required reactive power are established. Additionally, the use of self-commutated PWM converters by an control action allows the achievement of static compensators for generating or consuming reactive components faster than the fundamental system period. Based on the reliable high-speed power electronics, efficient analytical boxes, intelligent control Flexible AC and microcomputer devices, Flexible AC Transmission Systems (FACTS), are presented as a recent idea for the operation of power networks.

Inside these concepts, static VAR compensation uses fast response times and plays an important role in improving the amount of total power transfer through a transmission line, near its thermal rate, without violation in its stability boundary. These techniques arise through the power of special static VAR compensators to adapt the related parameters that control the performance of transmission systems with the reactance, current, resistances, voltage, load angle and oscillations damping [1].

This thesis presents an overview of FACTS technologies, their operation concepts, also compensation procedure and performance are presented and analyzed. FACTS are

categorized according to the technology and implementation and the connection method in the power system, where they are shunted or seriesed.

Conventionally steady-state reactive compensators are not powerful in controlling the transmission power when the network is subjected to disturbances. For explanation, a fault into the transmission grid disrupts the equilibrium between the mechanical input power for the generating units and the electrical output power of the generating units that is directed by the faulted area [2].

Even with sufficient transient stability margin, the power system may not become stable if its steady state stability is insufficient; that is, if the power system has negative damping. It has been shown that both the transient and steady state stabilities of the power system can be improved if the reactive compensation of the transmission system is made rapidly variable.

However, the present conventional transmission means were not applied to deal with the stressed required criteria of an interconnected power system. The power flow in the single lines of the transmission grid is calculated by their impedance and it cannot be limited to the required power packages. Consequently, power flow circuits are affected and some transmission circuits get over-loaded due to changes and fluctuations in the voltage profiles and impairs system stability. Furthermore, while the power transmission requirements have been rapidly growing, the difficulties and escalating cost of right-of-ways have serious effect on the construction of new lines [3].

The general layout wants a review of the conventional power transmission principle and practice, and the creation of new technologies that give the complete benefits of current power generation and transmission facilities without effecting system availability and security. The Electric Power Research Institute (EPRI) has developed the Flexible AC Transmission Systems (FACTS) in which power flow is effectively controlled by various power electronic devices. The core of FACTS technology contains high power electronics, a variety of thyristor devices, micro-electronics, communications and advanced control actions [4].

By FACTS, operator governs the phase angle, the voltage profile at certain buses and line impedance. Power flow is controlled and it flows by the control actions using FACTS devices, which include

- Static VAR Compensators (SVC)
- Thyristor Controlled Series Capacitors (TCSC)
- Static Compensators (STATCOM)
- Static Series Synchronous Compensators (SSSC)
- Unified Power Flow Controllers (UPFC)

1.2 FACTS Concept

From the general point of view, the FACTS principle is mainly depend on the advanced technologies of power electronic techniques and algorithms into the power system, to make it electronically controllable.

Much of the research upon which FACTS rests evolved over a period of many years. Nevertheless, FACTS, an integrated technology, is a novel concept that was brought to fruition during the 1980s at the Electric Power Research Institute (EPRI) for applications of North American army objectives [5]. FACTS can capitalize on the many ideas taking place in the area of high-voltage and high-current power electronics, to improve the control of power flows in networks during both steady-state and transient conditions. The recent reality of making the power network electronically controllable has initiated a change in the way that power plant equipment is designed and built as well as the technology that goes into the planning and operation of transmission and distribution networks. These achievements may also enhance the method energy exchanges are done, as high-speed control of the path of the energy flow is now feasible. FACTS own a lot of promising benefits, technical and economical, which get the benefits of electrical equipment devices, operators, and research groups around the world [6]. FACTS controllers have been installed in various regions of the world. The well known types are: load tap-changers transformer, static VAR compensators, phase-angle regulators, thyristor-controlled series compensators, static compensators, inter-phase power controllers and unified power flow controllers.

This thesis covers in breadth and depth the modeling and simulation methods required for a thorough study of the steady-state and dynamic operation of electrical power systems with FACTS controllers. The characteristics of a given power system evolve with time, as load grows and generation is added. If the transmission grid capacity is not updated sufficiently the power network becomes vulnerable to steady state and transient stability problems, as stability margins will be narrower [7].

The powerful of the transmission grid to transmit power has constraint by one or more of the following steady-state and dynamic limitations: Angular stability, Voltage stability, Thermal limits, Transient stability, and Dynamic stability.

These limits affect the packages of the power to be transferred without blockout to transmission lines and electric apparatuses. Mainly restrictions on power exchange can be controlled by installing new transmission and generation circuits. Also, FACTS controllers can achieve the same tasks to be met with no huge changes to system layout. FACTS controllers save a lot of benefits such as reduction of operation and transmission investment cost, increased system security and system reliability, maximize power transfer capabilities, and an overall enhancement of the quality of the electric energy delivered to customers [8].

From the operational point of view, FACTS technology is concerned with the ability to control, in an adaptive trend, the directions of the power flows throughout the network, where before the advent of FACTS, high-speed control was very limited. The ability to control the line impedance and the buses voltage magnitudes and phase angles at both the sending and the receiving ends of transmission lines, with almost no delay, has significantly increased the transmission capabilities of the network while considerably enhancing the security of the system. In many practical situations, it is desirable to include

economical and operational considerations into the power flow formulation, so that optimal solutions, within constrained solution spaces, can be obtained.

The main objective of this thesis is concerned with enhancing the steady state and dynamic performance of the Flexible AC Transmission System (FACTS) using Computational Intelligence methods, like Genetic Algorithms (GA), Fuzzy Logic (FL), Neural Networks, (NN), and Adaptive Neuro-Fuzzy Inference Systems (ANFIS).

1.3 Literature Survey on FACTS

There is a vast amount of work reported in the literature in the area of Reactive Power Control and FACTS devices. The reactive Power control concepts and methods, as well as FACTS devices research at the initial stage, clarified of the principles of FACTS devices functions. Later, modeling, analysis and control were investigated, resulting in the recent application tests.

In [9], there is a presentation of Parallel Optimal Reactive Power Flow Based on Cooperative Co-Evolutionary Differential Evolution and Power System Decomposition. Differential evolution (DE) is an effective evolutionary technique for solving optimal reactive power flow problems, but it needs mainly a large population to prevent convergence in the suitable time. To recover this disadvantage, a new decomposition and coordination technique, which depends on the cooperative co-evolutionary architecture and the voltage-var sensitivity-based power system decomposition method is applied and united with DE. It is achieved with a three-level parallel computing topology on a PC-cluster. Based on the IEEE 118-bus system test case, the power of the applied method has been tested by comparison with the parallel basic DE, that not employing the decomposition and coordination technique. The limitation of that paper that the application of DE to large-scale systems was not investigated and recommended as a future area of research.

In [10], a hybrid genetic algorithm–interior point method for optimal reactive power flow is presented. By combining a genetic algorithm (GA) with a non-linear Interior Point Method (IPM), a new hybrid technique for the Optimal Reactive Power Flow (ORPF) application is presented in that research. The applied technique can be essentially divided into two sections. The first section is to solve the ORPF with the IPM by releasing the discrete variables. The second section is to divide the original ORPF into two sub-problems: continuous optimization and discrete optimization. The optimal solution can be achieved by solving separately the two sub-problems. A dynamic updating strategy is also presented to make the GA and the IPM complement each other and to improve the efficiency of the hybrid proposed method. The GA is applied to solve the discrete optimization with the continuous variables being fixed, whereas the IPM handles the continuous optimization with the discrete variables being constant.

In [11], a new optimal reactive power flow (ORPF) model in rectangular form is proposed. Where the load tap changing (LTC) transformer element is considered as an ideal transformer and the series impedance becomes a dummy point placed between them. The terminal voltages of the ideal transformer winding are then utilized to exchange the turn ratio of the LTC for making the ORPF model quadratic. The Hessian matrices in this model are constants and require being determined only once inside the optimal procedure, which reduces the required time for the calculation. The solution of the ORPF problem by the predictor corrector primal dual interior point method is presented in this research. Two separate modules for the new and the traditional methods are developed in MATLAB in

order to compare the performances. The limitation on this method that it takes in some cases the same identical iteration counts as the conventional method to reach the solution.

In [12], a presentation of an easy, rapid, and powerful method for calculating the maximum loading point (MLP) and the voltage stability security limit of electric power networks. The presented technique depends on nonlinear programming methods. The MLP is accurately achieved after some demand change steps. The computational procedure has two kinds of power changes. Primary, load increases towards to the MLP are applied for reducing an fitness function based on sensitivities. In case an overestimated load increase moves the system outside the stable feasible operating region, another very simple optimization-based process lead to minimize the power mismatches that to calculate the load adjustment curtailment to pull the system back onto the feasible area. Cases results for small scale to large realistic networks are indicated to validate the presented technique. The limitation is that the simulation results were for small IEEE test systems. A possible shortcoming of the proposed approach would have been the need of setting parameter *t*. However, all simulations that have been carried out showed that its setting is straightforward, since it lies within a narrow range for all systems.

In [13], the maximum loading margin (MLM) method is presented in determining generation directions to maximize the static voltage stability margin, where the MLM is calculated at different possible generation tends in the generation space. An easy and short formula indicating the link between the generation direction and the LM is applied to get the MLM point. The presented technique is tested on the modified IEEE 14-bus system and applied for the Thailand power network. LMs of the system with the generation steps are compared for different generator combinations by the presented technique.

In [14], the Tellegen's theorem and adjoint networks are applied to derive a novel, local voltage-stability index. The new technique makes it available to calculate the Thevenin's values in a various method than adaptive curve-fitting techniques, from two consecutive phasor measurements. The new index was verified on various test systems. The results were achieved on a static two-bus test system and on the dynamic Belgian–French 32-bus test system that contains complete dynamic models of all power-system components crucial to the voltage instability analysis. The simulations indicate the advantages of the presented index: it is simple, computationally very fast, and easy to implement in wide-area monitoring and control center or locally in a numerical relay.

In [15], there is a proposal for a recent optimal technique to minimize power loss and at the same moment to enhance the voltage stability in radial networks. The resultant characteristics of this research can be presented as follows.

• An powerful a voltage stability index (VSI) has been applied to determine the voltage stability that is more suitable for constant switching characteristics. As indicated in the results, the voltage stability for the radial networks can be ranked by the presented VSI. Furthermore, data of the buses through the critical transmission path (CTP) and the critical bus can be automatically evaluted through the BE method. So utility can use a predictive action profile in a current contingency or disturbance condition that may lead to the voltage sag in a regional distribution network.

• The method can use both dual and single optimization based on operational conditions priority, which may be ill conditions distribution network, utility can adapt the network configuration by the VSI only, or dual optimization for VSI and loss minimization. While in the well conditions system, it may be sufficient only to use the losses fitness function. Utility can setup ranked tables analyze the ill conditions of the system that could supply

them with operational data to enhance the voltage stability while servicing the loss minimization target.

• In addition to, the improved branch exchange (IBE) approach is presented to decrease the computational time. The IBE method depends on the losses determination index. The index is applied as an efficient judge to evaluate the change of power losses without trying the iterations for power studies while the BEs in a ring system. For determination of the new tie-branch load flow coming from power exchange during the BEs, the recently derived TBP balance is applied with significant accuracy.

• The optimal routing algorithm (ORA) also has applied the GA as a global search technique to search an initial radial system. As indicated in numerical results, this hybrid method is very powerful in large-scale systems.

In [16], a new criterion of voltage stability margin is proposed. Voltage instability is usually leading to participating in the disturbances progress of power networks. While raising of load admittance, bus voltage decreases to certain level, which the total power (V^2Y) does not go up. Therefore, voltage sags with the consequences coming from it. the load shedding is an important defenses for the stations that the stability margin start to be low, and has bad effects on the large-scale power system disturbance. For executing that, there is a plan to make automatic apparatuses, which generate local signals, determine the decreased margin, and initiate the load shedding. One of the operating requirements for theses devices is measuring the voltage level. The negative point of that approach is the dependency between the voltage profile and the stability limit that depends mainly on the power factor of the load. To handle this issue, this research proposes a criterion, which has solid dependence on the concept of voltage stability. It determines the derivative of VA power with respect to the admittance ($\Delta S/\Delta Y$). It can be rapidly accomplished, by both the power and the admittance are measured, and the changes in load are because switching on and off the impedances, and process of the transformer on tap-changer sources. The limitation of this method, however, is that it is not performed in a real power system, Also there is no comparison between this method and others.

In [17], a proposal of a novel method to determine the optimal SVC allocation to enhance the voltage stability of power systems is presented. By concerning the second-order term of the Taylor's series expansion, the nonlinear bus voltage participation factor is calculated in this research. It gets the nonlinear features of power systems into the process. When we make a comparison between those that are available and the traditional linear technique, some advantages are available when the proposed nonlinear method is used.

1) By use of the normal forms of the proposed method, more details about the nonlinearity of the power system can be considered. Therefore, it is more accurate to analyze the complex nonlinear characteristics of power systems.

2) For the power systems operating under the light loading condition, as the nonlinearity of the system is not very high, the results from both the nonlinear bus voltage PF and the linear bus voltage PF lead to well outputs. When the power networks are working under stressed conditions, the nonlinearity has an essential role in the power system response. In this condition, the nonlinearity of the system cannot be ignored. The nonlinear bus voltages PF will lead to results that are more accurate related to the steady-state voltage stability index.

In [18], the modeling of FACTS devices for power flow studies and the role of that modeling in the study of FACTS devices for power flow control are discussed. Three essential generic models of FACTS devices are presented and the combination of those devices into load flow analysis, studies relating to wheeling, and interchange power flow

control is explained. The determination of the voltage magnitude and phase angle of the FACTS bus is provided by solving two simultaneous nonlinear equations. These equations are solved with a separate Newton-Raphson approach within each iteration of the large load flow analysis. Therefore, another set of mismatch equations must be met for each iteration of the larger study. It is possible that this smaller Newton-Raphson study will not converge, particularly when voltage magnitudes are significantly less than rating. Therefore, the resultant solution may not converge due to divergence of the internal search. The disadvantage of those models is due to the firing angle corresponding to such a compensation level should be calculated by reordering to an iterative process, in addition to the load flow solution. Moreover, it is not possible to evaluate within the load flow solution whether or not the solution is occurring near of a resonant point of a TCSC. The only indication would be a divergent iterative process.

In [19], the issue of UPFC modeling within the context of optimal power flow solutions is addressed. The UPFC model has been presented to control active and reactive power flow at the buses of the sending or receiving end. The UPFC model suitable for optimal power flow solutions is presented for the first time in this study.

In [20], the main characteristics of controllable reactive series elements (CRSE), which sometimes called controllable series compensation (CSC) and a static synchronous series compensator (SSSC)) for power system analysis and control are shown. Modeling of CRSE, containing a simple representation of the transmission system, have been developed. According to theses concepts, the CRSE effect on a longitudinal transmission system was analyzed. The theory of physics and the basic difference shown by a CSC and an SSSC related load flow control are explained. Due to conceptual principles, by the of ability of load flow control, SSSC is considered as more promising than CSC at low power angles. Therefore, SSSC is more suitable in cases where power flow requires to be controlled in short lines or under light-load conditions. The disadvantage of this paper is that the difference between an SSSC and a CSC has been studied on the basis of a static model.

In [21], a nouvel method to incorporate the power flow control needs of FACTS in analyzing the optimal active power flow problem is indicated. The linearized (DC) system model is applied. Three essential kinds of FACTS devices, namely TCSC, TCPS, and the UPFC, are concerned. The proposed method decomposes the solution of such modified optimum power flow (OPF) problem into the iteration of two problems. The first problem is a load flow control sub-problem and the second one is a normal OPF analysis. Further research work is needed for other OPF algorithms with an AC network model.

In [22, 23], a new and comprehensive load flow model for the TCSC and the UPFC is presented. For the TCSC, the state variable is the TCSC's firing angle, which is linked with the nodal voltage magnitudes and angles of the grid in a single format for a combined iterative process through a Newton-Raphson method. Under different operation of the TCSC models, this model develops account of the loop current that exists in the TCSC under both partial and full conduction operating modes. Also, the model provides proper care of the resonant points characterized by the TCSC fundamental frequency impedance. A group of analytical equations has been derived to make good UPFC initial conditions. Suitable guidelines are proposed for an efficient control coordination of two or more UPFCs operating in series or parallel arrangements.

In [24], using the FACTS devices steady sate models, the control ranges and controllability of the power flow on the transmission line occupied by single FACTS device are studied. That paper mainly concerns with the commitment of several FACTS

devices. To handle this issue, a new method based on genetic algorithm (GA) has been presented. With this presented technique, we analyze the number of FACTS to maximum range of the power flow control. It is found that the controllability of the power flow is based on the number of FACTS devices in the system and power flow control range with multiple FACTS devices is larger than that with only one such device. Therefore, the commitment of control performances of various devices is a very essential issue for future power system planning and operation.

A linear optimal controller is proposed [25] to enhance the system dynamics and to coordinate three SVCs depending on two control levels, the local control to insure optimum Performance at the local level and the global control to make the coordination by decoupling the state equation for each area. Also a state observer is suggested to obtain the unmeasured states. PSCAD/MTDC is used to simulate the system. The problem of coordination is also handled in [26], a coordinated controller is designed according to the linear quadratic problem; the gain matrix is modified to allow the controller to depend on output feedback. In addition, the system states are reduced since the controller is concerned with the range of frequencies of the inter-area modes.

A methodology to obtain the robust locations and feedback signals of FACTS controllers is proposed in [27]. The criteria proposed insure good performance for the controller not only at the designed operating condition but also at the different operating conditions of the power system. An eigen-free index is introduced to evaluate the performance of the controller.

In [28], it proposed the application of a Takagi-Sugeno (TS) fuzzy controller to provide regulation of a series and a shunt voltage source inverter of UPFC to damp the inter-area and local modes in a multi-machine power system. The UPFC injection model, which consists of two controllable loads, was used and the dynamics of the DC voltage was expressed by a differential equation. The reactive and active power deviations, which were feedback signals to the active and reactive components of the series voltage source respectively, were fuzzefied using two fuzzy sets, positive and negative. By applying Zadeh's rules for AND operation and the general defuzzifier, the output of the controller was obtained. In [29], it proposed a conventional lead-lag controller for UPFC to improve the oscillation damping of a single-machine infinite bus system. The generator speed deviation is the controller input signal. Based on the linearized model, the damping function of the UPFC is investigated.

A robust fixed-structured power system damping controllers using genetic algorithm is indicated in [30]. The designed controllers have a classical structure structuring from a gain, a washout stage and two lead-lag stages. The GA searches for an optimum solution over the controller's parameter space. The approach is applied to design SVC and TCSC damping controllers to improve the damping of the inter-area modes. Local voltage and current measurements are used to synthesis remote feedback signals.

In [31], various control methods for damping undesirable inter-area oscillations by PSSs, SVCs and STATCOMs are discussed. The oscillation problem is studied from Hopf bifurcations perspective. It is observed that the damping introduced by the SVC and STATCOM controllers with only voltage control was lower than that provided by the PSSs and the STATCOM provides better damping than the SVC as this controller is able to transiently exchange active power with the system.

A supplementary damping controller for a UPFC had been proposed in [32]. The gains of the UPFC supplementary damping controller are adjusted in real time, based on online measured real and reactive power flows in transmission lines. To decrease the time

required for the online gain adaptation process, an artificial neural network is designed. Power flows over the transmission line are used as inputs to the adaptive controller. The proposed damping compensator has effectively damped the electromechanical mode with an oscillation frequency of around 0.78 Hz.

In [32], it concerns with minimizing the active losses in the power systems using installation of UPFC in the network. The applications of UPFC in that paper are as series element to work as a series compensator and/or to work as a phase shifter; Genetic Algorithm (GA) is used to find the optimal values of the phase angles for the phase shifters and the optimal values of series reactance for the series compensators to achieve the required criteria. The simulations are applied on IEEE 30-bys system.

In [33], it focuses on optimal power flow with presence of UPFC in the system. And then it apples Genetic Algorithm (GA) to find the optimal dispatch of the generation powers of the generating units in the network to achieve the minimum total cost ($/hr). The model, which is used in modeling, is the injected model of FACTS device. The simulations are applied on IEEE 14-bys system. The results show that FACTS device doesn't lead to a significant reduction in the cost of the generating power. It can be used in controlling and increase the feasibility of the power network.

In [34], a design of fuzzy damping controller of UPFC through genetic algorithm is presented. It applies a fuzzy controller as external controller provides supplementary damping signal to UPFC. The design includes the shape and the number of membership functions for the input and the output variables. The genetic algorithm is applied to optimize the scaling factors, which are used in the scaling portion of the fuzzy controller. The simulations are applied on four machines interconnected power system, which used as a test system. A comparison between the fuzzy controller and the conventional controller and also without presence of controller is performed.

In [35], it studies the optimal location of FACTS devices, in general way. It compares between the simulated annealing method, Tabu search method, and genetic algorithm method; to find the optimal location for some FACTS devices like TCSC, TCVR, TCPST, SVS and UPFC. The study is performed on the steady-state models, and the simulations are occurred on IEEE 118-bus system. The problem is that, this paper represents UPFC as two separated devices, without modeling the UPFC itself as stand-alone device. It presents a limitation of the number of FACTS devices. It states that GA is better in the simulations.

In [36], it studies the application of harmony search algorithm and genetic algorithm in optimal installation of FACTS devices related to voltage stability and losses issues. It concerns with determining the optimal location of FACTS devices. The applied devices, which are used in that paper, are TCPAR, UPFC, and SVC. The concerning criteria are the loss and the voltage stability. The used mathematical model of FACTS devices is the power-injected model. The simulations are applied on IEEE 30-bys system.

In [37], it presents a control method on UPFC based on genetic algorithm, but applied on a single-machine infinite-bus system. The aim of UPFC installation on that system is to damp the system oscillations. The UPFC voltage sources are converted into three power injections at the receiving and sending buses. The applied controller is an external genetic algorithm PI controller trying to return the response deviation to zero. The fitness function is termed on the real and imaginary parts of the dominant eigenvalues.

In [38], it proposes a micro genetic algorithm based fuzzy logic controller to coordinate between TCSC and UPFC in the system. The micro genetic controller is designed to operate to reach the optimal criteria as fast as possible without enhancing the performance. The micro genetic algorithm is applied when it available to use small size and value of

population not more than 10. These characteristics direct the simulations to be executed on three-machine power system. The genetic algorithm search for the optimal membership functions. In [39], it studies the same application, in addition to use parallel micro genetic algorithms to speed up the initialization process covering the search-space, also it uses neuro-fuzzy technique to escape from dropping in the local minimum.

In [40], it concerns with enhancement of voltage stability and reduction in investment cost by installing multi-type FACTS devices using genetic algorithm. The fitness functions is termed by the FACTS devices cost functions and the system losses. Three different FACTS devices are used: TCSC, SVC, and UPFC. The paper uses the decoupled model for UPFC, which it less complex but it lacks to the modifications in Jacobian matrix. Multi.-type FACTS devices can achieve the required criteria but the economic aspects must be considered.

In [41], it studies the congestion management in deregulated power system; and how to utilize the FACTS devices in that application. It uses the static modeling of TCSC and the static modeling of UPFC, specially for UPFC modeling, it uses the injection model of UPFC. The fitness function is termed by the loading of the transmission lines in exponential mathematical formula. According to the proposed fitness function, to reduce more significantly the loading of the lines, we want to install more than FACTS devices, which may give reflection for the cost of the power in the system. The simulations are applied on IEEE 30-bys system.

In [42, 43], they present a method for optimal location of UPFC in power systems to increase the loadability using genetic algorithm. The model for UPFC, which is used in the papers, is the injection model of UPFC. The analysis studies the comparison of installing one, two or three UPFC in the system. The objective function concerns with maximizing the loadability of the transmission lines, and that is the only technical benefit is taken into consideration. The objective function is termed by exponential mathematical formula to describe the required criteria. The process depends on increase the number of UPFC installed in the system. The simulations are occurred on high loading operating conditions for the transmission lines. The simulations are applied on IEEE 14-bus system. Specially [43], it takes the same area and analysis with some more case studies for increasing the active power and the reactive power.

In [44], it concerns with a hybrid genetic algorithm for determining UPFC optimal control setting. The injected-power model is the static modeling of UPFC, which is the used in the simulations. The objective function is related to optimal power flow to minimize the operating cost especially for the power of the generating units. The optimization process searches the control setting of UPFC to minimize the cost of the operation. The results is achieved by first finding the optimal setting of UPFC using genetic algorithm, then simulate the system and UPFC with that setting to get the objective. The simulations are applied on IEEE 14-bus system.

Also, in [45], it discusses the same concept for a hybrid genetic algorithm for optimal power flow included FACTS devices. The static models of FACTS devices, which are used, are for TCSC and UPFC. The objective is to minimize the overall cost. The simulations are applied on IEEE 14-bus system with different loading conditions by increasing loading value at certain one bus.

In [46], it proposes ANFIS system to find the optimal setting UPFC during the static operation of the system. The objective is described in the difference of the desired parameter and the actual one. The analysis concerns with the normal increase in the loading conditions. The method is simulated in many small networks configurations. The approach

needs a continusly update in the patterns. The UPFC is installed in the system to control the power flow in certain transmission line.

In [47], it presents an external ANFIS controller on UPFC to enhance the stability of the system. The objective is mainly described to maximize the energy function of UPFC. The method is applied for a single-machine infinite-machine bus system. The generating units in the simulations are represented in classical model. The energy function is termed by the total reactive power injected into the network by the UPFC, that energy functions is used as the core of the neuro-fuzzy system; and is applied to generate the input/output patterns of the method.

1.4 Contribution of the Thesis

The contributions of the thesis start with formatting, deriving, coding and programming the network equations required to link UPFC steady-state and dynamic models to the power systems. One of the other contributions of the thesis is deriving GA applications on UPFC to achieve real criteria on a real world sub-transmission network.

An enhanced GA technique is proposed by enhancing and updating the working phases of the GA including the objective function formulation and computing the fitness using the diversity in the population and selection probability. The simulations and results show the advantages of using the proposed technique. Integrating the results by linking the case studies of the steady-state and the dynamic analysis is achieved. In the dynamic analysis section, a new idea for integrating the GA with ANFIS to be applied on the control action procedure is presented.

In addition to, packages of Software for genetic algorithm and adaptive neuro-fuzzy system are developed. In other related work, GA only was used to enhance the system dynamic performance considering all working range of power system at a time that gave a difficulty and inability in some cases to reach the solution criteria. In this thesis, for every operating point GA is used to search for controllers' parameters, parameters found at certain operating point are different from those found at others. ANFISs are required in this case to recognize the appropriate parameters for each operating point.

2 FACTS Devices Modeling

2.1 Introduction

This chapter presents an overview of the most prominent characteristics of the power electronic equipment currently used in the electricity supply industry for the purpose of voltage regulation, active and reactive power flow control, and power quality enhancement.

A study of the models and procedures with which to assess the steady-state operation of electrical power systems at the fundamental frequency is made.

The modeling of FACTS controllers in both the phase domain and the sequence domain is addressed in this chapter. All models are developed from the first principles, with strong reference to the physical structure of the equipment.

The focus is on steady-state operation and a distinction has been made between power electronic devices, which uses conventional power semiconductor equipments (i.e. thyristors) and the new generation of power system controllers, which use complete controllable semiconductor devices such as GTOs thyristors and IGBTs. Also the latter devices work well with fast switching control techniques, such as the sinusoidal PWM control scheme, and, from the power system perspective, operate like voltage sources, having an almost delay-free response. Devices based on thyristors have a slower response, more than one cycle of the fundamental frequency, and use phase control as opposed to PWM control. From the power system point of view, thyristor-based controllers behave like controllable reactances as opposed to voltage sources.

This chapter presents the structure, operation and the steady state characteristics of FACTS devices that depend in its operation on the Thyristor Controlled Reactor (TCR) or the Synchronous Voltage Source (SVS).

2.2 The Thyristor Controlled Reactor (TCR)

The main components of the basic TCR are shown in Figure 2.1. The controllable element is the antiparallel thyristor pair, Th1 and Th2, which conducts on alternate half cycles of the supply frequency. The other key component is the linear (air-core) reactor of inductance L. In a practical valve, many thyristors (typically 10 to 40) are in series connection to handle the desired blocking voltage levels [48, 49]. A gate pulse is activated to all thyristors of a thyristor valve brings the valve into conduction. The valve will automatically block approximately at the zero crossing of the AC current, in the absence of the firing signal. Thus, the controlling element is the thyristor valve. The TCR current is essentially reactive, lagging the voltage by nearly 90^o. The active component of the current is very small and the losses of the device are of the order of 0.5 – 2 % of the reactive power. Therefore, one of the modeling assumptions is that the resistance of the inductor may be neglected [50].

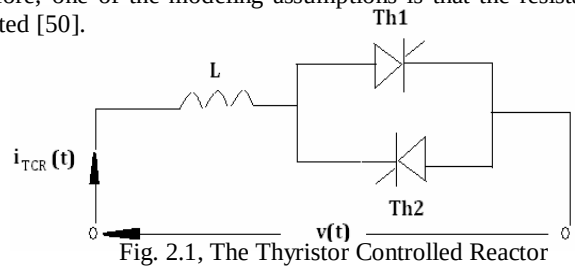

Fig. 2.1, The Thyristor Controlled Reactor

The firing angle α is defined as the angle in electrical degrees between the positive going zero-crossing of the voltage across the inductor and the positive going zero-crossing of the current through it. The thyristors are fired symmetrically; therefore, the maximum possible firing angle is 180^o. Complete conduction is achieved with a angle of gate of 90^o. Partial conduction is achieved with angles of gates between 90^o and 180^o with zero current at 180^o. Firing angles less than 90^o are not allowed, as they generate unsymmetrical currents with a high DC component [51]. The fundamental component of the reactor current is decreased as the firing angle increases. That means an increase in the reactor inductance, reducing both of its reactive power and its current.

In Figure 2.2a, the voltage across the TCR inductor and the current through it are shown at full conduction. The equivalent reactance of the TCR is equal to the inductor reactance. In Figure 2.2b, the current waveform is shown for a firing angle of 100^o. Only part of the sinusoidal voltage is applied to the inductor, the current and the voltage are not sinusoidal anymore. The fundamental component of the current is less than that the current at a 90^o firing angle, resulting in an equivalent reactance of the TCR higher than the inductor reactance. Figure 2.2c and 2.2d show the TCR current waveform for a firing angle of 130^o and 150^o. The fundamental component of the current through the inductor is very small, the equivalent reactance of the TCR is very high, and at 180^o it becomes practically infinite.

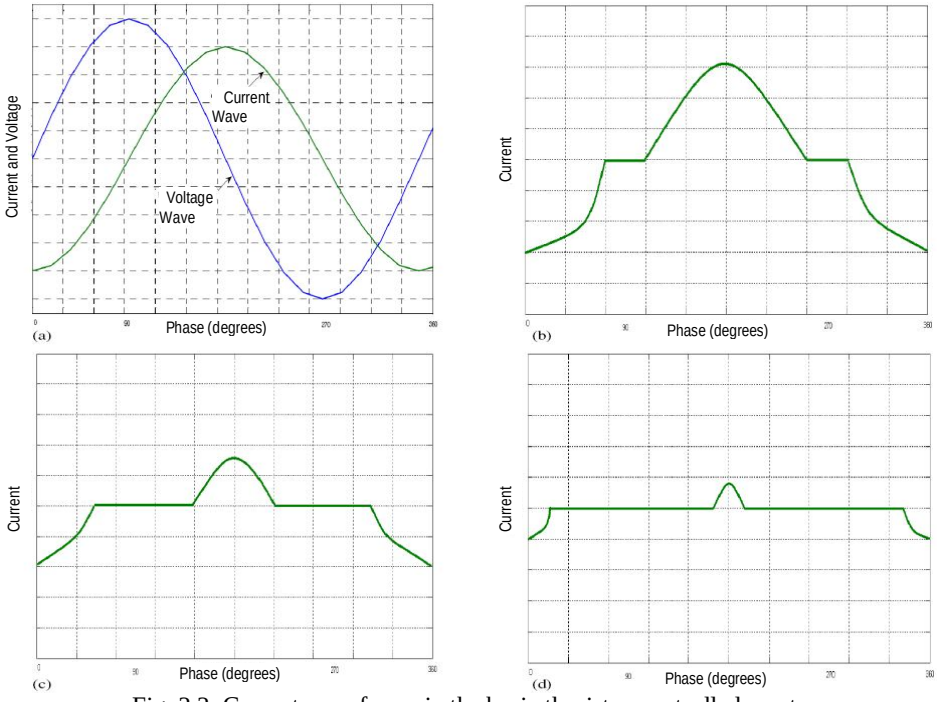

Fig. 2.2, Current waveforms in the basic thyristor-controlled reactor.

Using the Fourier series, the fundamental component of the controllable reactance of the TCR (X_v) is

$$x_v = x_l \frac{\pi}{2(\pi - \alpha) + \sin(2\alpha)} \qquad (2.1a)$$

Inside a 3-Φ network, three 1-Φ thyristor controlled reactors are utilized in delta connection. Subjecting to balanced conditions, the odd-order harmonic currents in zero sequence harmonic components flow in the delta linked TCRs and not flow to the power system. For the TCRs arranged in delta, the maximum total harmonic distortion coefficient is less than 10 % [2]. For being used with shunt devices, a step-down transformer is requested in high-vothage applications as the TCR voltages has a constraint for technical and economic reasons to values starting from 50 kV or below.

2.3 TCR Based FACTS Devices

Among the devices that depend on the TCR are Static Var Compensators (SVC), Thyristor Controlled Series Capacitor (TCSC).

2.3.1 Static Var Compensators (SVCs)

The construction of the SVC consists of a TCR in parallel with a capacitors bank. From a technical perspective, the SVC operates as a shunt-connected variable reactance that can produces or draws reactive power to regulate the voltage level at the location of the connection to the system. It is used efficiently to supply fast reactive power and voltage regulation support. The firing angle control of the thyristor provides the SVC with an instantaneous speed of response [5].

A graphical illustration of the SVC is shown in Figure 2.3, where a three-phase, three winding transformer is utilized to connect the SVC to the system. The transformer has two identical secondary windings: the first is for the delta connection, six-pulse TCR and the second for the star connection, is a three-phase bank of capacitors, with its star point floating. The three transformer windings are also taken to be star-connected, with their star points floating.

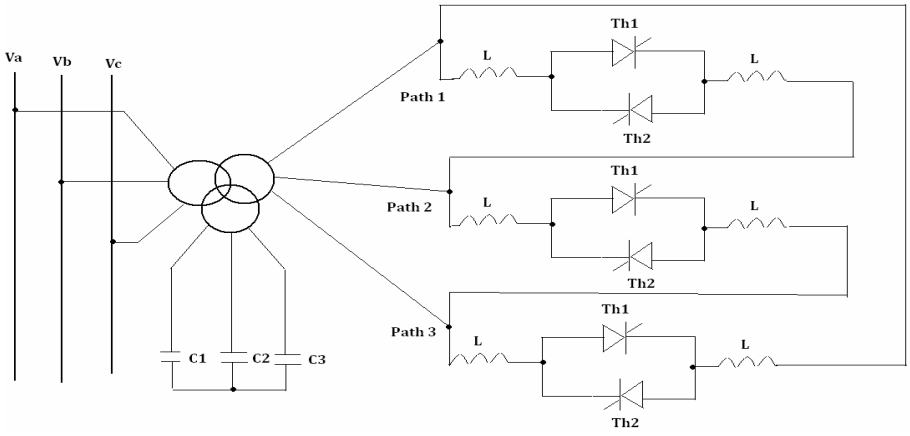

Fig. 2.3, three-phase static VAR compensator (SVC).

To regulate the transmission network voltage at a certain terminal is the main task of the compensator. Figure 2.4 clarifies the SVC V-I characteristic, indicating that regulation by a certain region near the nominal voltage can be done in the normal running range based on the maximum capacitive and inductive currents of the SVC. While the maximum capacitive current reduces linearly and the produced reactive power in quadrature with the voltage of the system, where the SVC does as a fixed capacitor at the maximum capacitive

output is presented. So the voltage support ability of the traditional thyristor-controlled static Var compensator speedily impairs with reducing system voltage [51].

Moreover, to voltage support, SVCs are applied for transient first swing and steady state stability damping improvements. SVC behaves like an ideal mid-point compensator until the maximum capacitive admittance BC_{max} is reached. From this point on, the power transmission curve becomes identical to that obtained with a fixed, mid-point shunt capacitor whose admittance is BC_{max}.

The steady state stability enhancement of power oscillation damping can be achieved by changing the result of the SVC from required capacitive and inductive levels to reverse the angular acceleration and deceleration of the machines presented. The issue is to increase the transferred electrical power by raising the transmission line voltage, through capacitive amount, when the units accelerate and to reduce it by reducing the voltage, through inductive amount, when the units decelerate. The powerful of the SVC in power oscillation damping is a function of the allowed voltage variation.

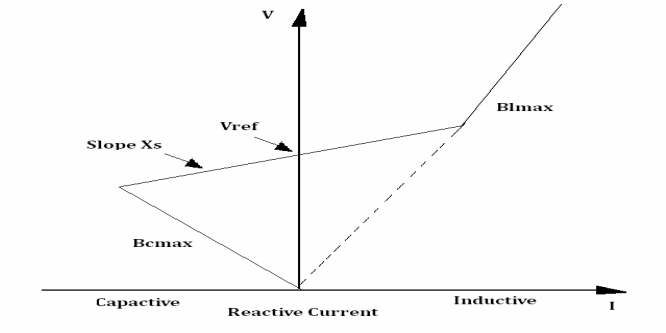

Fig. 2.4, Current V-I characteristics of a SVC.

2.3.2 Thyristor Controlled Series Capacitor (TCSC)

A basic TCSC module consists of a TCR in parallel with a capacitor. An actual TCSC comprises one or more modules. Figure 2.5 shows the layout of one phase of the TCSC installed in the Slatt substation on USA. The TCSC basically comprises a capacitor bank inserted in series with the transmission line, a parallel metal oxide varistor (MOV) to protect the capacitor against over-voltage and a TCR branch, with a thyristor valve in series with a reactor, in parallel with the capacitor. Mechanically bypass breakers are provided in parallel with the capacitor bank and in parallel with the thyristor valve. During normal operation, the bypass switch is open, the bank disconnect switches (1 and 2) are closed and the circuit breaker is open. When it is required to disconnect the TCSC, the bypass circuit breaker is switched on first, and then the bypass switch is switched on. The damping circuit is used to limit the current when the capacitor is switched on or when the by pass circuit breaker is switched on.

In the fixed-capacitor thyristor-controlled reactor scheme, the series compensation level in the capacitive operating area and the TCR admittance are saved under that of the parallel connection capacitor is changed with the change in the thyristor conduction angle and also with TCR current. Minimum series compensation is achieved when the TCR is off. The TCR can be selected to achieve the ability to restrict the voltage at the capacitor at faults and other system contingencies of similar effect.

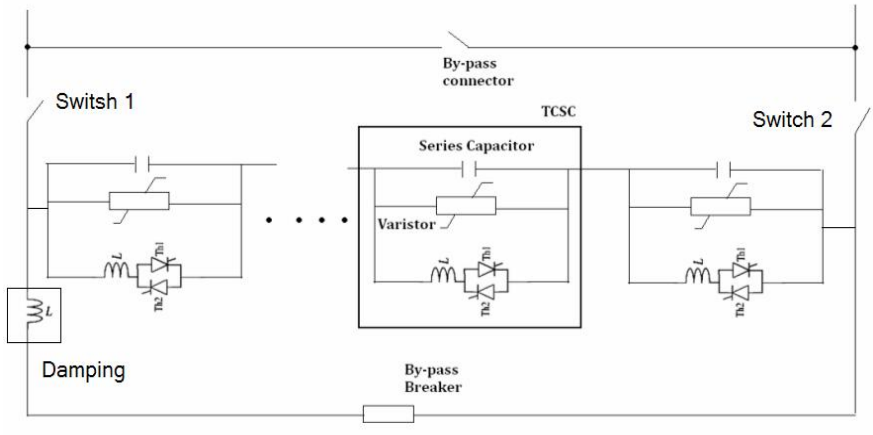

Fig. 2.5, Thyristor controlled series capacitor (TCSC).

The operating range curve of TCSC impedance against the line current is shown in Figure 2.6 [52]. The different operating limits of the TCSC can be explained as follows:

For low line current, the TCSC can provide maximum capacitive and inductive compensation according to the resonant firing angle. In the capacitive region, the minimum firing angle allowed is above the resonant firing angle (limit A). On the other hand, in the inductive region, the maximum firing angle allowed is lower than the resonant firing angle (limit E). In the capacitive region, as the line current increases, the voltage drop across the TCSC increases too. To prevent over-voltage across the TCSC during normal operation, the firing angle increases towards 180 to reduce the equivalent capacitive reactance of the TCSC, hence the voltage drop across it (limit c). In the inductive region, as the magnitude of the line current increases, the harmonic heating limit of the thyristor valves is reached. The firing angle should be reduced to reduce the equivalent inductive reactance of the TCSC so as not to exceed this limit (limit F). Limit G presents the thyristors current limits.

Figure 2.7 shows the block diagram for the TCSC operation under current control mode. The line current is measured and the magnitude of it is compared with the desired value of the line current, the error signal is passed to the TCSC controller to obtain the appropriate firing angle, which can be measured from the zero crossing of the line current. The model for balanced, fundamental frequency operation is shown in Figure 2.8 [53].

2.3.2.1 Equivalent impedance of the TCSC

Previously, attempts have been made to obtain the TCSC equivalent impedance. The overall impedance of the TCSC is given as:

$$X_{TCSC} = \frac{\pi X_C X_L}{X_C[2(\pi - \alpha) + \sin 2\alpha] - \pi X_L} \qquad (2.1b)$$

The problem of the last equation is that the harmonic analysis has only been conducted for the TCR while the analysis of the capacitor charging has been neglected. The total impedance has been obtained by paralleling the TCR equivalent impedance at the fundamental frequency and the fixed capacitor. This makes (2.1) only valid for the first cycle of the current. The reason is that after the first cycle has elapsed, the capacitor stores charge, leading to higher steady state voltages compared to cases when the capacitor charging effect is neglected.

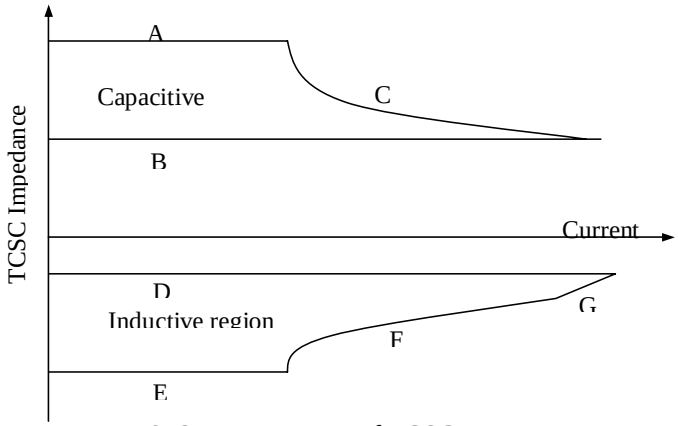

Fig. 2.6, Operating range of TCSC.

A: Firing angle limit - B: Thyristor blocked
C: Maximum voltage limit - D: Full thyristor conduction
E: Firing angle limit - F: Harmonic heating limit
G: Thyristor current limit

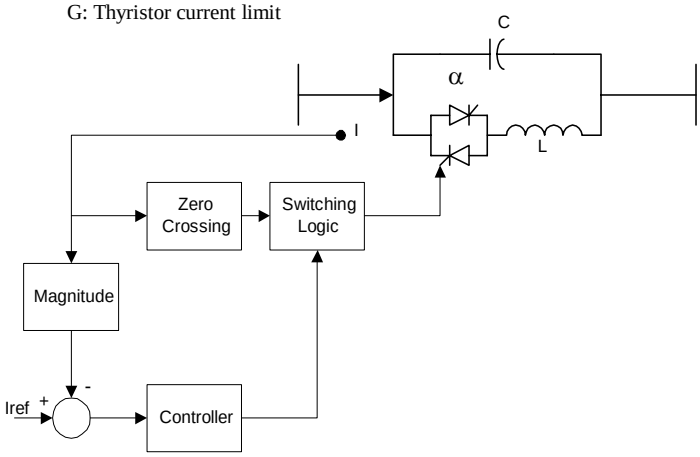

Fig. 2.7, Block diagram of a TCSC operating in current control.

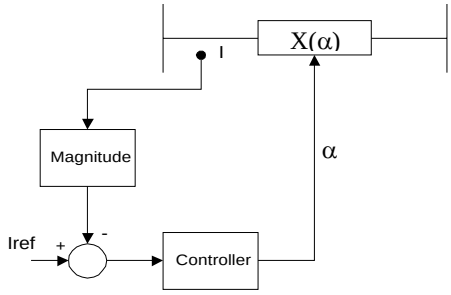

Fig. 2.8, Dynamic model of a TCSC.

The derivation of the TCSC impedance is started by examining the voltages and currents in the TCSC under the full range of operating conditions. The basic equation is:

$$Z_{TCSC(1)} = \frac{V_{TCSC(1)}}{I_{line}} \tag{2.2}$$

$V_{TCSC(1)}$ is the fundamental frequency voltage across the TCSC model, I_{line} is the fundamental frequency line current. The voltage $V_{TCSC(1)}$ is equal to the voltage across the TCSC capacitor and (2.2) can be written as:

$$Z_{TCSC(1)} = \frac{-jX_C I_{cap(1)}}{I_{line}} \tag{2.3}$$

If the external power network is represented by an idealized current source, as seen from the TCSC terminals, this current source is equal to the sum of the currents following through the TCSC capacitor and inductor. The TCSC can then be expressed as:

$$Z_{TCSC(1)} = \frac{-jX_C (I_{line} - I_{TCR(1)})}{I_{line}} \tag{2.4}$$

$I_{TCR(1)}$: The fundamental component of the TCR current, can be found by the following:

The line current is, $i_{line} = \cos(\omega t - \sigma) = \cos\omega t \cos\sigma + \sin\omega t \sin\sigma$ (2.5)

The voltage across the TCSC , $L\frac{di_{TCR}}{d} = \frac{1}{C}\int i_{cap} dt + V_C^o$ (2.6)

where V^o_C is the voltage across the capacitor when the thyristor turns on. In Laplace form equation (2.5) and (2.6) are

$$I_{line} = \cos\sigma \frac{s}{s^2 + \omega^2} + \sin\sigma \frac{\omega}{s^2 + \omega^2} \tag{2.7}$$

$$I_{cap} = s^2 LCI_{TCR} - CV_C^o \tag{2.8}$$

Applying Kirchhoff current low, $I_{TCR} = I_{line} - I_{cap}$ (2.9)

Substituting (2.7) and (2.8) into (2.9), and solving for I_{TCR},

$$I_{TCR} = \omega_o^2 \cos\sigma \frac{s}{(s^2 + \omega^2)(s^2 + \omega_o^2)} + \omega_o^2 \omega \sin\sigma \frac{1}{(s^2 + \omega^2)(s^2 + \omega_o^2)} + \frac{\omega_o^2 CV_C^o}{s^2 + \omega_o^2} \tag{2.10}$$

where $$\omega_o^2 = \frac{1}{LC} \tag{2.11}$$

Substituting the expression for $I_{TCR(1)}$ (The fundamental component of the TCR current) into (2.4) and assuming $I_{line} = I_m \cos\omega t$, leads to the fundamental frequency TCSC equivalent reactance, as a function of the TCSC firing angle α as:

$$X_{TCSC} = -X_C + C_1(2(\pi - \alpha) + \sin(2(\pi - \alpha))) - C_2 \cos^2(\pi - \alpha)(\overline{\omega}\tan(\overline{\omega}(\pi - \alpha)) - \tan(\pi - \alpha)) \tag{2.12}$$

Where

$$\overline{\omega} = \frac{\omega_0}{\omega} \quad , \quad \omega_o^2 = \frac{1}{LC} \quad , C_1 = \frac{X_C + X_{LC}}{\pi} \quad , \quad C_2 = \frac{4X^2{}_{LC}}{X_L \pi} \quad , X_{LC} = \frac{X_C X_L}{X_C - X_L}$$

Comparing Equations 2.1 and 2.12, the resonant firing angle in the two equations are not the same. Depending on the ratio between X_C and X_L, there could be more than one resonant angle for the TCSC expressed by Equation 2.5.

Figure 2.9 shows the TCSC equivalent reactances as a function of the firing angle. The TCSC capacitive and inductive reactance values should be chosen carefully in order to ensure that just one resonant point is present in the range of Π/2 to Π.

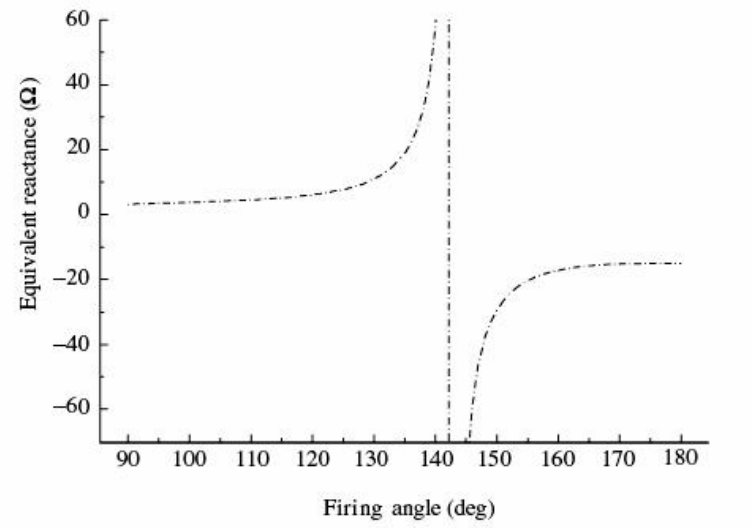

Fig. 2.9, Thyristor-controlled series capacitor (TCSC) fundamental frequency impedance [53].

2.3.2.2 Resonance firing angle:

Examining (2.5), the firing angle that cause resonance is obtained when

$$\cos(\pi - \alpha_{res}) \cos(\overline{\omega}(\pi - \alpha_{res})) = 0 \qquad (2.13)$$

$$\text{So} \quad \alpha_{res} = \pi - \frac{(n+1)\pi}{2} \sqrt{\frac{X_L}{X_C}} \qquad \textit{where } n = 0, 2, 4, ... \qquad (2.14)$$

Although of the effective enhancement on transmittable power, high levels of series compensation are not typically used. The feasible upper boundary to the limit of series compensation is about 70 % [53], as more steady state compensation may produce uncontrollable variations in the power for low alteration in terminal voltages or angles, and large transient currents and voltages during disturbances at series resonance conditions.

2.4 Synchronous Voltage Source (SVS)

Controllable solid-state synchronous voltage sources are employed for compensating the dynamic and controlling real-time the power flow in transmission systems. This method, when compared to conventional compensation approaches employing thyristor-switched capacitors and thyristor-controlled reactors, saves vastly premium performance characteristics and regular applicability for transmission voltage, reactance, and angle ability. It also gives the powerful tool to direct exchange active power with the AC grid, in addition to the independently controllable reactive power compensation, thereby giving a powerful new option for the counteraction of dynamic disturbances.

A functional model of the solid-state synchronous voltage source is shown in Figure 2.10. Reference signals Q_{ref} and P_{ref} define the output voltage amplitude with its phase angle of the generated voltage and also the reactive and real power flow between the solid-mention voltage source and the grid. If the goal of dynamic true power flow is not achieved, $P_{ref} = 0$, the SVS gets a self-sufficient reactive power source as an ideal synchronous condenser, and the external energy storage device can be disposed of.

Various switching power converters can implement the solid-state synchronous voltage source, although of the switching converter mentioned as the voltage-sourced inverter. This particular DC to AC switching power converter, which is based on gate turn-off (GTO) thyristors [54] in appropriate multi-pulse circuit configurations, is presently applied in the most practical for high power utility applications. The functional and operating characteristics of this type of inverter, which saves the basic functional building block for the comprehensive compensation and power flow control approach, are explained below.

An elementary, six-pulse, voltage-sourced inverter is shown in Figure 2.11. It consists of six self-commutated semiconductor (GTO) switches, each of which is shunted by a reverse-parallel connected diode. It should be noted that in a high power inverter, each solid-state switch consists of a number of series-connected GTO thyristor/diode pairs. With a DC voltage source (which may be a charged capacitor), the inverter can produce a balanced set of three quasi-square voltage wave-forms of a given frequency, as illustrated in Figure 2.12, by connecting the DC source sequentially to the three output terminals via the appropriate inverter switches.

There is exchange between the reactive power of the inverter and the AC system, which can be controlled by varying the magnitude of the produced three-phase output voltage. When the amplitude of the output voltage is raised over the system voltage, then the current flows via the reactance from the inverter to the AC system and the inverter produces capacitive power for the AC grid. If the output voltage amplitude is decreased under that of the AC grid, then the reactive current flows from the AC system to the inverter and the inverter draws inductive power. When the output voltage is balanced with the AC grid voltage, the reactive power flow becomes zero.

In the same way, the real power transfer between the SVS and the AC grid may be controlled by shifter of the phase voltage of the inverter related to the AC system voltage. That is, the inverter from its DC energy storage provides real power to the AC network if the voltage of the inverter is leading the corresponding AC network voltage. This is because this phase advancement results in a real component of current through the tie reactance that is in anti-phase with the AC network voltage. By the same way, the inverter draws real power from the AC grid for DC energy storage, when the voltage of the inverter is lagging the AC network voltage. The real component of current flowing trough the tie reactor is now in-phase with the AC system voltage.

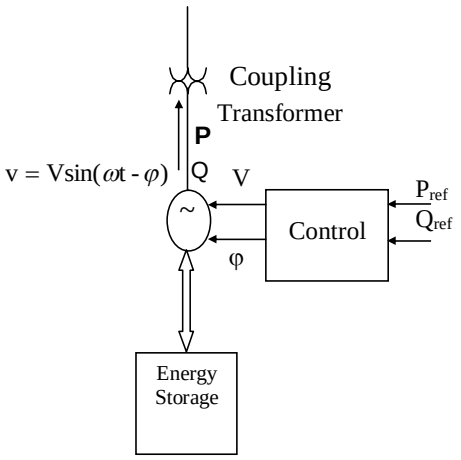

Fig. 2.10, generalized synchronous voltage source.

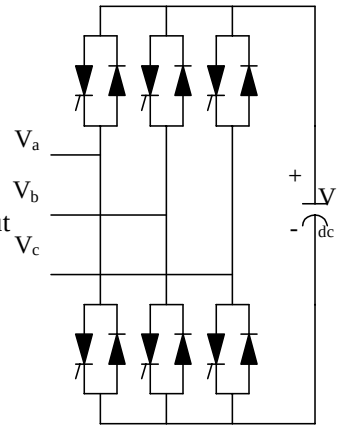

Fig. 2.11, Basic six-pulse voltage source.

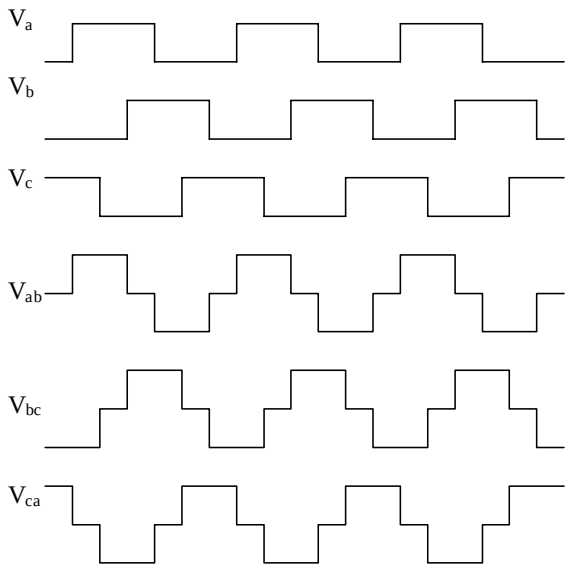

Fig. 2.12, Six pulse inverter output voltage waveforms.

The mechanism by which the inverter internally generates reactive power can be explained simply by considering the relationship between the output and input powers of the inverter. The base of the explanation depends on the physical rule that the process of energy transfer through the inverter, consisting of nothing but arrays of solid-state switches, is absolutely direct. Thus, it is clear that the resultant power at the AC output ports are always equal to the net resultant power at the DC input terminals when neglecting the losses.

Assume that the inverter is operated to supply only reactive output power. In this case, the active input power provided by the DC source has to be zero. Furthermore, where reactive power, at frequency equals zero, by basics will be zero, the DC source generates no input power and therefore it clearly has no part in the supplying of the reactive output power. In another meaning, the inverter connects internally the three output terminals, like a method, which the reactive currents may move easily between them. Concerning this with the terminals of the network, it could be seen that the inverter produces an exchanged circulating power among the phases [54].

Although reactive power is inherently produced by the action of the solid-state switches, it is still essential to have a relatively small DC capacitor connected across the input terminals of the inverter.

The importance for the DC capacitor is primarily requested to satisfy the above-stipulated the balance input power and output power. The waveform of the inverter output voltage is not a pure sine wave. It is a staircase approximation of a sine wave. However, the multi-pulse inverter absorbs a smooth, almost sinusoidal current from the network through the tie reactance. As a result, the resultant three-phase instantaneous apparent power (VA) at the output terminals of the inverter slightly fluctuates. Thus, for not violating the balance between of the real input power and output power, the inverter must draw a ripple current from the DC capacitor that keeps a regulated terminal voltage at the input.

The existence of ripple part of input current is mainly due to the ripple components of the output voltage, which depend on the used technique in the output waveform fabrication. In a high power inverter, using a sufficiently high pulse number, the output voltage distortion and, thereby, capacitor ripple current can be mainly decreased to any desired degree.

Thus, a perfect inverter would produce sinusoidal output voltage and draw pure DC input current without harmonics. To achieve purely reactive output, the input current of the perfect inverter is zero. Because of system unbalance and other unbalances like economic considerations, those ideal conditions are not practical, but approximated satisfactorily by inverters of sufficiently high pulse numbers (24 or higher).

2.5 SVS Based FACTS Device

Among the SVS based Facts devises are the STATCOM, the SSSC and the UPFC.

2.5.1 Static Compensator (STATCOM)

The STATCOM consists of one VSC and its associated shunt-connected transformer. It is the static form of the rotating synchronous condenser but it supplies or draws reactive power with a fast rate because there is no moving parts inside it. In principle, it performs the same voltage regulation function as the SVC but in a more robust manner because, unlike the SVC, its operation is not impaired by the presence of low voltages. A schematic representation of the STATCOM and the equivalent circuit are indicated in Figure 2.13.

If the energy storage is of suitable rating, the SVS can exchange both active and reactive power with the network. The active and reactive power, supplied or drawn by the SVS, can be controlled independently of each other, and any combination of active power, generated or absorbed, with active power, generated or absorbed, is possible. The active power that the SVS exchanges at its network terminals with the grid must, of course, be supplied to, or absorbed from, its DC terminals by the energy storage unit. In other way, the reactive power flow is internally developed by the SVS, without the DC energy storage device playing any significant part in it.

The bi-directional real power exchange capability of the SVS, that is, the ability to absorb energy from the AC system and deliver it to the DC energy storage device (large storage capacitor, battery, superconducting magnet) and to reverse this process and deliver power for the AC system from the energy storage device, makes complete, temporary system support possible. Specifically, this capability may be used to improve system efficiency and prevent power outages. In addition, in combination with fast reactive power control, dynamic active power exchange is considered as an extremely powerful method for transient and dynamic stability enhancement.

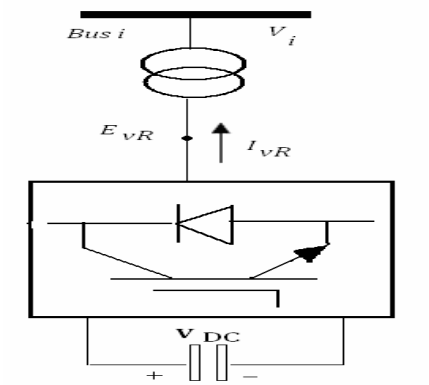

Fig. 2.13 Static compensator (STATCOM) system voltage source converter (VSC) connected to the AC network via a shunt-connected transformer.

When the SVS is applied in strict way for reactive shunt compensation, as a conventional static Var compensator, the DC energy storage device can be replaced by a relatively small DC capacitor, as shown in Figure 2.13. In this case, the steady-state power flow between the SVS and the AC grid become only in reactive form.

When the SVS is applied for reactive power supplying, the inverter itself can maintain the capacitor charged to the desired voltage level. This is achieved by making lagging in the output voltages of the inverter and the system voltages by a little angle. In this way, the inverter draws a small amount of active power from the grid to rebalance the inner losses and save the voltage of the capacitor at the required level. The same control procedure can be applied to raise or reduce the capacitor voltage, and then the inverter voltage magnitude, for achieving the control of the reactive power generation or absorption. The DC capacitor also owns a task of establishing a balance between the input energy and output energy at the dynamic changes of the Var output.

The STATCOM V-I characteristic is indicated in Figure 2.14 [55]. As can be seen, the STATCOM can act as both capacitive and inductive compensators and it is able to control its output current independently over the maximum range of the capacitive or inductive of the network voltage. That is, the STATCOM can produce complete capacitive output current at any grid voltage level. On the other side, the SVC can supply only output current with reducing system voltage as calculated by its maximum equivalent capacitive admittance. So the STATCOM is superior to the SVC in applying voltage support.

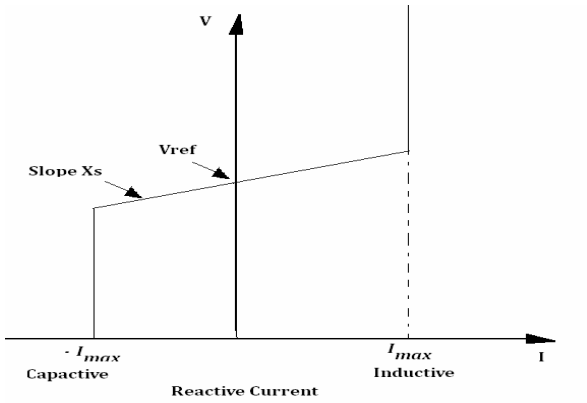

Fig. 2.14 V-I characteristic of a STATCOM.

2.5.2 Static Series Synchronous Compensator (SSSC)

The Static Synchronous Series Compensator (SSSC) is a series connection FACTS controller dependent on VSC and can be considered as an advanced kind of controlled series compensation, just as a STATCOM is an advanced SVC.

A SSSC own several merits over a TCSC such as (a) elimination of bulky passive components (capacitors and reactors), (b) improved technical characteristics (c) symmetric capability in both inductive and capacitive operating modes (d) the connection availability of an energy source on the DC port to exchange active power with the AC grid.

A solid-state synchronous voltage source, consisting of a multi-pulse, voltage-sourced inverter and a DC capacitor, is shown in series with the transmission line in Figure 2.15.

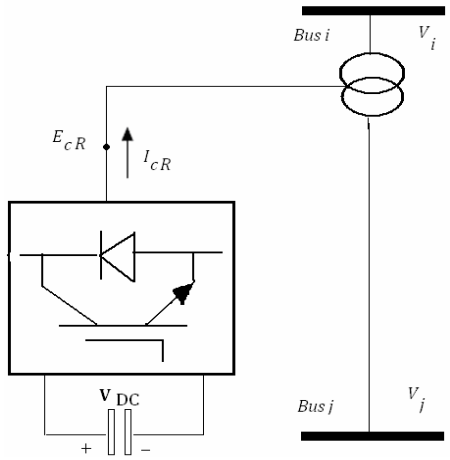

Fig. 2.15, Schematic diagram for the SSSC.

In general, the active and reactive power exchange is controlled by the phase displacement of the injected voltage related to the current. For example, when the injected voltage is in phase with the line current, then only active power is exchanged, and if it is in quadrature with the line current then only reactive power is exchanged

The series-connected synchronous voltage source is an extremely powerful tool for power flow control and, it is able to control both the transmission line impedance and angle. Its capability to exchange active power with the grid makes it very effective in enhancing dynamic stability by means of alternately inserting a virtual positive and negative damping resistance in series with the line by the disturbed generators angular deceleration and acceleration.

The idea of the solid-state synchronous voltage source for compensation of series reactive depends on the rule that the characteristic of the impedance with the frequency of the practically employed series capacitor, which is different than the filter techniques, has no role in achieving the required line compensation. The goal of the series capacitor is summarized to generate a suitable voltage at the fundamental AC network frequency in series with the line to eliminate the voltage drop produced via the inductive impedance of the line by the fundamental part of the line current. So that the resulting total voltage drop of the compensated line becomes electrically equivalent to that of a shorter line. Therefore, if an AC voltage supply with fundamental frequency, which has a quadrature lagging following to the line current and the magnitude depends on the line current is flowed in series with the line. A series compensation is equal to the one developed by a series capacitor during the fundamental frequency is supplied.

The voltage source can be described in mathematical form as follows:

$$V_n = -jkXI$$

Vn is the compensating value of the injected voltage, *I* is the phasor of the line current, *X* is the impedance of the series reactive line, and *k* is the series compensation degree. For conventional series compensation, *k* is defined as X_C /*X*, where X_C is the impedance of the series capacitor.

For regular capacitive compensation, the output voltage must lag the line current by 90 degrees, in order to directly oppose the inductive voltage drop of the line impedance. However, the output voltage of the inverter will be opposed by a proper control method to direct it to be leading the line current with 90 degrees. Then, the inserted voltage is in phase with the voltage developed by the inductive reactance of line. Therefore, the series compensation owns the equivalent effect as if the reactive impedance of the was raised. This capability can be invested to increase the effectiveness of power oscillation damping and, with sufficient inverter rating; it can be used for fault current limitation.

Series compensation by a synchronous voltage source that can be limited to the fundamental frequency is worthy to that provided with series capacitive compensation in that it cannot produce undesired electrical resonances with the transmission grid, and for this reason, it cannot cause sub-synchronous resonance. However, by appropriate control it can damp sub-synchronous oscillations, which may happen because of present series capacitive compensations by inserting non-fundamental voltage components with proper magnitudes, phase angles and frequencies, in addition to the fundamental component, in series with the line [55].

Due to the stipulated 90-degree phase relationship between the inverter output voltage and the line current, this, via the series insertion transformer, flows through the inverter as the load current, the inverter in the solid-state voltage source theoretically exchanges only reactive power with the AC system. As explained previously, the inverter can internally generate all the reactive power exchanged and thus can be operated from a relatively small DC storage capacitor charged to an appropriate voltage. In practice, however, the semiconductor switches of the inverter are not loss-less, and so the energy saved in the DC capacitor would be balanced through the inverter internal losses. Those losses will be provided by the AC system itself by acting the voltage of the inverter lags the current by less than 90 degrees. The typical deviation from 90 degrees is a fraction of a degree. In this way, the inverter draws a small value of active power from the AC network to balance the internal losses and save the DC capacitor voltage at the required level. That control procedure can also be applied to raise or reduce the DC capacitor voltage by making the inverter voltage lag the line current by an angle smaller or greater than 90 degrees. Thereby, control the magnitude of the AC output voltage of the inverter and the degree of series compensation.

2.5.3 Unified Power Flow Controller (UPFC)

The UPFC may be considered to be constructed of two VSCs sharing a common capacitor on their DC side and a unified control system. A simplified schematic representation of the UPFC is given in Figure 2.16.

The UPFC gives simultaneous control of real and reactive power flow and voltage amplitude at the UPFC terminals. Additionally, the controller may be adjusted to govern one or more of these criteria in any combination or to control none of them. This technique permits with the combined application of controlling the phase angle with controlled series reactive compensations and voltage regulation, but also the real-time change from one mode of compensation into another one to handle the actual system contingencies more effectively. For instance, series reactive compensation may be altered by phase-angle control or vice versa. This can become essentially important at relatively big numbers of FACTS devices will be applied in interconnected power grids, and compatibility and coordination control can own to be save in the face of devices failures and system changes.

The technique would also give significant flexible operation by the inner adaptability to power network expansions and changes no real hardware alterations.

The implementation problem of the unrestricted series compensation is simply that of supplying or absorbing the real power that it exchanges with the AC system at its AC terminals, to or from the DC input sides of the inverter applied in the solid-state synchronous voltage source. The implementation in the proposed configuration called unified power flow controller (UPFC) [55] employs two voltage source inverters applied with a common DC connected capacitor; it is shown schematically in Figure 2.16. That arrangement is practically an achievement of an AC to DC power converter with independently controllable input and output parameters.

Inverter 2 in the arrangement shown is used to generate voltage $V_B(t) = V_B \sin(\omega t - \delta_B)$ at the fundamental frequency with variable amplitude ($0 \leq V_B \leq V_{Bmax}$) and phase angle ($0 \leq \delta_B \leq 2\pi$), which is added to the AC system terminal voltage by the series connected coupling (or insertion) transformer. With these stipulations, the inverter terminal voltage injected in series way with the line will be applied for direct voltage control, series compensation, and phase-shift.

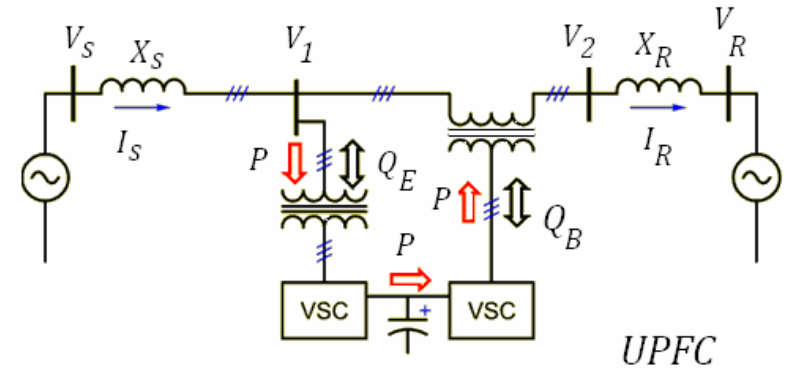

Fig. 2.16, Schematic diagram for the UPFC.

The inverter output voltage inserted in series with the line is considered mainly as an AC voltage source. The current flowing through the injected voltage source is the transmission line current; it depends on the transferred electric power and the transmission line impedance. The total of the maximum injected voltage defines the VA rating of the injected voltage source for Inverter 2 and the maximum line current during the power flow control is still developed.

This total VA consists of two components: the first is the maximum active power, which is calculated by the maximum line current, and the maximum injected voltage component that is in phase with this current. The second is the maximum reactive power, which is calculated by the maximum line current and the maximum injected voltage component that is in quadrature with this current.

As explained before, the voltage-sourced inverter applied in the technique can internally supply or draw, at grid side, the amount of reactive power required by the voltage/impedance/phase-angle control applied, and only the active power amount has to be generated at its DC input terminal.

Inverter 1 (shunt connection with the power network via a coupling transformer) provides primarily the active power required to Inverter 2 via the common DC link port

from the AC power grid. Since Inverter 1 can also supply or draw reactive power at its AC terminal, independently of the active power it transfers to (or from) the DC terminal, it follows that, with proper controls, it can also achieve the task of an independent static capacitor developing compensation for reactive power at the transmission line. So executing a regulation of indirect voltage where the input port of the unified power flow controller is achieved.

It is clear at the outset that Inverter 1 could be cancelled if a proper DC energy storage device was linked to Inverter 2, and the phase-shifting function of the unified power flow controller was applied only to deal with transient disturbances. That is, Inverter 2 would normally provide series reactive compensation and absorb real power at some pre-determined rate to keep the energy storage device charged. During the system disturbances, the UPFC would be controlled to provide phase angle control and/or direct active power to stabilize the network. With this arrangement, the UPFC would become a generalized solid-state series compensator discussed in the previous section.

The inherent control of the solid-state power flow controller is built so as to receive certain reference signals, in an order of designed criteria, for the required reactive shunt compensation, series compensation, transmission angle, and output voltage. These reference signals are used in closed control-loops to force the inverters to produce the AC voltages at the input (shunt-connected) terminals and output (series-connected) terminals of the power flow controller, and thereby establish the transmission parameters desired (Q_{Ref} , V_{Ref}, P_{Ref}, and φ_{Ref} at the output). The control also maintains the necessary DC link voltage and ensures smooth real power transfer between the two inverters.

It is evident that if the unified power flow controller is operated only with the phase angle reference input, it automatically acts as a perfect phase-shifter. It internally supplies the reactive power involved in the phase-shifting process and negotiates the necessary real power from the AC system. Since the active power component is generally smaller than the total VA demand resulting from phase-shifting, the rating of Inverter 1 would be normally less than that of Inverter 2, unless the “surplus” rating of Inverter 1 is, again, intentionally utilized for controllable reactive shunt compensation.

3 Artificial Intelligence Concept (AI)

3.1 Introduction

Soft computing (SC) is a promising new trend to build computationally intelligence systems. It is now recognized that complex real-world problems want intelligent systems that combine knowledge, techniques and methodologies from various sources. These intelligent systems are proposed to possess humanlike expertise within a specific domain, adjust themselves and learn to do better in changing environments, and explain how they make decisions or take actions. It is extremely beneficial to use several cooperatively computing techniques, resulting in the implementation of complementary hybrid intelligent systems.

This chapter introduces the concept of Artificial Intelligence especially the Genetic Algorithm (GA) and Adaptive Neuro-Fuzzy Inference System (ANFIS). Genetic algorithm is applied to the optimization process for optimal locations and optimal setting for FACTS Devices and also ANFIS to be applied in tuning the dynamics response.

3.2 AI Techniques Scope

During 1936, the concept of intelligence for devices is presented, Alan Turing explained the universal mathematics concept for machines, a basic theory in the computational mathematics. Turing and Emil Post indicated that finding the decidable mathematical formulas are equal to determine an abstract machine contains a package of guidelines could recognize the rank of sequences of a definite value of symbols. That procedure is related to the machine intelligence concept, assessing the arguments against the possibility of creating an intelligent computing machine and determining solutions to those disputations; in 1950, it is suggested the Turing test as an experiential measure of intelligence.

The Turing test judges the performance of a machine against that of a human being. Turing disputes that machines may be considered to be intelligent. In the 1960s, however, computers could not pass the Turing test due to the low processing speed of computers in those days.

The last few years had a novel concept of artificial intelligence (AI) concerning the principles, theoretical issues, and design methodology of algorithms simulated from the natural systems. Artificial neural networks based on neural systems, evolutionary computation based on biological natural selection, simulated annealing based on thermodynamics rules, and swarm intelligence based on the collective behavior of insects or microorganisms, and so on, interacting locally with their environment, has resulted in the emergence of coherent functional global patterns. These techniques have found their way into handling real-world problems in science, economics, technology and also to a great extent in measuring systems.

The new trend is to combine various algorithms to have advantage of integrated features and to produce a hybrid algorithm. Hybrid systems such as neuro-fuzzy systems, evolutionary-fuzzy systems, evolutionary-neural networks, evolutionary-neuro-fuzzy systems, are effectively used for handling real-world problems [56]. In the following sections, the main functional components of computational intelligence are introduced along with their key advantages and application domains.

3.2.1 Artificial Neural Networks

Artificial neural networks (ANN) have been appeared as general mathematical modules simulating biological nervous systems.

In the simple mathematical form of the neuron, the influence of the synapses are included by connection weights that regulate the influence of the corresponding input signals, and the non-linear behavior produced by neurons is presented by an activation function, which is usually the sigmoid, Gaussian-shaped, triangle-metric function, and others.

The neuron output is overall calculated by the weighting of inputs sum signals, being processed by the activation function.

The learning ability of an intelligent neuron is done by adapting the weights in accordance to the selected learning method. Most applications of neural networks fall into the following categories:

- **Prediction:** to predict the output variables using input values
- **Classification:** to process the classification stage using input values
- **Data Association:** it is as classification, plus recognizing data that has errors
- **Data conceptualization:** process the inputs to group relationships can be figured out

A typical multilayered neural network and an artificial neuron are illustrated in Figure 3.1. Each neuron is distinguished by an activity level; presenting the polarization status of a neuron; an output value; presenting the firing rate of the neuron; a set of input connections; presenting synapses on the neuron and its dendrite. In addition, bias value; presenting an inherent serene level of the neuron; and finally a set of output connections; presenting a neuron's axonal terms. Those components of the unit are described mathematically by real values. Thus, each connection owns a synaptic weight, strength, that defines the effect of the incoming input on the unit activation limit. The negative and positive weights can be used. Referring to Figure 3.1, the signal flow from inputs $x_1,\ldots\ldots,x_n$ is considered to be unidirectional, shown via arrows, like is a output neuron's signal flow (O). The signal of the neuron output O is determined by the following expression:

$$O = f(net) = f(\sum_{j=1}^{n} w_j x_j) \tag{3.1}$$

where w_j is the weight vector and the function $f(net)$ is pointed to an activation transfer function.

The variable *net* is defined as a sum product of the weight with input vectors

$$net = w^T x = w_1 x_1 + \ldots\ldots\ldots + w_n x_n \tag{3.2}$$

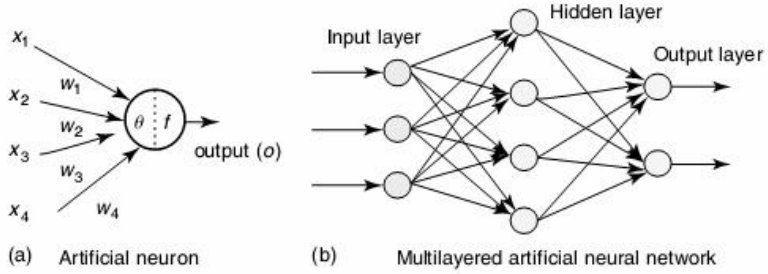

Fig. 3.1 An artificial neuron architecture and a multi layer neural network.

T is transpose of a matrix and in simple form the output O is computed as

$$O = f(net) = \begin{cases} 1 & if w^T x \geq \theta \\ 0 & otherwise \end{cases} \tag{3.3}$$

where θ is called the threshold level, and that node kind is named a linear threshold unit.

The feature of the neural network is significantly a function of the interaction between the different neurons. The main architecture contains three neuron layers types:

1. Input
2. Hidden
3. Output

In feed-forward networks, the signal flow is directed from the input to output layers, by constraint of the feed-forward direction. The data processing can be distribute over the multiple layers, but no feedback connections, that is, connections extending from the units outputs to units inputs in the identical or former layers.

Recurrent networks have feedback connections. Conflicting with feed-forward networks, the dynamical characteristics of the network are essential. In some states, the units' activation values subject to a relaxation action such that the system will extract a stable state that these activations are constant evermore. In some uses, the activation levels changes of the output neurons are essential, such that the dynamical behavior defines the network output [64].

There are many other neural network architectures such as Elman network, adaptive resonance theory maps, competitive networks, and others, depending on the characteristics and field of the application.

A neural network should be structured for that the use of input set develops the required set of outputs. There are many methods to adapt the strengths of the connections. The first technique is to adapt the weights in an explicit way based on a priori knowledge. Another technique is to learn the neural network through supplying it teacher patterns and adapting it to modify the weights based on some learning rules. The learning process of neural networks can be classified into three distinct sorts of learning:

1. Supervised
2. Unsupervised
3. Reinforcement

In supervised learning, an input vector is represented at the inputs nodes with a set of required performance; each node has one, at the output layer. A forward path is activated and the errors or discrepancies, between the desired and real response for each node in the output layer, are determined.

These values are then used to calculate weight changes in the network according to the governing learning rule.

The original of supervised learning is due to that the required signals on individual output neurons are available by an external teacher. The famous shapes of this technique are the back propagation training, the delta rule, and perceptron rule. In unsupervised learning or self-organization, an output unit has a training to respond to clustered pattern with the input. In that paradigm, the system is assumed to detect statistically clear characteristics for the input population. While in the supervised learning paradigm, there is not any priori categories set that the patterns are classified; rather, the system must produce its own organized self-map.

Reinforcement learning depends on learning the actions that should be done and the way to do the actions, by maximizing a well signal. The learner does not define the actions, as in most versions of training, but instead must detect the actions undergoing the most reward by activating them. In the most motivating and challenging situations, orders can affect not only the direct reward but also the next step and, through that, the subsequent rewards. Those two attribute trial and error option and shifted reward, are the most significant characteristics of reinforcement learning [57]-[60].

3.2.2 Fuzzy Logic Algorithm

In 1965, Zadeh presented the theory of fuzzy logic to present obscurity in linguistics and for more implementing and expressing human inference knowledge and ability in a natural way. Fuzzy logic begins by the theory of a fuzzy set. A fuzzy set is considered as a set has no a crisp defined boundary or limit. It can contain elements with a membership with partial degree.

A Membership Function (MF) is a plot that maps each input point in the space to a membership degree value, which is between 0, 1. Input space is usually named as the universe of discourse.

Let X be the universe of discourse and x be an inclusive part of X. A classical set A is considered as a group of elements $x \in X$, such that x may belong to or not belong to the set A.

By describing a characteristic membership function on each element x in X, a classical set A can be defined by a ordered pairs set $(x, 0)$ or $(x, 1)$, where 1 indicates membership and 0, non membership.

The fuzzy set is different from the normal set in expressing the degree that an element becomes in a set. Hence, the feature of a fuzzy set membership is permit to own a value between 0 and 1, referring to the membership degree for an element in a certain set. If X is a group of elements pointed to by x, then if a fuzzy set A in X is related to ordered pairs set:

$A = \{(x, \mu_A(x)) | x \in X\}$ (3.4)

$\mu_A(x)$ is the membership function of the linguistic variable x in A that moves X in the membership space M, for values between 0, 1. A is crisp and μ_A is coherent to the activation function in a crisp set.

Triangulated-shape and trapezoidal-shape membership functions are the most simple membership functions based on straight lines. Some of the other shapes are Gaussian, generalized bell, sigmoidal, and polynomial-based curves. Figure 3.2 illustrates the shapes of two commonly used MFs. The most significant issue to know about fuzzy logical reasoning is to understand of standard Boolean logic.

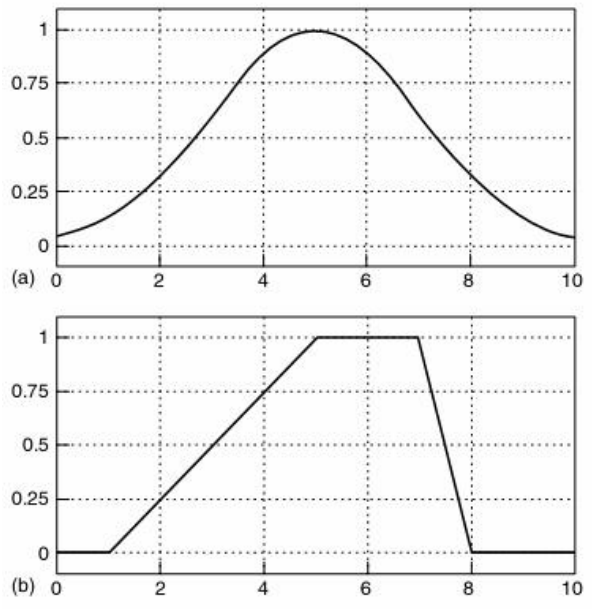

Fig. 3.2. Membership functions; (a) Gaussian and (b) trapezoidal.

3.2.2.1 Fuzzy Logic Operators

There is some coincidence between two-valued and multi-valued logic operations for the AND, OR, and NOT logical operators.

We can explain the expression *A* AND *B*, that *A* and *B* are between the range (0, 1) by using the operator minimum (*A*, *B*). By the way, we can alter the OR operator with the maximum operator, so that *A* OR *B* be equal to a maximum (*A*, *B*). Finally, the operation NOT *A* be equal to the operation *1–A*.

There are some terms related to fuzzy logic operators such as fuzzy intersection or con-junction for AND operation, fuzzy union or dis-junction for OR operation, and fuzzy complement for NOT operation. The intersection between two fuzzy sets *A* and *B* is generally described by a binary mapping *T* that merges two membership functions as follows:

$$\mu_{A \cap B}(x) = T(\mu_A(x), \mu_B(x)) \quad (3.5)$$

The fuzzy intersection operator is usually pointed to T-norm (Triangular norm) operator. The fuzzy union operator is generally addressed by a binary mapping *S*.

$$\mu_{A \cup B}(x) = S(\mu_A(x), \mu_B(x)) \tag{3.6}$$

This class of fuzzy union operators is often referred to as T-conorm (S-norm) operators.

3.3.2.2 If-Then Rules and Fuzzy Inference Systems

The fuzzy rule base is featured in the formula of if-then rules in which antecedent and conclusion having linguistic variables. The fuzzy rules format the rule bases for the fuzzy logic system. Fuzzy if-then rules are often applied to achieve the imprecise states of reasoning that have an important part in the human capability to take decisions in an condition of imprecision and uncertainty. A single fuzzy if-then rule supposes the form

If *x* is *A* then *y* is *B*

A and *B*: linguistic values are known by fuzzy sets in the ranges of universes of discourse, *X* and *Y*, respectively.

The "if" part of the rule '*x* is *A*' is called the antecedent or precondition, while the "then" part of the rule '*y* is *B*' is called the consequent or conclusion. Explaining an if-then rule has estimating the antecedent fuzzification of the input and activating any necessary fuzzy operators and then applying that result to the consequent known as implication. For rules with multiple antecedents, the terms of the antecedent are calculated simultaneously and merged to a single value by the logical operators. Similarly, all the consequents rules with multiple consequents are based equally on the antecedent result. The consequent defines a fuzzy set be addressed to the output.

Then Implication function upgrades the fuzzy set to the designed degree by the antecedent. For multiple rules, each rule output is a fuzzy set. The fuzzy outputs, defined for each rule, are then merged into a single output fuzzy set. Then, the resulted set is defuzzified to a single term.

The defuzzification interface is a map for a space of fuzzy processes known with an output universe of discourse to a space of non-fuzzy processes, due to the output from the inference engine is often a fuzzy set, but in most real problems, crisp numbers are the desired. The most famous defuzzification methods are maximum criterion, center of gravity, and the mean of maximum. The maximum criterion is the simplest one to apply. It develops the state for the possible distribution for achieving a maximum value [65] – [71].

It is basically benefit if the fuzzy rule base is adjustable to a certain application. The fuzzy rule base is often installed in manual or automatic way by some learning methods using evolutionary algorithms and/or neural network learning techniques.

3.2.3 Evolutionary Algorithms

Evolutionary Algorithm (EA) is an adaptive technique, which may provide solution search and optimization problems, related to the genetic processes and biological natural. According to the natural selection principles and the Charles Darwin rule of 'survival of the fittest', and by imitating this procedure, evolutionary algorithms are able to get solutions to real-world problems, provided they have been suitably encoded.

The genetic algorithms (GAs); evolution and evolutionary programming; and learning classifier systems are collections which belong to evolutionary algorithms or evolutionary

computation. They have the similar theoretical concept of emulating the evolution of individual structures by actions of selection, mutation, and reproduction. The processes depend on the realized characteristics of the individual construction as defined by the environment problem.

GA process parameters with finite length, which are programmed using a finite alphabet, not to manipulate the parameters in a direct way. This makes the search to be unrestricted by continuous function with investigation or by the existence of a derivative function.

Figure 3.3 depicts the functional block diagram of a genetic algorithm. It is supposed that an effective issue to a problem can be represented as a parameters set. Those parameters called genes are linked together to construct a string called a chromosome. A gene, also referred to as a feature, character, or detector, explains specific option that is coded inside the chromosome.

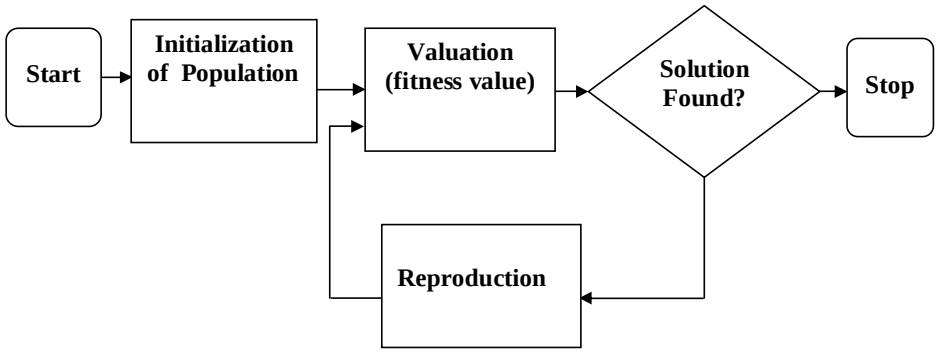

Fig. 3.3. Flowchart of genetic algorithm iteration.

The encoding process presents a solution in a chromosome and, there is no unique method solves the problems. A fitness function should be designed for the problem that required to be solved. For a certain single chromosome, the fitness function gives a single numerical fitness, which will determine and define the capability of the individual that the chromosome represents in the optimization process.

Reproduction is the second stage of GAs, which two individuals are chosen from the population are permitted to mate to develop an offspring, which will comprehend the next generation. Having selected the parents, the offsprings are generated, mainly by the procedure of crossover and mutation.

Selection is based on the survival of the fittest inside GAs. It explains the individuals that survive in the next generation. The selection phase contains 3 sections.

The first section determines the individual's fitness by the fitness function. A fitness function should be designed for the corresponding application; for a specific chromosome, the fitness function gives a single value, which is proportional to the capability, or utility, of the individual represented by that chromosome. The second stage transfers the fitness function into an expected value, and then is followed by the third and last stage where the expected value is then transferred to a discrete number of offspring.

Examples of the known applied selection techniques are the roulette wheel and stochastic universal sampling. The GA should be properly carried out, ensuring that the

population will involve sequential generations. The best fitness and the average individual in the generation are rised for the global optimal [61] – [63].

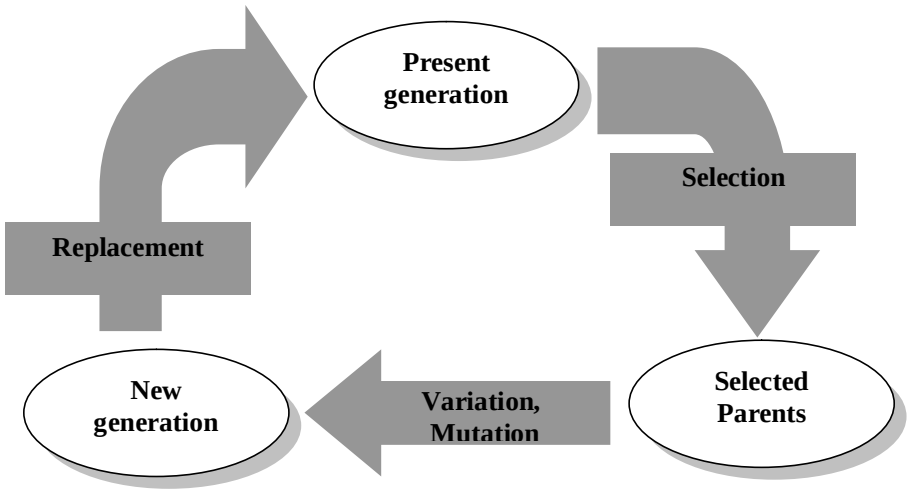

Fig. 3.4 Basic Evolution Cycle.

3.2.4 Components of GA

Major components of GA include initial population, natural selection, mating, and the mutations are explained next.

3.2.4.1 Initial Population

The genetic algorithm starts with a large commune of randomly selected chromosomes known as the initial population. A large initial population provides the genetic algorithm with a good sampling of search space; on the other hand, it increases the time of the search. Usually, not all the initial population chromosomes make the cut for the iterative portion of the genetic algorithm.

3.2.4.2 Natural Selection

A portion of the low fitness chromosomes is discarded through natural selection or survival of the fitness. Only the best members of the population are kept for each iteration of the genetic algorithm. Defining the numbers of the chromosomes to continue is mainly arbitrary. Leaving the survival of some chromosomes to the next generation controls the available genes in the offspring. Keeping too many chromosomes, on the other hand, allows bad performers a chance to contribute their traits to the next generation. 50 % of the population is often kept in the natural selection process.

3.2.4.3 Mating

Mating is the creating of one or more offspring from the parents chosen by natural selection stage. It is the first method a genetic algorithm discovers a fitness surface. The most common form of mating includes two parents that develop two offspring. A crossover point is selected between the first and last bits of the parents' chromosomes. The offspring contains portions of the binary codes of both parents.

3.2.4.4 Mutations

Random mutations change a small percentage of the bits in the last chromosomes. Mutations are the second method a genetic algorithm discovers a fitness surface. It can define attributes not in the master population and saves the genetic algorithm from converging too soon. Raising the number of mutations increases the algorithm freedom to search outside the current region of parameter space. It is also tends to divert the algorithm from converging on a solution. Typically, percentage about 1 % to 5 % of the bits mutate per iteration [76]. After mutations take place, the fitness associated with the offspring, mutated chromosomes are calculated, and the process described is iterated.

3.2.4.5 Continuous-Parameter Genetic Algorithm

When the fitness function parameters are continuous, it is logic to represent them by floating-point numbers. In addition, the binary genetic algorithm has its accuracy conditioned by the binary representation of parameters, using real number represent to the machine precision. This continuous parameter genetic algorithm owns the advantage of requesting less storage than the binary genetic algorithm. The other advantage is in the accurate representation of the continuous parameter, it follows that, representation of the fitness function is also more accurate [72] – [75]. The flow chart in Figure 3.4 provides an overview of a continuous GA.

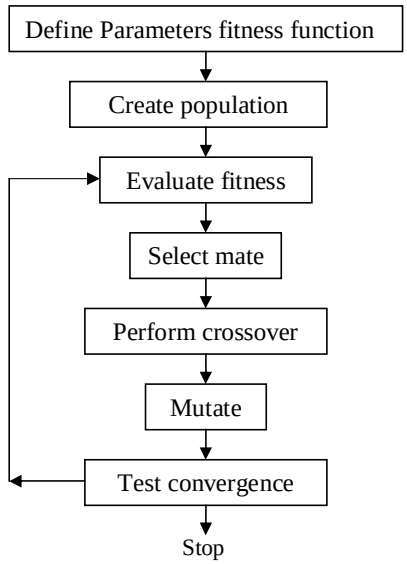

Fig. 3.5 Flow chart of a continuous GA.

The randomly selected initial population is sorted according to the fitness value. Selection is made randomly taking into consideration that the fittest individuals have the highest probability of being selected. If P_1 and P_2 are chosen to perform crossover, the resulting offspring according to the arithmetic crossover are:

$$P`_1 = r.P_1 + (1\text{-}r).P_2 \tag{3.7}$$
$$P`_2 = (1\text{-}r).P_1 + r.P_2 \tag{3.8}$$

Where r is a random number between 0 and 1.

Mutation introduces a new solution to the population for trial by producing spontaneous random change in various individuals. Non-uniform mutation is defined as follows, if an element P_k of a parent P is selected for mutation, the result would be:

$$P'_k = \begin{cases} P_k + (UB - P_k)\ f(gen) & if\ a\ random\ digit\ is\ 0 \\ P_k - (LB + P_k)\ f(gen) & if\ a\ random\ digit\ is\ 1 \end{cases} \tag{3.9}$$

LB and UB: the lower and upper bounds of the individual P_k. *gen* is the current generation. The function *f(gen)* should return a value in the range [0,1] such that the probability of *f(gen)* being close to 0 increases as *gen* increases. This insures the operator to search the space uniformly initially and very locally at later generations. The following function can be used

$$f(gen) = (r.(1 - \frac{gen}{gen\max}))^b \tag{3.10}$$

Where r is a random number in the range [0, 1], *genmax* is the maximum number of generation, and b is called the shape parameter that determines the degree of non-uniformity.

3.3 Hybrid Intelligent Systems

Various adaptive hybrid intelligent systems have been proposed in the last decades, for model expertise, image, and video process techniques, industrial control, mechatronics, robotics, automation applications and others.

Several of these systems combine different knowledge implementation schemes, decision-making modules, and learning strategies to handle a computational application. This integration overcomes the constraints of individual techniques by hybridization various methods.

These concepts direct to the emergence of many various types of intelligent system architectures. Many of the Hybrid Intelligent Systems (HIS) contain three necessary models: artificial neural networks, fuzzy inference systems, and global optimization algorithms as evolutionary algorithms. HIS is developing those appropriate techniques together with the essential advances in other new computing methods.

Experience has indicated that it is decisive for HIS designing to care primarily of the integration and interaction for various techniques rather than collect them to create ones from scratch. Techniques already well understood should be used to act certain domain problems in the system. The drawback can be defined to combine them with complementary methods.

Neural networks have a clear established architecture with learning and generalization power. The generalization capability for recent inputs depends on the internal algebraic structure of the neural network. However, it is very difficult to incorporate human a priori knowledge into a neural network.

In the opposite way, fuzzy inference systems show integral characteristics, allowing a very effective framework to actual reasoning as it attempts to model the human reasoning procedure at a cognitive scale. Fuzzy systems gain knowledge by domain experts and this is coded in the algorithm by the set of if-then rules. Fuzzy systems apply this rule-based approach and interpolative thinking with new inputs. The incorporation and knowledge interpretation is straightforward, whereas adaptation and learning handle major problems.

Global optimization is the task of getting the perfectly superior parameters set to optimize an objective function. Generally, it can be possible to own solutions that are locally optimum but not global optimum. Evolutionary Computing (EC) is based by simulating evolution on a processing device.

These techniques could be easily applied to optimize neural networks, fuzzy inference systems, and other applications. By the supplementary attributes and strengths of different systems, the new trends for hybrid system are to integrate various algorithms into a more efficient integrated system to overcome their individual weaknesses.

3.3.1 Adaptive Neuro-Fuzzy Inference Systems (ANFIS)

Jang and Sun [77] introduced the adaptive Neuro-Fuzzy inference system. This system makes use of a hybrid-learning rule to optimize the fuzzy system parameters of a first order Sugeno system. The Sugeno fuzzy model (also known as TSK fuzzy model) was presented to save a systematic method to produce fuzzy rules of a certain input-output data set. Figure 3.6 shows the architecture of two inputs, two-rule first-order ANFIS Sugeno system, the system has only one output.

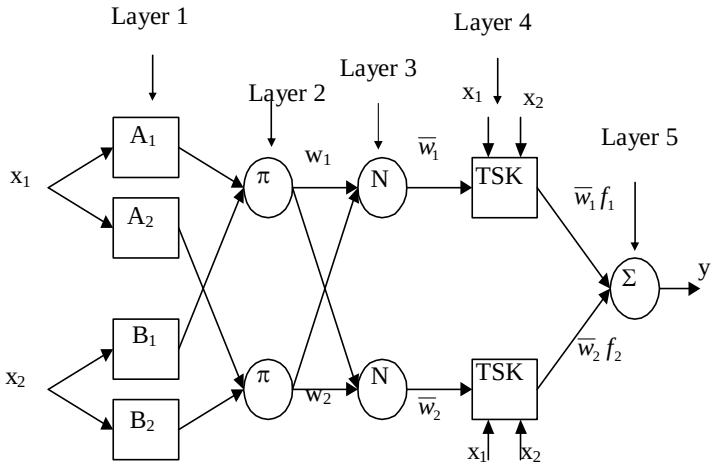

Fig. 3.6, Two input, two-rule first order Sugeno ANFIS system

The first layer of the ANFIS has adaptive nodes with each node has its function

$$O_{1,i} = \mu_A (x_1), \quad \text{for i = 1,2 or } \quad O_{1,i} = \mu_{B-2} (x_2), \qquad \text{for i = 3,4} \tag{3.11}$$

Where x_1 and x_2 are the inputs; and A_i and B_i are linguistic labels for the node. And $O_{1,i}$ is the membership grade of a fuzzy set A (= A_1, A_2, B_1 or B_2) to define the degree of applying the input to the set A.

The second layer has fixed nodes, where its output is the product of the present signals to act as the firing power of a rule.

$$O_{2,i} = w_i = \mu_A (x_1)\ \mu_B (x_2), \quad i = 1,2. \tag{3.12}$$

The third layer also has fixed nodes; the *i*th node computes the ratio of the *i*th rule's firing strength to the rules' firing strengths sum:

$$O_{3,i} = \overline{w}_i = \frac{w_i}{w_1 + w_2}, \qquad i = 1,2. \tag{3.13}$$

The nodes of the forth layers are adaptive nodes, each with a node function

$$O_{4,i} = \overline{w}_i f_i = \overline{w}_i (p_i x_1 + q_i x_2 + r_i) \tag{3.14}$$

Where $\overline{w}_i$ is a normalized firing strength produced by layer 3; $\{p_i, q_i, r_i\}$ is the parameter set of the node, and pointed to consequent parameters.

There is a single node in the fifth layer, which is a fixed node, which calculate the resultant output as the summation of all signals.

$$\text{Overall output} = O_{5,1} = \sum_i \overline{w}_i f_i = \frac{\sum_i w_i f_i}{\sum_i w_i} \tag{3.15}$$

3.3.2 ANFIS Hybrid Training Rule

The ANFIS architecture includes a two training parameter set

1. The antecedent membership function parameters
2. The polynomial parameters [*p, q, r*]

In [77], The ANFIS training systems applies a gradient descent algorithm to optimize the antecedent parameters and a least square algorithm to solve the consequent parameters. Due the reseaon that it utilizes two different algorithms to minimize the error, the training rule is reffered to as "hybrid". Firstly, The consequent parameters are updated using a least squares algorithm and the antecedent parameters are then updated by backpropagating the errors that still appear.

3.3.2.1 Training of the consequent parameters

Each output of ANFIS can be written as:

$$y_m = \overline{w}_1 f_{1m} + ... + \overline{w}_n f_{nm} \tag{3.16}$$

Where m is the output number and n the number of the input membership functions. The function f_{nm} in terms of the consequent parameters and two inputs is:

$$f_{nm} = p_{nm} x_1 + q_{nm} x_2 + r_{nm} \tag{3.17}$$

In this case, ANFIS outputs can be rewritten as:

$$y_m = [\overline{w}_1 x_1 \quad \overline{w}_1 x_2 \quad \overline{w}_1 \quad \cdots \quad \overline{w}_n x_1 \quad \overline{w}_n x_1 \quad \overline{w}_n] \begin{bmatrix} p_{1m} \\ q_{1m} \\ r_{1m} \\ \vdots \\ p_{nm} \\ q_{nm} \\ r_{nm} \end{bmatrix} = XW_m \tag{3.18}$$

If X is not invertable, Pseudo inverse can be used to calculate the vector W_m, i.e.

$$W_m = (X^T X)^{-1} X^T y_m \tag{3.19}$$

3.3.2.2 Training for the antecedent parameters

Each antecedent parameter updating rule can be written as:

$$a(T+1) = a(T) - \frac{\eta_a}{k} \frac{\partial E}{\partial a} \tag{3.20}$$

Where:

a: Parameter to be updated
T: Epoch number
η_a: Learning rate
k: Number of input patterns
E: Sum of square error (SSE)

To calculate the derivatives used to update the antecedent parameters, the chin rule is used which can be written as:

$$\frac{\partial E}{\partial a_{iL}} = \frac{\partial E}{\partial y} \cdot \frac{\partial y}{\partial w_i} \cdot \frac{\partial w_i}{\partial \mu_{iL}} \cdot \frac{\partial \mu_{iL}}{\partial a_{iL}} \tag{3.21}$$

Where i is the number of the membership function of input number L and y is the sum of ANFIS outputs. The partial derivatives are derived below:

$$E = \frac{1}{2}(y - y^t) \qquad \text{so} \qquad \frac{\partial E}{\partial y} = y - y^t = error \tag{3.22}$$

Where y^t is the target output.

$$y = \frac{w_1}{\sum_{j=1}^{n} w_j}(f_{11} + ... + f_{1m}) + ... + \frac{w_n}{\sum_{j=1}^{n} w_j}(f_{n1} + ... + f_{nm}) \tag{3.23}$$

so

$$\frac{\partial y}{\partial w_i} = \frac{\sum_{j=1}^{n} w_j - w_i}{(\sum_{j=1}^{n} w_j)^2}(f_{i1} + ... + f_{im}) = \frac{(f_{i1} + ... + f_{im}) - y_i}{\sum_{j=1}^{n} w_j} \tag{3.24}$$

$$w_i = \prod_{j=1}^{S} \mu_{ij} \qquad \text{so} \qquad \frac{\partial w_i}{\partial \mu_{iL}} = \prod_{\substack{j=1 \\ j \neq L}}^{S} \mu_{ij} = \frac{w_i}{\mu_{iL}} \tag{3.25}$$

Where *S* is the number of inputs.

The last term in Equation 3.16, $\frac{\partial \mu_{iL}}{\partial a_{iL}}$, depends on the membership function used. For example if the membership function is trapezoidal as shown in Figure 3.6, the derivatives of the membership function w.r.t. its parameters are:

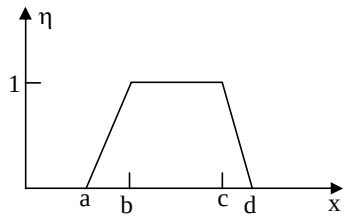

Fig. 3.7, Trapezoidal membership function

If the input pattern *x* lies between points *a* and *b*,

$$\frac{\partial \eta}{\partial a} = \frac{x-b}{(b-a)^2}, \quad \frac{\partial \eta}{\partial b} = \frac{a-x}{(b-a)^2}, \quad \frac{\partial \eta}{\partial c} = 0 \quad \text{and} \quad \frac{\partial \eta}{\partial d} = 0 \tag{3.26}$$

If the input pattern *x* lies between points *b* and *c*,

$$\frac{\partial \eta}{\partial a} = 0, \quad \frac{\partial \eta}{\partial b} = 0, \quad \frac{\partial \eta}{\partial c} = 0 \quad \text{and} \quad \frac{\partial \eta}{\partial d} = 0 \tag{3.27}$$

If the input pattern *x* lies between points *c* and *d*,

$$\frac{\partial \eta}{\partial a} = 0, \quad \frac{\partial \eta}{\partial b} = 0, \quad \frac{\partial \eta}{\partial c} = \frac{d-x}{(d-c)^2} \quad \text{and} \quad \frac{\partial \eta}{\partial b} = \frac{x-c}{(d-c)^2} \tag{3.28}$$

and if point *x* is outside the range from *a* to *d*, the partial derivatives of the membership function w.r.t its parameters are equal to 0.

4 Unified Power Flow Controller Scope

4.1 Introduction

The Unified Power Flow Controller (UPFC) is the promising FACTS controller to regulate the voltage and the power flow in the transmission grid.

This chapter analyzes the UPFC models (steady state and dynamic). The steady state model of the UPFC contains two equivalent voltage sources, those have controlled magnitude and phase angle in series with the transformers' impedance. These sources represent the shunt and the series branches of the UPFC. Incorporation of this model in the load flow of the power system will be discussed and applied.

4.2 Power Flow UPFC Modeling

Power flow UPFC model contains two voltage source converters (VSC), one has shunt connection and other has series connection. The converters have DC capacitors, which are connected in parallel as shown in Figure 4.1. When switches, 1 and 2 are open, the converters are STATCOM and SSSC, governing the injected reactive current and voltage in shunt and series of the line. At switches 1 and 2 are closed, enables the two converters to transfer real power of the two converters. The series connected converter can draw or generate the active power [78].

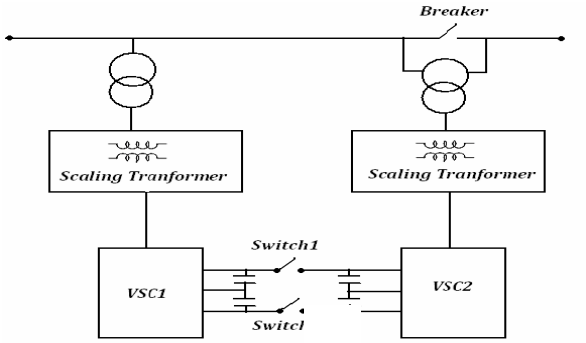

Fig. 4.1 A UPFC schematic.

The general transfer admittance matrix is obtained by applying Kirchhoff current and voltage laws to the electric circuit shown in Figure 4.2

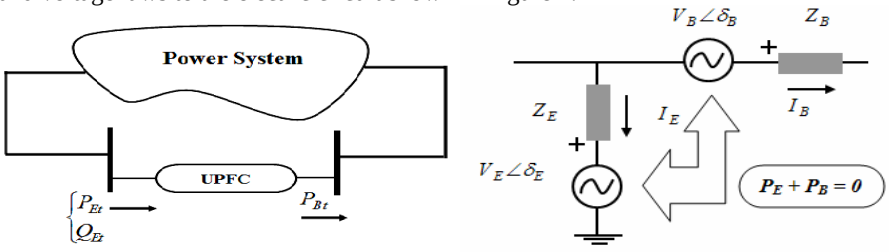

(a) (b)

Fig. 4.2 (a) UPFC Power Flow Model (b) UPFC Single Line Diagram.

Considering the sending shunt bus *k* and the receiving series bus *m*, and writing the injected currents at *m* and *k* buses:

$$\begin{bmatrix} I_k \\ I_m \end{bmatrix} = \begin{bmatrix} y_B + y_E & -y_B & -y_B & -y_E \\ -y_B & y_B & y_B & 0 \end{bmatrix} \begin{bmatrix} V_k \\ V_m \\ V_B \\ V_E \end{bmatrix} \tag{4.1}$$

$$\Delta Y_{bus} = \begin{bmatrix} Y_{kk} & Y_{km} & Y_{kB} & Y_{kE} \\ Y_{mk} & Y_{mm} & Y_{mB} & 0 \end{bmatrix} \tag{4.2}$$

The original Y_{bus} of the system before installing the UPFC is modified to include the UPFC model by adding ΔY_{bus} to it, and in this case the number of columns of the new Y_{bus} will be increased by two corresponding to V_B and V_E [79].

Considering a lossless converter operating, the UPFC will not draw nor supply real power with respect to the network. The real power demanded by the series converter is supplied from the network by the shunt converter via the common DC link voltage. The DC link voltage, V_{dc} , must remain constant so that the stored energy in the capacitor would not be changed. Hence, the active power supplied to the shunt converter, P_E, must satisfy the real power demanded by the series converter, P_B:

$$P_E + P_B = 0.0 \tag{4.3}$$

Where

$$\begin{aligned} P_B &= -real(V_B^* I_B) = -real(V_B^*(V_k - V_m - V_B)Y_{mB}) \\ &= V_B^2 G_{mB} - V_B Y_{mB} V_k \cos(\theta_{mB} + \delta_k - \delta_B) + V_B Y_{mB} V_m \cos(\theta_{mB} + \delta_m - \delta_B) \end{aligned} \tag{4.4}$$

$$\begin{aligned} P_E &= -real(V_E^* I_E) = -real(V_E^*(V_k - V_E)(-Y_{kE})) \\ &= -V_E^2 G_{kE} + V_E Y_{kE} V_k \cos(\theta_{kE} + \delta_k - \delta_E) \end{aligned} \tag{4.5}$$

$$\begin{aligned} P_B + P_E &= V_B^2 G_{mB} - V_E^2 G_{kE} - V_B Y_{mB} V_k \cos(\theta_{mB} + \delta_k - \delta_B) \\ &\quad + V_B Y_{mB} V_m \cos(\theta_{mB} + \delta_m - \delta_B) + V_E Y_{kE} V_k \cos(\theta_{kE} + \delta_k - \delta_E) \end{aligned} \tag{4.6}$$

The UPFC linearized power equations are combined with the linearized system equations corresponding to the rest of the network

$$[\Delta f(x)] = [J][\Delta x] \tag{4.7}$$

Where $[\Delta f(x)] = [\Delta P_k \ \Delta P_m \ \Delta Q_k \ \Delta Q_m \ \Delta P_{mk} \ \Delta Q_{mk} \ \Delta(P_B + P_E)]'$, $[\Delta x]$ is the solution and $[J]$ is the Jacobian matrix.

If both nodes *k* and *m* are PQ type and the UPFC is controlling active power, flowing from *m* to *k*, and reactive power injected at node *m*, the solution vector and the Jacobian matrix are defined as shown in Equation (4.8). Assuming the power controlled mentioned above and that the UPFC controls voltage magnitude at the AC system shunt converter terminal (node *k*), the solution vector and the Jacobian matrix are shown in Equation (4.9).

$$\begin{bmatrix} \Delta P_k \\ \Delta P_m \\ \Delta Q_k \\ \Delta Q_m \\ \Delta P_{mk} \\ \Delta Q_{mk} \\ \Delta (P_B + P_E) \end{bmatrix} = \begin{bmatrix} \frac{\partial P_k}{\partial \delta_k} & \frac{\partial P_k}{\partial \delta_m} & |V_k|\frac{\partial P_k}{\partial V_k} & |V_m|\frac{\partial P_k}{\partial V_m} & \frac{\partial P_k}{\partial \delta_B} & |V_B|\frac{\partial P_k}{\partial V_B} & \frac{\partial P_k}{\partial \delta_E} \\ \frac{\partial P_m}{\partial \delta_k} & \frac{\partial P_m}{\partial \delta_m} & |V_k|\frac{\partial P_m}{\partial V_k} & |V_m|\frac{\partial P_m}{\partial V_m} & \frac{\partial P_m}{\partial \delta_B} & |V_B|\frac{\partial P_m}{\partial V_B} & \frac{\partial P_m}{\partial \delta_E} \\ \frac{\partial Q_k}{\partial \delta_k} & \frac{\partial Q_k}{\partial \delta_m} & |V_k|\frac{\partial Q_k}{\partial V_k} & |V_m|\frac{\partial Q_k}{\partial V_m} & \frac{\partial Q_k}{\partial \delta_B} & |V_B|\frac{\partial Q_k}{\partial V_B} & \frac{\partial Q_k}{\partial \delta_E} \\ \frac{\partial Q_m}{\partial \delta_k} & \frac{\partial Q_m}{\partial \delta_m} & |V_k|\frac{\partial Q_m}{\partial V_k} & |V_m|\frac{\partial Q_m}{\partial V_m} & \frac{\partial Q_m}{\partial \delta_B} & |V_B|\frac{\partial Q_m}{\partial V_B} & \frac{\partial Q_m}{\partial \delta_E} \\ \frac{\partial P_{mk}}{\partial \delta_k} & \frac{\partial P_{mk}}{\partial \delta_m} & |V_k|\frac{\partial P_{mk}}{\partial V_k} & |V_m|\frac{\partial P_{mk}}{\partial V_m} & \frac{\partial P_{mk}}{\partial \delta_B} & |V_B|\frac{\partial P_{mk}}{\partial V_B} & \frac{\partial P_{mk}}{\partial \delta_E} \\ \frac{\partial Q_{mk}}{\partial \delta_k} & \frac{\partial Q_{mk}}{\partial \delta_m} & |V_k|\frac{\partial Q_{mk}}{\partial V_k} & |V_m|\frac{\partial Q_{mk}}{\partial V_m} & \frac{\partial Q_{mk}}{\partial \delta_B} & |V_B|\frac{\partial Q_{mk}}{\partial V_B} & \frac{\partial Q_{mk}}{\partial \delta_E} \\ \frac{\partial (P_B + P_E)}{\partial \delta_k} & \frac{\partial (P_B + P_E)}{\partial \delta_m} & |V_k|\frac{\partial (P_B + P_E)}{\partial V_k} & |V_m|\frac{\partial (P_B + P_E)}{\partial V_m} & \frac{\partial (P_B + P_E)}{\partial \delta_B} & |V_B|\frac{\partial (P_B + P_E)}{\partial V_B} & \frac{\partial (P_B + P_E}{\partial \delta_E} \end{bmatrix} \begin{bmatrix} \Delta\delta_k \\ \Delta\delta_m \\ \frac{\Delta V_k}{|V_k|} \\ \frac{\Delta V_m}{|V_m|} \\ \Delta\delta_B \\ \frac{\Delta V_B}{|V_B|} \\ \Delta\delta_E \end{bmatrix} \quad (4.8)$$

$$\begin{bmatrix} \Delta P_k \\ \Delta P_m \\ \Delta Q_k \\ \Delta Q_m \\ \Delta P_{mk} \\ \Delta Q_{mk} \\ \Delta (P_B + P_E) \end{bmatrix} = \begin{bmatrix} \frac{\partial P_k}{\partial \delta_k} & \frac{\partial P_k}{\partial \delta_m} & |V_E|\frac{\partial P_k}{\partial V_E} & |V_m|\frac{\partial P_k}{\partial V_m} & \frac{\partial P_k}{\partial \delta_B} & |V_B|\frac{\partial P_k}{\partial V_B} & \frac{\partial P_k}{\partial \delta_E} \\ \frac{\partial P_m}{\partial \delta_k} & \frac{\partial P_m}{\partial \delta_m} & |V_E|\frac{\partial P_m}{\partial V_E} & |V_m|\frac{\partial P_m}{\partial V_m} & \frac{\partial P_m}{\partial \delta_B} & |V_B|\frac{\partial P_m}{\partial V_B} & \frac{\partial P_m}{\partial \delta_E} \\ \frac{\partial Q_k}{\partial \delta_k} & \frac{\partial Q_k}{\partial \delta_m} & |V_E|\frac{\partial Q_k}{\partial V_E} & |V_m|\frac{\partial Q_k}{\partial V_m} & \frac{\partial Q_k}{\partial \delta_B} & |V_B|\frac{\partial Q_k}{\partial V_B} & \frac{\partial Q_k}{\partial \delta_E} \\ \frac{\partial Q_m}{\partial \delta_k} & \frac{\partial Q_m}{\partial \delta_m} & |V_E|\frac{\partial Q_m}{\partial V_E} & |V_m|\frac{\partial Q_m}{\partial V_m} & \frac{\partial Q_m}{\partial \delta_B} & |V_B|\frac{\partial Q_m}{\partial V_B} & \frac{\partial Q_m}{\partial \delta_E} \\ \frac{\partial P_{mk}}{\partial \delta_k} & \frac{\partial P_{mk}}{\partial \delta_m} & |V_E|\frac{\partial P_{mk}}{\partial V_E} & |V_m|\frac{\partial P_{mk}}{\partial V_m} & \frac{\partial P_{mk}}{\partial \delta_B} & |V_B|\frac{\partial P_{mk}}{\partial V_B} & \frac{\partial P_{mk}}{\partial \delta_E} \\ \frac{\partial Q_{mk}}{\partial \delta_k} & \frac{\partial Q_{mk}}{\partial \delta_m} & |V_E|\frac{\partial Q_{mk}}{\partial V_E} & |V_m|\frac{\partial Q_{mk}}{\partial V_m} & \frac{\partial Q_{mk}}{\partial \delta_B} & |V_B|\frac{\partial Q_{mk}}{\partial V_B} & \frac{\partial Q_{mk}}{\partial \delta_E} \\ \frac{\partial (P_B + P_E)}{\partial \delta_k} & \frac{\partial (P_B + P_E)}{\partial \delta_m} & |V_E|\frac{\partial (P_B + P_E)}{\partial V_E} & |V_m|\frac{\partial (P_B + P_E)}{\partial V_m} & \frac{\partial (P_B + P_E)}{\partial \delta_B} & |V_B|\frac{\partial (P_B + P_E)}{\partial V_B} & \frac{\partial (P_B + P_E}{\partial \delta_E} \end{bmatrix} \begin{bmatrix} \Delta\delta_k \\ \Delta\delta_m \\ \frac{\Delta V_E}{|V_E|} \\ \frac{\Delta V_m}{|V_m|} \\ \Delta\delta_B \\ \frac{\Delta V_B}{|V_B|} \\ \Delta\delta_E \end{bmatrix} \quad (4.9)$$

where

$$S_{mk}^{*} = V_m^{*} I_{mk} = V_m^{*}(V_m + V_B - V_k)Y_{mB} \tag{4.10}$$

$$P_{mk} = V_m^2 G_{mB} + V_m Y_{mB} V_B \cos(\theta_{mB} + \delta_B - \delta_m) - V_m Y_{mB} V_k \cos(\theta_{mB} + \delta_k - \delta_m) \tag{4.11}$$

$$Q_{mk} = -V_m^2 B_{mB} - V_m Y_{mB} V_B \sin(\theta_{mB} + \delta_B - \delta_m) + V_m Y_{mB} V_k \sin(\theta_{mB} + \delta_k - \delta_m) \tag{4.12}$$

4.3 Effective Initialization of UPFC Controllers

The modeling of UPFC controllers for application in power flow analysis results in highly nonlinear equations, which should be suitably initialized to ensure quadratic convergent solutions when using the Newton–Raphson method. This section concerns such as issue and makes well-grounded recommendations for the use of simple and effective initialization procedures for all FACTS models in power flow and related studies.

4.3.1 Controllers Represented by Shunt Synchronous Voltage Sources

Extensive application of FACTS devices represented by shunt voltage sources shows that elements such as the STATCOM, the shunt source of the UPFC, and the two-shunt sources representing the HVDC-VSC are suitably initialized by choosing 1 p.u. voltage magnitudes and 0 phase angles.

4.3.2 Controllers Represented by Series Synchronous Voltage Sources

Suitable initialization of series voltage sources in load flow analysis is obligatory to guarantee robust solutions. Examples of FACTS devices that use one or more series voltage sources are the static synchronous series compensator (SSSC) and unified power flow controller (UPFC).

Different equations exist for the purpose of initializing the series voltage source, depending on the operating condition exhibited by the controller. For example, for the case when active and reactive powers are specified at bus *k*, and assuming

$V_k = V_m = 1$ p.u., and $\theta_k = \theta_m = 0$, leads to the following simple expressions:

$$V_B = V_{cR} = X_B (P_{specified}^2 + Q_{specified}^2)^{1/2} \tag{4.13}$$

$$\theta_E = \theta_{cR} = \arctan\left(\frac{P_{specified}^2}{Q_{specified}^2}\right) \tag{4.14}$$

These equations are used to initialize the parameters of series voltage sources within the Newton–Raphson power flow solution.

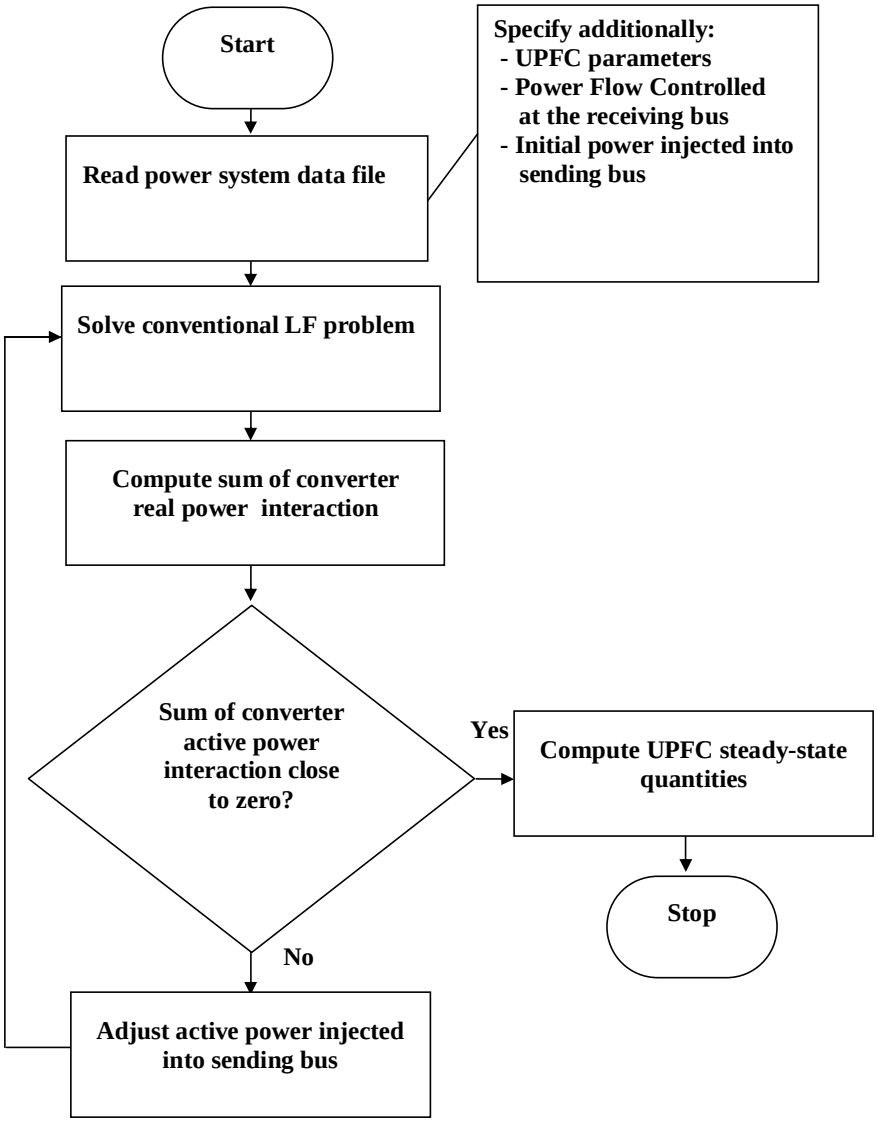

Fig. 4.3, General Load Flow Algorithm with UPFC.

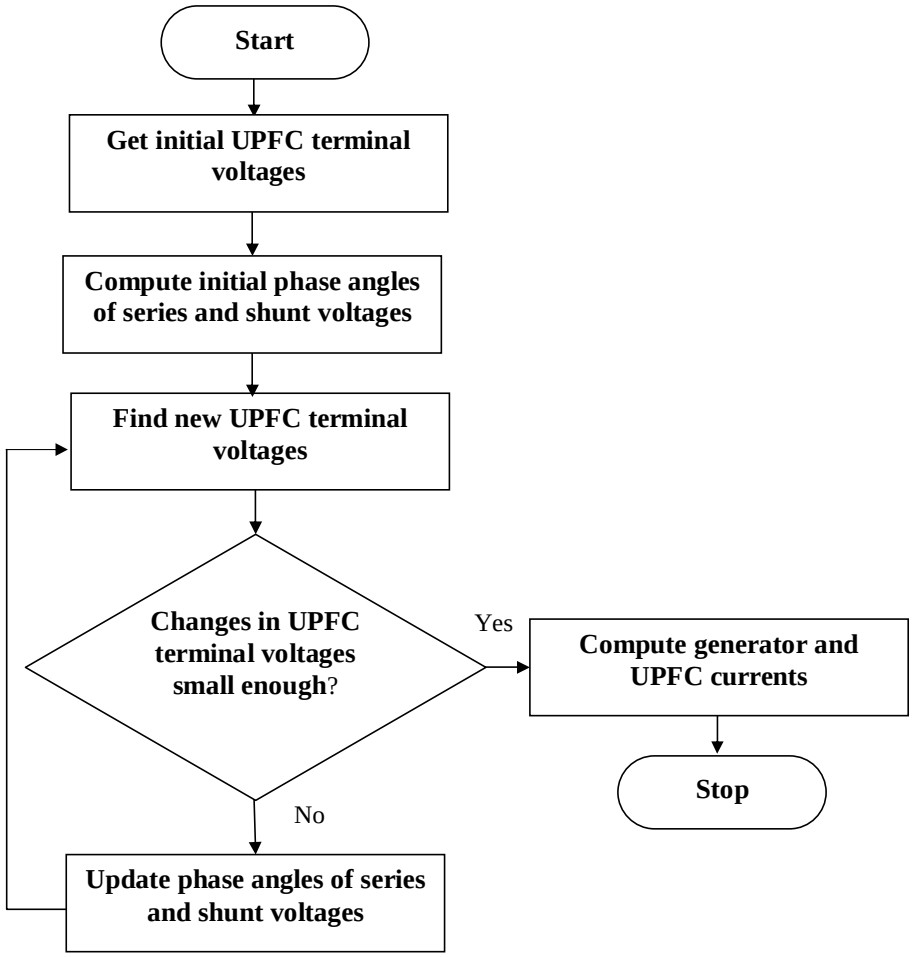

Fig. 4.4, Algorithm for Updating UPFC parameters.

4.4 Dynamic Modeling of UPFC

Figure 4.5 shows the UPFC schematic description. The two converters in the schematic own the same construction, but is varid in their rated values. The network voltages (magnitude, angles) of the two converters output can be updated according to the operating requests of the system [80].

Therefore, there are four control inputs : m_E, m_B and δ_E, δ_B, that are the amplitude modulation ratio and phase angle of the control signal of each VSC, as shown in Figure 4.5. In a practical system, the power flow of the transmission line, the voltage of the controlled bus, and the voltage on the DC link capacitor of the device itself can be controlled by regulating these four control variables.

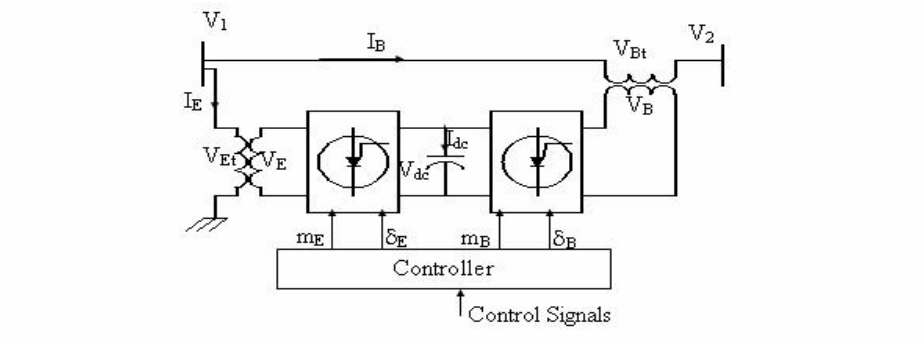

Fig. 4.5, Schematic diagram of the power circuit of a UPFC.

An equivalent UPFC model, which is based on the Pulse Width Modulation (PWM) approach, is shown in Figure 4.6.

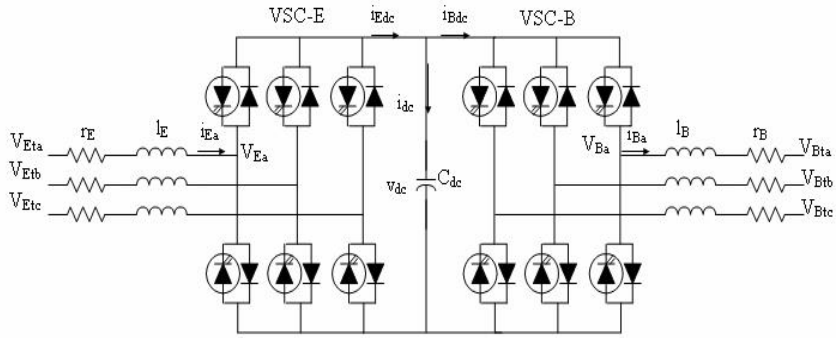

Fig. 4.6, Equivalent UPFC Model.

The three-phase dynamic differential equations of the UPFC are:

$$\begin{bmatrix} \frac{di_{Ea}}{dt} \\ \frac{di_{Eb}}{dt} \\ \frac{di_{Ec}}{dt} \end{bmatrix} = \begin{bmatrix} -\frac{r_E}{l_E} & 0 & 0 \\ 0 & -\frac{r_E}{l_E} & 0 \\ 0 & 0 & -\frac{r_E}{l_E} \end{bmatrix} \begin{bmatrix} i_{Ea} \\ i_{Eb} \\ i_{Ec} \end{bmatrix} + \begin{bmatrix} \frac{1}{l_E} & 0 & 0 \\ 0 & \frac{1}{l_E} & 0 \\ 0 & 0 & \frac{1}{l_E} \end{bmatrix} \begin{bmatrix} v_{Eta} \\ v_{Etb} \\ v_{Etc} \end{bmatrix} - \begin{bmatrix} \frac{1}{l_E} & 0 & 0 \\ 0 & \frac{1}{l_E} & 0 \\ 0 & 0 & \frac{1}{l_E} \end{bmatrix} \begin{bmatrix} v_{Ea} \\ v_{Eb} \\ v_{Ec} \end{bmatrix} \qquad (4.15)$$

$$\begin{bmatrix} \frac{di_{Ba}}{dt} \\ \frac{di_{Bb}}{dt} \\ \frac{di_{Bc}}{dt} \end{bmatrix} = \begin{bmatrix} -\frac{r_B}{l_B} & 0 & 0 \\ 0 & -\frac{r_B}{l_B} & 0 \\ 0 & 0 & -\frac{r_B}{l_B} \end{bmatrix} \begin{bmatrix} i_{Ba} \\ i_{Bb} \\ i_{Bc} \end{bmatrix} + \begin{bmatrix} \frac{1}{l_B} & 0 & 0 \\ 0 & \frac{1}{l_B} & 0 \\ 0 & 0 & \frac{1}{l_B} \end{bmatrix} \begin{bmatrix} v_{Bta} \\ v_{Btb} \\ v_{Btc} \end{bmatrix} - \begin{bmatrix} \frac{1}{l_B} & 0 & 0 \\ 0 & \frac{1}{l_B} & 0 \\ 0 & 0 & \frac{1}{l_B} \end{bmatrix} \begin{bmatrix} v_{Ba} \\ v_{Bb} \\ v_{Bc} \end{bmatrix} \qquad (4.16)$$

Where V_E , V_B and V_{dc} are given by:

$$\begin{bmatrix} v_{Ea} \\ v_{Eb} \\ v_{Ec} \end{bmatrix} = \frac{\sqrt{2} m_E v_{dc}}{2} \begin{bmatrix} \cos(\omega t + \delta_E) \\ \cos(\omega t + \delta_E - 120^0) \\ \cos(\omega t + \delta_E + 120^0) \end{bmatrix} \tag{4.17}$$

$$\begin{bmatrix} v_{Ba} \\ v_{Bb} \\ v_{Bc} \end{bmatrix} = \frac{\sqrt{2} m_B v_{dc}}{2} \begin{bmatrix} \cos(\omega t + \delta_B) \\ \cos(\omega t + \delta_B - 120^0) \\ \cos(\omega t + \delta_B + 120^0) \end{bmatrix} \tag{4.18}$$

V_E and V_B can be written as phasor quantities:

$$\mathrm{V_E} = \frac{m_E v_{dc}}{2} \angle \delta_E \tag{4.19}$$

$$\mathrm{V_B} = \frac{m_B v_{dc}}{2} \angle \delta_B \tag{4.20}$$

$$\begin{aligned} \frac{dv_{dc}}{dt} = {} & \frac{m_E}{2C_{dc}} [\cos(\omega t + \delta_E) i_{Ea} + \cos(\omega t + \delta_E - 120^0) i_{Eb} + \cos(\omega t + \delta_E + 120^0) i_{Ec}] \\ & + \frac{m_B}{2C_{dc}} [\cos(\omega t + \delta_B) i_{Ba} + \cos(\omega t + \delta_B - 120^0) i_{Bb} + \cos(\omega t + \delta_B + 120^0) i_{Bc}] \end{aligned} \tag{4.21}$$

4.5 UPFC Control

The structure of UPFC includes two converters, which are coupled at the DC side, the explaination of each converter control will be individually shown.

4.5.1 Shunt Converter Control

The shunt converter takes a controlled current from the network. A component of this current is I_P, which is automatically calculated by the requirement to balance the active power gone to the series converter by the DC link. This balancing of power is commanded through regulating the voltage of the DC capacitor via feedback controlling [81].

Other part of the current in the shunt converter is the reactive current, I_r that can be controlled with the same method as in a STATCOM.

There are two modes of the operating control for the shunt converter (STATCOM). which are,

1. Mode of VAR control that the reactive current reference is determined through the inductive or capacitive VAR order. Current transformers (CT), which positioned at the coupling step-down transformer, allocate the feedback signals.

2. Mode of automatic voltage control that the feedback voltage output controller, which has a droop characteristic as in the state of a SVC or a STATCOM, determines the reactive current reference. The voltage feedback signals are available from potential transformers (PT), which measure the voltage value V_1 of the substation which input of the coupling transformer.

The shunt converter controller consists of block diagram as shown in Figure 4.7.

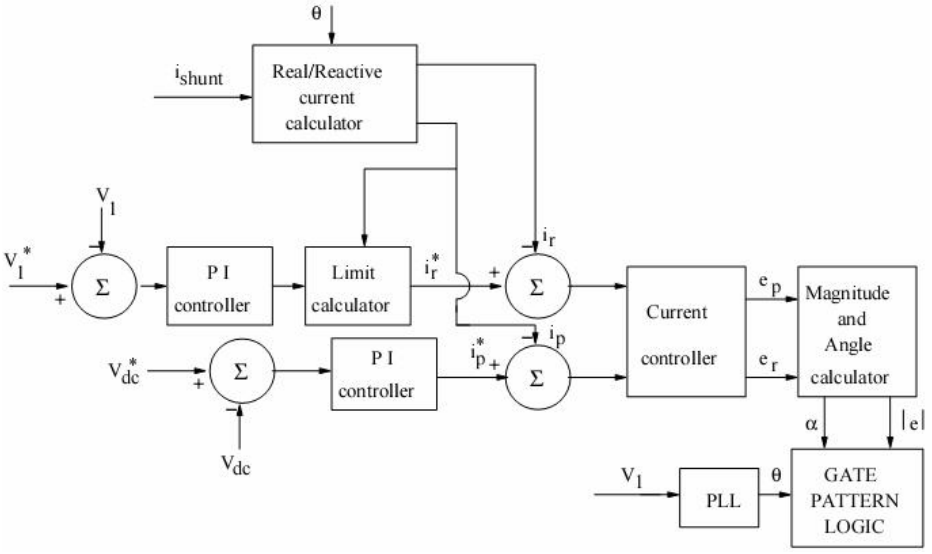

Fig. 4.7, Block diagram of shunt controller for UPFC.

4.5.2 Series Converter Control

The control of series converter cares with injecting a voltage, series, of the designed value and angle. There are many control modes for the series voltage [82].

1. Mode of direct voltage injection that the converter mainly generate a voltage phasor directed to the reference signal. Sometimes, the designed voltage is a reactive voltage and be in quadrature with the current.

2. Mode of Phase Angle Shifter that the injected voltage ($\hat{V}_C$) is phase shifted related to the voltage (V_1) by an angle determined by the reference input.

3. Mode of line impedance that the series injected voltage is governed related to the line current. The complex impedance that is determined by the relation of the injected voltage and the line current, through the reference inputs. It is necessary to consider in applying this control mode, to prevent instability or resonance. For example, resistance with negative value may produce instability. A high level of the capacitive, negative reactance, can make resonance case leading to very high current.

4. Mode of automatic power flow control that the reference inputs determine the require active power P and the reactive power Q at a certain line position. P and Q may be controlled separately in a feasible region determined by the achieving of different constraints.

During that control mode, the voltage of series injected is calculated by a vector control system to guarantee the flow of the required current phasor, which is kept even during system disturbances, unless the system control governs the modulation of the power, active and reactive. Although the nominal conditions control the regulation of the total power flow in the line, the contingency conditions want the controller to enhance the system stability through power oscillations damping.

CT and PTs achieve the feedback signals of the series converter controller, so there are measurements of current and voltages at the two terminals of the UPFC. The series converter controlling block diagram is indicated in Figure 4.8.

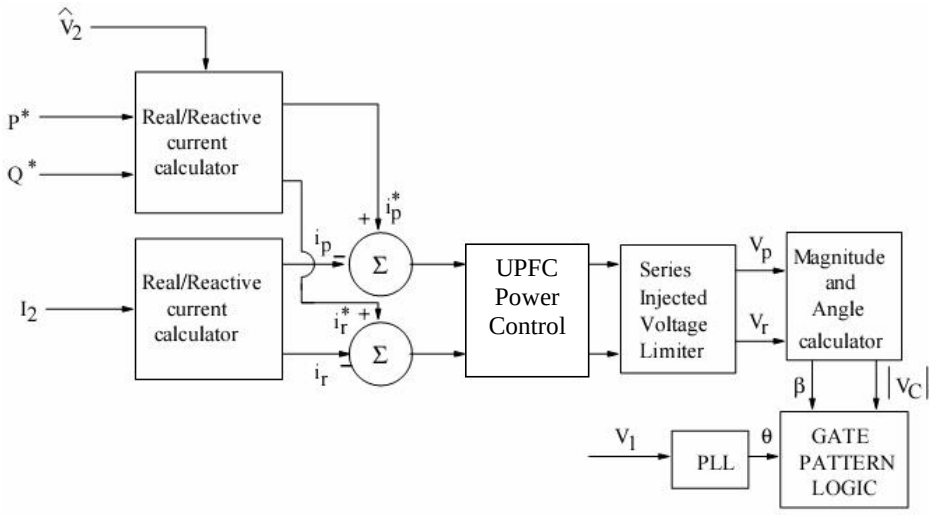

Fig. 4.8, Block diagram of series controller for UPFC.

5 Techniques for Optimal UPFC

5.1 Introduction

Unified Power Flow Controller (UPFC) was proposed as a family member of Flexible AC Transmission Systems (FACTS). This is a multiple functional FACTS controller with primary duty to control the power flow of the system. The secondary function of the UPFC can be voltage control, transient stability improvement, oscillation damping to enhance the dynamic stability of the system.

The applied proposed technique will be used to solve real problems in the power systems especially in a real Finnish network.

The optimal locations and the optimal settings will be detected using the AI concepts to reach the best performance area during the normal and the contingency operations of the network to solve the reliability issues in the line outage cases to improve the grid performance by finding the optimal locations and the settings for UPFC installation.

The criteria for the optimality will depend on some fitness functions, these fitness functions will involve in the indices terms to include the network buses voltage profile and how to reduce the voltage violations of the network, also the network line loading and how to reduce the lines overloading related to the network lines rate. UPFC own the capability to act both of SVC and SSSC performance simultaneously, and all of theses UPFC modes will be applied and investigated.

The effect of UPFC, in enhancing the dynamics performance of the system and in improving the oscillations damping of the system will be discussed. The link between the steady state and the dynamic analysis can be achieved by considering the results from the steady state coupled with the dynamic response analysis. Dynamic controller based modern control theory with damping effect will be designed to insure good damping under various operating conditions and disturbances.

5.2 Proposed Technique for Optimal Location and Optimal Setting

The UPFC installation scenario in the power network will be at the following phases:

- Normal operation (Base load pattern) with normal configuration
- Normal operation with load growth pattern (Load growth coefficients for the year 2020) with normal configuration
- Contingency analysis with elements outage (Base load and load growth)

At each phase, the installation of UPFC will be in the optimal locations and with optimal setting of parameters, which will be achieved according to the following procedure.

5.2.1 Problem Formulation

The regular operating of the power system depends on various items as the loading conditions, the system configuration and the current system operating point. All the former points affect the stability of the system and the trajectory of the system performance. A contingency can be considered to be the outage of a generator, a transformer or a line. The

system may become unstable and enter an insecure state when a contingency event has occurred.

Contingency analysis is one of the most important functions performed in power systems to establish appropriate preventive and/or corrective actions for each contingency.

Some indices will be proposed to indicate the overloaded lines and the bus voltage violations, and then ranking of the severest contingencies cases will be performed. For each line outage contingency in the system, we tabulate the all overloaded lines and the buses that have voltage violations, and then the lines are ranked with respect to the severity of the contingency, in another meaning, according to the total resultant number of the thermal and voltage violations limits. Then the most critical contingencies are calculated. After determining the most critical contingencies scenarios, the GA method is used to detect the optimal position and parameters setting of UPFC. Optimal installation of UPFC with these locations and parameters will prevent or reduce the overloading in lines and the violations of bus voltage to the minimum limit under these critical contingencies according to the proposed fitness function.

5.2.2. GA Fitness Functions

The task is concerned with finding the optimum position and the optimum parameter settings for the UPFC in the electric grid to minimize and eliminate the overloading in lines and the violations of bus voltage.

The solid layout description of the equations is:

$$\text{Min Fitness } F_t(X,U) \tag{5.1}$$

Subject to:

$$G_t(X,U) = 0.0 \tag{5.2}$$

$$H_t(X,U) \leq 0.\ 0 \tag{5.3}$$

Where

$F_t(X,U)$ describes the fitness function to be reduced and optimized;

$G_t(X,U)$ describes the group of the equality constraints directed to active and reactive power according to the balance equations;

$H_t(X,U)$ describes the group of the inequality constraints directed to UPFC parameter ranges limits, active and reactive power generation ranges limits, bus voltage ranges limits, and phase angles ranges limits;

X describes the group of the states of the power system containing voltage magnitude and phase angles; and

U describes the group of controlling variables to be optimized to become the output of the process, the UPFC positions and the parameters setting of UPFC.

The fitness function will depend on some performance indices; the fitness function and the performance index can be changed based on the scope region of interest as following:

I) <u>Optimizing with the bus voltage violations (No overloaded lines or out of interest zone):</u>

$$F_t(X,U) = \sum_{i=1}^{nbb:no.ofbuses} V(BV) \tag{5.4}$$

$$V(BV) = \begin{cases} 0 & ,if \quad 0.95 \le V_i \le 1.05 \\ Log\left(\Psi_{V(BV)} * abs\left(\frac{V_{\text{i nominal}} - V_i}{V_{\text{i nominal}}}\right)^{Q}\right) & ,otherwise \end{cases} \tag{5.5}$$

Where

$V(BV)$ represents the Bus Voltage Violation function;

V_i represents the voltage magnitude at bus i;

$V_{i\,nominal}$ represents the bus i nominal voltage;

$\Psi_{V(BV)}$ represents the weights and is calculated to have certain index value for covering various percentage of voltage difference, also applied to adjust the logarithm slope.

Q describes the integer coefficient is applied to penalize less or more voltage variations, it may be varied as 1, 2, 3, ….

nbb represent the number of the buses in the system.

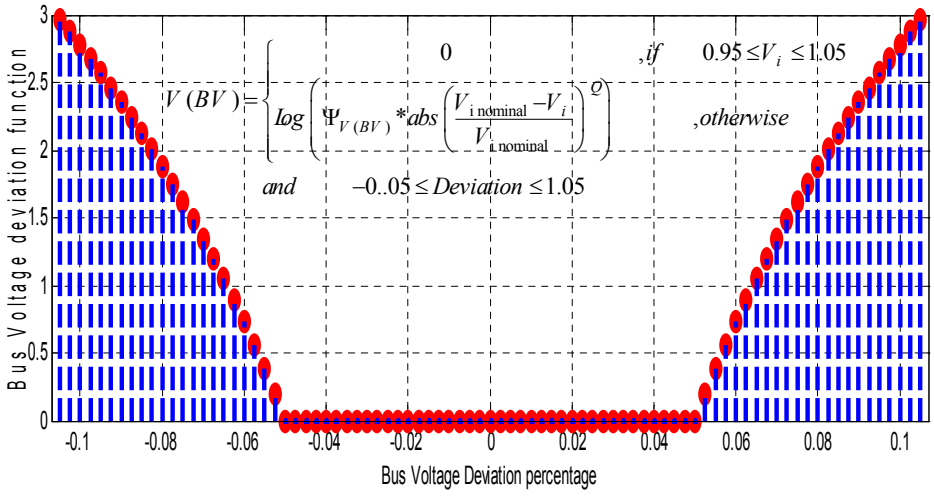

Fig. 5.1 Bus Voltage Violations function.

II) Optimizing with the overloaded lines (No bus voltage violations or out of interest zone):

$$F_t(X,U) = \sum_{i=1}^{ntl:no.of\ lines} L(OL) \tag{5.6}$$

$$L(OL) = \begin{cases} 0 & ,if\ S_{i\ \ operating} \le S_{\text{i max.}rate} \\ Log\left(\Psi_{L(OL)} * \left(\dfrac{S(MVA)_{i\ \ operating}}{S(MVA)_{\text{i max.}rate}} \right)^{2*\ R} \right) & ,if\ S_{i\ \ operating} > S_{\text{i max.}rate} \end{cases} \tag{5.7}$$

Where

$L(OL)$ represents the Over Loaded Line function;

S_i represents the current Volt-Ampere power in line i;

S_i represents the Volt-Ampere power rate of line

$\Psi_{L(OL)}$ represents the weights and is determined in order to have certain index value for various percentage of branch loading, in the same moment it applied to adjust the logarithm slope.

R describes the coefficient is applied to penalize less or more overloads.

ntl represent the total number of system transmission lines.

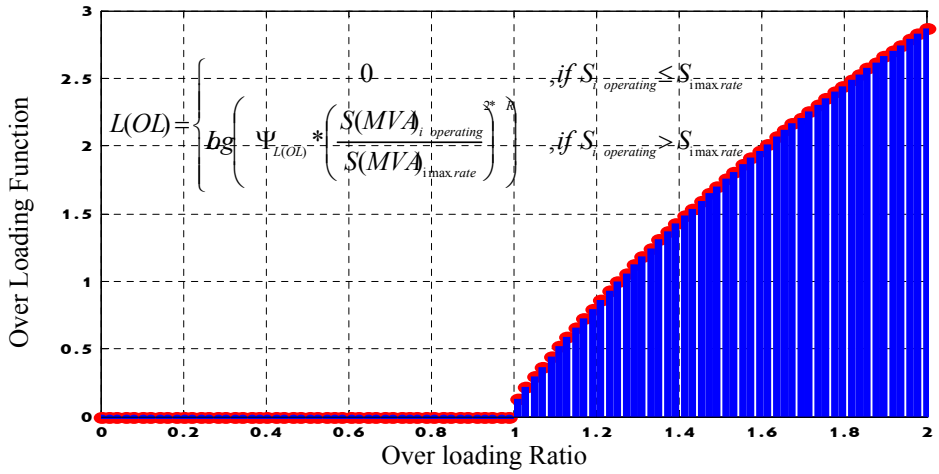

Fig. 5.2 Over Loaded Lines Function.

III) Optimizing both the overloading in lines and the bus voltage violations :

$$F_t(X,U) = \sum_{i=1}^{ntl\,:\,no.of\ lines} L(OL) + \sum_{j=1}^{nbb\,:\,no.of buses} V(BV) \tag{5.8}$$

As it is indicated in the Equation (5.4) and (5.5) and related variables

$$L(OL) = \begin{cases} 0 & ,if\ S_{i\ operating} \le S_{\text{i max.rate}} \\ Log\left(\Psi_{L(OL)} * \left(\dfrac{S(MVA)_{i\ operating}}{S(MVA)_{\text{i max.rate}}} \right)^{2*R} \right) & ,if\ S_{i\ operating} > S_{\text{i max.rate}} \end{cases}$$

$$V(BV) = \begin{cases} 0 & ,if \quad 0.95 \le V_j \le 1.05 \\ Log\left(\Psi_{V(BV)} * abs\left(\dfrac{V_{\text{j nominal}} - V_j}{V_j} \right)^{Q} \right) & ,otherwise \end{cases}$$

In some simulations, the (log) terms can be replaced with linear terms relation, based on the overloading penalty and values of voltage violations.

5.2.3. Power Flow UPFC Modeling

The equivalent circuit of UPFC will be attached to the power system equation, and programmed for output results, and is shown Figure (5.3). It structured from two synchronous voltage sources (SVS) that are simultaneously coordinated together to act the required performance mode.

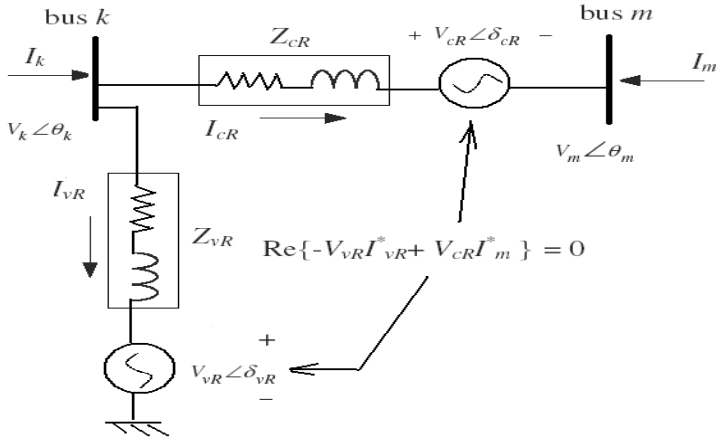

Fig. 5.3. Unified power flow controller equivalent circuit.

$$E_{vR} = V_{vR} * (\cos\delta_{vR} + j\sin\delta_{vR}) \tag{5.9}$$

$$E_{cR} = V_{cR} * (\cos\delta_{cR} + j\sin\delta_{cR}) \quad (5.10)$$

Where

V_{vR} describes the magnitude of the voltage for shunt SVS.

δ_{vR} describes the value of the angle for shunt SVS.

V_{cR} describes the magnitude of the voltage for series SVS.

δ_{cR} describes the value of the angle for series SVS.

Equations (5.4) and (5.5) will be adjusted to represent the active and reactive flow relations for bus *k* and *m*, then combined with Equations (5.9) and (5.10) to get:

$$\begin{aligned} P_{cR} = {} & V_{cR}^2 G_{mm} + V_{cR}V_k(G_{km}\cos(\delta_{cR}-\theta_k) + B_{km}\sin(\delta_{cR}-\theta_k)) \\ & + V_{cR}V_m(G_{mm}\cos(\delta_{cR}-\theta_m) + B_{mm}\sin(\delta_{cR}-\theta_m)) \end{aligned} \quad (5.11)$$

$$\begin{aligned} Q_{cR} = {} & -V_{cR}^2 B_{mm} + V_{cR}V_k(G_{km}\sin(\delta_{cR}-\theta_k) - B_{km}\cos(\delta_{cR}-\theta_k)) \\ & + V_{cR}V_m(G_{mm}\sin(\delta_{cR}-\theta_m) - B_{mm}\cos(\delta_{cR}-\theta_m)) \end{aligned} \quad (5.12)$$

$$P_{vR} = -V_{vR}^2 G_{vR} + V_{vR}V_k(G_{vR}\cos(\delta_{vR}-\theta_k) + B_{vR}\sin(\delta_{vR}-\theta_k)) \quad (5.13)$$

$$Q_{vR} = V_{vR}^2 B_{vR} + V_{vR}V_k(G_{vR}\sin(\delta_{vR}-\theta_k) - B_{vR}\cos(\delta_{vR}-\theta_k)) \quad (5.14)$$

Where

V_k and V_m : the magnitudes of the voltage at bus *k* and bus *m*.

θ_k and θ_m : the magnitudes of the voltage at bus *k* and bus *m*.

P_{cR} and Q_{cR} : the active and reactive power for series SVS.

P_{vR} and Q_{vR} : the active and reactive powers for shunt SVS.

G_{mm}, G_{kk}, G_{km} , G_{mk}: the conductance elements for bus *k* , *m* and for lines between buses.

B_{mm}, B_{kk}, B_{km} , B_{mk}: the susbtance elements for bus *k* , *m* and for lines between buses.

G_{vR}, B_{vR}, G_{cR}, B_{cR}: the susbtances & conductances for series SVS and series SVS.

5.2.4. Constraints of the Problem:

⇒ **Equality Constraints**

The active power and reactive power equations at all bus in the system, which are described as

$$\sum_{lines \Rightarrow busi} PowerLinesFlow = PowerGenerator_i - PowerDemand_i$$

$$P_{Gi} - P_{Di} - P_{Lines \Rightarrow busi}(V,\theta) = 0.0 \quad (5.15)$$

$$Q_{Gi} - Q_{Di} - Q_{Lines \Rightarrow busi}(V,\theta) = 0.0 \quad (5.16)$$

This is in addition to the active and reactive power flow equations for the series and shunt SVS for UPFC device, which is indicated from Equations (5.11) to (5.14).

$\Rightarrow$ **Inequality Constraints**

- Generation Power Limits:

$$P_{Gi}^{\min} \le P_{Gi} \le P_{Gi}^{\max} \text{ , } i=1, 2, \ldots\ldots\ldots\ldots n_G \quad (5.17)$$

$$Q_{Gi}^{\min} \le Q_{Gi} \le Q_{Gi}^{\max} \text{ , } i=1, 2, \ldots\ldots\ldots\ldots n_G \quad (5.18)$$

- Bus Voltage Limits:

$$V_i^{\min} \le V_i \le V_i^{\max} \text{ , } i=1, 2, \ldots\ldots\ldots nbb \quad (5.19)$$

- Phase Angles Limits:

$$\delta_i^{\min} \le \delta_i \le \delta_i^{\max} \text{ , } i=1, 2, \ldots\ldots\ldots nbb \quad (5.20)$$

- Parameters UPFC Constraints:

$$V_{vR}^{\min} \le V_{vR} \le V_{vR}^{\max}$$

$$V_{cR}^{\min} \le V_{cR} \le V_{cR}^{\max} \quad (5.21)$$

- Power Lines Limits:

$$P_{ij} \le P_{ij}^{\max} \text{ , } i=1, 2, \ldots\ldots\ldots ntl \quad (5.22)$$

5.3 Index for Performance Ranking

For installing UPFC, the optimum locations and optimum parameters setting (V_{cR} , V_{vR}) can be upgraded by the designed Genetics Algorithm which will be shown later. As indicated before, the installation of UPFC with optimal locations and optimal parameters setting will eliminate or at least reduce the overloading of the transmission lines and the violations of the bus voltage.

The achievement of UPFC can be executed on the system at the normal operations and also during contingency conditions. Ranking process is occurred on the network post the contingency study. There will be some single contingencies. We calculate the following performance indices at each single line outage:

- $\acute{K}_{(LOLN)}$: the index that describes the Lines Over Loaded Number.
- $\Gamma_{(VBVN)}$: the index which indicates the Violation of Voltage Buses Number.

Then we rank the lines according to the severity of the contingency, in other words, according to:

- The Performance Index $Я = \acute{K}_{(LOLN)} + \Gamma_{(VBVN)}$

As will be shown later in simulations and results, Performance Index $Я$ is zero for the remaining cases, which have no transmission line overloading nor buses voltage violation, as a short example for this process (as Numerical explanations):

Table 5.1 Ranking for the severity contingency cases

Ranking Case	Line Number	Connecting Bus		$\acute{K}_{(LOLN)}$	$\Gamma_{(VBVN)}$	$Я = \acute{K}_{(LOLN)} + \Gamma_{(VBVN)}$
		From	To			
1	11	9	2	3	2	5
2	15	8	5	2	1	3
3	1	6	12	2	0	2

5.4 The Proposed Genetics Algorithm

In the genetic algorithm, the individuals are coded to chromosomes that contain variables of the problem. The configuration of chromosomes to reach the optimal installation of the UPFC has two categories of parameters, those are UPFC location and parameters setting (V_{cR} *and* V_{vR}) as coherent model parameters for UPFC. the chromosome for the proposed algorithm has been indicated in Figure 5.4.

Objective Function	……..	**Location of UPFC**	V_{cR}	V_{vR}

Fig. 5.4 The Chromosome of Proposed GA.

- The first group of chromosomes inside the individual points to the positions locations of UPFCs hardware in the power system. This group defines in which transmission line the UPFCs should be structured.
- The second group (which starts from the first set end) describes the value of V_{cR} of series SVS. The limits for that set are randomly determined according to the working range [0.001, 0.3].
- At last, the third set (which starts form the second set end) describes the value of V_{vR} of shunt SVS. The limits for this set are randomly determined according to the range [0.8, 1.2].

Three items move a genetic algorithm: mutation rate, crossover rate and population size. The GA is a search procedure that can be used to constrained problems; the constraints can be concerned with the fitness function. In that algorithm, issues for optimization that should be executed on the fitness function and all equality and inequality constraints concerning the UPFC equations, these all explained in the previous sections. The structure of the GA execution can be separated into the following three constituent phases namely: initial population generation, fitness evaluation and genetic operations.

In the following steps, we describe the process of the implemented GA technique:

Phase 1: Definitions for the optimization controlling parameters such as the population size, crossover and mutation and their probabilities, maximum generation number, stopping criterion. In addition, the power flow data is defined.

Phase 2: Generation a primary population for individuals, this process performed for optimizing variables, which are the positions, and the parameters setting of UPFC. Three chromosomes for the individual show a meaningful point inside the optimization problem's region solution.

Phase 3: Using the objective function, we start to calculate the individual's fitness inside the population. The fitness is computed by considering the fitness function F_t. The population on-line performance *P(n)* is defined as

$$P(n) = \frac{1}{P} \sum_{p=1}^{N} F_t^n(p) \qquad n = 0, 1, \ldots\ldots, \quad T-1 \tag{5.23}$$

Where

N = Total population size;

T = total generations;

$F_t^n(p)$ = the fitness function of the pth chromosome in the nth generation.

Phase 4: GA depends on genes rules and the Darwin principle of the survival of the fittest, so we eliminate the worse individuals, and continue with the most highly fit members to generate a new population, keeping information for the next generation. That process is preformed by comprising selection, crossover, and mutation.

To maintain diversity in the population, we consider *dij* the variable distance between two solutions $X^{(i)}$ and $X^{(j)}$

$$d_{ij} = \sqrt{\sum_{k=1}^{S} \left(\frac{X_k^{(i)} - X_k^{(j)}}{X_k^{max} - X_k^{min}} \right)^2} \tag{5.24}$$

Where

S: the no. of the variables included in the optimizes

X_k^{max} and X_k^{min} respectively the upper and the lower bounds of variables of X_k

Phase 5: Trying multiplies epochs with the selection, crossover, and mutation until achieving the desired individuals for the new generation. Then we use the fitness values, which are the best and which are the worst, to rank the individuals, and use the ranking process to define the selection probability. Considering the individual at rank i:

$$\text{Probability}_i = \frac{1}{\|P\|} \left(2 - \alpha + (2\alpha - 1) \frac{i-1}{\|P\| - 1} \right) \tag{5.25}$$

Where α is the selection bias and its value between 1, 2; higher values for more directing the cursor on selecting only the well individuals. The best individual in the population is thus selected with the probability $\frac{\alpha}{\|P\|}$; the worst individual is selected with the probability $\frac{2-\alpha}{\|P\|}$. That procedure keeps the best individual in the new next generation.

Phase 6: Generation maximum number defines the stopping point of the system. Let z denote the bits number inside the chromosome and N population size as mentioned before, then the expected number of generations until convergence is,

$$E(N_G) = 1.4\, N\, (0.5 \ln(z) + 1) \tag{5.26}$$

This is valid for random mating with recombination but without selection and mutation. This procedure causes small selection intensities to decrease the probability to find the optimum. Reaching to the maximum number and achieving both function and constraints with the final best individual lead to end the procedure and prints the final result.

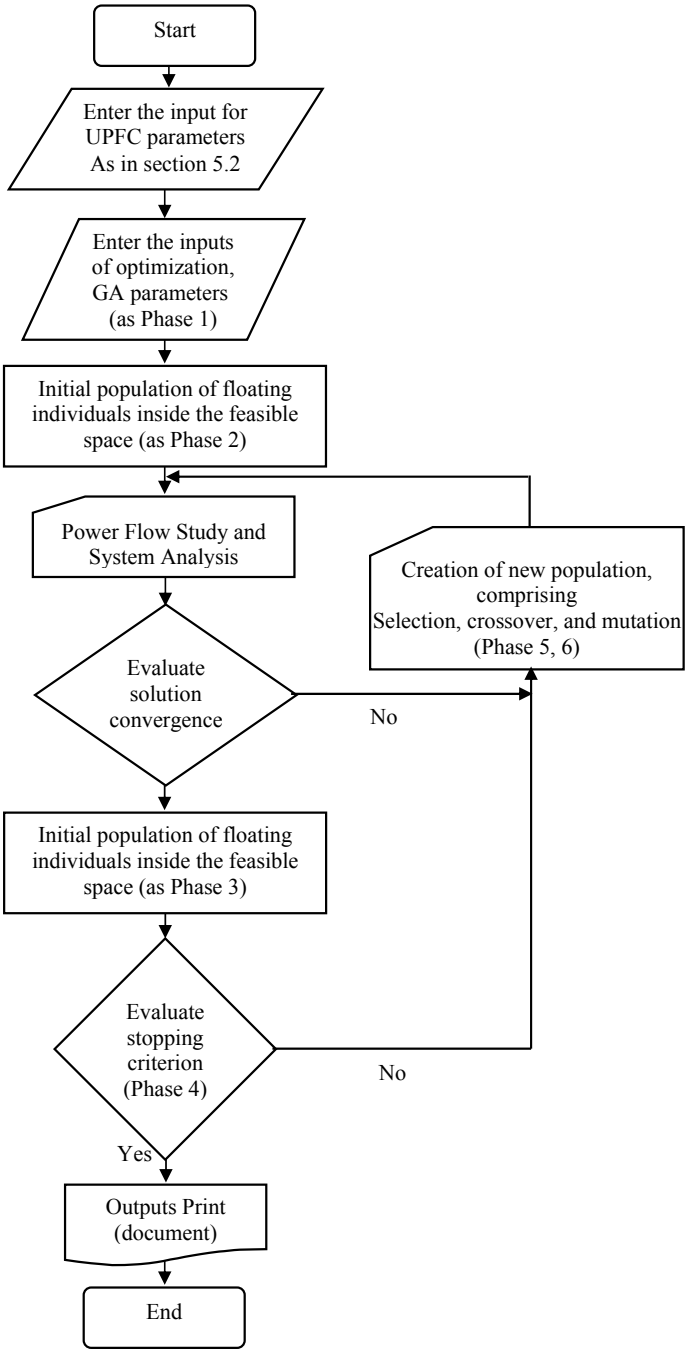

Fig. 5.5 Flowchart of optimization procedure for GA.

5.5 Scope on the Simulations Files (UPFC files , GA files)

Matlab programmed codes of GA (the main GA programming file, the fitness function and the constraints programming file) and a modified power flow algorithm to contain UPFC are established. M-files have been incorporated to contain the updates for adapt the algorithm based on the designed indices and terms. In addition, the automatic contingency analysis with performance indices and ranking the severity cases were developed and incorporated together for the simulation purposes. During the following sections, we will be concerned with the steady state data of the UPFC. That data affects the steady state performance of the UPFC and the power network; where the dynamics date will be concerned after in a later stage.

- **UPFC Data:**

% NUPFC : Number of UPFC's

% UPFCsend : Shunt converter's bus and series converter' sending bus

% UPFCrec : Series converter' receiving bus

%UPFCtln : UPFC Transmission Line Number (Insertion Location)

% Xcr : Inductive reactance of Shunt impedance (p.u.)

% Xvr : Inductive reactance of Series impedance (p.u.)

% Flow : Power flow direction

% Psp : Target active power flow (p.u.)

% PSta : control status for active power : 1 is on; 0 is off

% Qsp : Target reactive power flow (p.u.)

% QSta : control status for reactive power : 1 is on; 0 is off

% Vcr : Initial condition for the series source voltage magnitude (p.u.)

% Tcr : Initial condition for the series source voltage angle (rad.)

% VcrLo : Lower limit of series source voltage magnitude (p.u.)

% VcrHi : Higher limit of series source voltage magnitude (p.u.)

% Vvr : Initial condition to the shunt source voltage magnitude (p.u.)

% Tvr : Initial condition to the shunt source voltage angle (rad.)

% VvrLo : Lower limit of shunt source voltage magnitude (p.u.)

% VvrHi : Higher limit of shunt source voltage magnitude (p.u)

% VvrTar : Target nodal voltage magnitude to be controlled by shunt branch (p.u.)

% VvrSta : Control status for nodal voltage magnitude: 1 is on; 0 is off

- **Designed GA Program**

Table 5.2 the designed values for the GA parameters

GA Parameters	
Input Variables	x(1)= UPFCtln x(2)= Vcr(1) x(3)= Vvr(1)
Lower bound for Variables	LB = [1 1 0.001 0.8];
Upper bound for Variables	UB = [5 5 0.3 1.2];
Options. PopulationType	Double Vector
Options. PopulationSize	Adapted
Options. EliteCount	2
Options. CrossoverFraction	0.8
Options. MigrationDirection	Forward
Options. MigrationInterval	20
Options. MigrationFraction:	0.2
Options. Generations	200
Options. TimeLimit	Inf
Options. FitnessLimit	-Inf
Options. StallGenLimit	50
Options. StallTimeLimit	Inf
Options. TolFun	1e-6
Options. TolCon	1e-6
Options. InitialPenalty	10
Options. PenaltyFactor	100
Options. FitnessScalingFcn	‘Rank’
Options. SelectionFcn	‘Stochastic Uniform’
Options. CrossoverFcn	‘Scattered’
Options. MutationFcn	@mutationadaptfeasible

5.6 Dynamics Studies on the system (Concept and Building)

The unified power flow controller was proposed for flexible AC transmission systems applications. UPFC has various tasks, one of them as power flow controller. The secondary functions of the UPFC can be voltage control, transient stability improvement, oscillation damping, and others. UPFC can be very effective to damp power system oscillations.

Because FACTS devices have very fast dynamics compared to generators, they can play important roles in enhancing the dynamics response. This is usually accomplished through controls associated with theses devices.

Using a damping controller with the UPFC, it can enhance the electromechanical mode damping. That controller can be one of inherent UPFC PI damping controllers. UPFC main controllers can enhance system dynamics but first the dynamics parameters setting should be selected to damp and fine tuning the response. The damping controller for UPFC may affect the system response. The effect of different controllers as conventional and adaptive AI controllers can be compared to conclude the most effective controller.

The operating conditions can be changed according to the disturbance, which has an affect on the power system. In the steady state analysis section, we considered the increasing in loading conditions, which lead to a change from one certain operating condition to another operating point. In addition, we considered the contingency outage cases, which produce a loading increase in the power of all network elements.

For making stress on the correlation between the steady state and the dynamic analysis, we will consider the cases and the operating conditions from the steady state analysis. The steady state analysis leads to the importance of installing the UPFC in certain optimal locations with certain optimal settings. That may be considered as a comparison between installing and not installing the UPFC in the system. After we installed the UPFC at these optimal locations to achieve enhanced steady state performance, we should adapt the dynamic parameters to achieve also the optimal dynamic response, where UPFC at this location may not lead to prefect dynamics response. The mechanical modes of the generators in the system can be good indicator for the dynamic response; the speed deviation response ($\Delta\omega$) and the mechanical rotors angle dynamic response ($\Delta\delta$) can be shown.

The link between the steady state and the dynamic analysis can be achieved by considering the results from the steady state as a primary part to install the optimal UPFC in the system then we investigate the dynamics response analysis. Building and adapting the system configuration to be suitable for the dynamic response analysis will be achieved using the derivation and programming of dynamics equation in Chapter 4, Section 4.4 by m-file codes linked with simulink blocks models. Some scope on the dynamic model of UPFC and also dynamic model of multi-machine power system equipped with UPFC will appear in the Appendix section

5.6.1 Data for dynamics studying of UPFC installation

1- Synchronous Machine:

* Reactances d and q axis; steady state, transient and sub-transient

  $[X_d , X_d' , X_d'' , X_q , X_q' , X_q'']$.

* d and q axis time constants: (Short-circuit , Open-circuit)

  $[T_d' , T_d'' , T_{qo}'',\ldots]$.

* Stator resistance (R_s).

* Inertia coefficient, friction factor and pole pairs.

* Initial conditions [$\Delta\omega$, δ(deg), i_a, i_b, i_c ,ϕ_a,ϕ_b,ϕ_c(deg), V_{field}].

* Rotor Type : Salient-pole or Round.

2- Hydraulic Turbine and Governor:

* Servo-motor parameters [Ka , Ta].

* Gate opening limits [gmin , gmax , Vgmin , Vgmax].

* Permanent droop and regulator [Rp , Kp , Ki , Kd , Td].

* Hydraulic turbine settings [beta , Tw].

* Droop reference (0=power error , 1=gate opening).

* Initial mechanical power.

3- Excitation System:

* Low-pass filter time constant T_r.

* Regulator gain and time constant [K_a , T_a]

* Exciter parameters [K_e , T_e]

* Transient gain reduction [T_b , T_c]

* Damping filter gain and time constant [K_f , T_f]

* Regulator output limits and gain [E_{fmin} , E_{fmax} , K_p]

* Primary values of terminal and field voltage [V_{to} , V_{fo}]

4- ***Power System Stabilizer:***

* Sensor time constant

* Wash-out time constant

* Lead-lag time constant [T_{num} , T_{den}]

* Output limits [V_{smin} , V_{smax}]

5- Transformer Data:

* <u>Primary Winding parameters</u>:

Voltage, Resistance, Reactance, Magnetizing Resistance, Magnetizing reactance

* <u>Secondary Winding parameters</u>:

Voltage, Resistance, Reactance, Magnetizing Resistance, Magnetizing reactance

5.7 Importance of Dynamics Tuning

To show the importance of tuning the dynamic parameters of the UPFC, we will focus on a case study from the cases discussed before in steady state performance enhancing. In the previous cases, this stage concerned with enhancing the performance of the network related to the overloading of transmission lines and profile for violation of bus voltage. That task is performed on the normal configuration of the network at increasing the load pattern on the system until the year 2020. The results lead to optimal location and optimal settings of UPFC to be installed to achieve the required performance.

After installing the UPFC at these optimal locations with optimal settings, the dynamic parameters of the UPFC will have a significant effect on the dynamic response specially the mechanical variables response as the speed deviation response ($\Delta\omega$) and the mechanical rotor angle dynamic response ($\Delta\delta$) of the generating units. The dynamics parameters for the UPFC blocks should be well selected and be set to fine tune the response and damp the oscillation and enhance the settling time of the response.

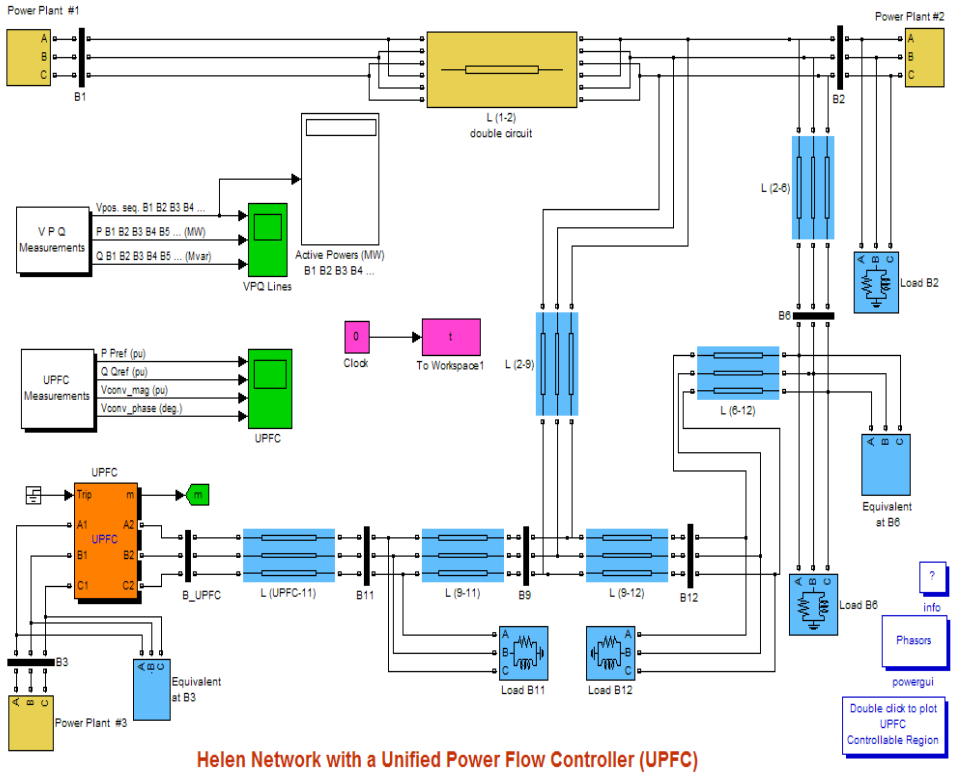

Fig. 5.6, Dynamic blocks for section of a real Finnish Network.

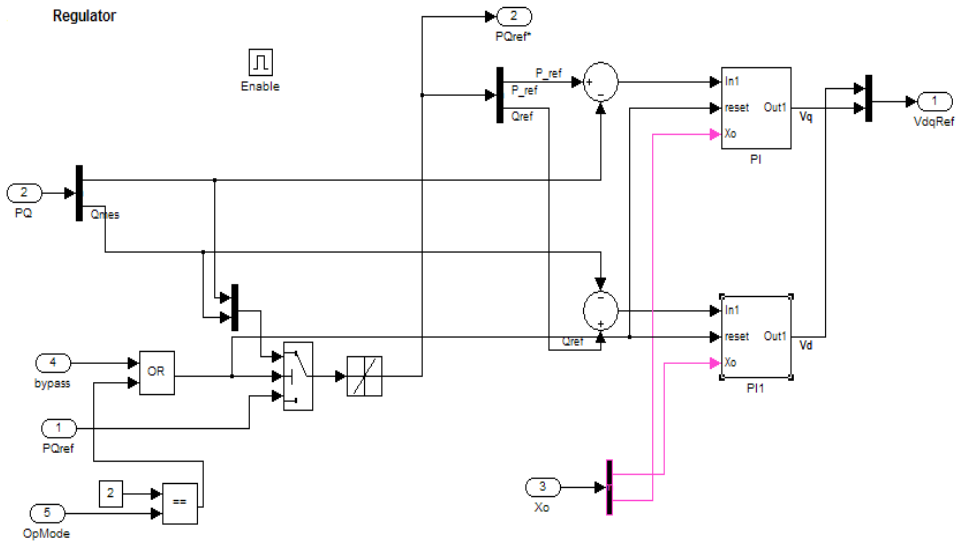

Fig. 5.7, General Structure for Dynamic Blocks for UPFC regulator (UPFC controller).

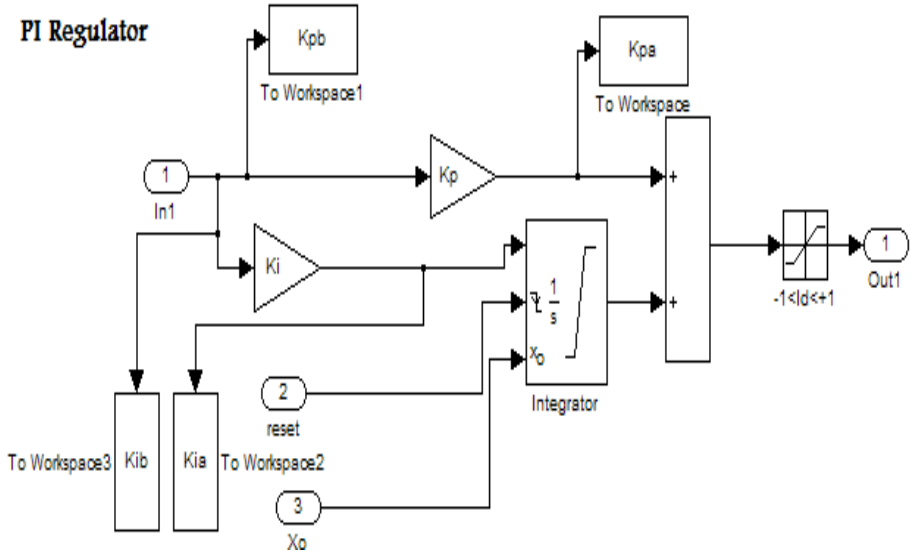

Fig. 5.8, Inherent Dynamic Blocks for UPFC regulator (UPFC controller).

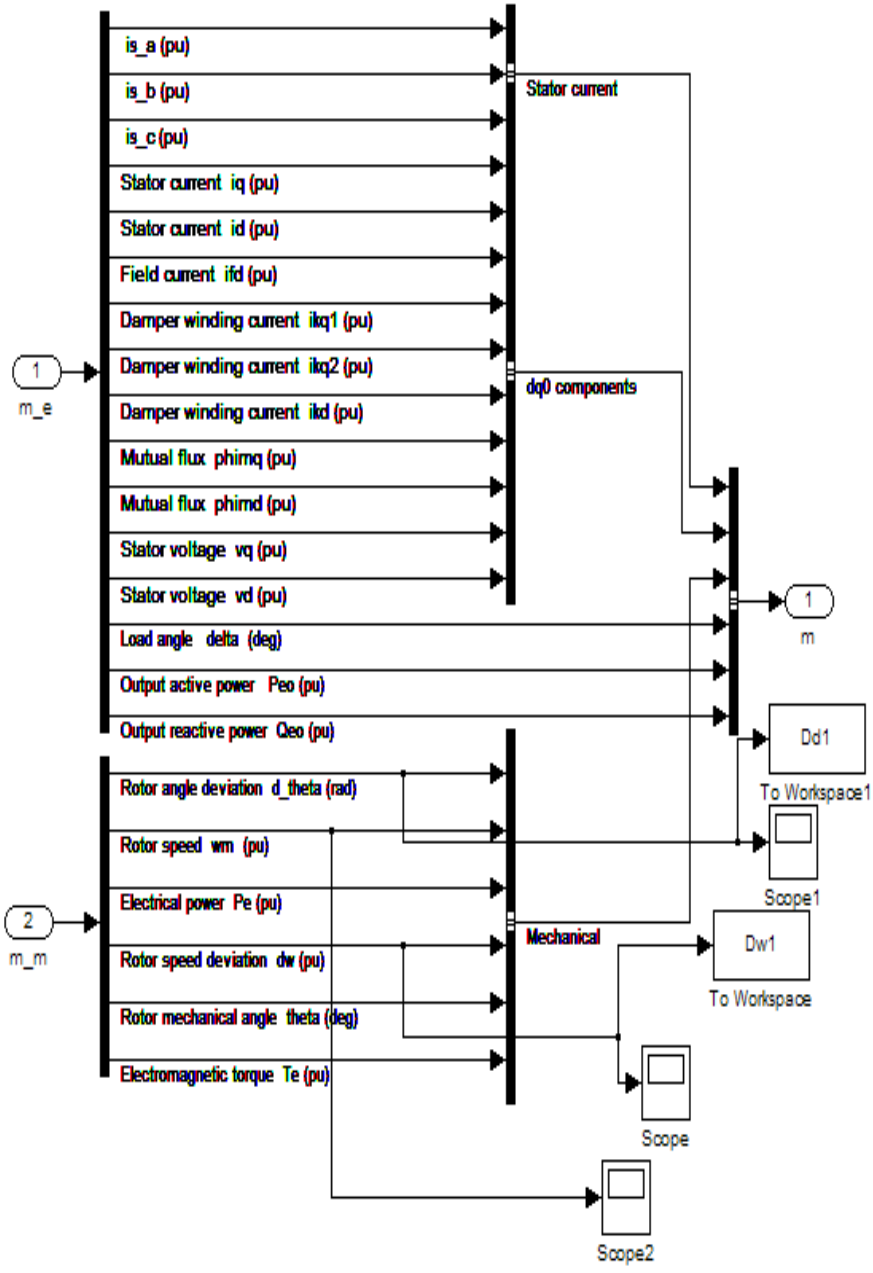

Fig. 5.9, Measurement variables prepared for Dynamic response.

The dynamic response of the mechanical variables as the speed deviation response (Δω) and the mechanical rotor angle (Δδ) of the generating units will be varied according to the adjusting of the dynamic parameters of the UPFC.

Some examples of the dynamic response for various operating cases with related UPFC dynamic parameters will show the improtance of getting the significant setting of that parameters to enhance the dynamic response.

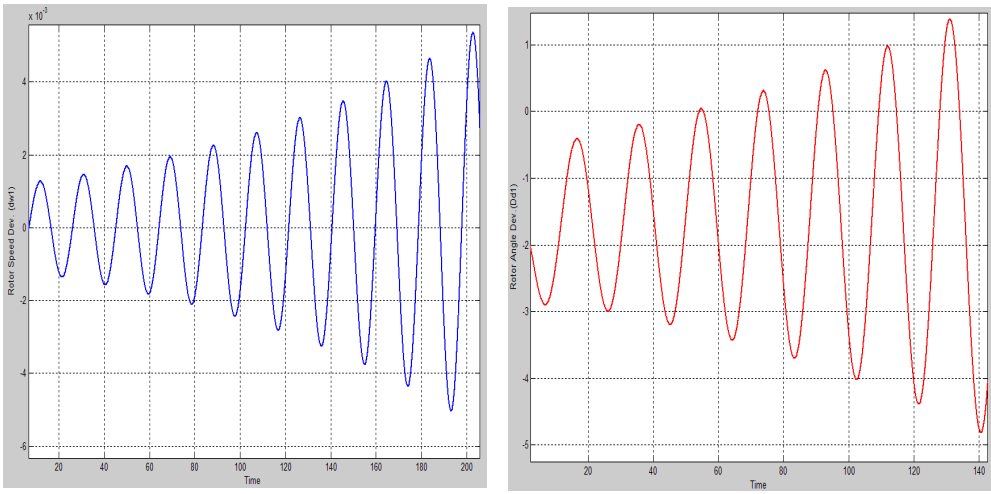

Fig. 5.10, Increased Instability Dynamic Response.

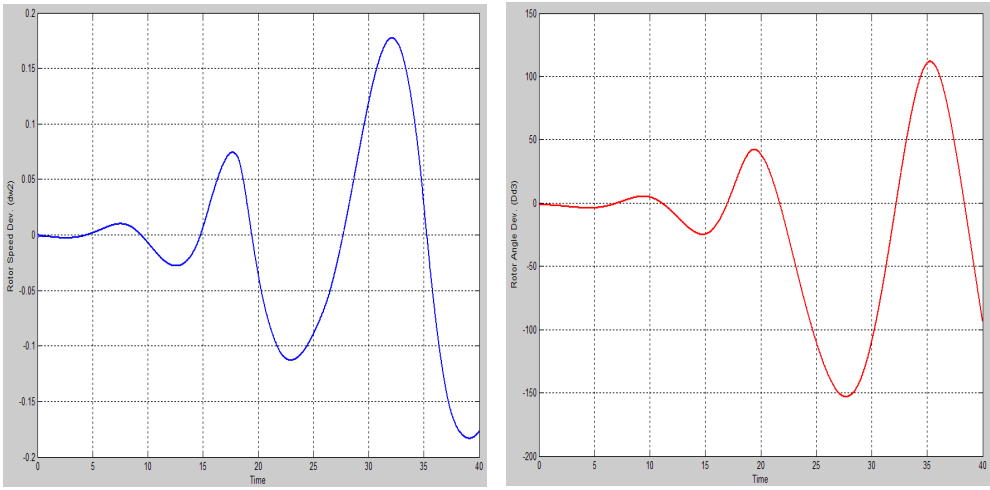

Fig. 5.11, Fast Instability Dynamic Response.

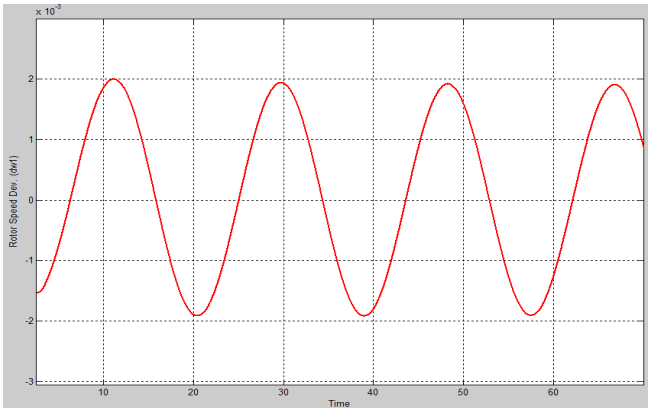

Fig. 5.12, Critical Stability (Naturally Damped) Dynamic Response.

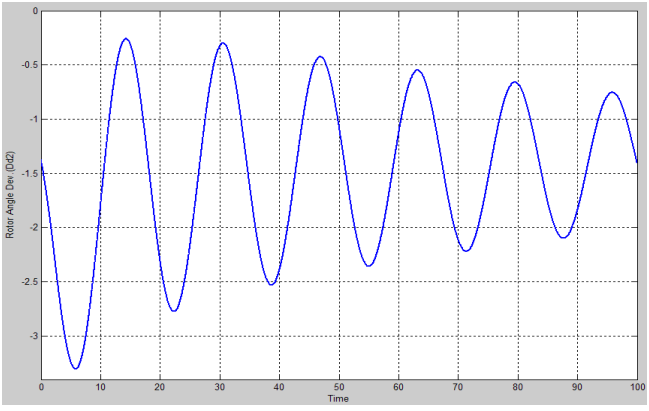

Fig. 5.13, High-Timed Damped Dynamic Response.

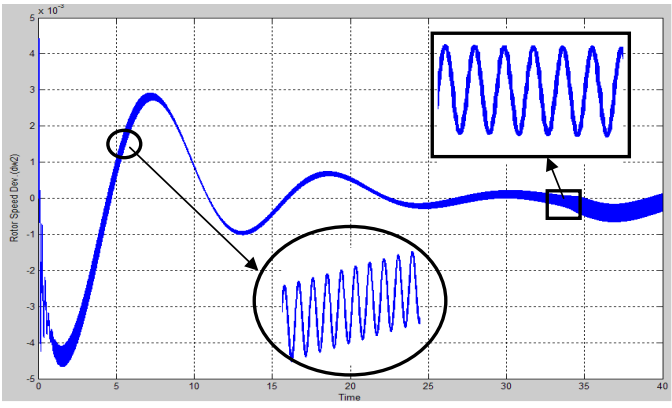

Fig. 5.14, High Oscillatory Dynamic Response.

5.8 Conventional PI Controller

The modelling of a PI controller can be considered mainly in software such as Simulink using Laplace operators:

$$C = \frac{G(1+\tau s)}{\tau s} \tag{5.27}$$

Where

G = Kp = proportional gain

G / τs = Ki = integral gain

G value set is usually varied between decreasing overshoot and increasing settling time, also finding a proper value for τs is an iterative process. The problem with using a PI controller is careful design considerations with respect to the gain must be considered.

- Proportional term

In the case of high value for the proportional gain, the performance can act in unstable mode. In the opposite situation, a small gain causes a small output performance to a large input difference, and a less sensitive controller. When the proportional gain is very low, the control action can be very small at occurence of network disturbances. Both tuning theory and industrial practice show that it is the proportional term, which should lead to the significant of the output change.

- Integral term

The goal of the integral part is proportional to both the value of the error and the time of the error. The magnitude of the integral part to the resultant control action is calculated using the integral gain (Ki). The integral part enhaces the motion speed in the direction of the set-point and minimizes the steady-state error that happens with only the proportional controller. However, the integral term is related to accumulated errors at the past, it may lead to the current value to overshoot the set-point.

- Loop tuning

The selection process of the PI controller parameters, which are the proportional and integral gains, should be chosen in a proper way that makes the controlled process more stable. Control loop tuning is upgrading the control parameters for the optimal values to the required control performance.

Stability of response is always required and the system must not oscillate under any circumstances. Increasing the value of the proportional gain, Kp, will make faster response, and more proportional term compensation. An increase in the proportional gain will direct to instable and oscillated behaviour. With respect to integral gain, Ki, larger values imply steady state errors are fast minimized. An integral control (Ki) will affect on eliminating the steady-state error, but it may worse the transient response.

There are many traditional manual techniques for tuning a PI loop. The most efficient techniques essentially have the investment of some phases of the process model, then select

P and I according to the parameters of dynamic model. Tuning methods by manual way may be inefficient.

The most effective tuning method has the effect of applying a step change in input to the system, evaluating the output as a dependent of time, and applying this response to calculate the control parameters.

- Manual tuning

The procedure to keep the system online starts with selecting one tuning method to set Ki values to zero. Larger the Kp value until the output oscillates, and then the Kp can be set to be roughly half of this value for a quarter amount decay response. And then raises Ki to any offset is proper in enough time for the process. We should note that too much Ki will lead to instability.

The tuning of the PI settings is quite a subjective procedure, depending mainly on the skill and experience of the control engineer and operator. Although tuning guidelines are available, the process of controller tuning takes some time with the result that many plant control loops are improperly tuned and the complete effect of the control system does not occurr.

Table 5.3 shows the effects of increasing a parameter independently on the system dynamics response.

Table 5.3 Effects of increasing a parameter independently

Parameter	Rise time	Overshoot	Settling time	Steady-state error	Stability
Kp	Decrease	Increase	Small change	Decrease	Degrade
Ki	Decrease	Increase	Increase	Decrease significantly	Degrade

Referring to the tables, these correlations may not be exactly accurate, because Kp and Ki are dependent on each other. In fact, altering one of them can change the effect of the another one. For this reason, the table should only be used as a reference when calculating the values for Ki and Kp.

- PI tuning software

Various modern industrial options no longer tune loops using the manual procedure shown above. Instead, PI tuning and loop optimization software is applied to achieve the desired results. These software packages will collect the information, develop process models, and suggest optimal tuning.

An impulse tuning is produced by a mathematical PI loop during the process, and then uses the controlled process's frequency response to get the PI loop values. The response times which take some minutes, mathematical loop tuning is better, due to trial and error can spend a long time just to get a stable group of loop values. Optimal values are more difficult to reach. Some digital loop controllers save self-tuning attributes in which very small set-point changes are activated in the process, leaving the controller itself to determine values of the optimal tuning. Other methods are possible to tune the loop related to different performance criteria.

5.9 UPFC Dynamic Controller

The shunt converter of UPFC operates as a STATCOM. The shunt converter governs the AC voltage of the terminals and the voltage of the DC bus. It uses a dual voltage regulation loops, where the inner current control loop and the outer loop regulating AC and DC voltages. The control system includes:

• A phase-locked loop (PLL) which handles the positive-sequence item of the three-phase AC voltage. The output of the PLL is applied to calculate the d-axis and q-axis items of the AC three-phase voltage and currents.

• Measuring devices for the d-axis and q-axis parts of the currents and voltages of AC positive-sequence to be under control like the DC voltage Vdc.

• An external regulation loop, with AC and DC voltage regulator.

• An internal current regulation loop has a current regulator.

That regulator controls the voltage supplied by the PWM converter. Control of the series branch inside a UPFC has two levels of functions where it is applied to control the active power and the reactive power. Figure 5.15 shows a schematic diagram of the series converter.

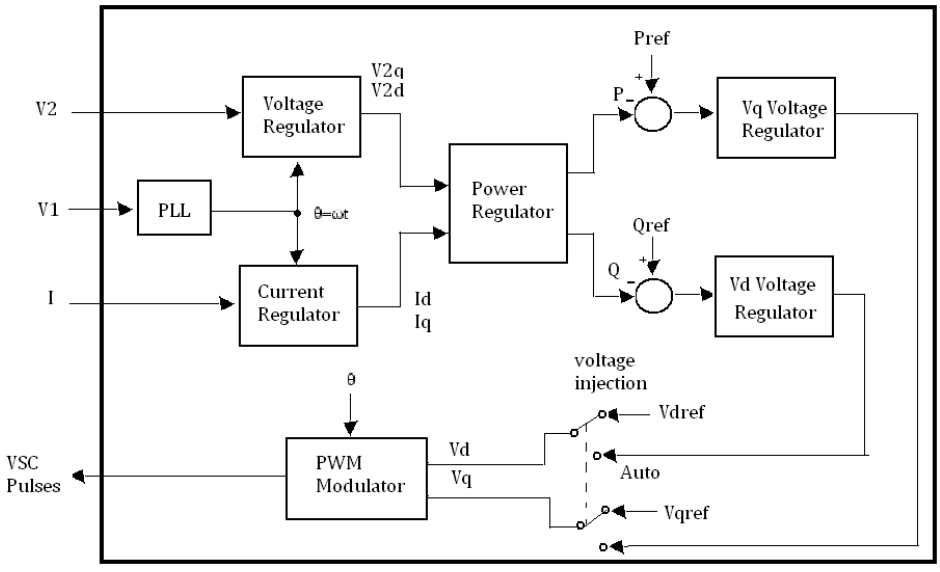

Fig. 5.15, Blocks Connections of the Series Converter Control System.

The series converter can work controlling the power flow and also in voltage control mode. During the power control mode, the real active power and reactive power are compared with reference values to generate P and Q signal errors. The P error and the Q

error are used by two PI regulators to get respectively the Vq and Vd parts of voltage to be applied by the VSC.

The analysis of a real Finnish Network during all the previous power flow studies and the corresponding results showed that the network has an efficient topology which is well tied and interconnected that made it always has no effectivly dangerous problems in its voltage profile. Under most operating conditions, the voltage of the majority of the system buses has high significant values near the required base values. So most of the problems which face the network are due to the power flow in the lines, not in the voltage profile of the buses. These options direct us to focus on examining the control elements, which mainly have a contribution and effect on the line power flow. According to the former statements, there are many control elements as Vac Regulator, Vdc Regulator and Power regulator and more. The most effective one on the power flow and its dynamics is the power flow regulator. So the main concerned control element will be inside the series SVS part to control the power flow which will be a power PI regulator containing Integral gain (Ki) and proportional gain (Kp).

We will try to adjust the values of the power PI regulator containing Integral gain (Ki) and proportional gain (Kp) to reach to optimum dynamic response. First we will use the conventional method described in the previous section to tune the parameters values of the PI controller. Then we will apply the Artificial Intelligence techniques to get the optimal tunning of the PI controller parameters values; this gives us all the options and benefits which are available in the AI concept and the controlling will gain process the required adaptivity, flexibility and intelligent characteristics.

5.10 Why AI?

In recent years, AI concept applications are appeared in an increasing attention in many sections of power networks such as planning, control and operation.

AI concepts own an important role in power network control and management. The electric power industry is always looking for methods to enhance the performance efficiency. Although the conventional concepts of power generation, transmission, and distribution vary in slow rate, the power industry moves quickly to explore new ideas, which can assist the search to show benefits.

The main description owns an effect on the layout of many artificial intelligence systems. Expert planning systems, artificial neural networks, fuzzy logic algorithms, genetic algorithms are applied almost AI benefits in at least prototype form to one or more problem applications in the power networks, and new practical uses of AI are with increasing frequency. In other cases, AI options vary existing techniques. In others, AI options give solutions to problems previously shown only by natural intelligence, creating new computers applications.

A number of research articles which have appeared recently indicate the applicability of AI methods to power networks for wider operating cases with uncertainties. Most of these methods are still under researching, however, there already current many practical applications of AI systems.

Because of multiple AI systems, they can be applied as a general methodology to provide knowledge or theory into controllers and decision makers. There are analytical solution techniques for power system problems. However, the mathematical formulations of power systems problems are derived during specific restrictive assumptions and even with these assumptions, the solution of large-scale power system problems is not simple.

On the other hand, there are various uncertainties in power system problems, due to those power systems are large-scale, complex, wide spread in geographical places, and affected by unplanned conditions. These reasons lead to difficultly in handling many power systems problems through strict mathematical formulations alone.

Therefore, the AI approach has emerged in recent years as a complement tool to mathematical approaches for solving power system problems. Since expert knowledge, experience, and intuition are essential in power systems operations, AI can be effectively used in power system problems to represent uncertainties based on preferences and/or experience.

Artificial intelligence (AI) analysis depends on the past history data of a system, the designer should understand and appreciate this data than other theoretical and experimental ways. AI can be used to give innovative methods of solving design applications and can make designers to find an almost instantaneous expert opinion on the effect of a proposed change in a design.

Figure 5.16 shows the percentages of some significant AI researches on applications to power systems.

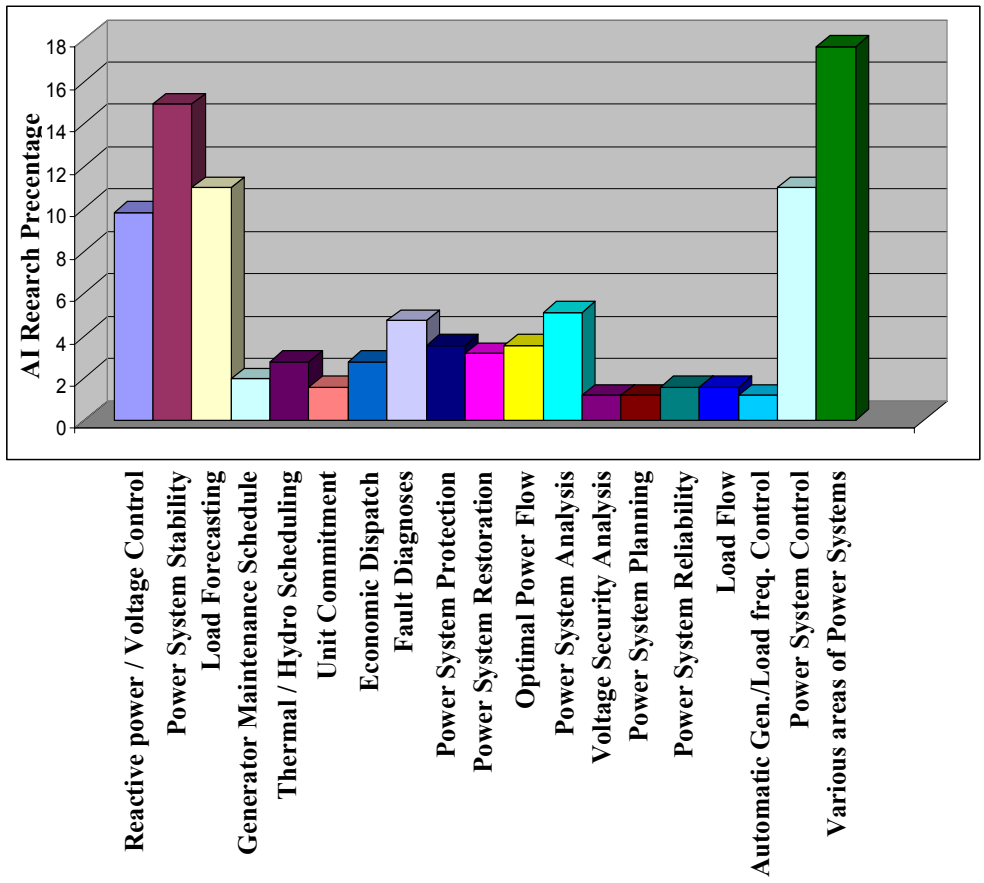

Fig. 5.16 Some Applications of AI in Power Systems [83].

5.10.1 Why GA with ANFIS?

Adaptive control is the updating of controller parameters online based on the changes in system operating conditions. Adaptive controllers based on analytical techniques can save wonderful response and enhance the dynamic performance of the plant by allowing the parameters of the controller to adapt the operating conditions change. Proper care is required to let them be robust, especially under large disturbances. Controller robustness can be enhanced by applying artificial intelligence (AI) techniques. It is available to achieve the entire algorithm using AI techniques or integrating analytical and AI techniques for executing some tasks using analytical approach and the rest using AI techniques.

The main benefit in using the genetics algorithm is the ability of GA to reach the optimal solution, which guarantee that if the GA is well self designed and trained that will lead to the most achieved level from the desired performance for the system under any problem space. About the Adaptive Neuro-Fuzzy Inference (ANFIS), we can first state that ANFIS is a merging system between the neural network system and fuzzy logic system. Therefore, it has the resultant benefits of both systems. The fuzzy system is a very efficient tool in the controlling actions and the neural networks (NN) are powerful in patterns classifications and patterns recognitions. The NN can be merged with the fuzzy system to adapt the parameters of the fuzzy systems to reach the best collection of fuzzy parameters leading to the required controlling procedure. Therefore, we get the positive options from each AI system and merge them to get the global benefits.

- **Why Fuzzy Logic?**

a list of general features about fuzzy logic:

- Fuzzy logic is basically easy to understand.

The theory behind fuzzy learning is very clear. Fuzzy logic is a better in self-evident methods without complex concepts.

- Flexibility of Fuzzy logic.

In any specific process, it is simple to apply on more flexibility without working from scratch.

- Fuzzy logic has more clearance to deal with imprecise data.

when we work closely enough, everything may be considered imprecise but not always, many issues are imprecise even on care inspection.

- Fuzzy logic can deal with nonlinear complex functions.

We can design a fuzzy system to any pattern of input and output data. This process is used particularly simply by adaptive methods as (ANFIS) systems.

- Fuzzy logic can be integrated with traditional control techniques.

Fuzzy systems do not necessarily exchange traditional controllers. In most situations, fuzzy systems link with them and enhance their implementation.

- Fuzzy logic building depends on natural language.

The core of fuzzy logic is the core of for people communication. This concept explains many features about fuzzy logic. Because fuzzy logic is structured on the structures of normal language description used in our life, the fuzzy logic algorithm is easy to apply.

- **Why Use ANFIS?**

The fuzzy logic has processed only certain membership functions that were selected at the beginning of the design. The fuzzy system is used to only handling processes, those have rules are basically determined by the user's design of the features of the variables in the system.

During the fuzzy logic design, the shape of the membership functions is based on parameters, and altering these parameters alters the shape of the membership function. In some modeling cases, we can select the shapes of the membership functions simply from looking at data. Considering selecting the parameters with respect to a specific membership function initially, those parameters can be chosen to tailor the membership functions to the input and output pattern for those kinds of values variations in the data. In such situations, we can apply the Neural networks; neuro-adaptive learning techniques (ANFIS) to allow a way for the fuzzy modeling process to learns information about a data set and to calculate the membership function parameters, which allow the best associated fuzzy inference to reach the given input and output pattern.

The ANFIS establishes a fuzzy inference system (FIS), which has membership function parameters that are updated. This updating permits fuzzy systems to know from the data that are modeled. The parameters of the membership functions change through the learning process. A gradient vector processes the updating of these parameters. This gradient vector saves a judge of the quality of the fuzzy inference system by handling the input/output data for a certain group of parameters. When the gradient vector occurrs, various optimization actions can be used in order to update the parameters to minimize some error measure.

- **Why Use GA?**

The genetic algorithm is a technique for solving optimization problems that depend on natural selection, the procedure that simulates biological evolution. The genetic algorithm repeatedly adapts a population of individual solutions. In each phase, the genetic algorithm chooses individuals randomly from the exist population to be parents and uses them to generate the children at the next generation. By next generations, the population flows toward an optimal solution.

We can use the genetic algorithm to solve many optimization problems that are not solved by standard optimization algorithms, especially problems, have an extremely nonlinear objective function.

5.10.2 Construction of the adaptive intelligent Controller

ANFIS will be used in this work to adapt the dynamic controllers' gains of the UPFC controllers in real time. Before ANFIS can be used, it is necessary to determine a proper set of training patterns. Each training pattern comprises a set of input data and corresponding output data. For UPFC controller, an ANFIS will be designed to update its gains. The inputs for ANFIS will be the desired line active power and line reactive power, and also the operating line active power and line reactive power.

To obtain this data, the operating conditions of the power system is varied covering the situations of light loaded system (25 % of the normal loading) to 150 over loading. Also conditions such as different generation levels are included. The training data contains the

training patterns obtained by GA for ANFIS. The GA feeds the ANFIS with the training patterns. The GA itself has been trained and designed well to guarantee the achieving and validation of the data [84]. That procedure gives the controller high power characteristics; where it focuses on the optimal solutions using the inherent structure of the GA system. Another power characteristic of the proposed controller is that ANFIS has the option to cover very wide operating conditions and it continuously adapts itself where there some operation conditions that GA cannot reach, the ANFIS can reach in fast action. In addition, the connection between the GA and ANFIS achieves that each one of them corrects and helps the another one where each one can be considered as a checker tool for its neighbor system.

The structure of the adaptive controller can be presented in working layers. As the neural network layer can be considered as co-operative with the fuzzy logic layer to construct the ANFIS system. Where the genetics algorithm system is a co-operative layer for the totally ANFIS system as a pre-training tool, it provides the ANFIS with the training patterns. The above structure can be indicated in the following Figure 5.17, which gives more details about the connection and link between the adaptive controller sections.

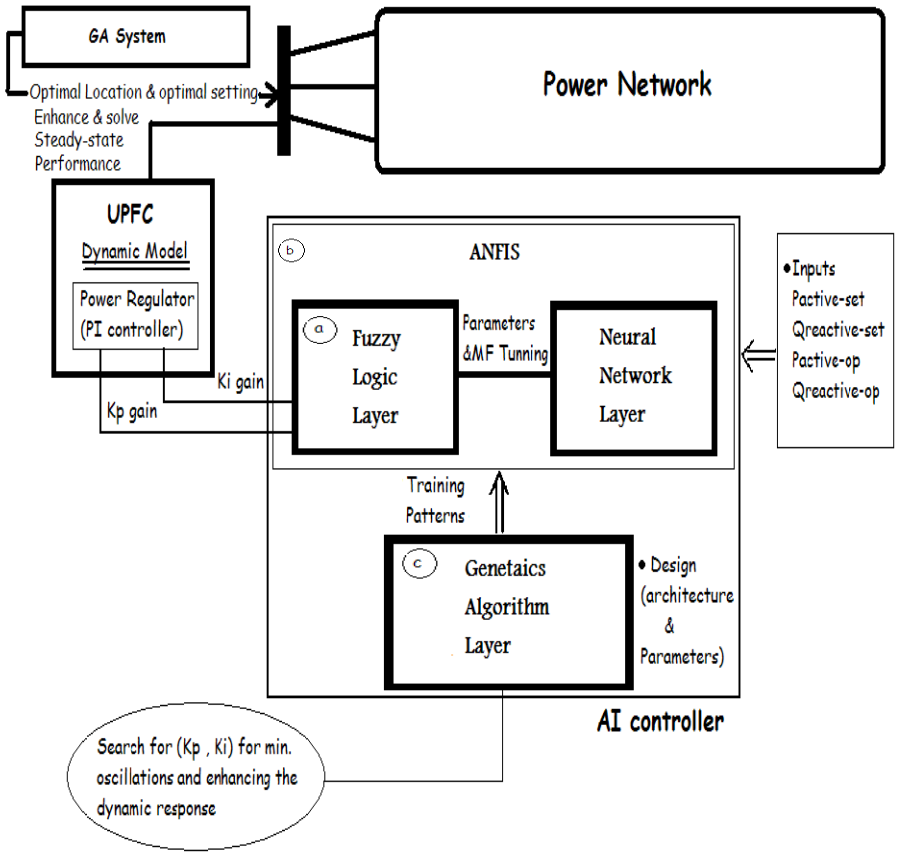

Fig. 5.17 Structure of UPFC adaptive controller.

More details of the inherent structure of the blocks and systems in the general structure of the adaptive controller can be indicated in the following figures.

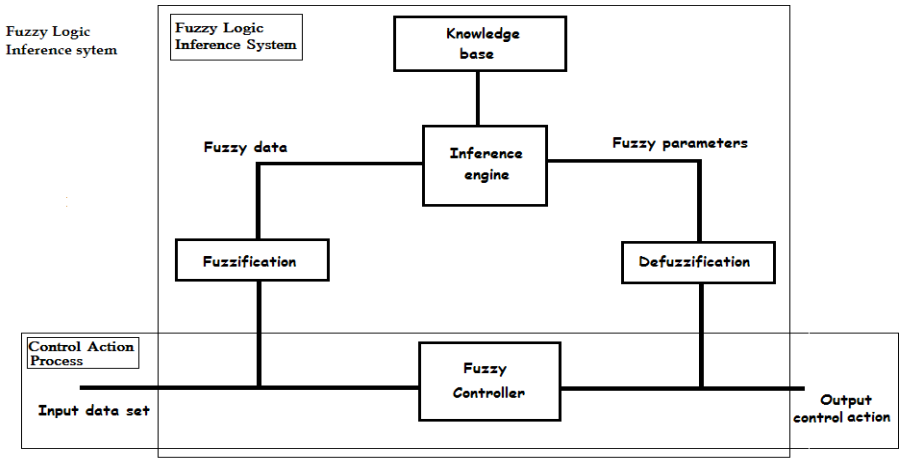

Fig. 5.18 Structure of Fuzzy logic control, section (a).

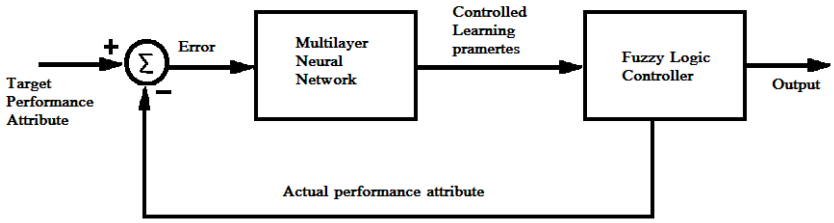

Fig. 5.19 Fuzzy Logic controlled multilayer neural network, section (b).

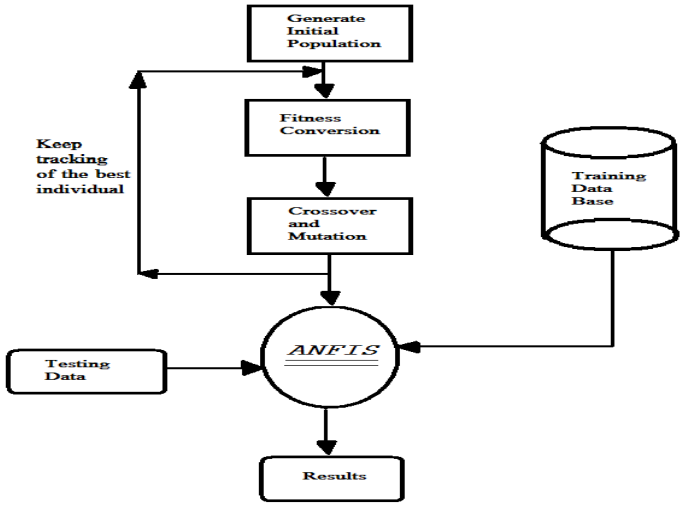

Fig. 5.20 Genetic algorithm linked ANFIS, section (c).

The following flow charts indicate the algorithms of the ANFIS procedure for designing, training and testing. In addition, it shows section of the genetic algorithm, which describes the fitness function.

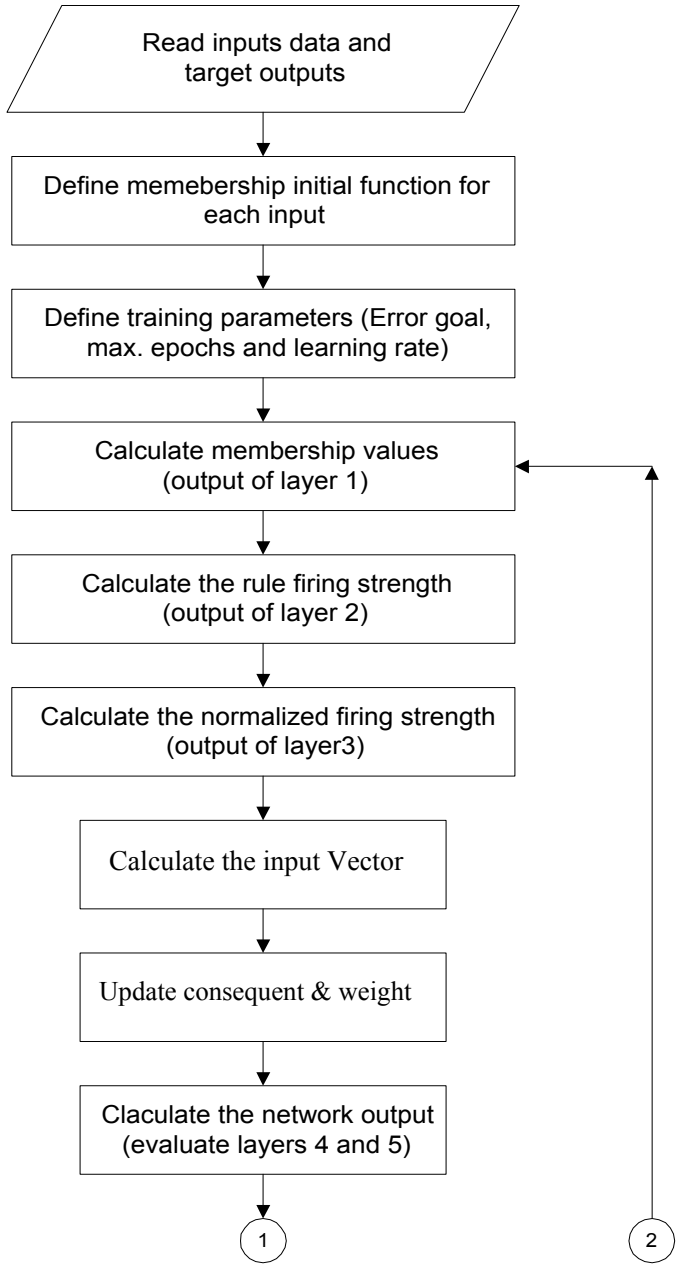

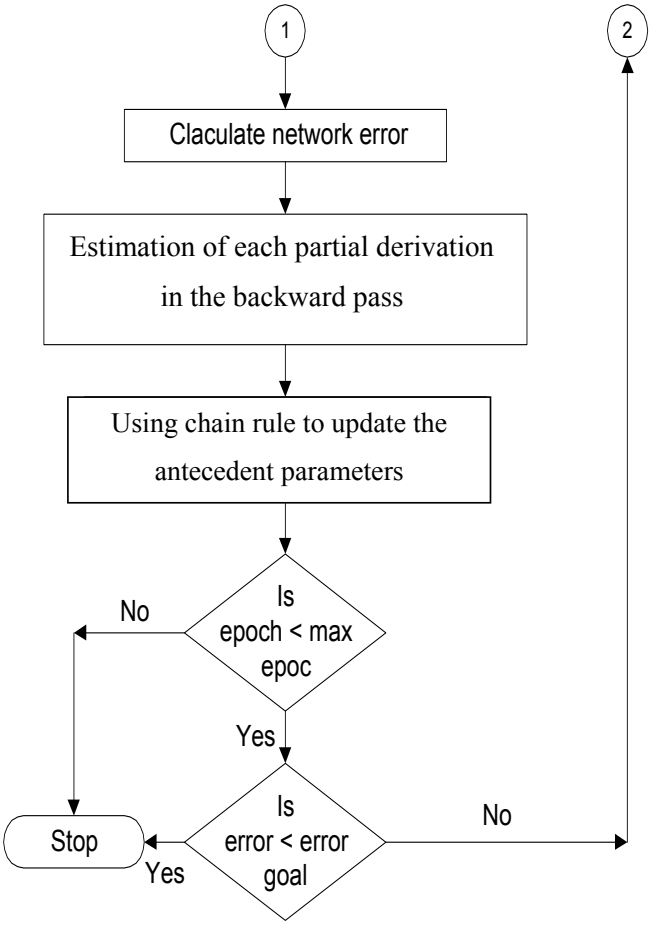

Fig. 5.21 ANFIS Flow chart structure.

Referring to Chapter 3, it describes all the details about ANFIS. Definitions, parameters, equations, relations and procedure sequence are indicated.

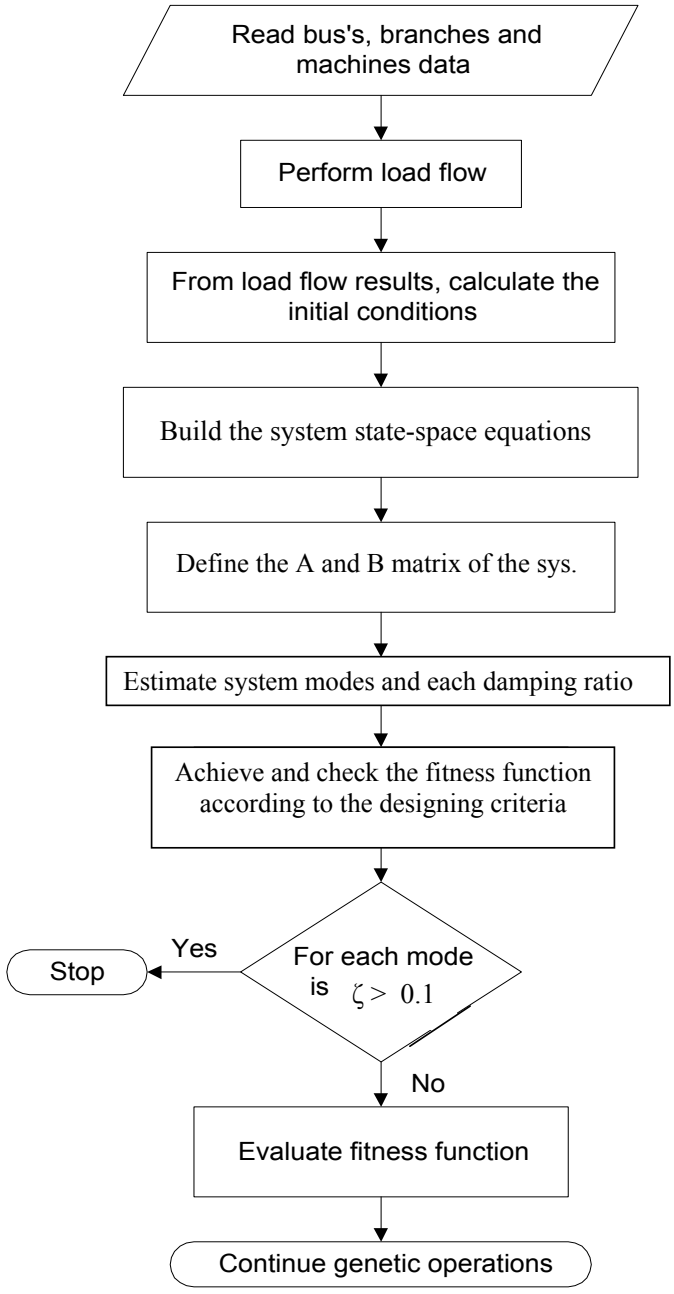

Fig. 5.22 Flow chart for genetic algorithm, describe the fitness function

- **GA System.**

The Genetic algorithm is used to tune the parameters of the P-I controller to obtain the optimal dynamic response for the system. The fitness function of the genetic controller is to minimize the difference between the required designed performance and the current actual performance

$$\text{Fitness function} = Min\left[\beta * e^{-\alpha * t} R_i(X,U) - R_i(X,U)\right] \qquad (5.28)$$

Where

$R_i(X,U)$: The current actual performance of the dynamic variable *i*

$\beta * e^{-\alpha * t} R_i(X,U)$: The required designed performance; damped performance of the dynamic variable *i*. The dynamic variable are the variables as the speed deviation response ($\Delta\omega$) and the mechanical rotor angle ($\Delta\delta$) of the generating units and others, which will be varied according to the adjusting of the dynamic parameters of the UPFC.

U : The designed control variables, the parameters of UPFC controller.

β *and* α : parameters used for Tuning the controller issue.

According to the operating conditions, you can add some constraints:

- Damping ratio for all modes is not less than 0.1.

- The searching space of K_P and K_I is between ± 3.

One of operating patterns, Floating point GA with a maximum generation number of 200, population size of 20 and a shape parameter b = 3 is used. The solution converged after 120 generations to K_P = 0.02421 and K_I = 0.4514. The fitness function versus the generation number is shown in Figure 5.23, Because GA minimizes the difference between the required designed performance and the current actual performance, system response with GA based damping controller is a superior based UPFC controller.

The results show the ability of the UPFC to improve power network performance by controlling the power flow. The GA controller is applied to make the UPFC more flexibility and to raise its ability to damp the oscillations of the power system; where the GA technique is used for tuning of UPFC.

GA will search the parameters space (K_P and K_I) to find the optimal values of the damping controller gains to achieve the fitness function. The floating point GA with maximum generation number of 200 is used. The solution converged after 120 generations to K_P and K_I, these parameters will applied to the system to realize the required dynamic performance.

Table 5.4. Designed values for the GA

GA Parameters	
Input Variables	x(1)= K_P x(2)= K_I
Variables Lower bound	LB = [-3 -3];
Variables Upper bound	UB = [3 3];
Options. PopulationType	Double Vector
Options. PopulationSize	20
Options. EliteCount	Adapted (in the simulations)
Options. CrossoverFraction	Adapted (in the simulations)
Options. MigrationDirection	Forward
Options. MigrationInterval	20
Options. MigrationFraction:	0.2
Options. Generations	200

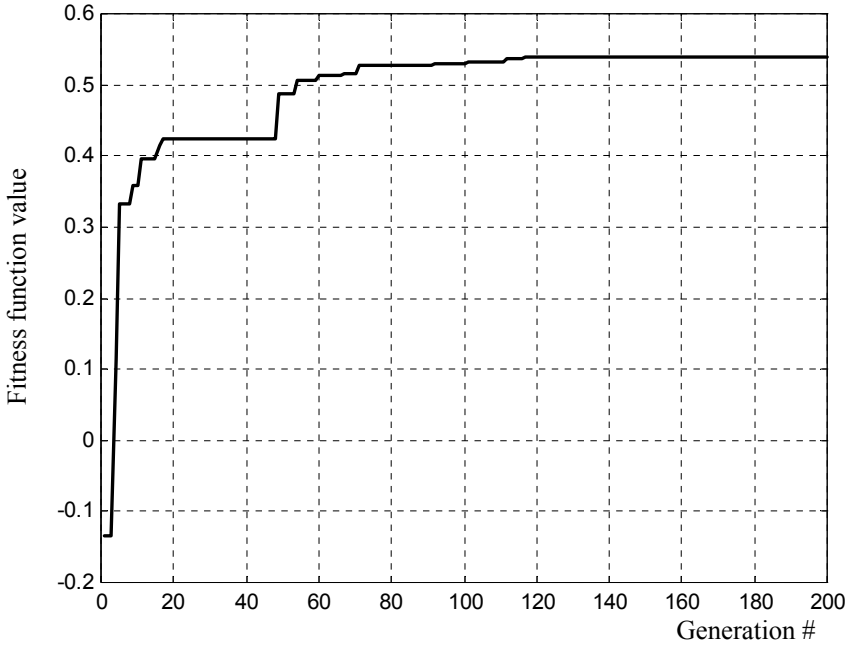

Fig. 5.23, Variation of the fitness function with the generations.

- **ANFIS System.**

In reality, the operating conditions change with time and, as a result, the dynamic performance of the system will change. Thus, to maintain good dynamic response under all possible operating conditions, the controllers' gains need to be adapted based on system operating conditions. ANFIS will be used in this work to adapt the controllers' gains of UPFC controllers in real time. Before ANFIS can be used, it is necessary to determine a proper set of training patterns. Each training pattern comprises a set of input data and corresponding output data. The inputs for ANFIS will be the line active and reactive power (current operating and settled).

For input patterns, we can proceed to determine a set of PI controllers' gains using GA, and the results are employed as the ANFIS outputs. To obtain this data, the operating conditions of the power system is varied covering the situations of light loaded system (25 % of the normal loading) to the highest loading of Year 2020. In addition, conditions such as different generation levels are included.

Trials should be done to choose a suitable number of membership functions to represent the inputs. A low number of membership functions leads to bad learned network, and high error in the network outputs, while a high number of membership functions leads to a complicated structure, to many parameters which have to be updated and a long training time. Input data is represented by a different number of membership functions and finally each input universe of discourse is represented by gaussian membership functions. The training algorithm is used with the following training parameters: learning rate (η) = 0.0001:0.0006, error goal of 0.05 and maximum epochs of 3000. There will be a noticeable change in the membership functions levels before and after training, the training process of adapting the shape and the number of membership functions during the training epochs.

The following figures will indicate the structure and the procedure of the ANFIS system.

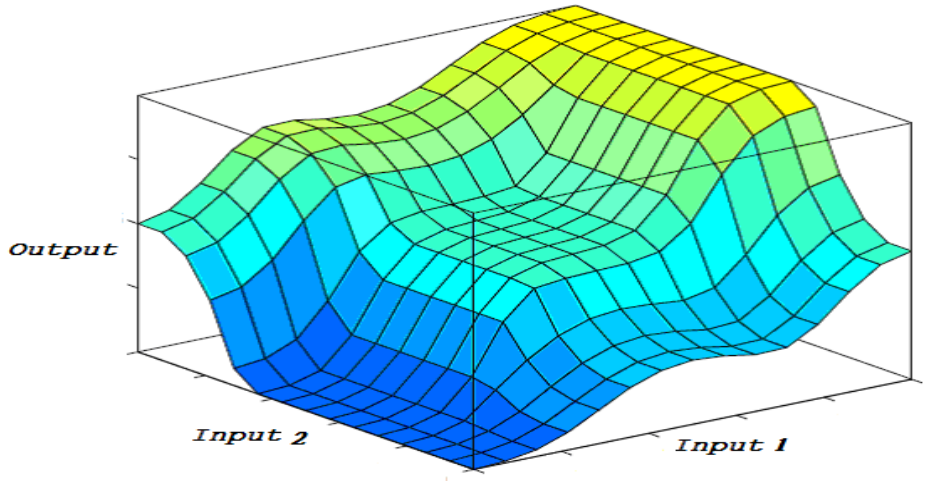

Fig. 5.24 Surface 3D for some input/output relations of ANFIS system.

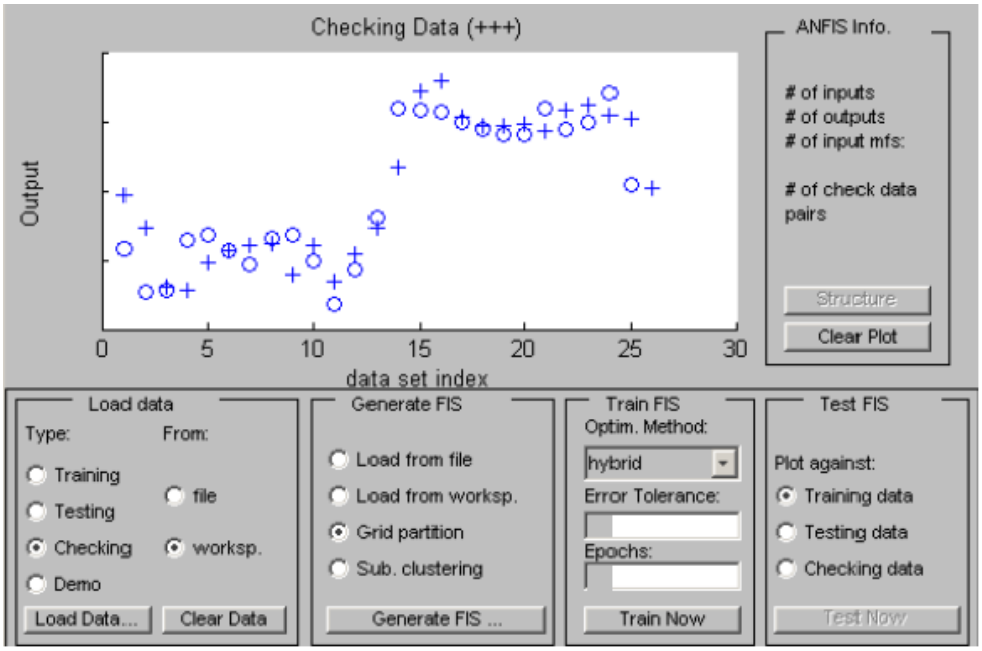

Fig. 5.25 Samples of the training Data, checked and training.

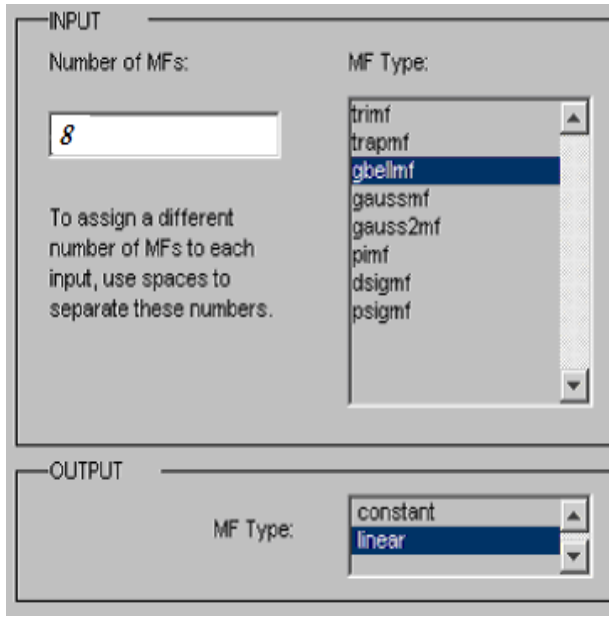

Fig. 5.26 Initial Membership number and shapes for one of inputs.

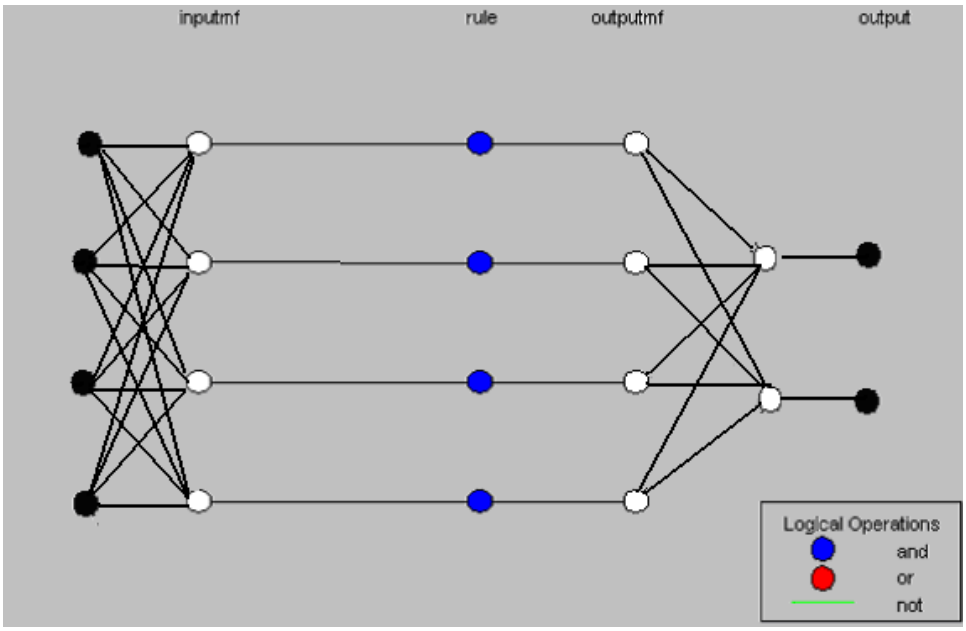

Fig. 5.27 Initial structure of the connected training neural network.

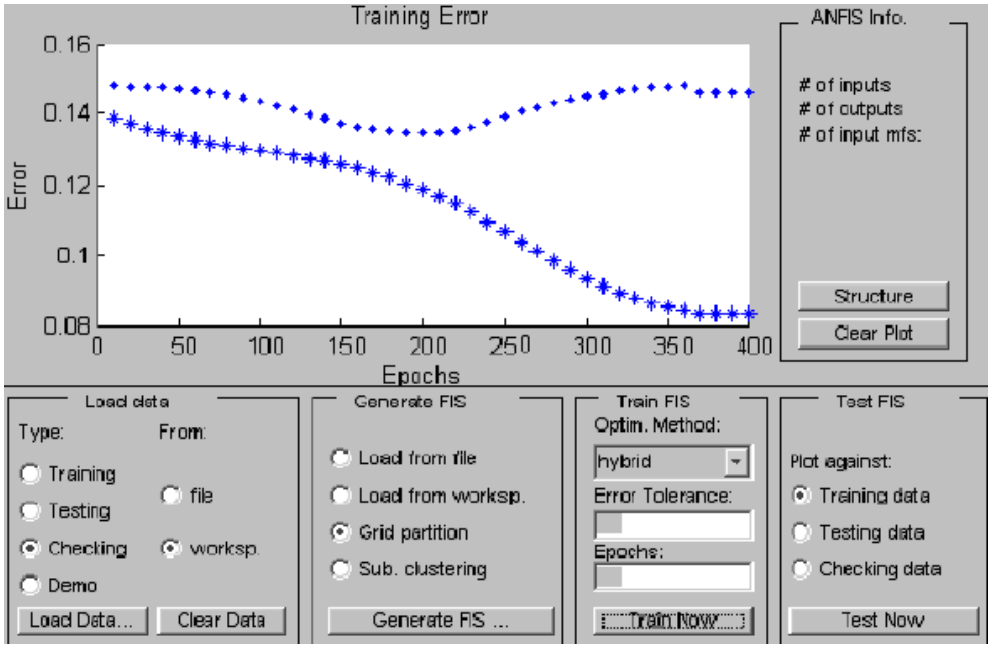

Fig. 5.28 Training and updating of the errors.

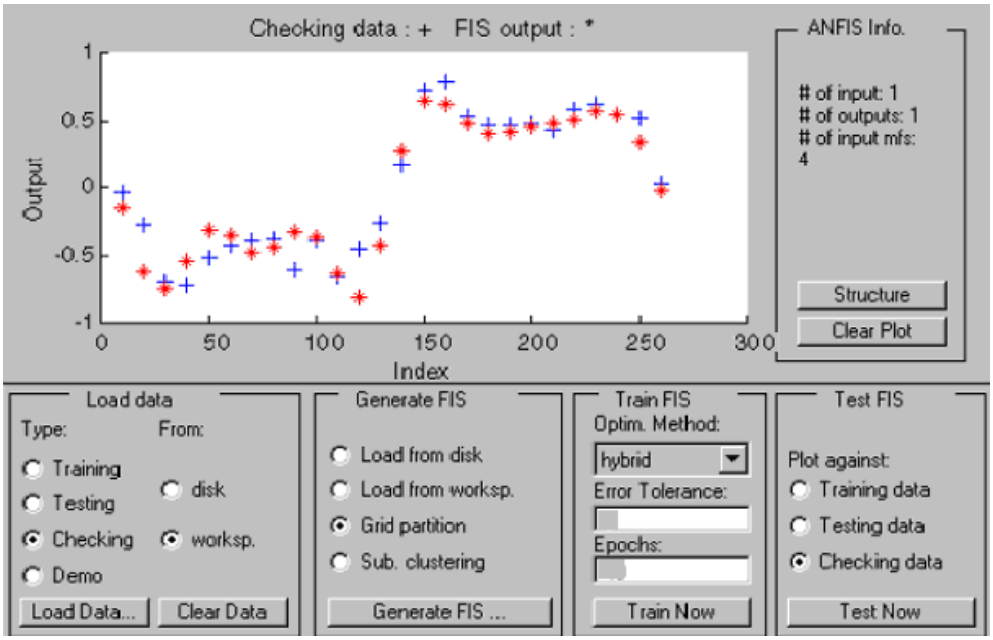

Fig. 5.29 Snapshot of training and updating of the output, checking patterns.

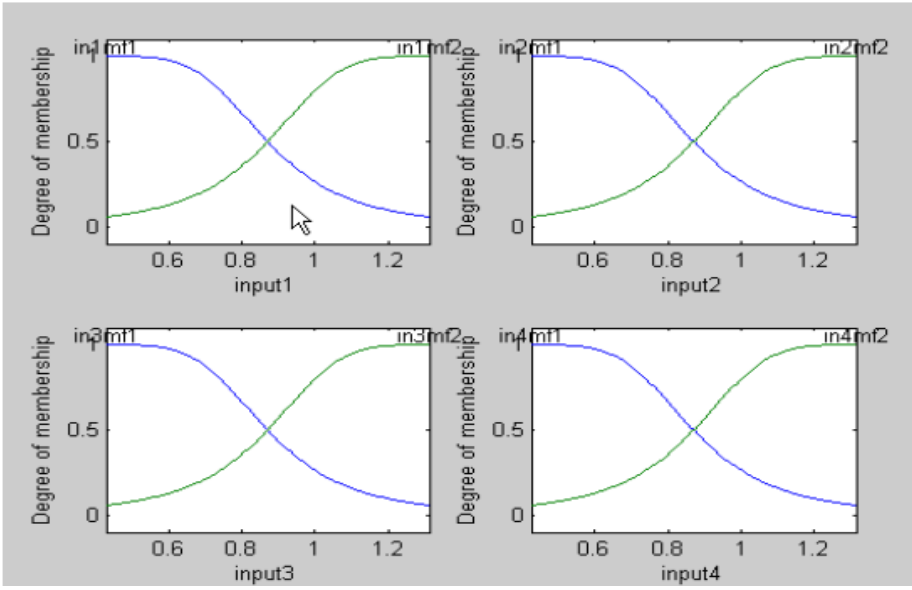

Fig. 5.30 Sample of inputs membership functions during training and updating.

Table 5.5 Snapshot of training of the ANFIS

ANFIS info:
Number of nodes: 55 Number of linear parameters: 80 Number of nonlinear parameters: 24 Total number of parameters: 104 Number of training data pairs: 30 Number of checking data pairs: 21 Number of fuzzy rules: 16 number of data is related to number of modifiable parameters
Start training ANFIS ... 1 1.41227e-005 1.38815e-005 2 1.34061e-005 1.31808e-005 3 1.27213e-005 1.25105e-005 4 1.2068e-005 1.18707e-005 5 1.14463e-005 1.12615e-005 :: :: ::
Step size increases to 0.011000 after epoch 15. 16 1.08566e-005 1.06836e-005 17 1.02456e-005 1.00849e-005 18 9.67494e-006 9.52589e-006 19 9.14526e-006 9.00735e-006 :: :: :: **Step size increases to 0.012100 after epoch 22.** 23 8.65688e-006 8.52974e-006 :: :: :: **Designated epoch number reached --> ANFIS training completed at epoch 400.**

6 Case Studies

6.1 Introduction

The primary function of the UPFC devices is to control the load flow of the power system. An additional function of them is to add a damping torque component to enhance the dynamic stability of the system. In this chapter, UPFC devices will be generally applied to the power network and especially to real electric power, the Finnish network, a real type Finnish transmission system. The applied algorithm and technique will be used to solve real problems in this Finnish network.

The optimal locations and the optimal settings will be detected using the AI concepts to reach the best performance area during the normal operation of the network. In addition, the technique will merged with the contingency analysis to solve the overloading issues in the line outage cases and to enhance the network response by detecting the optimal positions and the settings for UPFC. The cases of the contingency study will be ranked with respect to the severity of the outage case, the ranking will be indicated by indices to show the bus voltage profile and the lines rating, the most sever cases will be handled by using the applied technique.

The criteria for the optimality will depend on some fitness functions, these fitness functions will involve the indices terms to include the network buses voltage profile and explain how to reduce the voltage violations of the network. In addition to, the network line loading and explain how to reduce the lines overloading related to the network lines rate. Some comparisons will be achieved in the UPFC settings and locations when we use the bus voltage index only and when we use the line-loading index only and at including both of them.

The mode of UPFC application can be adjusted according to the required characteristics where the UPFC can work as an SVC to improve the network voltage profile by controlling the shunt elements of the UPFC only. And also it can work as an SSSC to improve the network lines loading by controlling the series element of the UPFC only. UPFC has the ability to handle both of SVC and SSSC performance simultaneously, and all of theses UPFC modes will be applied and investigated. The multiple optimal operation issues will be achieved for the UPFC installing by multiple optimization to achieve the optimum technical aspects, and this procedure will be applied for both the normal operation of the network and the contingency operation of the network to keep the performance of the network in a stable range.

The effect of UPFC, in enhancing the dynamics of the system performance and in improving the oscillations damping of the system will be discussed. The dynamic controller will be based on modern control theory with a damping effect and will be designed to insure good damping under various operating conditions and disturbances.

Steady state and dynamic simulation results throughout the thesis are obtained by using the Matlab environment and its various toolboxes such as the Control System Toolbox, Genetic Algorithm and Direct Search and Simulink, and others tools; all the required codes for the simulations are programmed in m-files.

6.2 Real Finnish Network Definition

The main task of the thesis is to solve real problems in a real Finnish network, so we will first present our main network that is our objective application. The Finnish network

has a total number of buses equal to 24, and the total number of the generators equal five generators. The network has in total 42 transmission lines.

Table 6.1 indicates the data for the network transmission lines, which the transmission line connecting buses, transmission line resistance, transmission line reactance, transmission line substance, and also it indicates MVA rates for the transmission lines. The configuration of the network is indicated in Figure 6.1, showing the type and the length for each line.

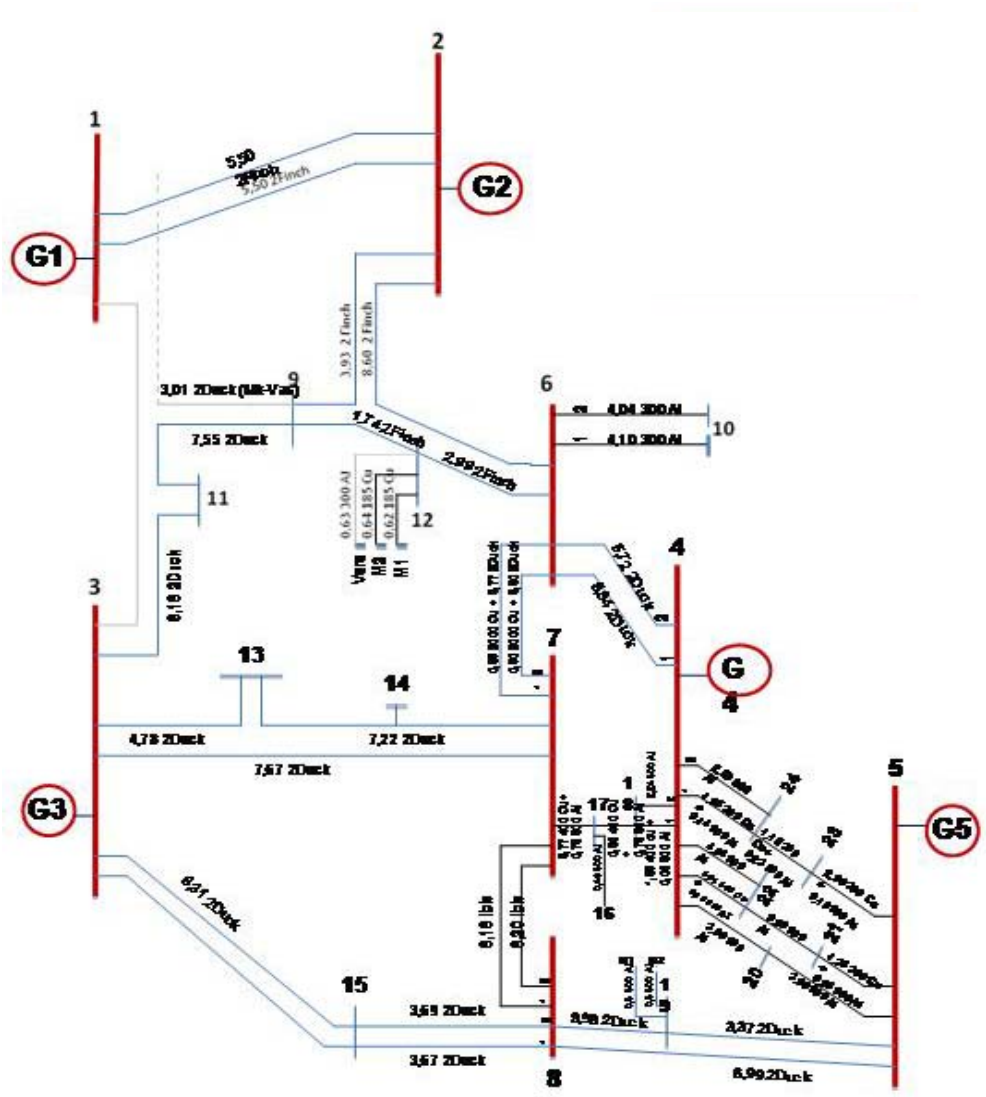

Fig. 6.1 the configuration of a real type Finnish Transmission Network.

Table 6.1 Base Transmissions Data for the System

T. L. No.	From Bus	To Bus	Impedance		Shunt Susceptance (μS)	T. L. Rate (MVA)
			R Series Resistance (Ω)	X Series Reactance (Ω)		
1	6	12	0.0820	0.7800	6.5000	410
2	6	4	0.2880	1.6640	11.8000	281
3	6	4	0.2830	1.6390	11.6000	281
4	6	7	0.2710	1.1720	17.2600	225
5	6	7	0.2700	1.1770	17.4000	225
6	6	2	0.2330	2.2850	18.2000	410
7	15	8	0.1810	1.0400	7.5000	281
8	15	8	0.1810	1.0400	7.5000	281
9	15	3	0.4080	2.4400	16.1000	281
10	15	3	0.4080	2.4400	16.1000	281
11	9	2	0.1060	1.0280	8.4000	410
12	19	8	0.1760	1.0300	7.1000	281
13	19	5	0.1640	1.0000	6.4000	281
14	12	9	0.0480	0.4500	3.9000	410
15	8	5	0.3410	2.0700	13.3000	281
16	8	7	0.8760	2.4000	8.8000	110
17	8	7	0.8810	2.4200	8.9000	110
18	3	7	0.3760	2.2100	15.1000	281
19	13	14	0.1775	1.0400	14.3000	281
20	14	7	0.1775	1.0400	14.3000	281
21	3	13	0.2350	1.3700	9.5000	281
22	11	3	0.4040	2.6620	15.7000	281
23	9	11	0.3690	2.2170	14.7000	281
24	2	1	0.1480	1.4560	11.0000	410
25	2	1	0.1480	1.4560	11.0000	410
26	6	10	0.5130	0.5780	97.0000	82
27	6	10	0.5050	0.5700	95.0000	82

Continue Table 6.1 Base Transmissions Data for the System

Trans. Line No.	From Bus	To Bus	Impedance		Shunt Susceptance (μS)	T. L. Rate (MVA)
			R Series Resistance (Ω)	X Series Reactance (Ω)		
28	21	22	0.0520	0.1140	32	134
29	22	4	0.2670	0.4630	191	104
30	22	4	0.2460	0.5820	143	134
31	23	24	0.1020	0.1960	65	104
32	24	4	0.1590	0.2770	102	104
33	24	4	0.1390	0.3260	81	134
34	23	5	0.2590	0.4070	155	104
35	17	18	0.0890	0.1960	76	120
36	17	7	0.2960	0.5110	243	120
37	17	16	0.0650	0.0880	11	134
38	21	5	0.1780	0.3060	98	104
39	5	20	0.1640	0.3590	102	134
40	4	20	0.1820	0.4430	119	134
41	18	4	0.1130	0.2310	112	134
42	18	4	0.1190	0.2870	70	120

6.3 Application Results on IEEE 6-Bus System

For the validation of the proposed techniques, the GA algorithms have been tested on the following test system, an IEEE-6 bus system (shown in Figure 6.2).

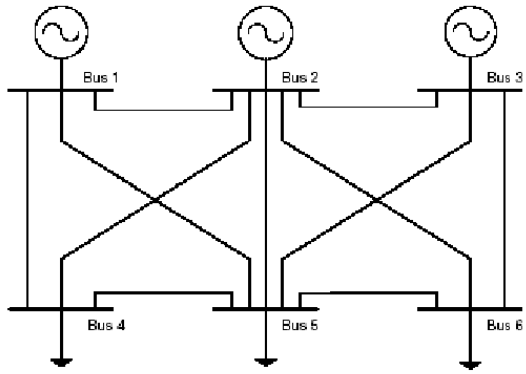

Fig. 6.2, The IEEE 6-Bus System.

This system consists of three generators, six buses, eleven transmission lines, and three loads; the data of the system is shown in Table 6.2.

Table 6.2 the data of IEEE 6-Bus System

From Bus	To Bus	Resistance	Reactance	Susbtance	Line Rate(Mw)	Bus	VM
1	2	0.10	0.20	0.02	30		
1	4	0.05	0.20	0.02	50		
1	5	0.08	0.30	0.03	40	1	1.05
2	3	0.05	0.25	0.03	22	2	1.05
2	4	0.05	0.10	0.01	45	3	1.07
2	5	0.10	0.30	0.02	20	4	1.00
2	6	0.07	0.20	0.025	40	5	1.00
3	5	0.12	0.26	0.025	20	6	1.00
3	6	0.02	0.10	0.01	60		
4	5	0.20	0.40	0.04	20		
5	6	0.10	0.30	0.03	20		

Matlab Codes for the techniques were developed for simulation purposes. The following variables are considered as the optimization variables:

a) The location of the UPFC in the power grid is the first variable in the GA process, and the position for this variable is a certain transmission line in the system where the UPFC should be located.

b) The series voltage value of the UPFC is the second parameter in the optimization, and the operating range for this parameter is [0.001, 0.3]

c) The shunt voltage value of the UPFC is considered as the third parameter to be optimized, and the operating range for this parameter is [0.8, 1.2].

6.3.1 Normal Operating with Heavy Loading Pattern

The increasing in the complexity of AC power networks requires a high-performance power flow control system in order to obtain the desired power flow and to enhance static and dynamic stability. One of the most efficient power electronics systems, to satisfy these requirements, is a UPFC (Unified Power Flow Controller) employing self-commutated converters. UPFCs are proven to be effective in power grids in well-developed countries (e.g. USA, Canada, Sweden). The economical viability of these controllers is justified through the long list of benefits that these controllers have, compared to the traditional controllers. UPFC technology can boost power transfer capability by increasing the flexibility of the systems. Power interchange with neighboring countries becomes easier and effective with these controllers.

UPFC can also increase the loadability and the distance to voltage collapse of a power network to additional loads can be exist in the system without the installation of new transmission and generating units. Moreover, the current trend of the deregulated electricity market also favors UPFC in many ways. UPFC in the deregulated electricity market allow the system to be used in a way that is more flexible with increases in various stability margins.

This stage will concern the solving the problems of the network related to overloading of transmission lines and violation of bus voltage profile. This task will be performed on the normal configuration of the system with an increase in the load pattern on the system.

During the results, the index $\acute{K}_{(LOLN)}$ indicates the Lines Over Loaded Number and $\Gamma_{(VBVN)}$: the index which indicates the Violation of Voltage Buses Number. While Y1 will penalize the value of overall overloading for all lines of the system and Y2 will penalize the value of overall voltage violations for all buses of the system. The calculations for Y1 and Y2 will depend on Equations (5.4) and (5.6).

The loading pattern will be increased in uniform rate to create the overloading of the transmission lines, starting from one overloading for one transmission line and so on for multiple overloading in the system. The results will concern comparing the performance of the system before installing UPFC and after installing UPFC at optimal location with optimal settings to achieve the required performance criteria, enhancing the operating conditions of the power system.

Table 6.3 Case Study (1) of IEEE 6-Bus System

Case Study 1

⇒ ***Increasing Load Pattern at each bus with 140% (for all Load buses)***

⇒ ***Before UPFC Installation***

$\acute{K}_{(LOLN)}$	*Y1*	Overloaded Line	Connecting Bus		Overloading %	$Я = \acute{K}_{(LOLN)}+\Gamma_{(VBVN)}$	$Y = Y1+Y2$
			From	To			
1	0.144	1	1	2	109.56%	1	0.144

⇒ ***After UPFC Installation***

⇒ ***Optimal Location Line (10) ≡ Buses (4-5), Optimal Setting (0.0023 , 1.1057)***

$\acute{K}_{(LOLN)} = 0$	$Y1 = 0$	$\Gamma_{(VBVN)} = 0$	$Y2 = 0$	$Я = 0$	$Y = 0$

⇒ ***No Overloading , No Voltage Violation*** $0.95 \le V_i \le 1.05$

Table 6.4 Case Study (2) of IEEE 6-Bus System

Case Study 2

⇒ ***Increasing Load Pattern at each bus with 143% (for all Load buses)***

⇒ ***Before UPFC Installation***

$\acute{K}_{(LOLN)}$	*Y1*	Overloaded Line	Connecting Bus		Overloading %	$Я = \acute{K}_{(LOLN)}+\Gamma_{(VBVN)}$	$Y = Y1+Y2$
			From	To			
1	0.1595	1	1	2	112.38%	1	0.1595

⇒ ***After UPFC Installation***

⇒ ***Optimal Location Line (1) ≡ Buses (1-2), Optimal Setting (0.0242 , 1.1911)***

$\acute{K}_{(LOLN)} = 0$	$Y1 = 0$	$\Gamma_{(VBVN)} = 0$	$Y2 = 0$	$Я = 0$	$Y = 0$

⇒ ***No Overloading , No Voltage Violation*** $0.95 \le V_i \le 1.05$

Table 6.5 Case Study (3) of IEEE 6-Bus System

Case Study 3			
⇒ ***Increasing Load Pattern at each bus with 145% (for all Load buses)***			
⇒ ***Before UPFC Installation***			
$\acute{K}_{(LOLN)} = 2$	$Y1 = 0.2804$	$Я = \acute{K}_{(LOLN)} + \Gamma_{(VBVN)} = 2$	$Y = Y1 + Y2 = 0.2804$

Overloaded Line	Connecting Bus		Overloading %
	From	*To*	
1	1	2	115.2%
3	1	5	102%

⇒ ***After UPFC Installation***

⇒ ***Optimal Location Line (1) ≡ Buses (1-2), Optimal Setting (0.008 , 1.1923)***

$\acute{K}_{(LOLN)} = 0$	$Y1 = 0$	$\Gamma_{(VBVN)} = 0$	$Y2 = 0$	$Я = 0$	$Y = 0$

⇒ ***No Overloading , No Voltage Violation*** $0.95 \le V_i \le 1.05$

Table 6.6 Case Study (4) of IEEE 6-Bus System

Case Study 4			
⇒ ***Increasing Load Pattern at each bus with 146% (for all Load buses)***			
⇒ ***Before UPFC Installation***			
$\acute{K}_{(LOLN)} = 3$	$Y1 = 0.4072$	$Я = \acute{K}_{(LOLN)} + \Gamma_{(VBVN)} = 3$	$Y = Y1 + Y2 = 0.4072$

Overloaded Line	Connecting Bus		Overloading %
	From	*To*	
1	1	2	118.04%
2	1	4	101%
3	1	5	102.77%

⇒ ***After UPFC Installation***

⇒ ***Optimal Location Line (2) ≡ Buses (1-4), Optimal Setting (0.0425 , 1.194)***

$\acute{K}_{(LOLN)} = 0$	$Y1 = 0$	$\Gamma_{(VBVN)} = 0$	$Y2 = 0$	$Я = 0$	$Y = 0$

⇒ ***No Overloading , No Voltage Violation*** $0.95 \le V_i \le 1.05$

Table 6.7 Case Study (5) of IEEE 6-Bus System

Case Study 5

⇒ ***Increasing Load Pattern at each bus with 150% (for all Load buses)***

⇒ ***Before UPFC Installation***

$\acute{K}_{(LOLN)}= 3$	$Y1 = 0.4775$	$Я = \acute{K}_{(LOLN)}+\Gamma_{(VBVN)} = 3$	$Y = Y1+Y2 = 0.4775$

Overloaded Line	Connecting Bus		Overloading
	From	*To*	%
1	1	2	123.74%
2	1	4	103.69%
3	1	5	107.29%

⇒ ***After UPFC Installation***

⇒ ***Optimal Location Line (1) ≡ Buses (1-2), Optimal Setting (0.0195 , 1.1868)***

$\acute{K}_{(LOLN)}= 0$	$Y1 = 0$	$\Gamma_{(VBVN)} = 0$	$Y2 = 0$	$Я = 0$	$Y = 0$

⇒ ***No Overloading , No Voltage Violation*** $0.95 \le V_i \le 1.05$

Table 6.8 Case Study (6) of IEEE 6-Bus System

Case Study 6

⇒ ***Increasing Load Pattern at each bus with 182% (for all Load buses)***

⇒ ***Before UPFC Installation***

$\acute{K}_{(LOLN)}= 4$	$Y1 = 2.6363$	$Я = \acute{K}_{(LOLN)}+\Gamma_{(VBVN)} = 4$	$Y = Y1+Y2 = 2.6363$

Overloaded Line	Connecting Bus		Overloading
	From	*To*	%
1	1	2	198.90%
2	1	4	146%
3	1	5	150.3%
7	2	6	101%

⇒ ***After UPFC Installation***

⇒ ***Optimal Location Line (1) ≡ Buses (1-2), Optimal Setting (0.001 , 1.2)***

$\acute{K}_{(LOLN)}= 0$	$Y1 = 0$	$\Gamma_{(VBVN)} = 0$	$Y2 = 0$	$Я = 0$	$Y = 0$

⇒ ***No Overloading , No Voltage Violation*** $0.95 \le V_i \le 1.05$

From the previous results, we can note that all line overloading is cancelled by positioning UPFC in an optimal location with optimal parameters setting by GA. While for the bus voltage profile, the optimal location and settings resulted from the GA keep the voltage profile for all the buses in the system inside the required limit.

6.3.2 Contingency Operating with Outage Pattern

According to the change in network configuration caused by the outage, undesired high or low voltage conditions can appear and thermal limits may be exceeded. Low voltage following an outage may lead to transmission limitations. The maximum acceptable voltage drop sets most major transmission line loading levels and the minimum voltage at line loss would appear at other locations in the network, and may in neighboring systems. The voltage drop due to the loss of a major line can be accompanied by circuit overloads, at the same voltage or at lower voltage levels. The introduction of the FACTS devices extends the possibility that current through a line can be controlled at a reasonable cost enables the large potential of increasing the capacity of existing lines, and the use of one of the FACTS devices to enable corresponding power to flow through such lines under normal and contingency conditions.

This stage is concern with solving the problems of the network related to overloading of transmission lines and the violation of bus voltage profile during the contingency operating with an outage pattern.

A ranking process is performed on the network after the contingency analysis. There will be some single contingencies. For each single line outage, we find the following performance indices $\acute{K}_{(LOLN)}$ and $\Gamma_{(VBVN)}$, which are described in Chapter 5.

Then we rank the lines according to the severity of the contingency, in other words, according to $Я = \acute{K}_{(LOLN)} + \Gamma_{(VBVN)}$. The remaining cases will not be concerned where the total performance indices equal zero.

Table 6.9 Ranking for the severity contingency cases for IEEE 6-bus system

Ranking Case	Line Number	Connecting Bus		$\acute{K}_{(LOLN)}$	$\Gamma_{(VBVN)}$	$Я = \acute{K}_{(LOLN)} + \Gamma_{(VBVN)}$
		From	To			
1	9	3	6	3	1	4
2	5	2	4	2	1	3
3	2	1	4	1	1	2
4	6	2	5	1	0	1
5	3	1	5	1	0	1
6	4	2	3	1	0	1
7	11	5	6	1	0	1

Table 6.10 Outage Case Study (1) of IEEE 6-Bus System

Outage Case Study 1					
⇒ ***Outage of Line (9) ≡ (3-6), Severity Rank =1***					
⇒ ***Before UPFC Installation***					
$\acute{K}_{(LOLN)}= 3$	*Y1 = 1.3040*	$\Gamma_{(VBVN)}=1$	*Y2=0.0115*	*Я = 4*	*Y = 1.3155*

Overloaded Line	Connecting Bus		Overloading %
	From	*To*	
4	2	3	108.63%
7	2	6	101%
8	3	5	180.51%
Bus Violation		Bus 6	

⇒ ***After UPFC Installation***			
⇒ ***Optimal Location Line (4) ≡ (2-3), Optimal Setting (0.008 , 0.9931)***			
$\acute{K}_{(LOLN)}= 1$	***One Overloading***	***Line (8)***	***Eliminate Overloading at line 4, 7***
$\Gamma_{(VBVN)} = 0$	***No Voltage Violation***		$0.95 \le V_i \le 1.05$

Table 6.11 Outage Case Study (2) of IEEE 6-Bus System

Outage Case Study 2					
⇒ ***Outage of Line (5) ≡ (2-4), Severity Rank =2***					
⇒ ***Before UPFC Installation***					
$\acute{K}_{(LOLN)}= 2$	*Y1=0.3205*	$\Gamma_{(VBVN)} = 1$	*Y2=0.0103*	*Я = 3*	*Y = 0.3308*

Overloaded Line	Connecting Bus		Overloading %
	From	*To*	
6	2	5	101%
8	3	5	121.53%
Bus Violation		Bus 4	

⇒ ***After UPFC Installation***			
⇒ ***Optimal Location Line (3) ≡ (1-5), Optimal Setting (0.1779 , 0.977)***			
$\acute{K}_{(LOLN)}= 0$	***No Overloading***	$\Gamma_{(VBVN)} = 0$	***No Voltage Violation*** $0.95 \le V_i \le 1.05$

Table 6.12 Outage Case Study (3) of IEEE 6-Bus System

Outage Case Study 3					
⇒ ***Outage of Line (2) ≡ (1-4), Severity Rank =3***					
⇒ ***Before UPFC Installation***					
$\acute{K}_{(LOLN)}= 1$	*Y1=0.1560*	$\Gamma_{(VBVN)} = 1$	*Y2=0.0068*	*Я = 2*	*Y = 0.1628*

Overloaded Line	Connecting Bus		Overloading %
	From	*To*	
5	2	4	111.75%
Bus Violation		Bus 4	

⇒ ***After UPFC Installation***

⇒ ***Optimal Location Line (1) ≡ (1-2), Optimal Setting (0.012 ,1.1903)***

$\acute{K}_{(LOLN)}= 0$	***No Overloading***	$\Gamma_{(VBVN)} = 0$	***No Voltage Violation*** $0.95 \le V_i \le 1.05$

Table 6.13 Outage Case Study (4) of IEEE 6-Bus System

Outage Case Study 4					
⇒ ***Outage of Line (6) ≡ (2-5), Severity Rank =4***					
⇒ ***Before UPFC Installation***					
$\acute{K}_{(LOLN)}= 1$	*Y1=0.1716*	$\Gamma_{(VBVN)} = 0$	*Y2=0.0*	*Я = 1*	*Y = 0.1716*

Overloaded Line	Connecting Bus		Overloading %
	From	*To*	
8	3	5	114.45%
Bus Violation		---	

⇒ ***After UPFC Installation***

⇒ ***Optimal Location Line (3) ≡ (1-5), Optimal Setting (0.1297 ,0.8758)***

$\acute{K}_{(LOLN)}= 0$	***No Overloading***	$\Gamma_{(VBVN)} = 0$	***No Voltage Violation*** $0.95 \le V_i \le 1.05$

Table 6.14 Outage Case Study (5) of IEEE 6-Bus System

Outage Case Study 5					
⇒ ***Outage of Line (3) ≡ (1-5), Severity Rank =5***					
⇒ ***Before UPFC Installation***					
$\acute{K}_{(LOLN)}= 1$	*Y1=0.1880*	$\Gamma_{(VBVN)} = 0$	*Y2=0.0*	*Я = 1*	*Y = 0.1880*

Overloaded Line	Connecting Bus		Overloading %
	From	*To*	
8	3	5	117.09%
Bus Violation		---	

⇒ ***After UPFC Installation***

⇒ ***Optimal Location Line (9) ≡ (3-6), Optimal Setting (0.1349 ,0.9185)***

$\acute{K}_{(LOLN)}= 0$	***No Overloading***	$\Gamma_{(VBVN)} = 0$	***No Voltage Violation*** $0.95 \le V_i \le 1.05$

Table 6.15 Outage Case Study (6) of IEEE 6-Bus System

Outage Case Study 6					
⇒ ***Outage of Line (4) ≡ (2-3), Severity Rank =6***					
⇒ ***Before UPFC Installation***					
$\acute{K}_{(LOLN)}= 1$	*Y1=0.1031*	$\Gamma_{(VBVN)} = 0$	*Y2=0.0*	*Я = 1*	*Y = 0.1031*

Overloaded Line	Connecting Bus		Overloading %
	From	*To*	
8	3	5	101%
Bus Violation		---	

⇒ ***After UPFC Installation***

⇒ ***Optimal Location Line (1) ≡ (1-2), Optimal Setting (0.001 ,0.8)***

$\acute{K}_{(LOLN)}= 0$	***No Overloading***	$\Gamma_{(VBVN)} = 0$	***No Voltage Violation*** $0.95 \le V_i \le 1.05$

Table 6.16 Outage Case Study (7) of IEEE 6-Bus System

Outage Case Study 7					
⇒ ***Outage of Line (11) ≡ (5-6), Severity Rank =7***					
⇒ ***Before UPFC Installation***					
$\acute{K}_{(LOLN)}= 1$	$Y1=0.1014$	$\Gamma_{(VBVN)} = 0$	$Y2=0.0$	$Я = 1$	$Y = 0.1014$

Overloaded Line	Connecting Bus		Overloading %
	From	*To*	
8	3	5	101%
Bus Violation		---	

⇒ ***After UPFC Installation***

⇒ ***Optimal Location Line (2) ≡ (1-4), Optimal Setting (0.012 ,0.9015)***

$\acute{K}_{(LOLN)}= 0$	***No Overloading***	$\Gamma_{(VBVN)} = 0$	***No Voltage Violation*** $0.95 \leq V_i \leq 1.05$

From the previous tables, we can find that all bus voltage violations are eliminated by placing UPFC in an optimal location with optimal parameter settings by GA. While for overloaded lines, despite that, placing UPFC in the system did not result in eliminating all of them, but most of overloaded lines are eliminated and the power flow distribution in the rest-overloaded lines is significantly reduced.

The optimal installation of FACTS devices plays a key role in achieving the proper functionality of these devices. The tables, we have simulated, show that the application can efficiently get the proper settings and locations of UPFC. Optimal UPFC in these locations can enhance the performance of a power system by preventing the overloading in lines and the bus voltage violations.

6.3.3 Genetic Algorithms Versus another advanced optimization tool (PSO)

Particle Swarm Optimization (PSO) is a technique based on a stochastic optimization process presented by Kennedy and Eberhart in Year of 1995 without clear data of the gradient of the optimization problem. PSO is mainly attributed first to be requested for simulating social behavior. The algorithm was summarized and it was stated to be performing optimization.

PSO applies optimization by keeping a population of proposed issues named particles and moving those particles through the search-space with respect to simple formulae. The motions of the particles are directed by the best locations in the search space that are continually upgraded as better locations are determined by the particles.

Concept of Particle Swarm Optimization (PSO)

PSO participate various identical feature with evolutionary computation methods like Genetic Algorithms (GA). The system is started with a population of stochastic solutions and looks for optimality by updating generations. However, PSO doesnot have evolution process like crossover and mutation. In PSO, the potential solutions are the particles, which move in the problem space by succeeding the real optimum particles.

All particles maintain trend of the coordinates in the space-solution that is accompanied with the best record it has occurred. The fitness is also memorized. This value is called P_{best}. The second best value that is followed by each particle swarm optimizer is the best amount, reulted by any particle in the neighbors of the particle. This location is named as L_{best}. During a particle gets all the population as its topological neighbors, the best is the global and is named g_{best}.

The particle swarm optimization idea depends on changing the speed of accelerating of each particle directed to its P_{best} and L_{best} positions. Acceleration is controlled by a random parameter, with separate random values being determined for acceleration directed to P_{best} and L_{best} locations.

Many publications are concerned with choosing well PSO parameters. The method for tuning PSO parameters is called meta-optimization because another optimization method is used in an overlapping way to tune the PSO parameters. The best performing PSO parameters were found to be contrary to the guidelines in the literature and often yielded satisfactory optimization performance for simple PSO variants.

PSO Technique

There is a randomized velocity corresponding to a potential solution, called a particle, and harmonized with individuals. Each particle in PSO moves in the D-dimensional problem space with a speed dynamically adapted with respect to the flying experiences of particles.

The position of the *ith* particle is described as $X_i = [x_{i1}, x_{i2}, \ldots, x_{iD}]$, where, $x_{id} \in [l_d, u_d]$, $d \in [1,D]$. l_d *and* u_d , are the lower and upper bounds for *dth* dimension, respectively. The best previous position, which calculates the best fitness value of the *ith* particle is saved and represented as $P_i = [P_{i1}, P_{i2}, \ldots, P_{iD}]$, which is also called P_{best}.

The index of the best particle between all particles in the population is described by the symbol g . The location P_g is also called as g_{best} . The speed of the *ith* particle is described as $V_i = [v_{i1}, v_{i2}, \ldots, v_{iD}]$ and is clamped to a maximum speed $V_{max} = [v_{max1}, v_{max2}, \ldots, v_{maxD}]$ which is defined by the designer. At each time step, the particle swarm optimization concept regulates the velocity and location of each particle toward its P_{best} and g_{best} locations according to the following equations

$$v_{id}^{n+1} = w v_{id}^{n} + c_1 r_1^n (P_{id}^n - x_{id}^n) + c_2 r_2^n (P_{gd}^n - x_{id}^n)$$

$$x_{id}^{n+1} = x_{id}^{n} + v_{id}^{n+1}$$

$i = 1,2,\ldots,m$, $\quad d = 1,2,\ldots,D$

Where:

c_1 and c_2 are two positive constants, called cognitive and social parameters respectively, m is the size of the swarm,

D is the number of members in a particle,
r_1 and r_2, are random numbers, uniformly distributed in [0,1],
n is the pointer of iterations (generations), and
w is the inertia weight, which achieve a balance between global and local investigation and thus leading to lower iteration to calculate a appropriate optimal solution.

It is specified by the following equation:

$$w = w_{\max} - \frac{w_{\max} - w_{\min}}{iter_{\max}} \times iter$$

Where:
w_{max} is the initial weight,
w_{min} is the final weight,
$iter$ is the current iteration number, and
$iter_{max}$ is the maximum iteration number (generations).

We can summery particle swarm optimization algorithm in steps:

1. Initialise particles in the search space at random.
2. Assign random initial velocities for each particle.
3. Evaluate the fitness of each particle according a user defined objective function.
4. Calculate the new velocities for each particle.
5. Move the particles.
6. Repeat steps 3 to 5 until a predefined stopping criterion is satisfied.

Particle Swarm: Controlling Velocities

- During PSO, it is available for increasing the magnitude of the speed.
- Performance can be improper if V_{max} is set in the wrong way.
- Several techniques were proposed for controlling the growth of velocities:
  - A effectively updated inertia weight factor,
  - A effectively updated acceleration coefficients
  - Re-initialization of stagnated particles and swarm size.
  - Robust Settings for (c_1 and c_2).

Outline of the Basic Genetic Algorithm

The concept of Genetic algorithms is simulated to Darwin's theory of evolution. GAs were appeared and promoted by John Holland with his research group.
The outline of the GA technique is:
1. Produce stochastic population of n chromosomes (proper solutions for the problem).
2. Calculate the fitness of each chromosome x in the population.
3. Produce a new population by sequencing following actions for ending the new population process.

a. Refer to two parent chromosomes from a population with respect to their fitness (the more well fitness, the higher chance to be chosen).
b. With a crossover probability cross over the parents to generate new offspring (new children). If no crossover was occurred, children are the exact copies of parents.
c. With a mutation probability mutate new offspring at each location in chromosome.

4. Locate new offspring in the new population.
5. Apply new generated population for a further run of the algorithm.
6. If the end condition is satisfied, stop, and return the best solution in current population.
7. Go to step 2.

Case Study: IEEE 6-bus System

This system consists of three generators, six buses, eleven transmission lines, and three loads; the data of the system is shown in Table 6.2. Eleven possible single outage contingencies are included. Ranking process is performed on the network after the contingency analysis. The applied GA and PSO algorithms were implemented to find the optimal values of UPFC variables.

The GA parameters and PSO parameters are:

GA parameters	
Parameter	Value
Variables Numbers	3
Population Size	40
Generations Number	100
Crossover Probability	0.85
Mutation Probability	0.1

PSO parameters	
Parameter	Value
Variables Numbers	3
Max. weight	0.8
Min. weight	0.1
Max. iteration	100
c1 , c2	0.5
r1 , r2	[0, 1]
Swarm beings Number	25

Table 6.17: Overloaded lines and bus voltage violations before and after Placing UPFC for IEEE 6-bus system with optimal location and optimal parameters setting of UPFC by GA

Severity	Outaged Line	Without UPFC			UPFC Optimal Location Line No.	UPFC Optimal Settings		With Optimal UPFC		
	Line No. ≡ (From – To) Buses	Voltage Violation Buses	Overloaded Lines	Overloading %		V_{CR}	V_{VR}	Voltage Violation Buses	Overloaded Lines	Overloading %
1	2 ≡ (1 – 4)	Bus 4	1-5 1-2 2-4	106.64 123.53 117.95	10≡(4–5)	0.0517	1.098	-	- - 2-4	- - 111.1
2	3 ≡ (1 – 5)	-	1-4 1-2 3-5	116.24 109.14 104.85	11≡(5–6)	0.1142	1.089	-	1-4 - -	109.1 - -
3	5 ≡ (2 – 4)	Bus 4	1-4 3-5	159.95 105.85	10≡(4–5)	0.0769	1.059	-	1-4 -	112.8 -
4	9 ≡ (3 – 6)	Bus 6	2-6 3-5	128.97 145.39	11≡(5–6)	0.2169	1.090	-	-	-
5	7 ≡ (2 – 6)	-	2-3 3-6	137.25 115.35	11≡(5–6)	0.0534	1.099	-	-	-
6	6 ≡ (2 – 5)	-	3-5	103.54	2 ≡ (1–4)	0.2010	1.088	-	-	-

Table 6.18: Overloaded lines and bus voltage violations before and after placing UPFC for IEEE 6-bus system with optimal location and optimal parameters setting of UPFC by PSO

Severity	Outaged Line	Without UPFC			UPFC Optimal Location Line No.	UPFC Optimal Settings		With Optimal UPFC		
	Line No. ≡ (From – To) Buses	Voltage Violation Buses	Overloaded Lines	Overloading %		V_{CR}	V_{VR}	Voltage Violation Buses	Overloaded Lines	Overloading %
1	2 ≡ (1 – 4)	Bus 4	1-5 1-2 2-4	106.64 123.53 117.95	6≡(2–5)	0.2081	1.041	-	- - 2-4	- - 116.2
2	3 ≡ (1 – 5)	-	1-4 1-2 3-5	116.24 109.14 104.85	10≡(4–5)	0.2035	1.1	-	1-4 - -	114.7 - -
3	5 ≡ (2 – 4)	Bus 4	1-4 3-5	159.95 105.85	10≡(4–5)	0.1424	1.0291	-	1-4 -	124.1 -
4	9 ≡ (3 – 6)	Bus 6	2-6 3-5	128.97 145.39	11≡(5–6)	0.1173	1.0564	-	-	-
5	7 ≡ (2 – 6)	-	2-3 3-6	137.25 115.35	11≡(5–6)	0.0946	1.0361	-	-	-
6	6 ≡ (2 – 5)	-	3-5	103.54	10≡(4–5)	0.0776	1.0913	-	-	-

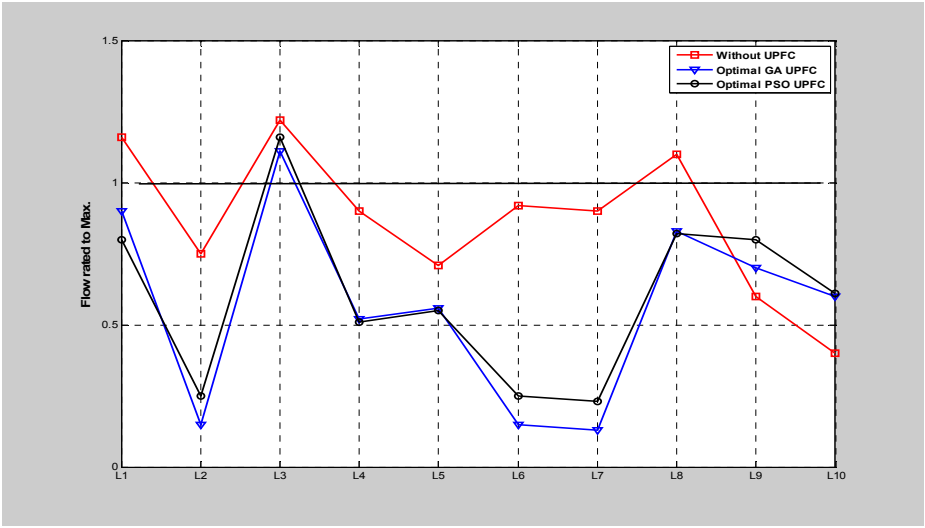

Fig. 6.3: Power flow distribution for IEEE 6-bus system when line 2 is outage by GA and PSO.

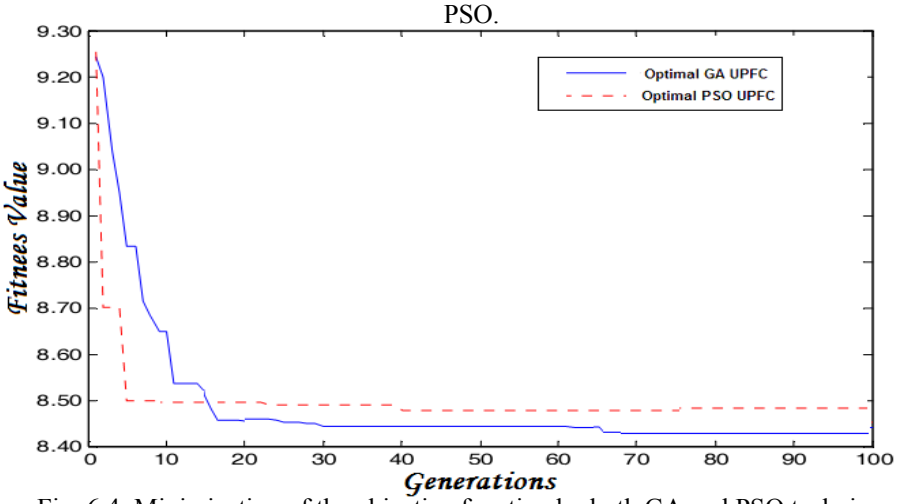

Fig. 6.4: Minimization of the objective function by both GA and PSO techniques for IEEE 6-bus system when line 2 is outage.

Analyzing the simulation results, from the convergence point of view, it is clear that with the increase of generation, it can be noted that the performance of GA is better than the performance of PSO as indicated. This is because the GA technique has selection, crossover, and mutation actions, while PSO doesnot have such actions; the GA more efficient and effective to achieve the optimal solution. The solutions, which we got from the GA, minimize the overloading better than the ones through PSO. The most advantageous part in GA that we apply the rules of evolution to the individuals. GA finds the individuals with the best suggestions to the problem and then combine these individuals into new individuals. Using this method repeatedly, the population will evolve good solutions. Specifically, the elements of a GA are: selection, cross-over, and mutation. As we can see, Darwin's principles have been a major inspiration to GAs.

A GA owns many advantages. It can quickly scan a vast solution group. Unwell solutions do not affect the final results negatively as they are simply disappearing.

6.4 Application Results on IEEE Large Scale 57-Bus System

For the validation of the proposed technique on a large-scale power system, it has been tested on the following test system, an IEEE-57 bus system [85]. This system consists of seven generators, fifty-seven buses, and eighty transmission lines.

6.4.1 Normal Operating with Heavy Loading Pattern

This stage concerns solving a network problem related to the overloading of transmission lines. This will performed on the normal configuration of the system with increasing the load pattern on the system.

Table 6.19 Case Study (1) of IEEE 57-Bus System

⇒ ***Increasing Load Pattern at each bus with 120% (for all Load buses)***					
⇒ ***Before UPFC Installation***					
$\acute{K}_{(LOLN)}$	*Y1*	Overloaded Line	From Bus	To Bus	Overloading %
1	0.1573	8	8	9	112%
⇒ ***After UPFC Installation***					
⇒ ***Optimal Location Line (18) ≡ (3-15), Optimal Setting (0.2997, 1.1995)***					
$\acute{K}_{(LOLN)} = 0$	*Y1 = 0*	***- No Overloading***			

Table 6.20 Case Study (2) of IEEE 57-Bus System

⇒ ***Increasing Load Pattern at each bus with 150% (for all Load buses)***					
⇒ ***Before UPFC Installation***					
$\acute{K}_{(LOLN)}$	*Y1*	Overloaded Line	From Bus	To Bus	Overloading %
1	0.236	8	8	9	103.77 %
		15	1	15	104.82 %
⇒ ***After UPFC Installation***					
⇒ ***Optimal Location Line (18) ≡ (3-15), Optimal Setting (0.13241 , 1.2)***					
$\acute{K}_{(LOLN)} = 0$	*Y1 = 0*	***- No Overloading***			

From the previous simulations, we can note that all line overloading is prevented by applying an optimal installation of UPFC using GA. That means the applied technique is successful in achieving the desired performance.

6.4.2 Contingency Operating with Outage Pattern

This stage is to do with solving the problems of the network related to overloading of transmission lines during the contingency operating with a single outage pattern.

Table 6.21 Outage Case Study (1) of IEEE 57-Bus System

Outage Case Study 1		
⇒ ***Outage of Line (8) ≡ (8-9)***		
⇒ ***Before UPFC Installation***		
$\acute{K}_{(LOLN)}$= *1*	*Y1 = 0.1558*	*- One overloading*

Overloaded Line	Connecting Bus		Overloading %
	From	*To*	
21	7	8	111.73 %

⇒ ***After UPFC Installation***

⇒ ***Optimal Location Line (6) ≡ (6-7), Optimal Setting (0.02387 , 0.8002)***

$\acute{K}_{(LOLN)}$= *0*	*Y1 = 0.0*	***- No Overloading***

Table 6.22 Outage Case Study (2) of IEEE 57-Bus System

Outage Case Study 2		
⇒ ***Outage of Line (15) ≡ (1-15)***		
⇒ ***Before UPFC Installation***		
$\acute{K}_{(LOLN)}$= *2*	*Y1 = 0.2452*	*- Two overloading*

Overloaded Line	Connecting Bus		Overloading %
	From	*To*	
1	1	2	102 %
8	8	9	108.37 %

⇒ ***After UPFC Installation***

⇒ ***Optimal Location Line (8) ≡ (8-9), Optimal Setting (0.10438 , 0.8)***

$\acute{K}_{(LOLN)}$= *0*	*Y1 = 0.0*	***- No Overloading***

6.5 Application Results on a Real Finnish Transmission Network

The data of a real Finnish Transmission Network was introduced in Table 6.1. In addition, the configuration of the network was indicated in Figure 6.1. The load and generation data are valid through Aalto (TKK) University. The data is taken for 24 hours each day monthly for twelve months. The applications of UPFC for this network will be studied until the year 2020 using the load forecasting coefficient which will be available until the year 2020. To show the effectiveness of the UPFC installation, the design of the UPFC will be applied for the worst cases, which are the highest loading conditions, of each loading value at each bus at the same time. This procedure will be applied for current loading pattern and also for the worst cases of the year 2020. Increasing load patterns will be performed with two procedures, the first one is multiplying all the entire loads in the system by increasing the percentage factor. The second one is multiplying all the entire loads in the system by their individual forecasted load coefficient for the future year. The contingency analysis with outage cases will be enhanced through the UPFC installation. This analysis will also be studied through the worst case scenario with the maximum load value at each bus at the same time in the current loading pattern until the year 2020 conditions. Estimating loadability of a generation and transmission system is practically important in power system operations and planning. Increasing the loadability of the system will be indicated during the analysis to measure the utilization of the network after the UPFC installation. The loadability of the transmission grid will be calculated according to the transmission lines flow related to the transmission lines maximum capacity, for all the transmission lines, considering the number of the lines to get the total average loadability. The enhancement in the loadability is achieved in some cases as additional benefits besides the main objective of minimizing overloading and voltage violations. Simulations show that UPFC can be used to enhance loadability in the power system even with solving one, two or more in overloading boundaries. UPFC is a powerful control device that can efficiently control powerful, both transmitted real and reactive flows power as well as bus independently voltages.

6.5.1 Normal Operating with Heavy Loading Pattern until 2020

This stage deals with enhancing the performance of the network related to the overloading of the transmission lines and violation of the bus voltage profile. This task will be performed on the normal configuration of the system with an increasing load pattern on the system until the year 2020.

Table 6.23 Case Study (1) of the real Finnish Network

Case Study 1					
- Normal Loading (Base Case) Max. Load for each load bus at the same time ***- Before UPFC Installation***					
$\acute{K}_{(LOLN)} = 0$	$Y1 = 0$		$Я = \acute{K}_{(LOLN)} + \Gamma_{(VBVN)} = 0$		$Y = Y1 + Y2 = 0$
Loadability			24.04 %		
⇒ ***After Optimal UPFC Installation: Location (4 ≡ 6-7), Setting (0.1219 , 0.996)***					
$\acute{K}_{(LOLN)} = 0$	$Y1 = 0$	$\Gamma_{(VBVN)} = 0$	$Y2 = 0$	$Я = 0$	$Y = 0$
Loadability			24.1512%		
- No Overloading , No Voltage Violation $0.98 \le V_i \le 1.02$					

Table 6.24 Case Study (2) of the real Finnish Network

Case Study 2			
⇒ ***Max. Load for each load bus at the same time with 110% increase for all.***			
⇒ ***Before UPFC Installation***			
$\acute{K}_{(LOLN)}=0$	$Y1=0$	$Я=\acute{K}_{(LOLN)}+\Gamma_{(VBVN)}=0$	$Y=Y1+Y2=0$
Loadability		28.17%	
⇒ ***After UPFC Installation***			
⇒ ***Optimal Location Line (2) ≡ (6-4), Optimal Setting (0.0573 , 0.8286)***			

$\acute{K}_{(LOLN)}=0$	$Y1=0$	$\Gamma_{(VBVN)}=0$	$Y2=0$	$Я=0$	$Y=0$
Loadability			30.5788%		
⇒ ***No Overloading , No Voltage Violation*** $0.98 \le V_i \le 1.02$					

Table 6.25 Case Study (3) of the real Finnish Network

Case Study 3			
⇒ ***Max. Load for each load bus at the same time with 115% increase for all.***			
⇒ ***Before UPFC Installation***			
$\acute{K}_{(LOLN)}=0$	$Y1=0$	$Я=\acute{K}_{(LOLN)}+\Gamma_{(VBVN)}=0$	$Y=Y1+Y2=0$
Loadability		30.26%	
⇒ ***After UPFC Installation***			
⇒ ***Optimal Location Line (2) ≡ (6-4), Optimal Setting (0.0036 , 0.934)***			

$\acute{K}_{(LOLN)}=0$	$Y1=0$	$\Gamma_{(VBVN)}=0$	$Y2=0$	$Я=0$	$Y=0$
Loadability			31.454%		
⇒ ***No Overloading , No Voltage Violation*** $0.98 \le V_i \le 1.02$					

Table 6.26 Case Study (4) of the real Finnish Network

Case Study 4			
⇒ ***Max. Load for each load bus at the same time with 118% increase for all.***			
⇒ ***Before UPFC Installation***			
$\acute{K}_{(LOLN)} = 1$	$Y1 = 0.1124$	$Я = \acute{K}_{(LOLN)} + \Gamma_{(VBVN)} = 1$	$Y = Y1 + Y2 = 0.1124$
Loadability		31.52%	
Overloaded Line (11) ≡ (9-2)		102.96%	
⇒ ***After UPFC Installation***			
⇒ ***Optimal Location Line (22) ≡ (11-3), Optimal Setting (0.1366 , 1.1958)***			

$\acute{K}_{(LOLN)} = 0$	$Y1 = 0$	$\Gamma_{(VBVN)} = 0$	$Y2 = 0$	$Я = 0$	$Y = 0$
Loadability			34.8819%		
⇒ ***No Overloading , No Voltage Violation*** $0.98 \le V_i \le 1.02$					

Table 6.27 Case Study (5) of the real Finnish Network

Case Study 5			
⇒ ***Max. Load for each load bus at the same time with 120% increase for all.***			
⇒ ***Before UPFC Installation***			
$\acute{K}_{(LOLN)} = 1$	$Y1 = 0.1242$	$Я = \acute{K}_{(LOLN)} + \Gamma_{(VBVN)} = 1$	$Y = Y1 + Y2 = 0.1242$
Loadability		32.37%	
Overloaded Line (11) ≡ (9-2)		105.56%	
⇒ ***After UPFC Installation***			
⇒ ***Optimal Location Line (22) ≡ (11-3), Optimal Setting (0.1508 , 0.9716)***			

$\acute{K}_{(LOLN)} = 0$	$Y1 = 0$	$\Gamma_{(VBVN)} = 0$	$Y2 = 0$	$Я = 0$	$Y = 0$
Loadability			37.1451%		
⇒ ***No Overloading , No Voltage Violation*** $0.98 \le V_i \le 1.02$					

Table 6.28 Case Study (6) of the real Finnish Network

Case Study 6			
⇒ ***Max. Load for each load bus at the same time multiplied by 96% of 2020 coefficient.***			
⇒ ***Before Optimal UPFC (UPFC at line 13, for case 90% of 2020 coefficient)***			
$\acute{K}_{(LOLN)} = 2$	$Y1 = 0.2328$	$Я = \acute{K}_{(LOLN)} + \Gamma_{(VBVN)} = 2$	$Y = Y1 + Y2 = 0.2328$
Loadability		35.42%	
Overloaded Line (11) ≡ (9-2) Overloaded Line (36) ≡ (7-17)		107% 101%	
⇒ ***After UPFC Installation***			
⇒ ***Optimal Location Line (22) ≡ (11-3), Optimal Setting (0.1812 , 0.9356)***			

$\acute{K}_{(LOLN)} = 0$	$Y1 = 0$	$\Gamma_{(VBVN)} = 0$	$Y2 = 0$	$Я = 0$	$Y = 0$
Loadability			37.23%		
⇒ ***No Overloading , No Voltage Violation*** $0.98 \le V_i \le 1.02$					

Table 6.29 Case Study (7) of the real Finnish Network

Case Study 7			
⇒ ***Max. Load for each load bus at the same time multiplied by 98% of 2020 coeff.***			
⇒ ***Before Optimal UPFC (UPFC at line 22, for case 96% of 2020 coefficient)***			
$\acute{K}_{(LOLN)} = 2$	$Y1 = 0.2068$	$Я = \acute{K}_{(LOLN)} + \Gamma_{(VBVN)} = 2$	$Y = Y1 + Y2 = 0.2068$
Overloaded Line (11) ≡ (9-2) Overloaded Line (36) ≡ (7-17)		102.07% 101%	
⇒ ***After UPFC Installation***			
⇒ ***Optimal Location Line (14) ≡ (12-9), Optimal Setting (0.196 ,1.0928)***			

$\acute{K}_{(LOLN)} = 0$	$Y1 = 0$	$\Gamma_{(VBVN)} = 0$	$Y2 = 0$	$Я = 0$	$Y = 0$
⇒ ***No Overloading , No Voltage Violation*** $0.98 \le V_i \le 1.02$					

Table 6.30 Case Study (8) of the real Finnish Network

Case Study 8			
⇒ ***Max. Load for each load bus at the same time multiplied by 98% of 2020 coefficient.***			
⇒ ***Before UPFC installation.***			
$\acute{K}_{(LOLN)} = 1$	$Y1 = 0.1487$	$Я = \acute{K}_{(LOLN)} + \Gamma_{(VBVN)} = 1$	$Y = Y1 + Y2 = 0.1487$
Overloaded Line (11) ≡ (9-2)		110.42%	
⇒ ***After UPFC Installation***			
⇒ ***Optimal Location Line (14) ≡ (12-9), Optimal Setting (0.2032 , 0.8447)***			

$\acute{K}_{(LOLN)} = 0$	$Y1 = 0$	$\Gamma_{(VBVN)} = 0$	$Y2 = 0$	$Я = 0$	$Y = 0$

⇒ ***No Overloading , No Voltage Violation*** $0.98 \le V_i \le 1.02$

Table 6.31 Case Study (9) of the real Finnish Network

Case Study 9			
⇒ ***Max. Load for each load bus at the same time multiplied by 100% 2020 coeff.***			
⇒ ***Before Optimal UPFC (UPFC at line 14, for case 98% of 2020 coefficient)***			
$\acute{K}_{(LOLN)} = 2$	$Y1 = 0.2091$	$Я = \acute{K}_{(LOLN)} + \Gamma_{(VBVN)} = 2$	$Y = Y1 + Y2 = 0.2091$
Overloaded Line (6) ≡ (6-2) Overloaded Line (11) ≡ (9-2)		103% 101%	
⇒ ***After UPFC Installation***			
⇒ ***Optimal Location Line (14) ≡ (12-9), Optimal Setting (0.215 ,0.9883)***			

$\acute{K}_{(LOLN)} = 0$	$Y1 = 0$	$\Gamma_{(VBVN)} = 0$	$Y2 = 0$	$Я = 0$	$Y = 0$

⇒ ***No Overloading , No Voltage Violation*** $0.98 \le V_i \le 1.02$

Table 6.32 Case Study (10) of the real Finnish Network

Case Study 10			
⇒ ***Max. Load for each load bus at the same time multiplied by 100% 2020 coeff.***			
⇒ ***Before UPFC installation.***			
$\acute{K}_{(LOLN)} = 1$	$Y1 = 0.1577$	$Я = \acute{K}_{(LOLN)} + \Gamma_{(VBVN)} = 1$	$Y = Y1 + Y2 = 0.1577$
Overloaded Line (11) ≡ (9-2)		112.07%	
⇒ ***After UPFC Installation***			
⇒ ***Optimal Location Line (14) ≡ (12-9), Optimal Setting (0.215 , 0.9629)***			

$\acute{K}_{(LOLN)} = 0$	$Y1 = 0$	$\Gamma_{(VBVN)} = 0$	$Y2 = 0$	$Я = 0$	$Y = 0$
⇒ ***No Overloading , No Voltage Violation*** $0.98 \le V_i \le 1.02$					

The tables show that the UPFC can enhance the performance of power systems with optimal location and optimal settings. Locating UPFC in the network prevents all of the overloading in the lines. However, all of the bus voltage violations are eliminated, or the technique can achieve the solution region to eliminate the overloaded lines and at the same moment keeping the voltage profile. Increasing the system loadability of a power system as an index to evaluate the impact of UPFC in power system is achieved with respect to the line thermal limits and the bus voltage magnitude limits. Loading increase studies on the system can be applied at different cases and aspects. UPFC in optimal placement can restore the system operating condition to the steady state point.

Figure 6.5 shows the effect of the UPFC at an optimal location with optimal settings on the transmission line flow at the maximum loading pattern of the year 2020.

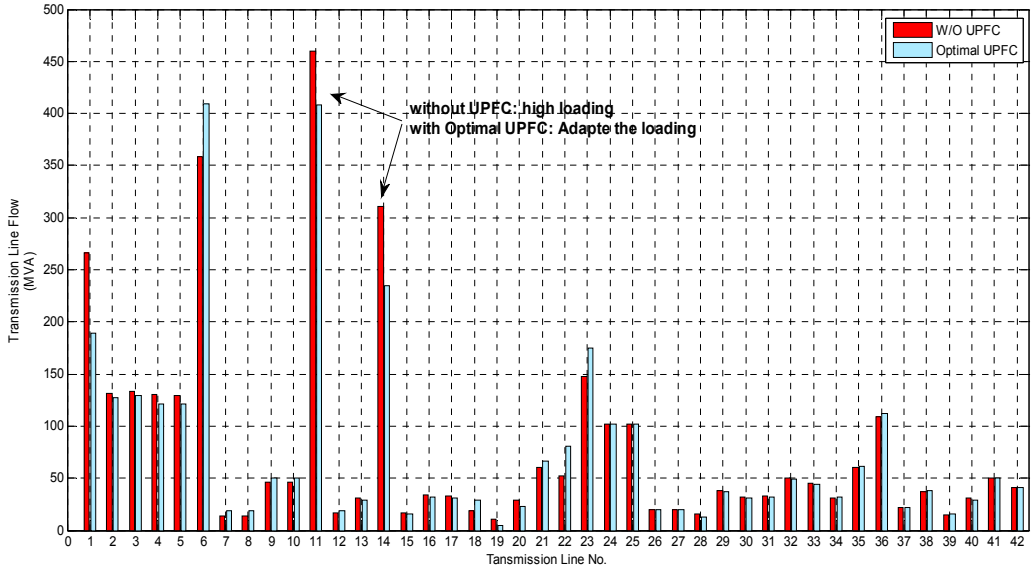

Fig. 6.5 the effect of the UPFC at the maximum loading pattern of the year 2020.

6.5.2 Contingency Operating with Outage Pattern

Most electric power grids are widely interconnected, and are extend to inter-utility interconnections and then to inter-regional and internal connections. That is because of economic issues, to minimize the cost of electricity, and to enhance the reliability of the power supply. However, as power transfer grows, the power system becomes increasable more operation that is complex and the system can be less secure for operating through the sever outages. It may lead to a large power flow with enough control, excessive reactive power in many sections of the system, large dynamic swings between different portions of the networks. Therefore, the full powerful of transmission networks cannot be utilized. Power system stability and thermal constraints restrict the transmission capacity. To meet the increasing load demand and satisfy the stability and reliability criteria, both existing transmission and generation facilities must be utilized more efficiently, or new facilities should be added to the systems. Given the constraints, such as lack of investment and difficulties in getting new transmission line right-of ways, the later is often difficult. The former can be achieved by using UPFC as seen in well-developed power systems throughout the world.

This stage is related to enhancing the performance of the real Finnish Network with regard to the overloading of transmission lines and violation of bus voltage profile during the contingency operating with an outage pattern.

A ranking process is performed on the network after the contingency analysis. There will be some single contingencies. For each single line outage, we will find the following performance indices $\acute{K}_{(LOLN)}$ and $\Gamma_{(VBVN)}$.

Then we rank the lines according to the severity of the contingency, in other words, according to $Я = \acute{K}_{(LOLN)} + \Gamma_{(VBVN)}$. The remaining cases will not be of concern where the totally performance indices equal zero.

The results will be performed on the real Finnish Network with the maximum loading value for each bus individual at the same time to achieve the worst loading pattern of the system. Also using these conditions, the simulation and the analysis will be verified on the maximum loading pattern of the year 2020 to improve the performance and solve the related problems in the network.

Table 6.33 Ranking for the severity contingency cases for the real Finnish Network (*Max. Load for each load bus at the same time multiplied by Year 2020 coefficient)*

Ranking Case	Line Number	Connecting Bus		$\acute{K}_{(LOLN)}$	$\Gamma_{(VBVN)}$	$Я = \acute{K}_{(LOLN)} + \Gamma_{(VBVN)}$
		From	To			
1	6	2	6	3	0	3
2	11	9	2	1	0	1
3	14	12	9	1	0	1
4	3	6	4	1	0	1
5	2	6	4	1	0	1
6	1	12	6	1	0	1

Table 6.34 Outage Case Study (1) of the real Finnish Network

Outage Case Study 1			
⇒ ***Outage of Line (6) ≡ (2-6), Severity Rank =1***			
⇒ ***Before UPFC Installation***			
$\acute{K}_{(LOLN)} = 3$	$Y1 = 1.2227$	$Я = \acute{K}_{(LOLN)} + \Gamma_{(VBVN)} = 3$	$Y = Y1 + Y2 = 1.2227$
Loadability		32.74%	
Overloaded Line (1) ≡ (6-12)		115.72%	
Overloaded Line (11) ≡ (9-2)		168.2%	
Overloaded Line (14) ≡ (12-9)		125.3%	
⇒ ***After UPFC Installation***			
⇒ ***Optimal Location Line (22) ≡ (11-3), Optimal Setting (0.2546 , 0.98)***			

$\acute{K}_{(LOLN)} = 1$	$Y1 = 0.8$	$\Gamma_{(VBVN)} = 0$	$Y2 = 0$	$Я = 1$	$Y = 0.8$
Loadability			33.85%		
⇒ ***One Overloading***	***Line (11)***	***Eliminate Overloading at line 1, 14***			
⇒ ***No Voltage Violation*** $0.98 \le V_i \le 1.02$					

Table 6.35 Outage Case Study (2) of the real Finnish Network

Outage Case Study 2			
⇒ ***Outage of Line (11) ≡ (9-2), Severity Rank =2***			
⇒ ***Before UPFC Installation***			
$\acute{K}_{(LOLN)} = 1$	$Y1 = 0.8053$	$Я = \acute{K}_{(LOLN)} + \Gamma_{(VBVN)} = 1$	$Y = Y1 + Y2 = 0.8053$
Overloaded Line (6) ≡ (6-2)		168.46 %	
⇒ ***After UPFC Installation***			
⇒ ***Optimal Location Line (6) ≡ (6-2), Optimal Setting (0.20 , 0.80)***			

$\acute{K}_{(LOLN)} = 1$	$Y1 = 0.15$	$\Gamma_{(VBVN)} = 0$	$Y2 = 0$	$Я = 1$	$Y = 0.15$
- One Overloading	***Line (6)***	***Reduced Overloading (168.46% to 110%)***			
⇒ ***No Voltage Violation*** $0.98 \le V_i \le 1.02$					

Table 6.36 Outage Case Study (3) of the real Finnish Network

Outage Case Study 3			
⇒ ***Outage of Line (14) ≡ (12-9), Severity Rank =3***			
⇒ ***Before UPFC Installation***			
$\acute{K}_{(LOLN)} = 1$	$Y1 = 0.1762$	$Я = \acute{K}_{(LOLN)} + \Gamma_{(VBVN)} = 1$	$Y = Y1 + Y2 = 0.1762$
Loadability		27.88%	
Overloaded Line (6) ≡ (6-2)		115.21%	
⇒ ***After UPFC Installation***			
⇒ ***Optimal Location Line (22) ≡ (11-3), Optimal Setting (0.239 , 0.9525)***			

$\acute{K}_{(LOLN)} = 0$	$Y1 = 0$	$\Gamma_{(VBVN)} = 0$	$Y2 = 0$	$Я = 0$	$Y = 0$
Loadability			29.4468%		
⇒ ***No Overloading , No Voltage Violation*** $0.98 \le V_i \le 1.02$					

Table 6.37 Outage Case Study (4) of the real Finnish Network

Outage Case Study 4			
⇒ ***Outage of Line (3) ≡ (6-4), Severity Rank =4***			
⇒ ***Before UPFC Installation***			
$\acute{K}_{(LOLN)} = 1$	$Y1 = 0.1624$	$Я = \acute{K}_{(LOLN)} + \Gamma_{(VBVN)} = 1$	$Y = Y1 + Y2 = 0.1624$
Loadability		30.9%	
Overloaded Line (36) ≡ (7-17)		112.89 %	
⇒ ***After UPFC Installation***			
⇒ ***Optimal Location Line (15) ≡ (8-5), Optimal Setting (0.0872 , 0.9260)***			

$\acute{K}_{(LOLN)} = 0$	$Y1 = 0$	$\Gamma_{(VBVN)} = 0$	$Y2 = 0$	$Я = 0$	$Y = 0$
Loadability			32.4554%		
⇒ ***No Overloading , No Voltage Violation*** $0.98 \le V_i \le 1.02$					

Table 6.38 Outage Case Study (5) of the real Finnish Network

Outage Case Study 5			
⇒ ***Outage of Line (2) ≡ (6-4), Severity Rank =5***			
⇒ ***Before UPFC Installation***			
$\acute{K}_{(LOLN)} = 1$	$Y1 = 0.1578$	$Я = \acute{K}_{(LOLN)} + \Gamma_{(VBVN)} = 1$	$Y = Y1 + Y2 = 0.1578$
Loadability		30.85%	
Overloaded Line (36) ≡ (7-17)		112.07%	
⇒ ***After UPFC Installation***			
⇒ ***Optimal Location Line (15) ≡ (8-5), Optimal Setting (0.1104 , 0.8402)***			

$\acute{K}_{(LOLN)} = 0$	$Y1 = 0$	$\Gamma_{(VBVN)} = 0$	$Y2 = 0$	$Я = 0$	$Y = 0$
Loadability			34.100%		
⇒ ***No Overloading , No Voltage Violation*** $0.98 \le V_i \le 1.02$					

Table 6.39 Outage Case Study (6) of the real Finnish Network

Outage Case Study 6			
⇒ ***Outage of Line (1) ≡ (6-12), Severity Rank =6***			
⇒ ***Before UPFC Installation***			
$\acute{K}_{(LOLN)} = 1$	$Y1 = 0.1386$	$Я = \acute{K}_{(LOLN)} + \Gamma_{(VBVN)} = 1$	$Y = Y1 + Y2 = 0.1386$
Loadability		27.57%	
Overloaded Line (6) ≡ (6-2)		108.5%	
⇒ ***After UPFC Installation***			
⇒ ***Optimal Location Line (23) ≡ (9-11), Optimal Setting (0.2912 , 0.8249)***			

$\acute{K}_{(LOLN)} = 0$	$Y1 = 0$	$\Gamma_{(VBVN)} = 0$	$Y2 = 0$	$Я = 0$	$Y = 0$
Loadability			28.9328%		
⇒ ***No Overloading , No Voltage Violation*** $0.98 \le V_i \le 1.02$					

The results indicate that the UPFC can efficiently enhance the characteristics of power systems with optimal position and optimal parameter settings. Positioning UPFC in the network cancels the overloading in the lines in most of the conditions. In other cases, most of the overloaded lines are cancelled and the power flow in the rest-overloaded lines is efficiently decreased.

Increasing of the system loadability of a power system as an index to evaluate the impact of UPFC in power system is achieved with respect to the line thermal limits and the bus voltage magnitude limits. Load increasing studies on the system can be applied at different cases and aspects. Figure 6.6 shows the effect of the Optimal UPFC on the transmission line flow at the year 2020 during the Outage of Line (14).

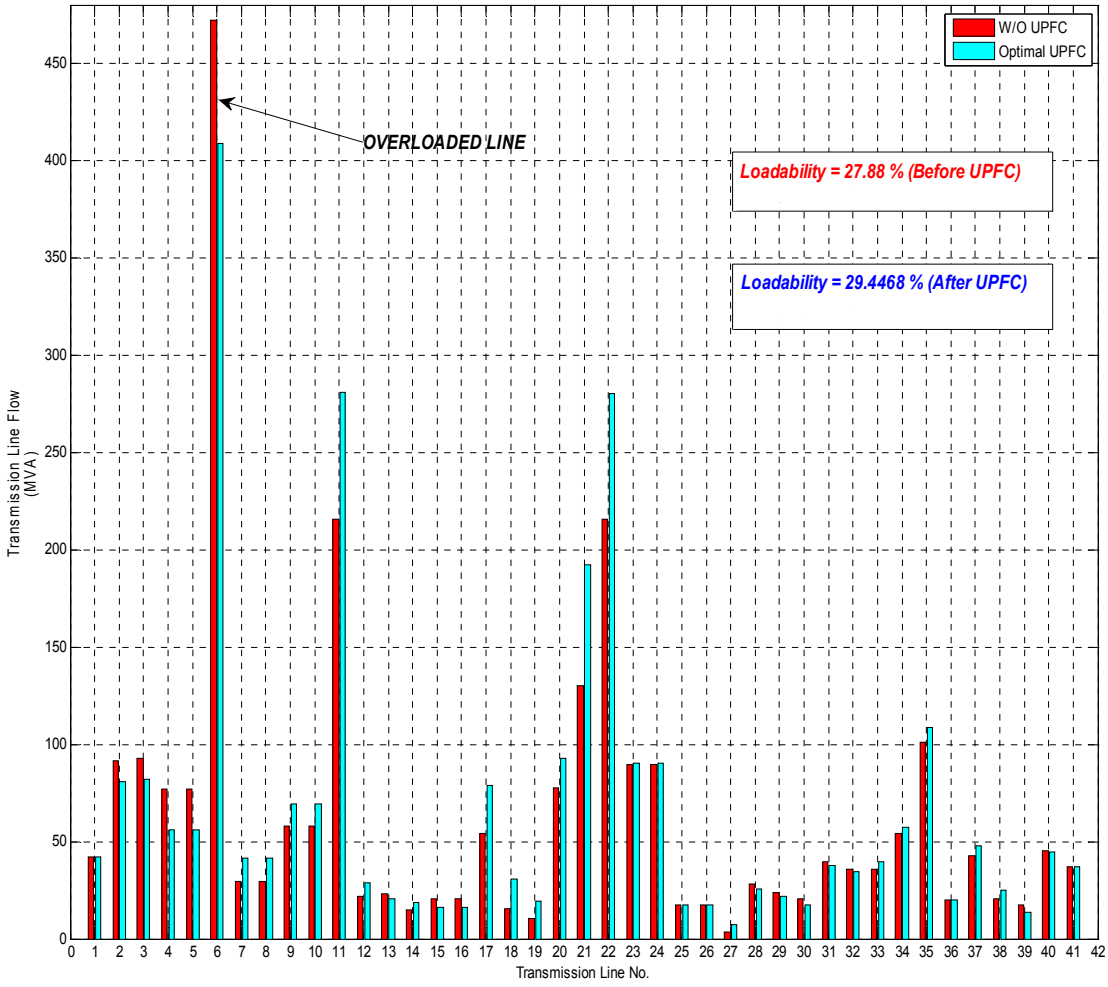

Fig. 6.6 the effect of the Optimal UPFC on the transmission line flow at Year 2020 during the Outage of Line (14).

6.6 Cases Study: Optimal Installation for Load Profile Period

6.6.1 Normal Configuration with high loading

We will start by selecting one of the highly loading conditions for the real Finnish Network in the year 2020, using the hourly loading profile and forecasting the coefficient for the year 2020. Then, to generate the load profile period for that highly loaded condition, we will focus on the week that contains that highly case.

Table 6.40, Case (1) Normal Configuration

➔ ***Without UPFC*** :

- For a given loading scenario in 2020, one loading pattern on the week that contains highly loading conditions.

(Considering 168 loading cases with one-hour load steps for the 42 lines of the real Finnish Network)

- Total number of overloads (out of a possible number of 168 loading cases x 42 lines) = 179
- Number of overloads in current concerned scenario = 2.

$K_{(LOLN)}$=2	Y1=2.7	$\Gamma_{(VBVN)}$=0	Y2=0	Я =2	Y=Y1
Overloaded Line 17-18			121.67 %		
Overloaded Line 17-7			224.58 %		

➔ ***With UPFC*** :

- For the same load scenario
- The optimal location is on line (36) and the optimal setting is: [0.097257 , 0.93716]
- Total number of overloads (out of a possible number of 168 loading cases x 42 lines) with UPFC = 2
- Number of overloads in current concerned scenario = 0

$K_{(LOLN)}$=0	Y1=0	$\Gamma_{(VBVN)}$=0	Y2=0	Я =0	Y=0

➔ No overloading, no voltage violation $0.95 \leq V_i \leq 1.05$

Naturally, the study forms required part for planning the upgrading of a sub-transmission network that will cope with future load and contingency requirements in the most effective manner. We will simply state that the line is secure for the future load scenario. Optimal location and the optimal parameter settings of the UPFC in the power network eliminate or minimize the overloaded lines and the bus voltage violations. These results prove to be successful in solving the steady-state problems and in enhancing performance in the majority of the cases. UPFC is already kept in its optimum location, as in table 6.40 where considering 168 loading cases with one-hour load steps for the 42 lines of the Network, so it is kept for one week with 168 cases. The following tables will have their description about the cases.

Table 6.41, Case (2) Normal Configuration

➔ ***Without UPFC*** :

- For another given loading scenario in 2020, which is the maximum loading Pattern.

(Considering 168 loading cases with one-hour load steps for the 42 lines of the real Finnish Network)

- Total number of overloads (out of a possible number of 168 x 42) with UPFC = 179
- Number of overloads in current concerned scenario = 2

$Ќ_{(LOLN)}$=2	Y1=1.76	$Γ_{(VBVN)}$=0	Y2=0	Я =2	Y=Y1
Overloaded Line 17-18			105.73 %		
Overloaded Line 17-7			201.18 %		

* Without UPFC line 17-7 exceeds the thermal limit given by a transient thermal analysis, i.e., the overload percentage of 201% exceeds the cyclic rating factor of approximately 155%.

➔ ***With UPFC*** :

- For the same load scenario
- Optimal location at line (36) with optimal setting: [0.097257 , 0.93716]
- Total no. of overloads (out of 168 x 42) with UPFC = 2
- Number of overloads in current concerned scenario = 1

Overloaded Line 21-5			104.22 %		
$Ќ_{(LOLN)}$=1	Y1=0.12	$Γ_{(VBVN)}$=0	Y2=0	Я =1	Y=Y1

➔ No voltage violation $0.95 \leq V_i \leq 1.05$

The thermal overload, which occurs on 38, is only slight. This line is split between an old oil cable, which will most likely have been upgraded by the time this simulation is valid for, and a 3 x AHXLMK 800 installation, which are more modern XLPE cables with 800 mm^2 stranded aluminum conductors. If the entire overloaded line section has been upgraded by 2020, then the projected overload will not be an overload at all, even in steady-state terms, but if the old oil cables still remain in use, a transient rating shows that they are, at least thermally, in no danger. The cyclic loading factor for these cables is approximately 155%, which is much greater than the projected overload based on a steady-state rating of 104.22%. Thus, we can safely say, for this case the projected thermal overload is not a thermal overload when a full transient analysis is performed.

6.6.2 The contingency Study

During the same load profile for the highly loaded conditions, The total number of overload cases for each of 42 single contingency outage cases. Each contingency case has 168 loading patterns $\Rightarrow$ 3677 cases. The most severe case is the outage of line 24, which

gives rise to the highest number of overloaded lines – 140 overloaded cases from the 168 loading cases.

The second most severe case is the outage of line 2, which has the second highest number of overloaded lines – 106 overload cases from the 168 loading cases.

Table 6.42 Contingency Case (1)

➔ ***Without UPFC*** :

- Severity case Rank 1 = outage of line 24, For a given loading scenario in 2020, one loading pattern on the week that contains highly loading conditions.
- Total number of overloads (out of 168 x 41) without UPFC = 140
- Number of overloads in current concerned scenario = 3

$Ќ_{(LOLN)}$=2	Y1=0.56	$Γ_{(VBVN)}$=0	Y2=0	Я =2	Y=Y1
Overloaded Line 1-2			102.18 %		
Overloaded Line 23-5			127.65 %		
Overloaded Line 17-18			115.29 %		

➔ ***With UPFC*** :

- For the same loading scenario; with outage of line 24.
- Optimal location at line (4) with optimal setting: [0.24324 , 0.98349]
- Total number of overloaded lines (out of 168 x 41) when there is an outage of line 24 with UPFC = 13
- Number of overloads in current concerned scenario = 0

$Ќ_{(LOLN)}$=0	Y1=0	$Γ_{(VBVN)}$=0	Y2=0	Я =0	Y=Y1
➔ No overloading, no voltage violation $0.95 \le V_i \le 1.05$					

Table 6.43, Contingency Case (2)

One of the (13) cases with overloads after UPFC Optimal placement

➔ ***Without UPFC*** :

- Severity case Rank 1 = outage of line 24, for the given loading scenario, which the maximum loading pattern.
- Total number of overloads (out of 168 x 41) without UPFC = 140

➔ ***With UPFC*** :

- For an outage of line 24
- Optimal location at line (4) with optimal setting: [0.24324 , 0.98349]
- Total number of overloads (out of 168 x 41) with UPFC = 13
- One of the (13) cases, after UPFC Optimal placement

Overloaded Line 17-18		106.23%			
$Ќ_{(LOLN)}$=0	Y1=0.13	$Γ_{(VBVN)}$=0	Y2=0	Я =1	Y=Y1
➔ No voltage violation $0.95 \le V_i \le 1.05$					

In this case, the cyclic rating factor is only 107.5 % and so the full thermal response is shown in Fig. 6.7.

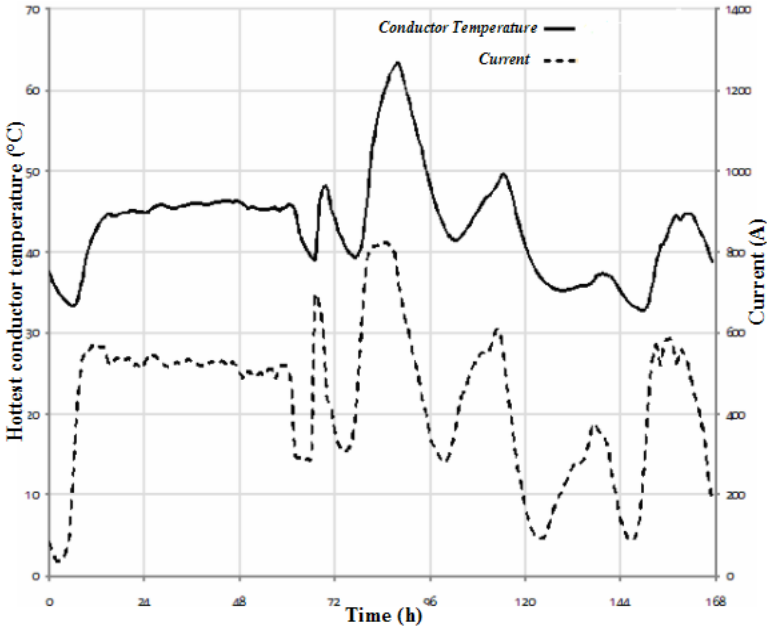

Fig. 6.7. Temperature response of cable for the 1st severity case (Contingency Case (2)).

As can be seen in Fig. 6.7, the temperature does not rise above 65 °C in the hottest conductor, so we can conclude that even with conservative thermal modeling, the cables will not overheat in the projected future loading scenario due to this contingency. The second severity case is the outage of line 2; it has the second highest number of overloaded lines, 106 out of a possible 168 loading cases.

Table 6.44, Contingency Case (3)

➔ ***Without UPFC*** :
- Severity case Rank 2 = outage of line 2
- Total number of overloaded lines (out of 168 x 41) without UPFC = 106

➔ ***With UPFC*** :
- at outage of line 2
- Optimal location at line (4) with optimal setting: [0.24324 , 0.98349]
- Total number of overloaded lines (out of 168 x 41)
  at outage of line 2 with UPFC = 38
- One of these cases, after UPFC Optimal placement

Overloaded Line 17-18			117.65 %		
$\acute{K}_{(LOLN)}=0$	Y1=0.36	$\Gamma_{(VBVN)}=0$	Y2=0	Я =1	Y=Y1
➔ No voltage violation $0.95 \leq V_i \leq 1.05$					

This thermal overload is the most severe out of the cases considered and its thermal response is given below in Fig. 6.8.

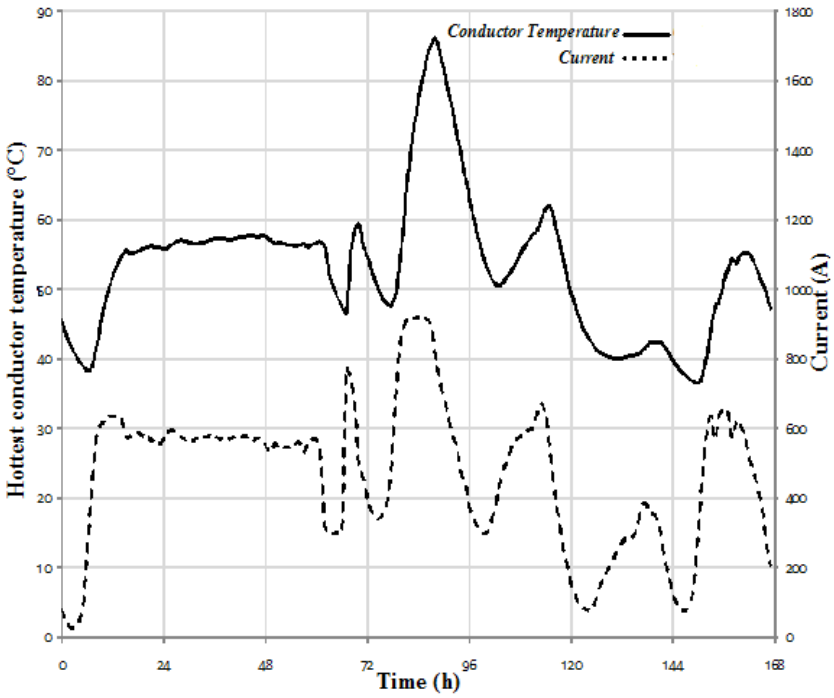

Fig. 6.8. Temperature response of cable for the 2nd severity case (Contingency Case (3)).

It can be seen that the temperature exceeds 65 °C in contingency 2. 65 °C has normally been used as the maximum allowable conductor temperature in underground cables in order to avoid moisture migration problems. Now, however, we have conservatively modeled moisture migration in the transient analysis, which means that the catalogue maximum temperature for continuous operation of 90 °C can be considered – and, as Fig. 6.8 shows, the temperature stays below 90 °C. If moisture migration occurs at lower temperatures, however, 90 °C will be exceeded.

Some publications for the author are done using the previous sections and previous results in this chapter [86] – [90].

6.7 Case Study: Fixed Location with Optimal Setting

The following case study involves studying the effect of searching for only the optimal settings at fixed locations of UPFC. To achieve a link between the results, we will use the results of Section 6.5.1; Table 6.28 indicates that using proposed GA the optimal UPFC is in location of line 13, for case 90 % of operating conditions of the year 2020. However, for the loading pattern of 96 % of operating conditions of the year 2020, this location should be modified using the proposed GA to location of line 22 with optimal settings of (0.1812 , 0.9356) to solve the problem of overloading of line 11 and line 36 and also to enhance the loadability. The analysis now will study fixing the location of UPFC at line 13 for the two cases 90 % and 96 % of operating conditions of the year 2020, and search for the optimal settings only.

Table 6.45 Case Study (1) for optimal settings of UPFC only.

<table>
<tr><td colspan="6">Case Study</td></tr>
<tr><td colspan="6">⇒ Max. Load for each load bus at the same time multiplied by 96% of 2020 coeff.</td></tr>
<tr><td colspan="6">⇒ Before Optimal Process , UPFC at Line (13) , Setting (0.001 , 0.800)
(UPFC at Optimal Location and settings of previous pattern 90 % of year 2020)</td></tr>
<tr><td colspan="2">$\acute{K}_{(LOLN)} = 2$</td><td colspan="2">Y1 = 0.2328</td><td>$Я = \acute{K}_{(LOLN)} + \Gamma_{(VBVN)} = 2$</td><td>Y = 0.2328</td></tr>
<tr><td colspan="3">Loadability</td><td colspan="3">35.42%</td></tr>
<tr><td colspan="3">Overloaded Line (11) ≡ (9-2)</td><td colspan="3">107%</td></tr>
<tr><td colspan="3">Overloaded Line (36) ≡ (7-17)</td><td colspan="3">101%</td></tr>
<tr><td colspan="6">⇒ Performing Optimal Process for UPFC settings with fixed Location
⇒ UPFC at Location Line (13) , Optimal Setting (0.0750 , 0.8000)</td></tr>
<tr><td colspan="2">$\acute{K}_{(LOLN)} = 1$</td><td colspan="2">Y1 = 0.1310</td><td>$Я = \acute{K}_{(LOLN)} + \Gamma_{(VBVN)} = 1$</td><td>Y = 0.1310</td></tr>
<tr><td colspan="3">Loadability</td><td colspan="3">35.48%</td></tr>
<tr><td colspan="3">Overloaded Line (11) ≡ (9-2)</td><td colspan="3">106%</td></tr>
<tr><td colspan="6">⇒ With UPFC for Optimal Location Line (22), Optimal Setting (0.1812 , 0.9356)</td></tr>
<tr><td>$\acute{K}_{(LOLN)} = 0$</td><td>Y1 = 0</td><td>$\Gamma_{(VBVN)} = 0$</td><td>Y2 = 0</td><td>Я = 0</td><td>Y = 0</td></tr>
<tr><td colspan="3">Loadability</td><td colspan="3">37.23%</td></tr>
<tr><td colspan="6">⇒ No Overloading , No Voltage Violation $0.98 \le V_i \le 1.02$</td></tr>
</table>

Also, Table 6.29 indicates the optimal location and settings for 98% of operating conditions of the year 2020; this loading pattern will be used again but with fixing the location of UPFC and uses the optimal process for the optimal settings only.

Table 6.46 Case Study (2) for optimal settings of UPFC only.

Case Study			
⇒ ***Max. Load for each load bus at the same time multiplied by 98% of 2020 coefficient.***			
⇒ ***Before Optimal Process , UPFC at Line (22) , Setting (0.1812 , 0.9356) (UPFC at Optimal Location and settings of previous pattern 96 % of year 2020)***			
$\acute{K}_{(LOLN)} = 2$	$Y1 = 0.2068$	$Я = \acute{K}_{(LOLN)} + \Gamma_{(VBVN)} = 2$	$Y = 0.2068$
Overloaded Line (11) ≡ (9-2)		101.07%	
Overloaded Line (36) ≡ (7-17)		101%	
⇒ ***Performing Optimal Process for UPFC settings with fixed Location***			
⇒ ***UPFC at Location Line (22) , Optimal Setting (0.1784 , 1.1980)***			
$\acute{K}_{(LOLN)} = 1$	$Y1 = 0.1048$	$Я = \acute{K}_{(LOLN)} + \Gamma_{(VBVN)} = 1$	$Y = 0.1048$
Overloaded Line (11) ≡ (9-2)		101.119%	
⇒ ***Performing Optimal Process, for Optimal Location and Optimal Setting***			
⇒ ***With UPFC for Optimal Location Line (14), Optimal Setting (0.1960 , 1.0928)***			

$\acute{K}_{(LOLN)} = 0$	$Y1 = 0$	$\Gamma_{(VBVN)} = 0$	$Y2 = 0$	$Я = 0$	$Y = 0$
⇒ ***No Overloading , No Voltage Violation*** $0.98 \le V_i \le 1.02$					

The previous results show that the effective actions of UPFC are achieved when performing the optimal process for the optimal location and the optimal settings together. Table 6.45 indicates that the optimal process for the optimal setting with fixed location from the previous loading pattern does not achieve the maximum benefits where the network will still have overloaded lines. In addition, the enhancing in the loadability is significantly slight low with searching for the optimal settings only, where with optimal location and optimal settings together the enhancing in the loadability is clearer. In addition, Table 6.46 shows that the optimal process for the optimal setting with fixed location from the previous loading pattern does not get the desired performance for totally no overloading.

6.8 Case Study: Multiple Optimal UPFC Installation

The following case study is concerned with modifying the proposed GA to install multiple UPFCs according to optimal locations and optimal settings for each UPFC in order to enhance the network performance. To achieve a link between the results, we will use the results of Section 6.5.1. Table 6.29 indicates that used proposed GA, the optimal UPFC is in the location of line 14 for case of 98 % of operating conditions for the year 2020, with optimal settings of (0.1960 , 1.0928) to solve the problem of the overloading of line 11 and line 36 with one optimal UPFC. The analysis now will study installing multiple UPFCs instead of only of only a single UPFC.

Table 6.47 Case Study (1) for Multiple Optimal UPFC Installation

Case Study

⇒ ***Max. Load for each load bus at the same time multiplied by 98% of 2020 coeff.***

⇒ ***Before Optimal Process for Multiple UPFC.***

⇒ ***UPFC at Line (22) , Setting (0.1812 , 0.9356)***

(UPFC at Optimal Location and settings of previous pattern 96 % of year 2020)

$\acute{K}_{(LOLN)} = 2$	$Y1 = 0.2068$	$Я = \acute{K}_{(LOLN)} + \Gamma_{(VBVN)} = 2$	$Y = 0.2068$
Overloaded Line (11) ≡ (9-2)		101.07%	
Overloaded Line (36) ≡ (7-17)		101%	

- Performing Optimal Process for Multiple UPFC (optimal locations & settings)

⇒ ***UPFC(1) at Location Line (39) , Optimal Setting (0.0138 , 0.8975)***

⇒ ***UPFC(2) at Location Line (14) , Optimal Setting (0.2228 , 0.9238)***

$\acute{K}_{(LOLN)} = 0$	$Y1 = 0$	$\Gamma_{(VBVN)} = 0$	$Y2 = 0$	$Я = 0$	$Y = 0$

⇒ ***No Overloading , No Voltage Violation*** $0.98 \le V_i \le 1.02$

In addition, Table 6.32 indicates the optimal location and settings for 100% of operating conditions of the year 2020, this loading pattern will be used again but with installing multiple UPFCs with optimal locations and setting for each UPFC.

Table 6.48 Case Study (2) for Multiple Optimal UPFC Installation.

Case Study			
⇒ ***Max. Load for each load bus at the same time multiplied by 100% of 2020 coefficient.***			
⇒ ***Before Optimal Process for Multiple UPFC.***			
⇒ ***Without UPFC Installation***			
$\acute{K}_{(LOLN)} = 1$	$Y1 = 0.1577$	$Я = \acute{K}_{(LOLN)} + \Gamma_{(VBVN)} = 1$	$Y = Y1 + Y2 = 0.1577$
Overloaded Line (11) ≡ (9-2)		112.07%	
- Performing Optimal Process for Multiple UPFC (optimal locations & settings)			
⇒ ***UPFC(1) at Location Line (14) , Optimal Setting (0.2186 , 0.9657)***			
⇒ ***UPFC(2) at Location Line (10) , Optimal Setting (0.0282 , 0.8620)***			

$\acute{K}_{(LOLN)} = 0$	$Y1 = 0$	$\Gamma_{(VBVN)} = 0$	$Y2 = 0$	$Я = 0$	$Y = 0$
⇒ ***No Overloading , No Voltage Violation*** $0.98 \le V_i \le 1.02$					

The previous tables state that multiple optimal UPFC can fulfill the required performance and enhance the features of the grid. However, by comparing Table 6.29 with 6.48 and Table 6.32 with 6.49, we can note that one optimal UPFC will achieve the same outputs of multiple optimal UPFCs. In addition, the tables show that the process of one optimal UPFC reaches the same optimal location that multiple optimal UPFC reach. However, with tuning the optimal settings of one optimal UPFC, it achieves the objective function without installing more UPFCs. From an economical point of view, when one optimal UPFC can fulfill the required performance, so there is no need for multiple optimal UPFC, due to the high cost of installing more UPFC devices. Also, from a technical perspective, more UPFC installation may cause itself to overloading.

6.9 Optimal Power Flow Case

The FACTS technology is a solution for the transmission level in the power system. Due to the power market and Deregulated power system concepts, which are now applicable in most of real power networks, we should obtain many solution related to each power system level and section. The power market concept divides the power system operation into many levels and sections. Each level is controlled by a certain authority or company. There are many principles, which consider that the ultimate open supplier is the Transmission System Operator (TSO). The optimal power flow sometimes is unable to solve the technical problems of the power network; also in some cases it strikes or hits the bounds of the system variables. Some variables needs to lambda multiplier to just be kept

at the limits. The main issue is that the optimal power flow requires actions from the generation, transmission and distribution levels.

Table 6.49 IEEE 30-Bus Case [85], Study OPF and Optimal UPFC

System Summary					
Buses No. 30		Generators No. 6		Lines No. 41	
Loads No. 20		Shunts No. 2			
I. OPF Simulation					
Objective Function Value = 576.89 $/hr					
Lambda P Lambda Q	(min) 3.66 $/MWh @ bus 1 (min) -0.06 $/MWh @ bus 29		(max) 5.38 $/MWh@bus 8 (max) 1.40 $/MWh@bus 8		
Voltage Constraints					
Bus #	Vmin mu	Vmin	|V|	Vmax	Vmax mu
29	-	0.950	1.050	1.050	29.810
Line Flow Constraints					

Line #	From Bus	"From" End |Sf| mu	"From" End |Sf|	Limit |Smax|	"To" End |St|	"To" End |St| mu	To Bus
10	6	2.387	32.00	32.00	31.63	-	8
35	25	-	15.62	16.00	16.00	0.024	27

II. Optimal UPFC Placement					
- After UPFC Installation *- Optimal Location Line (10) ≡ (6-8), Optimal Setting (0.0023794 , 0.99983)*					
$\acute{K}_{(LOLN)} = 0$	*Y1 = 0*	$\Gamma_{(VBVN)} = 0$	*Y2 = 0*	*Я = 0*	*Y = 0*
- No Overloading , No Voltage Violation $0.95 \le V_i \le 1.05$					

6.10 Dynamics of the system (Concept and Building)

The unified power flow controller was proposed as a device of flexible AC transmission systems. This is a multiple functional FACTS controller with the main task to control the power flow. The additional jobs of UPFC are to provide voltage control, transient stability enhancement, oscillation damping. UPFC can be very effective to damp power system oscillations.

Because FACTS devices have very fast dynamics compared to generators, they can play important roles to enhance the dynamics response. This is usually accomplished through controls associated with theses devices. Using a damping controller with the UPFC can enhance the electromechanical mode damping. That controller can be one of inherent UPFC PI damping controller. UPFC main controllers can enhance system dynamics but the dynamics parameters setting should first be selected to damp and fine tuning the response. Damping controller for UPFC may affect the system response.

The effect of different controllers as conventional and adaptive AI controllers can be compared to conclude the most effective controller. The operating conditions can be changed according to the disturbance, which affect the power system response. In the steady state analysis section, we considered the increasing in loading conditions, which lead to a change from one certain operating condition to another operating point. In addition, we considered the contingency outage cases, which produce an increase in the loading of all network elements.

For making stress on the correlation between the steady state and the dynamic analysis, we will consider the cases and the operating conditions from the steady state analysis. The steady state analysis leads to the importance of installing the UPFC in certain optimal locations with certain optimal settings. That may be considered as a comparison between installing and not installing the UPFC in the system. After we installed the UPFC at these optimal locations to achieve enhanced steady state performance, we should adapt the dynamic parameters to achieve also the optimal dynamic response.The mechanical modes of the generators in the system can be good indicators for the dynamic response; the speed deviation response ($\Delta\omega$) and the mechanical rotor angle dynamic response ($\Delta\delta$) can be shown.

The link between the steady state and the dynamic analysis can be achieved by considering the results from the steady state as a part for the dynamic response analysis. So the same operating conditions will be assumed, we will select some different cases and patterns from the previous analysis in Sections 6.5.1 and 6.5.2 to complete the analysis with the dynamic response analysis. Building and adapting the system configuration to be suitable for the dynamic response analysis will be achieved using the derivation and programming of dynamics equation in Chapter 4, Section 4.4 by m-file codes linked with Simulink blocks models. Some scope on the dynamic model of UPFC, as in Fig. 6.9 and the dynamic model of a multi-machine power system equipped with UPFC will appear in the Appendix section.

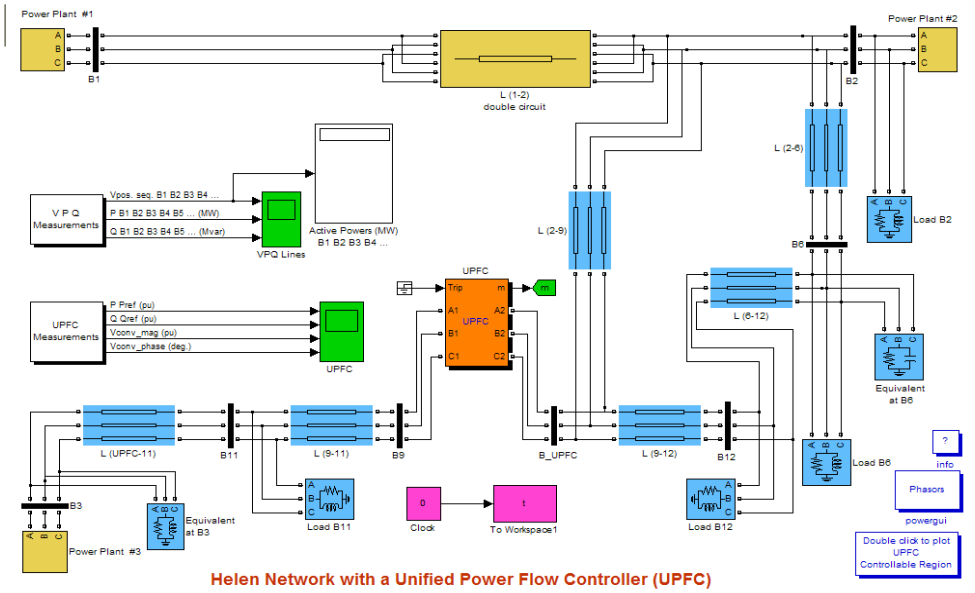

Fig. 6.9, a zone scope of dynamic blocks for the real Finnish Network at certain case study from steady state analysis.

6.11 Importance of Dynamics Tuning

To show the importance of tuning the dynamic parameters of the UPFC, we will introduce a case study from the cases indicated before in steady state performance enhancing. In the previous cases, this stage was concerned with enhancing the performance of the network related to overloading of the transmission lines and violation of the bus voltage profile. This task performed on the normal configuration of the system with an increasing the loading pattern until the year 2020. The results lead to optimal location and optimal settings of UPFC to be installed to achieve the required performance.

After installing the UPFC at these optimal locations with optimal settings, the dynamic parameters of the UPFC will have a significant effect on the dynamic response especially the mechanical variables response as the speed deviation response ($\Delta\omega$) and the mechanical rotor angle dynamic response ($\Delta\delta$) of the generating units. The dynamic blocks of the UPFC are indicated in Chapter 4, Section 4.5. The dynamics parameters for the UPFC blocks should be well selected and be set to fine tune the response and damp the oscillation and enhance the settling time of the response. More focus on the UPFC parameters, and the ones which should be adapted, will be shown in the following sections.

Table 6.50 indicates the case study, which will be the start to show the importance of adapting the dynamic parameters of the UPFC after its installation in the optimal location with the optimal settings.

Table 6.50 Case Study for the optimal location and setting of UPFC on the real Finnish network (Start Point).

<table>
<tr><th colspan="6">Case Study</th></tr>
<tr><td colspan="6">- Max. Load for each load bus at the same time multiplied by 97% of 2020 coeff.
⇒ Before Optimal UPFC.</td></tr>
<tr><td>Ќ (LOLN)= 2</td><td colspan="2">Y1 = 0.24</td><td>Я = Ќ(LOLN)+Γ(VBVN) = 2</td><td colspan="2">Y =Y1+Y2 = 0.24</td></tr>
<tr><td colspan="3">Loadability</td><td colspan="3">33%</td></tr>
<tr><td colspan="3">Overloaded Line (11) ≡ (9-2)</td><td colspan="3">108%</td></tr>
<tr><td colspan="6">⇒ After UPFC Installation
- Optimal Location Line (22) ≡ (3-11), Optimal Setting (0.1812 , 0.9356)</td></tr>
<tr><td>Ќ (LOLN)= 0</td><td>Y1 = 0</td><td>Γ(VBVN) = 0</td><td>Y2 = 0</td><td>Я = 0</td><td>Y = 0</td></tr>
<tr><td colspan="3">Loadability</td><td colspan="3">37.63%</td></tr>
<tr><td colspan="6">⇒ No Overloading , No Voltage Violation $0.98 \le V_i \le 1.02$</td></tr>
</table>

After installing the UPFC at the optimal location line (22) ≡ (3-11), with optimal setting (V_{VR} = 0.1812 , V_{CR} = 0.9356), we should build up the dynamic model of the Finnish network including UPFC at the optimal location, as in Fig. 6.10. That building will use the dynamic equations of UPFC from Equations (4.5) to (4.21) incorporated with the block models for the Finnish network elements and UPFC blocks; the Appendix section will present a part of equations and programming codes for constructing the model.

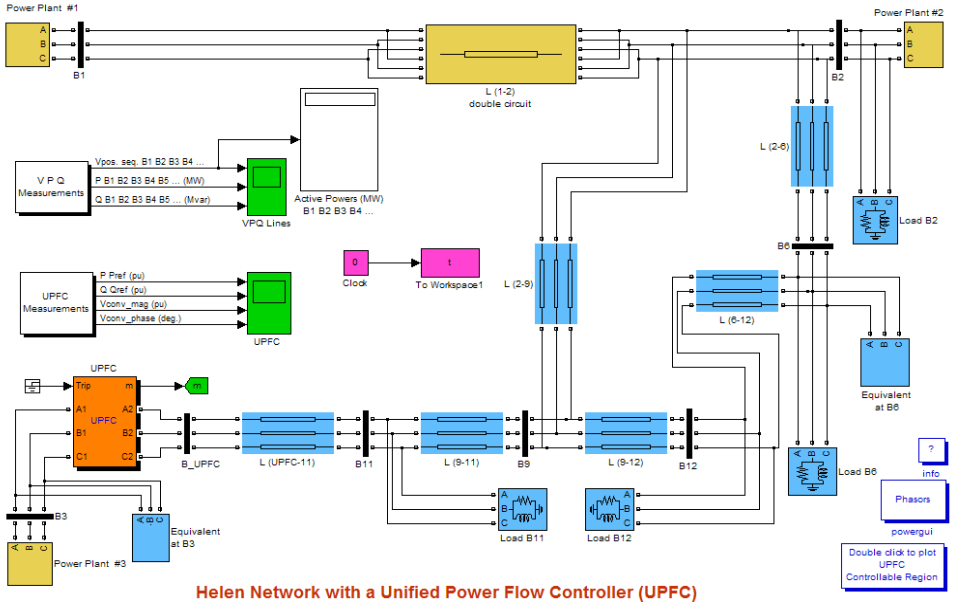

Fig. 6.10 Dynamic blocks zone for the Finnish Network for above mentioned case.

The dynamic response of the mechanical variables as the speed deviation response ($\Delta\omega$) and the mechanical rotor angle ($\Delta\delta$) of the generating units will be varied according to the adjusting of the dynamic parameters of the UPFC, as in Fig. 6..11.

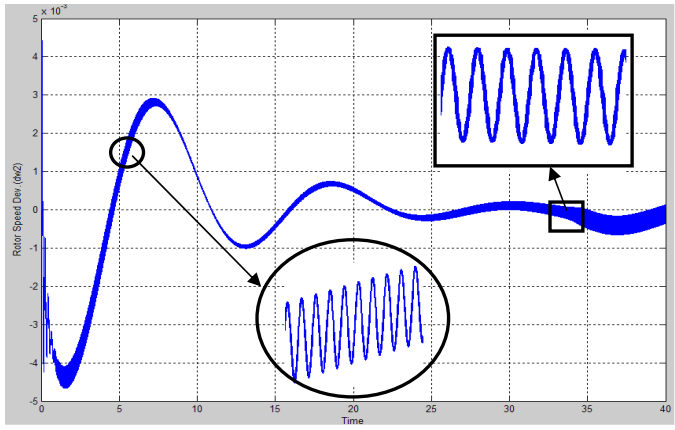

Fig. 6.11, Highly Oscillatory Dynamic Response

6.12 Effect of Adjusting PI Controller on Dynamics

To show the effect of tuning the dynamic parameters of the UPFC, we examine the case study from the cases indicated before in the steady state performance enhancing. The simulations calculate the optimal location and optimal settings of the UPFC to be installed to achieve the required performance.

The dynamic buildings of the network and the UPFC are constructed. The dynamics parameters for the UPFC blocks will be adapted according to the conventional manual tuning method described in Section 5.8. As in Section 5.9, the main concerned control element will be inside the series SVS part to control the power flow, which will be power PI regulator containing Integral gain (Ki) and propotional gain (Kp). That will be the controlling element, which will be adapted to enhance the dynamic response for the system. According to Table 6.50 that shows the case study, which will be the used to demonstrate the effect of adapting the dynamic parameters of the UPFC after its installation in the optimal location with the optimal settings.

The simulation of the case study indicated that the operating loading conditions are considered as follows: the loading of each load bus is the maximum loading values at all of them then multiplying that loading pattern in the load forecasting coefficients of the year 2020 to achieve most loading constraints. That operating conditions leads to some overloading cases. After applying the GA technique to reach the optimal location and settings which are optimal location line (22) ≡ (3-11), optimal settings (0.1812 , 0.9356), there will be no overloading in the network with keeping the voltage profile of the network in the required limits.

The dynamic response for that operating case with related UPFC dynamic parameters, in Fig. 6.12, 6.13 and 6.14, will show the effect to get the significant setting of that parameters to enhance the dynamic response. Without adapting the UPFC paramerters, we may lose the benefits that we got from installing the UPFC in the optimal location, where may lead to instability or osclliations in the dynamic response which means that we enhanced certain performance and impaired another one.

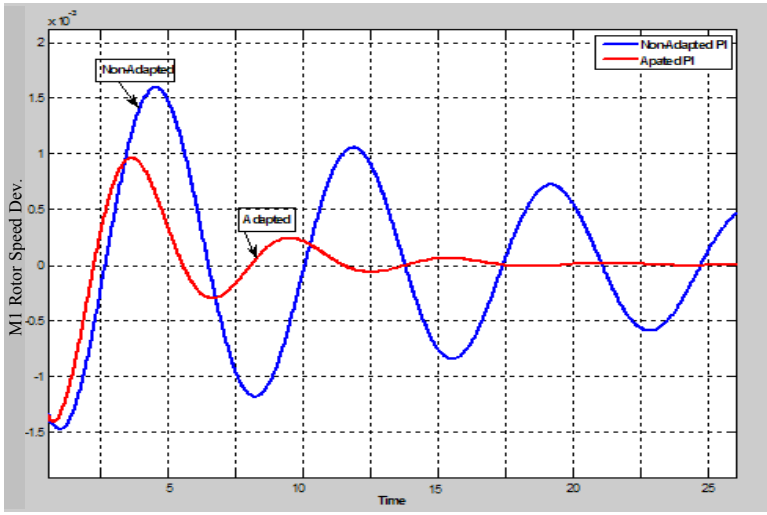

Fig. 6.12, Rotor Speed Deviation of Machine #1.

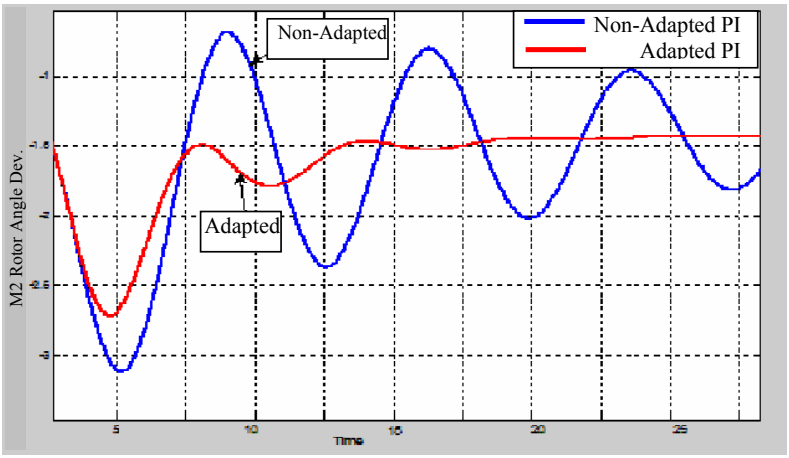

Fig. 6.13, Rotor Angle Deviation of Machine #2.

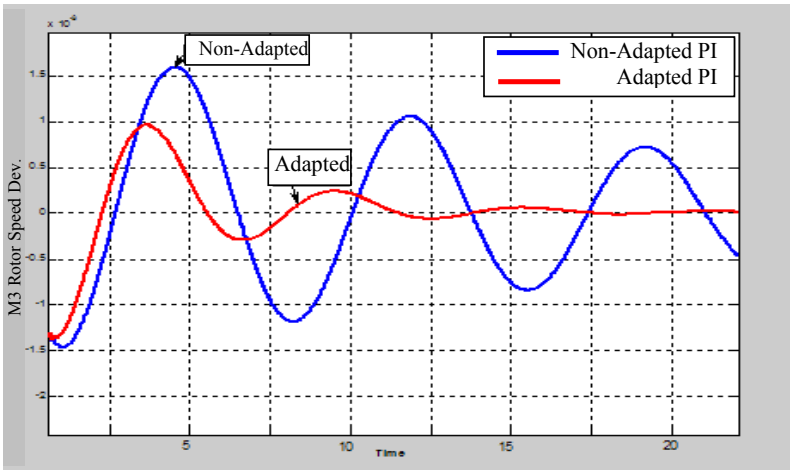

Fig. 6.14, Rotor Speed Deviation of Machine #3.

6.13 Effect of AI Controller Installation on the System

We select a case study from the cases indicated before in steady state performance enhancing, to study the effect of adaptive controller installation to adapt the dynamic parameters of the UPFC. In that case, we will enhance the performance of the network related to the overloading of transmission lines and violation of the bus voltage profile, during the normal configuration of the system with an increasing load pattern on the system until the year 2020. The results lead to optimal location and optimal settings of UPFC to be installed to achieve the required performance.

After installing the UPFC at these optimal locations with optimal settings, the dynamic parameters of the UPFC will have a significant effect on the dynamic response specially the mechanical variables response as the speed deviation response ($\Delta\omega$) and the mechanical

rotor angle dynamic response (Δδ) of the generating units. The dynamics parameters for the UPFC blocks should be well-selected and setted to fine tune the response and damp the oscillation and enhance the settling time of the response. Table 6.51 indicates the case study, which will be concerned to show the effect of adapting the dynamic parameters of the UPFC after its installation in the optimal location with the optimal settings.

Table 6.51 Case Study of the Finnish Network for optimal UPFC.

Case Study			
- Max. Load at all load bus at the same time multiplied by 98% of 2020 coeff.			
⇒ Before Optimal UPFC (UPFC at line 22, for case 96% of 2020 coefficient)			
$\acute{K}_{(LOLN)} = 2$	$Y1 = 0.2068$	$Я = \acute{K}_{(LOLN)} + \Gamma_{(VBVN)} = 2$	$Y = Y1 + Y2 = 0.2068$
Overloaded Line (11) ≡ (9-2)		101.07%	
Overloaded Line (36) ≡ (7-17)		101%	
⇒ After UPFC Installation			
- Optimal Location Line (14) ≡ (12-9), Optimal Setting (0.196 ,1.0928)			
$\acute{K}_{(LOLN)} = 0$	$Y1 = 0$	$\Gamma_{(VBVN)} = 0$	$Y2 = 0$
$Я = 0$	$Y = 0$		
⇒ No Overloading , No Voltage Violation	$0.98 \le V_i \le 1.02$		

After installing the UPFC at the optimal location line (14) ≡ (9-12), with optimal setting (V_{VR} = 0.196 , V_{CR} = 1.0928), we will build up the dynamic model of the Finnish network including UPFC at the optimal location.

The dynamic behavior aspects of the systems that can be improved with the use of UPFC controllers include transient stability and dynamic stability for damping oscillations. Dynamic instability is characterized by sustained or growing power oscillations between generators or groups of generators. Application of UPFC to enhance the stability of the power system is an important issue. The problems faced in planning and operation are where to place, what size is the appropriate size for these controllers, and what appropriate control input signal should be used to improve dynamic performance.

Figures 6.15, 6.16 and 6.17 show the variation of the change in the generator speed deviation and generator angle deviation and in the generator speed respectively. In the dynamic system responses Δδ, Δω and ω, which will be shown in the following figures, the mechanical oscillations in addition to the system settling down times are noticed. To ensure the robustness of the proposed controller, the design process takes into account a wide range of operating conditions and system configurations.

While the major advantage of UPFC controllers is flexible power scheduling under various operating conditions, the fast controllability also ensures improvement of the dynamic of power systems where system stability is threatened. We take up the problem of oscillations and their damping by appropriate controllers. The UPFC controller damps out the oscillation effectively, which means that the presence of UPFC damping controller

enhances system dynamics. Demonstrating the effectiveness of the UPFC controller, the settling time of the system enhanced with the UPFC controller.

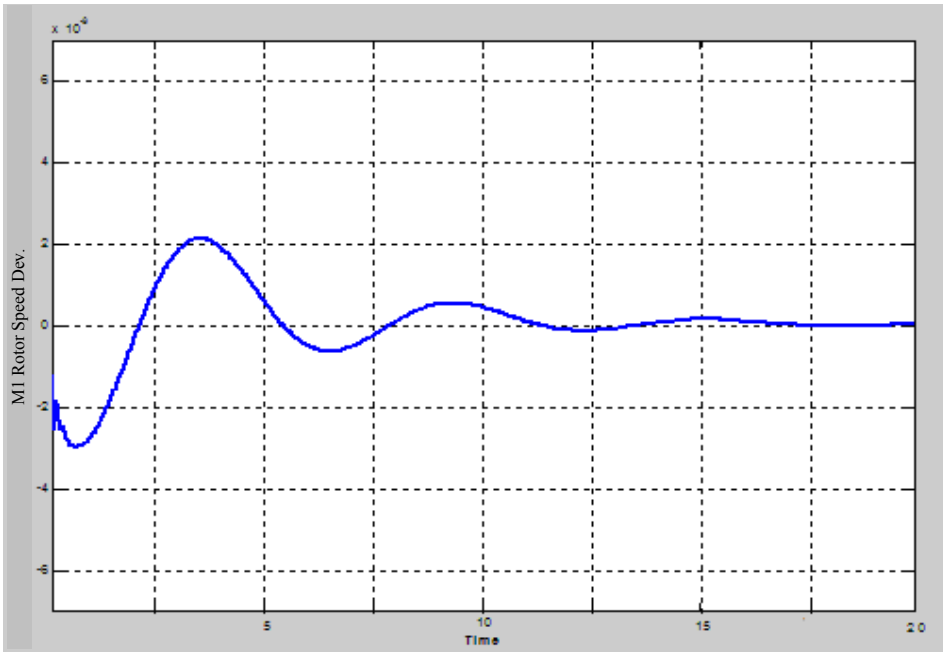

Fig. 6.15 Rotor Speed Deviation Response with AI-adapted optimal UPFC.

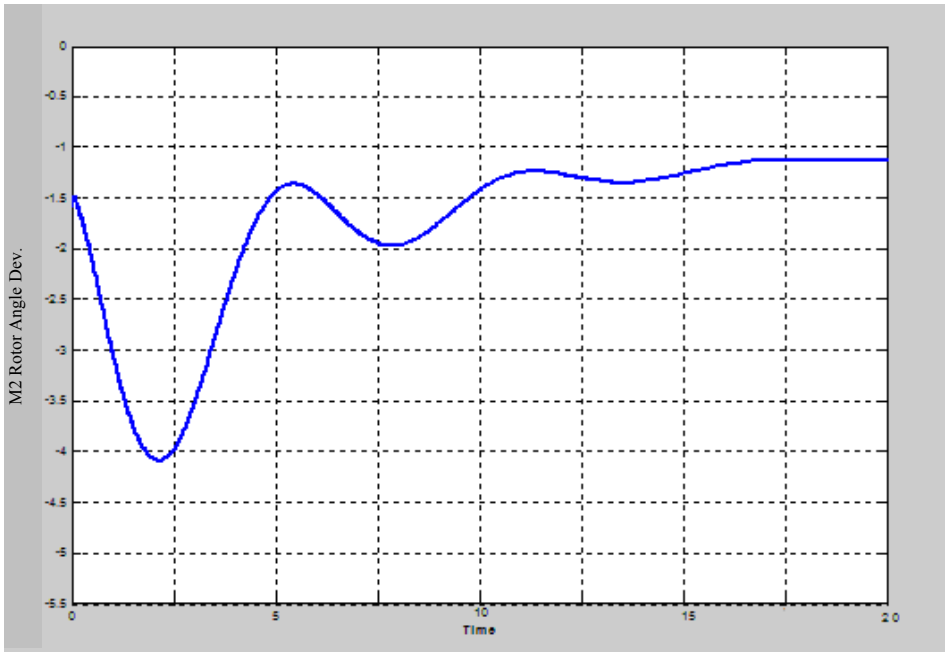

Fig. 6.16 Rotor Angle Deviation Response with AI-adapted optimal UPFC.

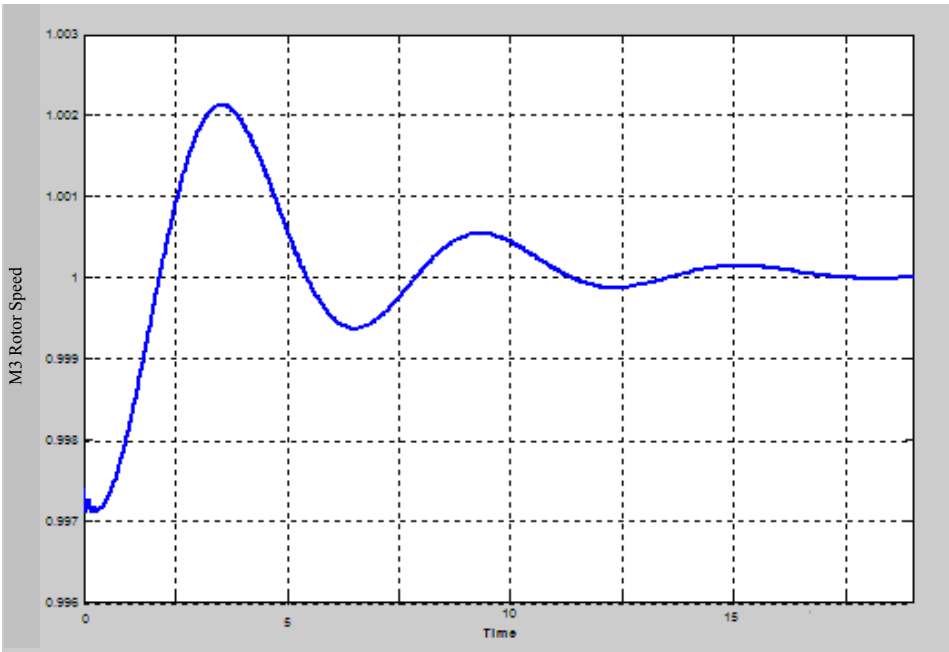

Fig. 6.17 Rotor Speed Response with AI-adapted optimal UPFC.

6.14 Comparing Conventional Fixed PI with Adaptive AI Controller

The performance of the proposed ANFIS controllers has been investigated. The response of the system with fixed-gain controllers designed by GA under normal operating conditions and with the adaptive ANFIS controllers is compared.

The controllers' gains as calculated by GA under normal operating conditions and are held constant and the system loading is increased by 30 %. System responses for this condition with fixed gains damping controllers and with ANFIS are shown in Figures from 6.18 to 6.20. System performance is greatly enhanced by the tuning action of ANFIS.

The figures will show the dynamic response of the system without and with installing an AI-adapted UPFC controller. The AI-adapted UPFC controller makes the system settle down in less cycles and less overshoot, which means the presence of the UPFC controller enhances the system dynamics. We considered the application of UPFC controllers for damping power oscillations in the system. The objective is to improve the stability of power systems that implies the ability of the power systems to maintain synchronism under disturbances that are always present. We are concerned with the improvement of the dynamic response of power systems by suitable control of UPFC controllers. To show the comparison effect of adaptive controller installation to adapt the dynamic parameters of the UPFC, we will now turn to another case study from the cases indicated before in steady state performance enhancing. After installing the UPFC in these optimal locations with optimal settings, the dynamic parameters of the UPFC will have a noticeable effect on the dynamic response. Transient stability is concerned with the stability of power systems when subjected to a severe or large disturbance such as a high increase in loading conditions. Transient stability depends on the location and nature of the disturbance in addition to the initial operating point.

Table 6.52 Outage Case Study, real Finnish Network

Outage Case Study			
⇒ ***Outage of Line (1) ≡ (6-12), Severity Rank =6***			
⇒ ***Before UPFC Installation***			
$\acute{K}_{(LOLN)} = 1$	$Y1 = 0.1386$	$Я = \acute{K}_{(LOLN)} + \Gamma_{(VBVN)} = 1$	$Y = Y1 + Y2 = 0.1386$
Loadability		27.57%	
Overloaded Line (6) ≡ (6-2)		108.5%	
⇒ ***After UPFC Installation***			
⇒ ***Optimal Location Line (23) ≡ (9-11), Optimal Setting (0.2912 , 0.8249)***			

$\acute{K}_{(LOLN)} = 0$	$Y1 = 0$	$\Gamma_{(VBVN)} = 0$	$Y2 = 0$	$Я = 0$	$Y = 0$
Loadability			28.9328%		
⇒ ***No Overloading , No Voltage Violation*** $0.98 \le V_i \le 1.02$					

After installing the UPFC at the optimal location line (23) ≡ (9-11), with an optimal setting (V_{VR} = 0.2912 , V_{CR} = 0.8249), we will build up the dynamic model of the Finnish network including UPFC at an optimal location.

Figures 6.18, 6.19, 6.20 and 6.21 show the variation of the change in the generator speed deviation and generator angle deviation and in the generator speed respectively. In the dynamic system responses Δδ, Δω and ω, which will be shown in the following figures, the mechanical oscillations in addition to the system settling down times are noticed. The figures will show the dynamic response of the system with a fixed controller (without the AI-adapted UPFC controller) and with an installed AI-adapted UPFC controller. The AI-adapted UPFC controller makes the system settle down in less cycles and less overshoot, which means the presence of UPFC controller enhances system dynamics. System performance is greatly enhanced by the tuning action of ANFIS.

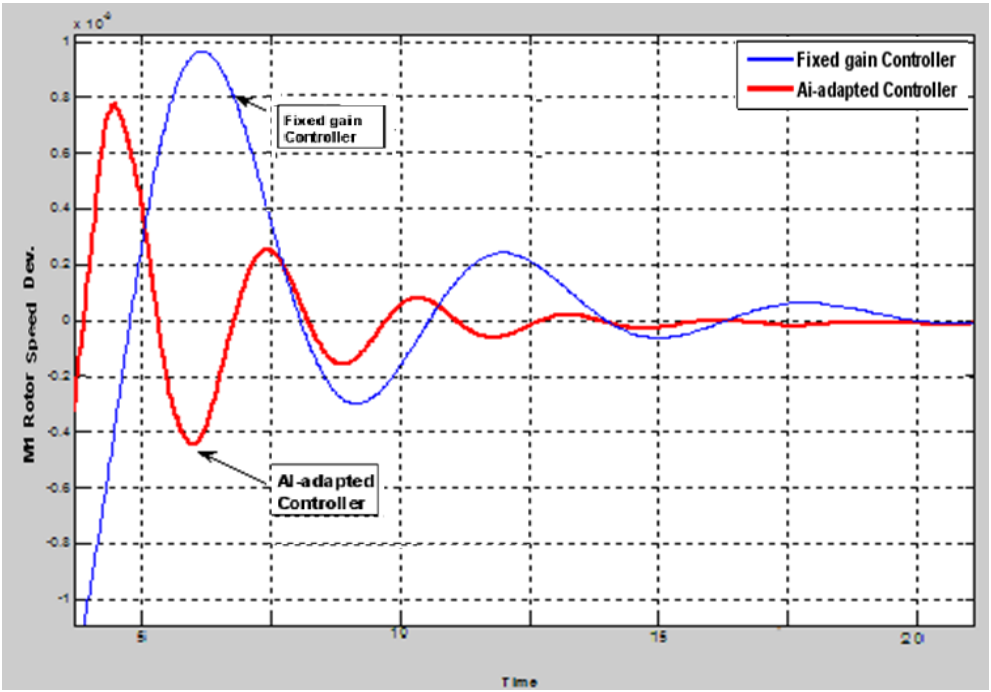

Fig. 6.18 Comparison of Rotor Speed Deviation Response**.**

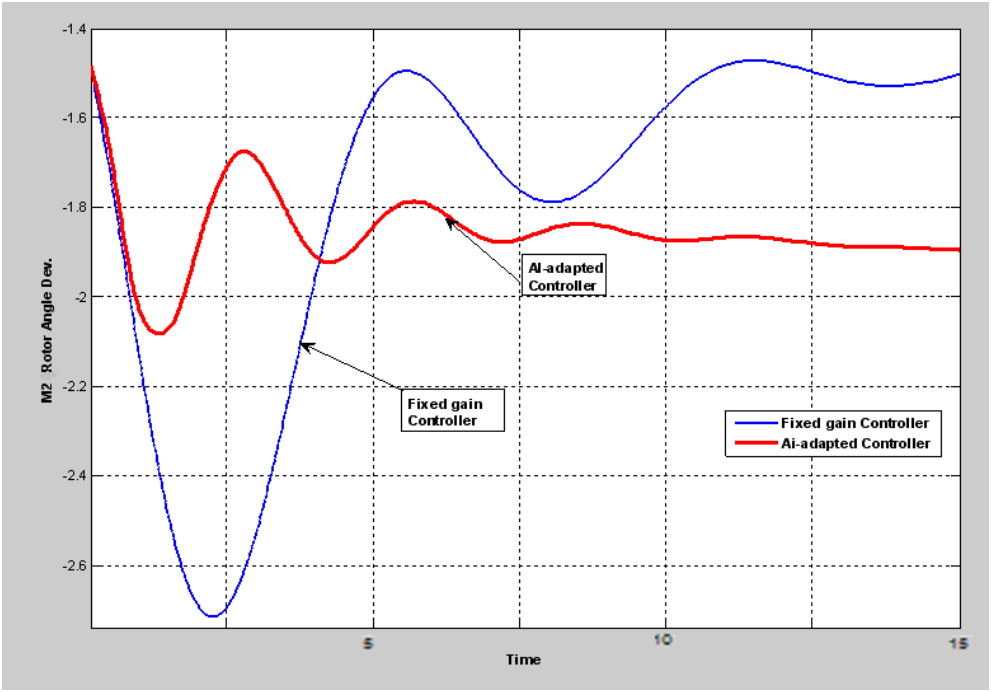

Fig. 6.19 Comparison of Rotor Angle Deviation Response.

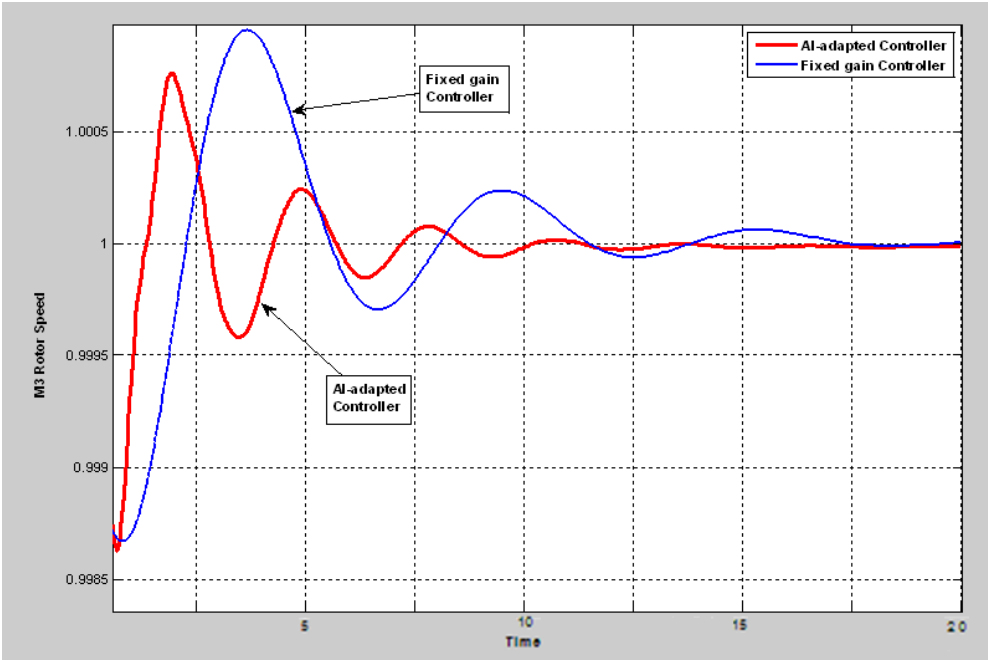

Fig. 6.20 Comparison of Rotor Speed Response.

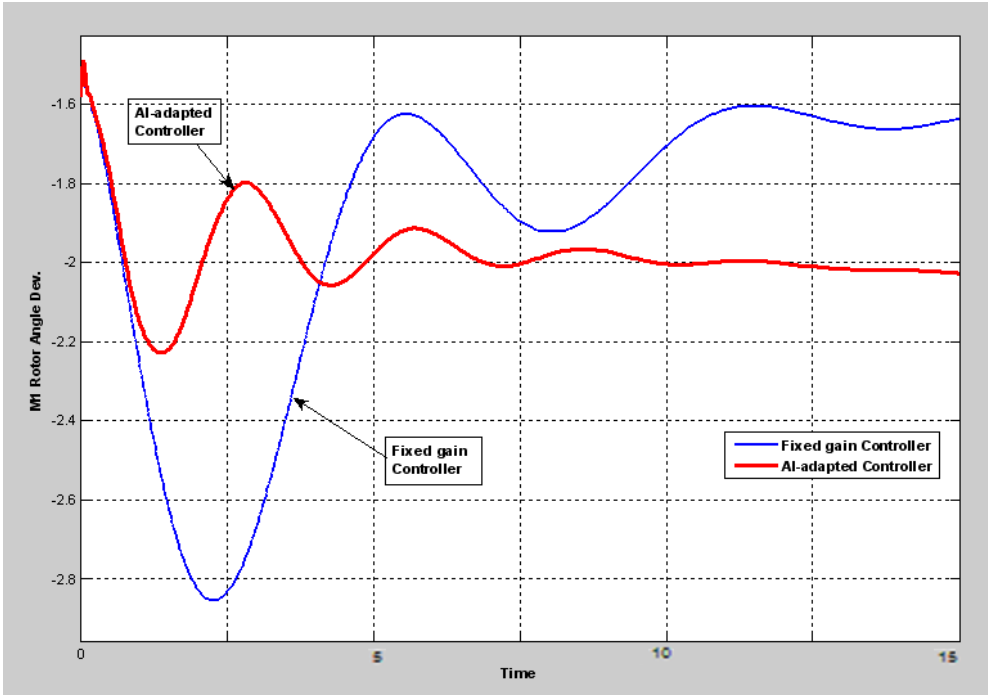

Fig. 6.21 Comparison of Rotor Angle Dev. Response.

7 Conclusions

- We can use the Genetic Algorithm (GA) to determine the optimal position and also the optimal settings of the UPFC to enhance the performance of the power network especially handling the transmission lines overloading and buses voltage violations during normal operation at increasing loading condition and during the contingency outage cases.

- The optimal UPFC is used to maximize the loadability of the transmission grid. Loadability is an index of the utilization of the transmissions lines and the capability of the power transfer.

- The proposed procedure, for achieving the optimal UPFC installation, is proposed to be applied on a real Finnish Transmission network, until the operating conditions of the year 2020. The validity of the technique can be shown by testing on the IEEE 6-bus, IEEE 30-bus and IEEE 57-bus system.

- Indices have been proposed to evaluate the performance and are used to determine the suitable location and parameter settings of the UPFC in the network.

- These optimal UPFCs enhance the steady-state performance of the network; but the dynamic performance needs another adaptive stage to improve it.

- The performance of the system is based on the model parameters and loading conditions, which varied according to operating point of the network. Therefore, the system performance is studied to get analysis before the control stage under different loading conditions on different system models parameters.

- A novel hybrid technique based on ANFIS, ANFIS merged with a GA system, is used to tune the dynamic parameters of the optimal UPFC to achieve the optimal characteristics; steady-state and dynamic.

- Simulation results show that the proposed genetic based ANFISs controller is a very effective means for enhancing the power grid dynamic performance compared to fixed-gains controllers.

Contributions of the Thesis

The contributions of the thesis start with formatting, deriving, coding and programming the network equations required to link UPFC steady-state and dynamic models to the power systems. One of the other contributions of the thesis is deriving GA applications on the UPFC to solve real problems on a real world sub-transmission network.

An enhanced GA technique is proposed by enhancing and updating the working phases of the GA; the simulations and results show the advantages of using the proposed technique. Integrating the results by linking the case studies of the steady-state and the dynamic analysis is achieved. In the dynamic analysis section, a new idea for integrating the GA with ANFIS to be applied on the control action procedure is presented.

In addition to, packages of Software for genetic algorithm and adaptive neuro-fuzzy system were developed. In other related works, GA only was used to enhance the system dynamic performance considering the whole working range of the power system at a time that made it difficult and unable in some cases to reach the solution criteria. In this thesis, for every operating point GA is used to search for the controllers' parameters, parameters found at a certain operating point are different from those found at other points. ANFISs are required in this case to recognize the appropriate parameters for each operating point.

FUTURE WORK

- Investigation of the economical issues should be applied to indicate the benefits of UPFC devices versus other options such as network reinforcement.

- Examination the relation and the effect of UPFC devices with magnetic energy storage elements on the system performance should be studied.

- Reliability analysis of the UPFC considering the outage cost analysis and Demand Not Supplied (DNS), Energy Not Supplied (ENS) indices.

8 References

[1] T. J. Miller, “Reactive power Control in Electric Systems”, John Wiley & Sons, 1982.

[2] E. Wanner, R. Mathys, M. Hausler, “Compensation Systems for Industry,” Brown Boveri Review, vol. 70, pp. 330-340, Sept./Oct. 1983.

[3] P. Kundur, “Power System Stability and Control”, McGraw-Hill, 1994.

[4] A. Hammad and B. Roesle, “New Roles for Static VAR Compensators in Transmission Systems,” Brown Boveri Review, vol. 73, pp. 314-320, June 1986.

[5] E. Acha, C. R. Fuerte, H. A. Pe´rez, and C. A. Camacho, “FACTS Modelling and Simulation in Power Networks”, John Wiley & Sons Ltd, West Sussex, ISBN 0-470-85271-2, pp. 9-12, 2004.

[6] N. G. Hingorani and L. Gyugyi, “Understanding FACTS: Concepts and Technology of Flexible AC Transmission Systems”, Institute of Electrical and Electronic Engineers (IEEE) Press, New York, pp. 16-20, 2000.

[7] C. R. Fuerte-Esquivel, “Steady State Modelling and Analysis of Flexible ac Transmission Systems”, Department of Electronics and Electrical Engineering, University of Glasgow, Glasgow, 1997.

[8] H. Ambriz-Perez, 1998, “Flexible AC Transmission Systems Modelling in Optimal Power Flows Using Newton's Method”, Department of Electronics and Electrical Engineering, University of Glasgow, Glasgow, 1998.

[9] C. H. Liang, C. Y. Chung, , K. P. Wong, and X. Z. Duan, “Parallel Optimal Reactive Power Flow Based on Cooperative Co-Evolutionary Differential Evolution and Power System Decomposition”, IEEE Transactions on Power Systems, Vol. 22, No. 1, pp. 249-253, February 2007.

[10] W. Yan, F. Liu, C. Chung, and K. Wong, “A Hybrid Genetic Algorithm–Interior Point Method for Optimal Reactive Power Flow”, IEEE Transactions on Power Systems, Vol. 21, No. 3, pp. 1163-1166, August 2006.

[11] W. Yan, J. Yu, D. C. Yu, and K. Bhattarai, “A New Optimal Reactive Power Flow Model in Rectangular Form and its Solution by Predictor Corrector Primal Dual Interior Point Method”, IEEE Transactions on Power Systems, Vol. 21, No. 1, pp. 61-64, February 2006.

[12] L. A. Zarate, C. A. Castro, J. L. Ramos, and E. R. Ramos, “Fast Computation of Voltage Stability Security Margins Using Nonlinear

Programming Techniques", IEEE Transactions on Power Systems, Vol. 21, No. 1, pp. 19-22, February 2006.

[13] A. Sode-Yome, N. Mithulananthan, and K. Y. Lee, "A Maximum Loading Margin Method for Static Voltage Stability in Power Systems", IEEE Transactions on Power Systems, Vol. 21, No. 2, pp. 799-802, May 2006.

[14] I. Smon, G. Verbiˇ, and F. Gubina, "Local Voltage-Stability Index Using Tellegen's Theorem", IEEE Transactions on Power Systems, Vol. 21, No. 3, pp. 1267-1270, August 2006.

[15] J. Shin, B. Kim, J. Park, and K. Y. Lee, "A New Optimal Routing Algorithm for Loss Minimization and Voltage Stability Improvement in Radial Power Systems", IEEE Transactions on Power Systems, Vol. 22, No. 2, pp. 648-651, May 2007.

[16] A. Wiszniewski, "New Criteria of Voltage Stability Margin for the Purpose of Load Shedding", IEEE Transactions on Power Delivery, Vol. 22, No. 3, pp. 1376-1370, July 2007.

[17] J. Zhang, J. Y. Wen, S. J. Cheng, and J. Ma, "A Novel SVC Allocation Method for Power System Voltage Stability Enhancement by Normal Forms of Diffeomorphism", IEEE Transactions on Power Systems, Vol. 22, No. 4, pp. 1819-1822, November 2007.

[18] C. W. Taylor, "Improving Grid Behavior", IEEE Spectrum, Vol. 36, No. 6, pp. 40-45, June 1999.

[19] Canadian Electrical Association, "Static Compensators for Reactive Power Control," Context Publications, 1984.

[20] L. Gyugyi, "Solid-State Synchronous Voltage Sources for Dynamic Compensation and Real-Time Control of AC Transmission Lines", Emerging Practices in Technology, IEEE Standards Press, 1993.

[21] G. Bonnard, "The Problems Posed by Electrical Power Supply to Industrial Installations," Proc. of IEE Part B, vol. 132, pp. 335-340, Nov. 1985.

[22] N. Mithulananthan, "Hopf Bifurcation Control and Indices for Power System with Interacting Generator and FACTS Controllers", Ph.D. Thesis, University of Waterloo, Ontario, Canada, 2002.

[23] "FACTS Technology for Open Access", CIGRE Report, August 2000.

[24] N. Li, Y. Xu, and H. Chen, "FACTS-Based Power Flow Control in Interconnected Power Systems", IEEE Transactions on Power System, Vol. 15, No. 1, pp. 257-262, Feb. 2000.

[25] R. Mihalic, "Power Flow Control with Controllable reactive series elements", IEE Proceeding., Generation, Transmission and Distribution, Vol. 145, No. 5, pp. 493-498, Sept. 1998.

[26] S. Y. Ge and T S Chung, "Optimal power flow incorporating Power Flow Control Needs in Flexible AC Transmission Systems", IEEE Transactions on Power System, Vol. 14, No. 2, pp. 738-744, May 1999.

[27] C.R. Fuerte-Esquivel, E. Acha, and H. Amprez-Pêrez, "A Thyristor Controlled Series Compensation Model for the Power Flow Solution of Practical Power Networks", IEEE Transactions on Power System, Vol. 15, No. 1, pp. 58-64, Feb. 2000.

[28] C.R. Fuerte-Esquivel, E. Acha, and H. Amprez-Pêrez, "A Comprehensive Newton-Raphson UPFC Model for the Quadratic Power Flow Solution of Practical Power Networks", IEEE Transactions on Power System, Vol. 15, No. 1, pp. 102-109, Feb. 2000.

[29] F. P. De Mello and T. F. Laskowski, "Concepts of Power System Dynamic Stability", IEEE Power Apparatus and Systems (PAS) Transactions, Vol. 94, pp. 827-833, May 1979.

[30] G. N. Taranto and D. M. Falcao, "Robust Decentralized Control Design Using Genetic Algorithm in power System Damping Control", IEE Proc. Generation, Transmission and Distribution, Vol. 145, No. 1, pp. 1-6, Jan. 1998.

[31] T. Luor, Y. Hsu, T. Guo, J. Lin, and C. Huang, "Application of Thyristor-Controlled Series Compensators to Enhance Oscillatory Stability and Transmission Capability of Longitudinal Power System", IEEE Transactions on Power System, Vol. 14, No. 1, pp. 179-185, Feb. 1999.

[32] L. L. Li and J. T. Ma, "Power Flow Control with UPFC Using Genetic Algorithms", International Conference on Intelligent Systems Applications to Power Systems, Orlando, FL, Feb 1996.

[33] H. C. Leung and T. S. Chung, "Optimal Power Flow with a Versatile FACTS controller by Genetic Algorithm Approach", Power Engineering Society IEEE Winter Meeting, Vol. 4, pp. 2806 – 2811, 2000.

[34] T. K. Mok, Y. Ni, and F. F. Wu, "Design of Fuzzy Damping Controller of UPFC through Genetic Algorithm", Power Engineering Society IEEE Winter Meeting, USA, Vol. 3, pp. 1889 - 1894, 16-20 July 2000.

[35] S. Gerbex, R. Cherkaoui, and A. J. Germond, "Optimal Location of FACTS Devices to Enhance Power System Security", IEEE PowerTech Conference, Bologna, pp.1 -7, June 2003.

[36] A. Parizad, A. Khazali, and M. Kalntar, "Application of HAS and GA in Optimal Placement of FACTS Devices Considering Voltage Stability and

Losses", Conference on Electric Power & Energy Conversion Systems, EPECS '09, Sharjah, pp. 1 - 7, 10-12 Nov. 2009.

[37] S. O. Faried and A. A. Eldamaty, "Damping Power System Oscillations Using A Genetic Algorithm Based Unified Power Flow Controller", Conference on Electrical & Computer Engineering, Canda, Vol. 1, pp. 65 - 68, 2-5 May 2004.

[38] L. Khan, K. L. Lo, and N. Ahmed, "Micro-GA based Fuzzy Logic Controllers for Coordinated FACTS Control", 7th International Conference on Multi Topic INMIC 2003, Islamabad, pp. 269 - 275, 8-9 Dec. 2003.

[39] L. Khan, N. Ahmed, and C. Lozano "GA Neuro-Fuzzy Damping Control System for UPFC to Enhance Power System Transient Stability", 7th International Conference on Multi Topic INMIC 2003, pp. 276 - 282 , Dec. 2003.

[40] H. R. Baghaee, M. Jannati, and B. Vahidi, "Improvement of Voltage Stability and Reduce Power System Losses by Optimal GA-based Allocation of Multi-type FACTS Devices", 11th International Conference on Optimization of Electrical and Electronic Equipment, OPTIM 2008, pp. 209 – 214, 22-24 May 2008.

[41] K. R. Saidi, N. P. Padhy, and R. N. Patel, "Congestion Management in Deregulated Power System using FACTS Devices", International IEEE Power India Conference, India, 10-12 April 2006.

[42] A. Kazemi, D. Arabkhabori, M. Yari, and J. Aghaei, "Optimal Location of UPFC In Power Systems for Increasing Loadability By Genetic Algorithm", Universities Power Engineering Conference, UPEC '06, UK, Vol. 2, pp. 774 – 779, 6-8 Sept. 2006.

[43] D. Arabkhabori, A. Kazemi, M. Yari, and J. Aghaei, "Optimal Placement of UPFC In Power Systems using Genetic Algorithm", IEEE International Conference on Industrial Technology (ICIT), India, pp. 1694 - 1699, 18-21 Dec. 2006.

[44] H. C. Leung, and T. S. Chung, "A Hybrid GA Approach for Optimal Control Setting Determination of UPFC", IEEE Power Engineering Review, Vol. 21, pp. 62 - 65, Dec. 2001.

[45] K. Vijayakunar, R. P. Kumudinidevi, and D. Suchithra, "A Hybrid Genetic Algorithm for Optimal Power Flow Incorporating FACTS Devices", Conference on Computational Intelligence and Multimedia Applications, India, Vol. 1, pp. 463 - 467, 13-15 Dec. 2007.

[46] B. Mahdad, T. Bouktir, and K. Srairi, "Dynamic Methodology for Control of Multiplie-UPFC to Relieve Overloads and Voltage Violations", The

International Conference on (Computer as a Tool) EUROCON 2007, Poland, Vol. 1, pp. 1579 – 1585, 9-12 Sept. 2007.

[47] F. Taki, S. Abazari, and G. R. Markadeh, "Transient Stability Improvement using ANFIS Controlled UPFC based on Energy Function", 18th Iranian Conference Electrical Engineering (ICEE), Iran, pp. 994 – 948, 11-13 May 2010.

[48] G. Li, T. T. Lie, G. B. Shrestha, and K. L. Lo, "Design and application of coordinated Multiple FACTS Controllers", IEE Proc., Generation, Transmission and Distribution, Vol. 147, No. 2, pp. 112-120, , March 2000.

[49] L. Gyugyi, "Power Electronics in Electric Utilities: Static Var Compensator", Proc. of the IEEE, Vol. 76, No. 4, pp. 483-494, April 1988.

[50] Z. T. Faur, "Effects of FACTS Devices on Static Voltage Collapse", Master Thesis, University of Waterloo, Ontario, Canada, 1996.

[51] T. J. E. Miller, "Reactive Power Control in Electric Systems", John Wiley & Sons, 1982.

[52] X. Zhou and J. Liang, "Overview of Control Methods for TCSC in Enhance the Stability of Power Systems", IEE Proc., Generation, Transmission and Distribution, Vol. 146, No. 2, pp. 125-130, March 1999.

[53] C. A. Canizares, "Power Flow and Transient Stability Models of FACTS Controllers for Voltage and Angle Stability Studies", IEEE/PES Panel on Modeling, Simulation and Application of FACTS Controller in Angle and Voltage Stability Studies, Singapore, pp. 1-8, Jan. 2000.

[54] E. Y. Ho and P. C. Sen, "Effect of Gate-Drive Circuits on GTO Thyristor Characteristics", IEEE Transaction on Industrial Electronics, Vol. IE-33, No. 3, pp. 325-331, August 1986.

[55] L. Gyugyi, "Solid-State Synchronous Voltage Sources for Dynamic Compensation and Real-Time Control of AC Transmission Lines", Emerging Practices In Technology, IEEE Standards Press, Vol. 9, pp. 904 – 911, April 1993.

[56] P. H. Sydenham and R. Thorn, "Handbook of Measuring System Design", John Wiley & Sons, Ltd. ISBN: 0-470-02143-8, 2005.

[57] A. Abraham, "Neuro-Fuzzy Systems: State-of-the-art Modeling Techniques, Connectionist Models of Neurons, Learning Processes, and Artificial Intelligence", Lecture Notes in Computer Science, Vol. 2084, Springer Verlag, Germany, pp. 269–276, 2001

[58] A. Abraham, "Intelligent Systems: Architectures and Perspectives, Recent Advances in Intelligent Paradigms and Applications, in Studies in Fuzziness and Soft Computing", Springer Verlag Germany, pp. 1–35, 2002.

[59] C.M. Bishop, “Neural Networks for Pattern Recognition”, Oxford University Press, UK, 1995.

[60] T. K. Mok, Yixin Ni and Flex F. Wu, “Design of Fuzzy Damping Controller of UPFC through Genetic Algorithm”, IEEE Transaction on Power Systems, Vol. 1, No. 2, pp. 1889-1894, Nov. 2000.

[61] D. B. Fogel, “Evolutionary Computation: Toward a New Philosophy of Machine Intelligence”, second ed., IEEE Press, Piscataway, NJ, 1999.

[62] L. J. Fogel, A.J. Owens, and M.J. Walsh, “Artificial Intelligence through Simulated Evolution”, John Wiley & Sons, New York, 1967.

[63] D. E. Goldberg, “Genetic Algorithms in Search, Optimization, and Machine Learning”, Addison-Wesley Publishing Corporation, Inc, Reading, MA, 1989.

[64] J. Holland, “Adaptation in Natural and Artificial Systems”, University of Michigan Press, Ann Harbor, MI, 1975.

[65] T. Kohonen, “Self-organization and Associative Memory”, Springer-Verlag, New York, 1988.

[66] J. R. Koza, “Genetic Programming”, MIT Press, Cambridge, MA, 1992.

[67] H. T. Nguyen and E. A. Walker, “A First Course in Fuzzy Logic”, CRC Press, USA, 1999.

[68] J. Pearl, “Probabilistic Reasoning in Intelligent Systems: Networks of Plausible Inference”, Morgan Kaufmann Publishers, San Francisco, CA, 1997.

[69] A. M. Turing, “Computing Machinery and Intelligence”, http://abelard.org /turpap/turpap.htm, VOL. LIX. No. 236, October 1950.

[70] Turing Machine, http://www.turing.org.uk/turing/, 2004

[71] L. A. Zadeh, “Fuzzy Sets”, Journal of Information and Control, Vol. 8, pp. 338–353, 1965.

[72] R. L. Haupt and S. E. Haupt, “Practical Genetic Algorithms”, John Wiley & Sons, 1998.

[73] S. Mitra and Y. Hayashi, “Neuro-Fuzzy Rule Generation: Survey in Soft Computing Framework”, IEEE Transaction on Neural Networks, Vol. 11, No. 3, pp. 748-768, May 2000.

[74] H. C. Chang and M. Wang, "Neural Network-Base Self-Organizing Fuzzy Controller for Transient Stability of Multi-machine Power Systems", IEEE Transaction on Energy Conversion, Vol. 10, No. 2, pp. 339-346, June 1995.

[75] J. W. Hines, "MATLAB Supplement to Fuzzy and Neural Approaches in Engineering", John Wiley & Sons, 1997.

[76] M. Reformat, E. Kuffel, D. Woodford and W. Pedrycz, "Application of Genetic Algorithm for Control Design in Power systems", IEE Proc., Generation, Transmission and Distribution., Vol. 145, No. 4, pp. 345-354, July 1998.

[77] J. R. Jang, C. Sun, and E. Mizutani, "Neuro-Fuzzy and Soft Computing", Prentice-Hall, 1997.

[78] P. M. Anderson and A. A. Fouad, "Power System Control and Stability", Iowa State University Press, Iowa, 1977.

[79] A. N. Niaki and M. R. Iravani, "Steady-State and Dynamic Models of Unified Power Flow Controller (UPFC) for Power System Studies", IEEE Transaction on Power Systems, Vol. 11, No. 4, pp. 1937-1943, Nov. 1996.

[80] H. Wang, "A Unified Model for the Analysis of FACTS Devices in Damping Power System Oscillations Part III: Unified power Flow Controller", IEEE Transaction on Power Delivery, Vol. 15, No. 3, pp. 978-983, July 2000.

[81] K. R. Padiyar, "FACTs Controllers in Power Transmission and Distribution", New Age International (P) Limited, Publishers, New Delhi, ISBN (13): 978-81-224-2541-3, 2007.

[82] K. Schoder, A. Hasanovic, and A. Feliachi , "Load-Flow and Dynamic Model of the Unified Power Flow Controller (UPFC) within the Power System Toolbox (PST) ", Circuits and Systems Proc. of the 43rd IEEE Midwest Symposium, USA, Vol. 2, pp. 634 – 637, 8-11 August 2000.

[83] I. Dahhaghchi, R.D. Christie, G. W. Rosenwald, and C. Liu, "AI application areas in power systems", IEEE Expert Magazine, Volume: 12, pp. 58 – 66, Jan/Feb 1997.

[84] D. Radu and Y. Besanger, "Blackout prevention by optimal insertion of FACTS devices in power systems", International Conference on Future Power Systems, Amsterdam, Vol. 6, Issue 18, pp. 9-18, 18-19 Nov. 2005.

[85] http://www.ee.washington.edu/research/pstca/

[86] A. M. Othman, A. Gaun, M. Lehtonen, and M. M. Alarini, “Real World Optimal UPFC Placement and its Impact on Reliability”, 5th IASME / WSEAS International Conference on (EE'10), Cambridge University, UK, pp. 90-95, February 2010.

[87] A M. Othman, M. Lehtonen, and M. M. Alarini, “Enhancing the Contingency Performance by Optimal Installation of UPFC based on Genetics Algorithm”, IEEE Power & Energy Society General Meeting, USA, pp. 1-8, 24-28 July 2010.

[88] A. M. Othman, M. Lehtonen, and M. M. Alarini, “Optimal UPFC based on Genetics Algorithm to Improve the Steady-State Performance at Increasing the Loading Pattern”, 9th International Conference on Electrical Engineering (EEEIC) , Prague, pp. 162-166, May 2010,

[89] A M. Othman, A. Gaun, M. Lehtonen, and M. M. Alarini, “Optimal UPFC Installation based on GA in a Real Finnish Sub-transmission Network considering Performance Measures and Reliability", WSEAS Journal Transactions on Power Systems, ISSN: 1790-5060, pp 1-10, May 2010.

[90] A. M. Othman, M. Lehtonen, and M. M. Alarini, “Heavy Loading Conditions Studies by Optimal UPFC on a Real Finnish 110 KV Network to Solve Technical Problems of 2020”, Electrical Review Journal, ISSN 0033-2097, Vol. 11, p.p 23-27, December 2010.

Appendix A – GA Programming

```
%Main GA core program
%PowerFlowsData; %Function to read network data
%UPFCdata; %Function to read the UPFC data

ObjectiveFunction = @UPFCobjective;
nvars = 3; % Number of variables
LB = [1 0.001 0.8]; % Lower bound
UB = [42 0.3 1.2]; % Upper bound
ConstraintFunction = @UPFCconstraint;

options = gaoptimset('MutationFcn',@mutationadaptfeasible,
'PopulationSize',500,'Generations',30);
options =
gaoptimset(options,'PlotFcns',{@gaplotbestf,@gaplotmaxconstr},'Display
','iter');

[X,FVAL,EXITFLAG,OUTPUT,POPULATION,SCORES] =
ga(ObjectiveFunction,nvars,[],[],[],[],LB,UB,[],options)
%[X,FVAL,EXITFLAG,OUTPUT,POPULATION,SCORES] =
GA(FITNESSFCN,NVARS,A,b,Aeq,beq,lb,ub,NONLCON,options)

% Objective function programming
function y = UPFCobjective(x)

UPFCtln(1)=x(1);
Vcr(1)=x(2);
Vvr(1)=x(3);

NetworkData; %Function to read network data

NUPFC=1;
UPFCrec(1)=25;

nbb=25;
bustype(25) = 3 ; VM(25) = 1 ; VA(25) =0 ;

Xcr(1)=0.1; Xvr(1)=0.1;
Psp(1)= -4.49 ; Qsp(1)=0.099;
Flow(1)=-1; PSta(1)=0; QSta(1)=0;
%Vcr(1)=     0.21855            ;
Tcr(1)=-87.13/57.3; VcrLo(1)=0.001; VcrHi(1)=0.3;
%Vvr(1)=     1.0155   ;
Tvr(1)=0.0; VvrLo(1)=0.8; VvrHi(1)=1.2;
VvrTar(1)=1.0; VvrSta(1)=0;

UPFCtln(1)=fix(UPFCtln(1));
UPFCsend(1)=tlsend(UPFCtln(1));
tlsend(UPFCtln(1))=25;

[YR,YI] = YBus(tlsend,tlrec,tlresis,tlreac,tlsuscep,tlcond,shbus,...
shresis,shreac,ntl,nbb,nsh);
```

```
[VM,VA,it,Vcr,Tcr,Vvr,Tvr,DPQ] =
UPFCNewtonRaphson(nmax,tol,itmax,ngn,nld,...
nbb,bustype,genbus,loadbus,PGEN,QGEN,QMAX,QMIN,PLOAD,QLOAD,YR,YI,...
VM,VA,NUPFC,UPFCsend,UPFCrec,Xcr,Xvr,Flow,Psp,PSta,Qsp,QSta,Vcr,...
Tcr,VcrLo,VcrHi,Vvr, Tvr,VvrLo,VvrHi,VvrTar,VvrSta);
[PQsend,PQrec,PQloss,PQbus] = PQflows(nbb,ngn,ntl,nld,genbus,...
loadbus,tlsend,tlrec,tlresis,tlreac,tlcond,tlsuscep,PLOAD,QLOAD,...
VM,VA);
tlflow=zeros(1,ntl);
for n=1:ntl
    if abs(PQsend(1,n)) >  abs(PQrec(1,n))
    tlflow(1,n)=abs(PQsend(1,n));
    else
      tlflow(1,n)=abs(PQrec(1,n));
    end
end
Vmref=ones(1,nbb);
q=2; r=2;
Q=2*q; R=2*r; wm=1 ; wl=0.1 ; y1=0; y2=0;
for i=1:nbb
    if VM(1,i) > 1.05 || VM(1,i) < 0.95
        y1=y1+(wm*((Vmref(1,i)-VM(1,i))./Vmref(1,i)).^R);
    else
       y1=y1+0;
    end
end
   for i=1:ntl
    if tlflow(1,i)*100 <= tlrate(1,i)
        y2=y2+0;
    else
        y2=y2+(wl*(tlflow(1,i)*100./tlrate(1,i)).^Q);
    end
  end
y = y1+y2;
%y(1)=abs(imag(sum(PQloss))); y(2)=real(sum(PQloss));
%End Main Program
function [x,fval,exitFlag,output,population,scores] =
ga(fun,nvars,Aineq,bineq,Aeq,beq,lb,ub,nonlcon,options)
%GA    Constrained optimization using genetic algorithm.
defaultopt = struct('PopulationType', 'doubleVector', ...
    'PopInitRange', [0;1], ...
    'PopulationSize', 20, ...
    'EliteCount', 2, ...
    'CrossoverFraction', 0.8, ...
    'MigrationDirection','forward', ...
    'MigrationInterval',20, ...
    'MigrationFraction',0.2, ...
    'Generations', 100, ...
    'TimeLimit', inf, ...
    'FitnessLimit', -inf, ...
    'StallGenLimit', 50, ...
    'StallTimeLimit', inf, ...
    'TolFun', 1e-6, ...
    'TolCon', 1e-6, ...
    'InitialPopulation',[], ...
    'InitialScores', [], ...
    'InitialPenalty', 10, ...
    'PenaltyFactor', 100, ...
    'PlotInterval',1, ...
```

```
    'CreationFcn',@gacreationuniform, ...
    'FitnessScalingFcn', @fitscalingrank, ...
    'SelectionFcn', @selectionstochunif, ...
    'CrossoverFcn',@crossoverscattered, ...
    'MutationFcn',{{@mutationgaussian 1  1}}, ...
    'HybridFcn',[], ...
    'Display', 'final', ...
    'PlotFcns', [], ...
    'OutputFcns', [], ...
    'Vectorized','off', ...
    'UseParallel', 'never');
% Check number of input arguments
errmsg = nargchk(1,10,nargin);
if ~isempty(errmsg)
    error('gads:ga:numberOfInputs',[errmsg,' GA requires at least 1
input argument.']);
end
 % If just 'defaults' passed in, return the default options in X
if nargin == 1 && nargout <= 1 && isequal(fun,'defaults')
    x = defaultopt;
    return
end
if nargin < 10,  options = [];
    if nargin < 9,  nonlcon = [];
        if nargin < 8, ub = [];
            if nargin < 7, lb = [];
                if nargin <6, beq = [];
                    if nargin <5, Aeq = [];
                        if nargin < 4, bineq = [];
                            if nargin < 3, Aineq = [];
                            end
                        end
                    end
                end
            end
        end
    end
end
 % Is third argument a structure
if nargin == 3 && isstruct(Aineq) % Old syntax
    options = Aineq; Aineq = []; end
% One input argument is for problem structure
if nargin == 1
    if isa(fun,'struct')
        [fun,nvars,Aineq,bineq,Aeq,beq,lb,ub,nonlcon,rngstate,options]
= separateOptimStruct(fun);
        % Reset the random number generators
        resetDfltRng(rngstate);
    else % Single input and non-structure.
        error('gads:ga:invalidStructInput','The input should be a
structure with valid fields or provide at least two arguments to GA.'
);    end
end
 % If fun is a cell array with additional arguments get the function
handle
if iscell(fun)
    FitnessFcn = fun{1};
else
    FitnessFcn = fun;
```

```
end
 % Only function handles or inlines are allowed for FitnessFcn
if isempty(FitnessFcn) ||  ~(isa(FitnessFcn,'inline') ||
isa(FitnessFcn,'function_handle'))
    error('gads:ga:needFunctionHandle','Fitness function must be a
function handle.');
end
 % We need to check the nvars here before we call any solver
valid =  isnumeric(nvars) && isscalar(nvars)&& (nvars > 0) ...
    && (nvars == floor(nvars));
if ~valid
    error('gads:ga:notValidNvars','Number of variables (NVARS) must be
a positive integer.');
end
user_options = options;
% Use default options if empty
if ~isempty(options) && ~isa(options,'struct')
        error('gads:ga:optionsNotAStruct','Tenth input argument must
be a valid structure created with GAOPTIMSET.');
elseif isempty(options)
    options = defaultopt;
end
% Take defaults for parameters that are not in options structure
options = gaoptimset(defaultopt,options);
 % All inputs should be double
try
    dataType = superiorfloat(nvars,Aineq,bineq,Aeq,beq,lb,ub);
    if ~isequal('double', dataType)
        error('gads:ga:dataType', ...
            'GA only accepts inputs of data type double.')
    end
catch
    error('gads:ga:dataType', ...
        'GA only accepts inputs of data type double.')
end
[x,fval,exitFlag,output,population,scores,FitnessFcn,nvars,Aineq,bineq
,Aeq,beq,lb,ub, ...
    NonconFcn,options,Iterate,type] =
gacommon(nvars,fun,Aineq,bineq,Aeq,beq,lb,ub,nonlcon,options,user_opti
ons);
if exitFlag < 0
    return;
end
% Call appropriate single objective optimization solver
switch (output.problemtype)
    case 'unconstrained'
        [x,fval,exitFlag,output,population,scores] =
gaunc(FitnessFcn,nvars, ...
            options,output,Iterate);
    case {'boundconstraints', 'linearconstraints'}
        [x,fval,exitFlag,output,population,scores] =
galincon(FitnessFcn,nvars, ...
            Aineq,bineq,Aeq,beq,lb,ub,options,output,Iterate);
    case 'nonlinearconstr'
        [x,fval,exitFlag,output,population,scores] =
gacon(FitnessFcn,nvars, ...

Aineq,bineq,Aeq,beq,lb,ub,NonconFcn,options,output,Iterate,type);
end
```

Appendix B– Network, UPFC Model Programming

```
  SavedCharacterEncoding  "US-ASCII"
  SaveDefaultBlockParams  on
  ScopeRefreshTime    0.035000
  OverrideScopeRefreshTime on
  DisableAllScopes    off
  DataTypeOverride    "UseLocalSettings"
  MinMaxOverflowLogging   "UseLocalSettings"
  MinMaxOverflowArchiveMode "Overwrite"
  Creator         "hyp01"
  UpdateHistory       "UpdateHistoryNever"
  ModifiedByFormat    "%<Auto>"
  LastModifiedBy      "Amo"
  ModifiedDateFormat      "%<Auto>"
  RTWModifiedTimeStamp    0
  ModelVersionFormat      "1.%<AutoIncrement:1027>"
  ConfigurationManager    "None"
  SampleTimeColors    off
  SampleTimeAnnotations   off
  LibraryLinkDisplay      "none"
  WideLines       off
  ShowLineDimensions      off
  ShowPortDataTypes   off
  ShowLoopsOnError    on
  IgnoreBidirectionalLines off
  ShowStorageClass    off
  ShowTestPointIcons      on
  ShowSignalResolutionIcons on
  ShowViewerIcons     on
  SortedOrder         off
  ExecutionContextIcon    off
  ShowLinearizationAnnotations on
  BlockNameDataTip    off
  BlockParametersDataTip  off
 Array {
    Type            "Handle"
    Dimension           1
    Simulink.ConfigSet {
      $ObjectID           1
 Array {
    Type            "Handle"
    Dimension       8
    Simulink.SolverCC {
      $ObjectID       2
      Version         "1.6.0"
      StartTime       "0"
      StopTime        "40"
      AbsTol          "1e-3"
      FixedStep       "auto"
      InitialStep         "auto"
      MaxNumMinSteps      "-1"
      MaxOrder        5
      ZcThreshold         "auto"
      ConsecutiveZCsStepRelTol "10*128*eps"
      MaxConsecutiveZCs   "1000"
      ExtrapolationOrder      4
      NumberNewtonIterations  1
```

```
      MaxStep         "1/60"
      MinStep         "auto"
      MaxConsecutiveMinStep   "1"
      RelTol          "1e-4"
      SolverMode          "SingleTasking"
      Solver          "ode23tb"
      SolverName          "ode23tb"
      ShapePreserveControl    "DisableAll"
      ZeroCrossControl    "UseLocalSettings"
      ZeroCrossAlgorithm      "Nonadaptive"
      AlgebraicLoopSolver     "TrustRegion"
      SolverResetMethod   "Fast"
      PositivePriorityOrder   off
      AutoInsertRateTranBlk   off
      SampleTimeConstraint    "Unconstrained"
      InsertRTBMode       "Whenever possible"
      SignalSizeVariationType "Allow only fixed size"
    }
PropName        "Components"
      }
      Name            "Configuration"
      CurrentDlgPage          "Real-Time Workshop/Interface"
      ConfigPrmDlgPosition    " [ -2, 26, 927, 740 ] "
    }
    PropName            "ConfigurationSets"
  }
  Simulink.ConfigSet {
    $PropName           "ActiveConfigurationSet"
    $ObjectID           1
  }
  BlockDefaults {
    ForegroundColor     "black"
    BackgroundColor     "white"
    DropShadow          off
    NamePlacement       "normal"
    FontName            "Helvetica"
    FontSize            10
    FontWeight          "normal"
    FontAngle           "normal"
    ShowName            on
    BlockRotation       0
    BlockMirror         off
  }
  AnnotationDefaults {
    HorizontalAlignment     "center"
    VerticalAlignment       "middle"
    ForegroundColor     "black"
    BackgroundColor     "white"
    DropShadow          off
    FontName            "Helvetica"
    FontSize            10
    FontWeight          "normal"
    FontAngle           "normal"
    UseDisplayTextAsClickCallback off
  }
  LineDefaults {
    FontName            "Helvetica"
    FontSize            9
    FontWeight          "normal"
```

```
  FontAngle           "normal"
}
BlockParameterDefaults {
  Block {
    BlockType           BusCreator
    Inputs              "4"
    DisplayOption       "none"
    UseBusObject        off
    BusObject           "BusObject"
    NonVirtualBus       off
  }
  Block {
    BlockType           Outport
    Port            "1"
    UseBusObject        off
    BusObject           "BusObject"
    BusOutputAsStruct       off
    PortDimensions          "-1"
    SampleTime          "-1"
    OutMin              "[]"
    OutMax              "[]"
    DataType            "auto"
    OutDataType         "fixdt(1,16,0)"
    OutScaling          "[]"
    OutDataTypeStr          "Inherit: auto"
    LockScale           off
    SignalType          "auto"
    SamplingMode        "auto"
    SourceOfInitialOutputValue "Dialog"
    OutputWhenDisabled      "held"
    InitialOutput       "[]"
    DimensionsMode          "auto"    }
  Block {
    BlockType           PMComponent
    SubClassName        "unknown"    }
  Block {
    BlockType           PMIOPort
  }
  Block {
    BlockType           Product
    Inputs              "2"
    Multiplication          "Element-wise(.*)"
    CollapseMode        "All dimensions"
    CollapseDim         "1"
    InputSameDT         on
    OutMin              "[]"
    OutMax              "[]"
    OutDataTypeMode         "Same as first input"
    OutDataType         "fixdt(1,16,0)"
    OutScaling          "[]"
    OutDataTypeStr          "Inherit: Same as first input"
    LockScale           off
    RndMeth             "Zero"
    SaturateOnIntegerOverflow on
    SampleTime          "-1"    }
  Block {
    BlockType           RateLimiter
    RisingSlewLimit         "1"
    FallingSlewLimit        "-1"
```

```
      SampleTimeMode          "continuous"
      InitialCondition        "0"
      LinearizeAsGain         on
    }
    Block {
      BlockType           RealImagToComplex
      Input           "Real and imag"
      ConstantPart        "0"
      SampleTime          "-1"
    }
    Block {
      BlockType           RelationalOperator
      Operator            ">="
      InputSameDT         on
      LogicOutDataTypeMode    "Logical (see Configuration Parameters:
Optimization)"
      LogicDataType       "uint(8)"
      OutDataTypeStr          "Inherit: Logical (see Configuration
Parameters: Optimization)"
      ZeroCross           on
      SampleTime          "-1"
    }
    Block {
      BlockType           Saturate
      UpperLimit          "0.5"
      LowerLimit          "-0.5"
      LinearizeAsGain         on
      ZeroCross           on
      SampleTime          "-1"
      OutMin              "[]"
      OutMax              "[]"
      OutDataTypeMode         "Same as input"
      OutDataType         "fixdt(1,16,0)"
      OutScaling          "[]"
      OutDataTypeStr          "Inherit: Same as input"
      LockScale           off
      RndMeth             "Floor"    }
    Block {
      BlockType           Scope
      ModelBased          off
      TickLabels          "OneTimeTick"
      ZoomMode            "on"
      Grid            "on"
      TimeRange           "auto"
      YMin            "-5"
      YMax            "5"
      SaveToWorkspace         off
      SaveName            "ScopeData"
      LimitDataPoints         on
      MaxDataPoints       "5000"
      Decimation          "1"
      SampleInput         off
      SampleTime          "-1"    }
    Block {
      BlockType           Selector
      NumberOfDimensions      "1"
      IndexMode           "One-based"
      InputPortWidth          "-1"
      SampleTime          "-1"    }
```

This work is a joint supervision between ZAGAZIG UNIVERSITY, EGYPT and AALTO UNIVERSITY, FINLAND. Professor Mahdi El-Arini participated from Zagazig University and Professor Matti Lehtonen participated from Aalto University. The concept of FACTS technology has the ability to deal with many fields of both system and customer problems, where the power control can solve many of these problems with enhancing the quality of the performance. The subject of the thesis is to study applications of FACTS to control an electric power system. There are some problems like the inability to achieve full utilizing of the capacity of the transmission lines, undesirable voltage levels, higher losses, high or low voltages, blocking and outages that must be solved. The thesis derives the criteria to install the UPFC in an optimal location with optimal parameters and then designs an AI based damping controller for enhancing power system dynamic performance.

Aalto-DD 55/2011

ISBN 978-952-60-4176-6 (pdf)
ISBN 978-952-60-4175-9
ISSN-L 1799-4934
ISSN 1799-4942 (pdf)
ISSN 1799-4934

Aalto University
School of Electrical Engineering
Department of Electrical Engineering
www.aalto.fi

BUSINESS + ECONOMY

ART + DESIGN + ARCHITECTURE

SCIENCE + TECHNOLOGY

CROSSOVER

DOCTORAL DISSERTATIONS